

**Cytoskeletal Remodeling and Exocytosis During Mast Cell
Activation is Controlled by the RhoA GEF, GEF-H1**

by

Yitian Guo

A thesis submitted in partial fulfillment of the requirements for the degree of

Doctor of Philosophy

Department of Medicine

University of Alberta

© Yitian Guo, 2021

Abstract

Mast cells are tissue-resident immune cells that play important roles in health and diseases. Mast cells release their granule contents under antigen-stimulation via the FcεRI signaling pathway. The process of regulated exocytosis in mast cells is known as degranulation which participates in allergic and inflammatory disorders, such as asthma. Therefore, it is important to elucidate the detailed mechanisms of mast cell exocytosis. Previously, we and others have shown that Rho proteins (Rac1, Cdc42, RhoA), members of small monomeric G proteins and molecular switches, regulate mast cell degranulation. Rho proteins are master regulators of the cytoskeleton including actin and microtubules, suggesting that cytoskeleton remodeling is involved in controlling granule transport in mast cells. Rho proteins are activated by RhoGEFs.

Here, we investigated the roles of cytoskeleton remodeling and RhoGEFs in regulating mast cell exocytosis. In **Chapter 3**, we primarily used live-cell imaging to analyze cytoskeleton remodeling and granule transport in real-time during antigen-stimulation of RBL-2H3 cells. Granule transport to the cell periphery was found to be coordinated with de novo microtubule formation rather than F-actin. Kinesore, a drug that activates the microtubule motor kinesin-1 in the absence of cargo, inhibited microtubule-granule association and significantly reduced exocytosis, but had no effect on cell morphology. Immunofluorescence microscopy showed granules accumulated in the perinuclear region after kinesore treatment. The depolymerization of microtubules with nocodazole or colchicine also resulted in a significant defect in exocytosis and prevention of granule movement; however, cell morphology was also significantly affected. Furthermore, enriched granule fractions showed kinesin-1 levels increased in antigen-stimulated cells, whereas they were reduced by kinesore pre-treatment. Results of granule co-fractionation assays suggested that cargo adaptors recruitment to granules was independent of the kinesin-1

motor association. Altogether, results in **Chapter 3** showed that mast cell granules associate with microtubules and are driven by kinesin-1 to facilitate exocytosis.

In **Chapter 4**, RhoGEFs required for mast cell exocytosis were investigated using RBL-2H3 cells as model mast cells. RT-PCR was used to profile the expression levels of RhoGEFs. High levels and selective mast cell expression suggested that Vav1, P-Rex1, α -PIX, β -PIX and GEF-H1 may act as candidates. Silencing of Vav1, P-Rex1, α -PIX, β -PIX expression by RNA interference (RNAi) did not alter granule movement or exocytosis in antigen-stimulated cells. The activation of Rac1 was downregulated, but not completely, in Vav1, P-Rex1, and α -PIX depleted cells. These results ruled out independent functional roles for these RhoGEFs in mast cell exocytosis. Importantly, silencing of GEF-H1 significantly disrupted cell spreading, granule movement and exocytosis. Re-introduction of an RNAi-resistant mutant of GEF-H1 restored cell morphology and granule localization in GEF-H1-depleted cells when stimulated. Moreover, RhoA, but not Rac1, was found to be a downstream target by GEF-H1. Morphologically, the knockdown of GEF-H1 suppressed stress fiber formation, a function of RhoA, without altering cell ruffling or lamellipodia formation. Re-introduction of Rho-G14V, a constitutively active mutant of RhoA, restored normal cell morphology in antigen-stimulated GEF-H1-depleted cells. In addition, focal adhesion (FA) formation was found to participate in granule exocytosis. Inhibition of FA formation by PF-573228 significantly reduced antigen-stimulated exocytosis. GEF-H1 depletion led to the reduced formation of FAs in antigen-stimulated cells, which correlated with defective exocytosis. Furthermore, GEF-H1 underwent activation via the Fc ϵ RI signaling pathway, but was found to be independent of microtubule dynamics. Activation of GEF-H1 was dependent on the Syk kinase regardless of other kinases including Src, Fyn, Lck, MEK1/2, PI3K and FAK. The Syk inhibitor, GS-9973, suppressed cell spreading, granule

movement and exocytosis in antigen-stimulated RBL-2H3 cells. Assays of co-localization and co-fractionation of enriched granules did not identify interactions between GEF-H1 and Exo70, an important component of the exocytosis machinery. Taken together, the GEF-H1-RhoA signaling axis transduces antigen stimulation signals from FcεRI to the exocytosis machinery in mast cells, which we show involves the formation of FAs.

Preface

This thesis contains the original work performed by Yitian Guo. **Chapter 3** and **Chapter 4** will be submitted for publication in open access scientific journals as co-authored papers. Experiments presented in **Chapter 3** were performed by Yitian Guo with the aid of Jeremies Ibanga, who was supervised primarily by Yitian Guo. Yitian's specific contributions to experiments presented in **Chapter 3** were the design of the research study, development of protocols, execution and analysis of experiments, collection of data and editing of the manuscript. Specific contributions to the data in **Chapter 3** by Jeremies Ibanga are as indicated in the figure legends. Experiments presented in **Chapter 4** were performed by Yitian Guo with the aid of Judeah Negre who was supervised primarily by Dr. Gary Eitzen. Yitian's specific contributions to experiments presented in **Chapter 4** were the design of the research study, development of protocols, execution and analysis of experiments, collection of data and writing and editing of the manuscript. Specific contributions to the data in **Chapter 4** by Judeah Negre are as indicated in the figure legends.

Acknowledgements

I would like to thank my supervisors Drs. Gary Eitzen and Paige Lacy from the bottom of my heart. They have guided me consistently and helped me toward earning this degree, without hesitating to train me as a qualified scholar even when I was switching labs. In the past five years of my graduate journey, I mostly appreciate all the efforts and help from Dr. Gary Eitzen, with whom I am lucky to share so many unforgettable experiences. All in my journey were indeed a life-long treasure. I have hugely transformed in a number of life aspects.

I am also thankful to my candidacy and PhD exam committee members including Drs. Nicolas Touret, Katalin Szaszi, Marianna Kulka, Adrian Wagg, Thomas Simmen, Harissios Vliagoftis for their valuable feedback and guidance. I am fortunate to receive intensive help from the colleagues at University of Alberta, including Drs. Andrew Simmonds, Paul LaPointe, Sarah Hughes, Qiumin Tan, Christine Webber, Julie Haskins, Jobey Wills, to name a few, including their generous reagents and comments. I am grateful to many students who worked with me during this journey.

Sincerely, a kind appreciation should be given to Jeremies Ibanga, Judeah Negre, Rowayna Shouib, Eric Zhang, Arthur Bassot, Kazuki Ueda, Nadia Daniel, Yuxiang Fan, Lucas Mina, Solomon Hussein and many others, for the collaboration and shared experiences. All of you are genuinely wonderful and very helpful. Moreover, even when I was suffering and lacked productivity during my former research time in the Mason lab, I still feel grateful to many members including Dr. Andy Mason, Gunagzhi Zhang, Kerolous Messeha, Filip Wysokinski, Tracy Jordan, Juan Jovel and others. I also greatly appreciate Julian Schulz and Gopinath Sutendra who are graduate coordinators in the Department of Medicine for their very supportive help and care. I thank all my course instructors at University of Alberta for the knowledge.

Being an international PhD student is even harder than what I thought before coming to Canada. There were always ups and downs in this journey, both academically and non-academically. I am so fortunate to survive and extend to a higher level. Life is challenging when studying overseas, but I could be fruitful due to my curiosity and strong willpower to keep learning and practicing. It is almost at the end of my graduate journey, but it is a new beginning of my resting life.

A lot of people in China have helped me incredibly in these years, including my family, many best friends and former colleagues. I owe my growth to all you guys, too. Thank you so much for such unwavering support and encouragement. I appreciate the funding sources of Natural Sciences and Engineering Research Council of Canada (NSERC) and China Scholarship Council (CSC) to support my research work.

Last but not least, my thesis work here is not a solo effort but instead a collection of contribution and efforts. Thank you to all the guys who helped me to learn and grow.

Table of Contents

Page #

Chapter 1 Background of Knowledge

<u>1.1</u> Mast cells	1
1.1.1 Overview of mast cells	1
1.1.2 Heterogeneity of mast cells	1
1.1.3 Development and isolation of mast cells (RBL-2H3 as a mast cell model)	2
1.1.4 Roles of mast cells in immunity, inflammation, and diseases	3
1.1.5 Regulation of mast cell activation	4
1.1.6 Mast cell granule exocytosis (degranulation)	5
<u>1.2</u> Cytoskeletal remodeling and its roles in mast cell degranulation	6
1.2.1 Overview of actin and microtubule polymerization	6
1.2.2 Actin in mast cell degranulation	8
1.2.3 Role of microtubule dynamics in mast cell granule motility and degranulation	9
<u>1.3</u> Rho signaling pathway in mast cells	9
1.3.1 Overview of Rho proteins	9
1.3.2 Regulation of Rho proteins	10
1.3.3 Rho proteins are cytoskeleton regulators	10
1.3.4 Rho proteins and mast cell degranulation	11
<u>1.4</u> Rho proteins upstream activators, RhoGEFs	12
1.4.1 Overview of RhoGEFs	12
1.4.2 Roles of RhoGEFs in immune cells and cell secretion	12
<u>1.5</u> GEF-H1, a RhoGEF involved in exocytosis	13
1.5.1 GEF-H1 overview	13
1.5.2 Roles of GEF-H1 in cellular processes and diseases	14
1.5.3 Regulation of GEF-H1	14
1.5.4 Interacting partners of GEF-H1	16
1.5.5 Roles of exocyst in exocytosis and membrane trafficking	16
1.5.6 The exocyst contributes to the function of GEF-H1	17
<u>1.6</u> Rationale and Hypothesis	18
1.6.1 Rationale	18
1.6.2 Hypothesis and Research Questions	18

Chapter 2 Materials and Methods

<u>2.1</u> Materials	20
2.1.1 Plasmids	20

2.1.2	Small molecules and drugs	21
2.1.3	Antibodies	22
2.1.4	Oligonucleotides	24
2.2	Methods	27
2.2.1	Cell culture	27
2.2.2	Drug and small molecule treatment	27
2.2.3	Total RNA extraction and cDNA synthesis	27
2.2.4	RT-PCR and qPCR	28
2.2.5	Knockdown of Vav1, P-Rex1, α -PIX, β -PIX and GEF-H1 expression	28
2.2.6	Competent cell preparation and plasmid isolation	29
2.2.7	Transfection of RBL-2H3 cells by electroporation of plasmids	30
2.2.8	Purification of recombinant protein probes	30
2.2.9	Detection of RhoA-GTP and Rac1-GTP by pulldown assay	31
2.2.10	Detection of active GEF-H1 by RhoA-G17A pulldown assay	31
2.2.11	Co-immunoprecipitation (co-IP) assay	31
2.2.12	Protein extraction and immunoblot analysis	32
2.2.13	Mast cell granule exocytosis assay (degranulation assay)	32
2.2.14	Immunofluorescence	33
2.2.15	Live-cell imaging	33
2.2.16	Molecular cloning of GEF-H1-RNAi resistant mutant	34
2.2.17	Focal adhesion isolation and staining	35
2.2.18	Cell size measurement by ImageJ	35
2.2.19	Granule enrichment and co-fractionation	35
2.2.20	Statistical analysis	36

Chapter 3 and 4 Results

[Chapter 3](#) Mast cell granule motility and exocytosis is driven by dynamic microtubule formation and kinesin-1 motor function

3.1	Introduction: microtubule dynamics, but not actin remodeling, regulate mast cell granule exocytosis	38
3.2	Live-cell imaging of cytoskeletal dynamics during mast cell stimulation implicates a role for microtubules in granule exocytosis	40
3.3	Effect of microtubule-targeted drugs on mast cell granule exocytosis	41
3.4	Effect of the microtubule motor modulator, kinesore, on mast cell granule trafficking and exocytosis	44

3.5	Microtubule-targeted drugs do not block cell transition to activated phenotype	49
3.6	Kinesore affects the association of granules with the microtubule motor, kinesin-1	51
3.7	Discussion: microtubule dynamics for granule trafficking in mast cells	52
3.8	Supplemental video list with links to online content	58

Chapter 4 The Role of RhoGEFs in mast cell exocytosis

4.1	Introduction: Signal transductions from RhoGEFs to Rho proteins in mast cell cytoskeleton remodeling and exocytosis	60
4.2	Profile of RhoGEF expression in mast cells	62
4.3	Knockdown of putative Rac1 RhoGEFs (Vav1, P-Rex1, α -PIX and β -PIX) and the effect on mast cell degranulation	64
4.4	Roles of Vav1, P-Rex1, α -PIX and β -PIX in granule trafficking during RBL-2H3 cell activation	68
4.5	Double knockdown of Vav1 and P-Rex1 and the effect on mast cell degranulation	72
4.6	Establishment of a role for GEF-H1 (ARHGEF2) in mast cell degranulation; depletion of GEF-H1 affects mast cell degranulation	72
4.7	Knockdown of GEF-H1 resulted in dysregulated cell activation/spreading and granule trafficking	74
4.8	RhoA, but not Rac1, is a downstream target of GEF-H1	82
4.9	The GEF-H1-RhoA signaling axis regulates focal adhesion (FA) formation; role of FAs in mast cell degranulation	90
4.10	GEF-H1 is activated in mast cells via the Fc ϵ RI antigen-stimulated signaling pathway	91
4.11	Regulation of GEF-H1 activation by kinases in mast cells	96
4.12	Interaction of GEF-H1 with Exo70 and its contribution to mast cell degranulation	108
4.13	Discussion: the roles of the GEF-H1-RhoA signaling axis in mast cells exocytosis	112
4.14	Supplemental video list with links to online content	117

Chapter 5 Discussion and Future directions

5.1	Discussion	119
5.1.1	Roles of microtubules (and associated motors) in mast cell degranulation	119
5.1.2	Microtubule-based motors and their cargo adaptor proteins	120
5.1.3	Roles of putative RhoGEFs in mast cell degranulation	121
5.1.4	GEF-H1 subcellular localization: interacted with microtubules	123
5.1.5	GEF-H1 in actin remodeling	123
5.1.6	GEF-H1-RhoA axis regulated focal adhesion	124
5.1.7	GEF-H1 activation by kinases in mast cells	125

5.1.8 Interactions of GEF-H1: and roles of Exo70	126
5.1.9 The crosstalk between microtubule dynamics and focal adhesions	127
5.2 Future directions	128
5.2.1 BioID/protein proximity ligation to dissect GEF-H1 interacting proteins	128
5.2.2 Biosensor of GEF-H1 to dissect its activation manner	128
5.2.3 Further investigate the role of Exo70 in mast cell degranulation	129
5.2.4 In vivo study: utilize primary mast cells of GEF-H1 knockout mice and dissect its role in allergic diseases	129
Bibliography	130

List of Figures

Figure 1.1	A mouse bone marrow-derived mast cell stained with toluidine blue.	1
Figure 1.2	Role of mast cells in airway hyper-responsiveness.	4
Figure 1.3	Mast cell antigen-activation and FcεRI signaling.	7
Figure 1.4	Features of the GEF-H1/ARHGEF2 protein.	15
Figure 1.5	A hypothesized model of RhoGEFs and cytoskeleton remodeling in mast cell exocytosis.	19
Figure 3.1	Live-cell imaging of cytoskeletal dynamics and granule movement during mast cell stimulation.	42
Figure 3.2	Microtubule drugs inhibit mast cell granule exocytosis and affect granule motility.	45
Figure 3.3	Kinesore, a small-molecule activator of microtubule motors, inhibits mast cell granule exocytosis.	47
Figure 3.4	Microtubule drugs and the microtubule motor drugs, kinesore, affects cell morphology and granule distribution but not F-actin remodeling.	50
Figure 3.5	Kinesore treatment of mast cells affects microtubule structures independent of its effect on granule distribution.	53
Figure 3.6	Kinesore inhibits granule association of the microtubule motor kinesin-1.	54
Figure 4.1	RhoGEFs (Rho guanine exchange factors) expressed in RBL-2H3 cells, NRK (normal rat kidney epithelial) cells, BMDCs, and bone marrow (BM) stromal cells.	63
Figure 4.2	Depletion of Vav1, P-Rex1, α-PIX and β-PIX by lentivirus-mediated shRNA knockdown (KD) in RBL-2H3 cells.	65
Figure 4.3	The effect of knockdown of Vav1, P-Rex1, α-PIX and β-PIX expression on mast cell exocytosis.	66
Figure 4.4	Rac1 activation in antigen-stimulated RBL-2H3 cells after the depletion of Vav1, P-Rex1, α-PIX and β-PIX.	69
Figure 4.5	Effect of knockdown of Vav1, P-Rex1, α-PIX and β-PIX in granule trafficking in antigen-stimulated RBL-2H3 cells.	70
Figure 4.6	Effect of double knockdown of Vav1 and P-Rex1 on mast cell exocytosis.	73
Figure 4.7	Knockdown of GEF-H1 in RBL-2H3 cells by lentivirus-mediated shRNA interference.	75
Figure 4.8	Depletion of GEF-H1 reduces antigen-stimulated exocytosis in RBL-2H3 mast cells.	76
Figure 4.9	Depletion of GEF-H1 causes cell morphology defects.	77
Figure 4.10	Depletion of GEF-H1 affects granule mobility.	79
Figure 4.11	Introduction of a GEF-H1 RNAi-resistant construct restores granule distribution and cell spreading in antigen-stimulated GEF-H1-depleted RBL-2H3 cells.	80
Figure 4.12	RhoA, but not Rac1, is a downstream effector of GEF-H1 in antigen-stimulated RBL-2H3 cells.	84
Figure 4.13	Depletion of GEF-H1 affects stress fiber formation in antigen-stimulated RBL-2H3 cells.	85
Figure 4.14	Depletion of GEF-H1 does not block membrane ruffling and lamellipodia formation.	86

Figure 4.15 Depletion of GEF-H1 does not affect F-actin remodeling at the cell periphery.	87
Figure 4.16 Expression of constitutively active RhoA-G14V restores the defects of granule distribution and cell spreading in GEF-H1-depleted cells.	88
Figure 4.17 Involvement of focal adhesion (FA) formation in RBL-2H3 cell granule exocytosis.	92
Figure 4.18 Quantification of focal adhesions (FAs) in antigen-stimulated RBL-2H3 cells.	93
Figure 4.19 Visualization of focal adhesions (FAs) in GEF-H1-depleted RBL-2H3 cells.	94
Figure 4.20 Focal adhesions (FAs) are reduced in GEF-H1-depleted RBL-2H3 cells	95
Figure 4.21 Assay for active GEF-H1.	97
Figure 4.22 Active GEF-H1 levels increase in antigen-stimulated RBL-2H3 cells.	98
Figure 4.23 Activation of GEF-H1 in stimulated RBL-2H3 cells is not affected by microtubule-targeted drugs.	99
Figure 4.24 Effect of microtubule-targeted drugs on GEF-H1 localization.	100
Figure 4.25 Tubulin was not detected in GEF-H1 immunoprecipitates.	101
Figure 4.26 Effect of kinase inhibitors on granule exocytosis.	103
Figure 4.27 Effect of inhibitors on GEF-H1 activation.	104
Figure 4.28 Effect of the Syk inhibitor, GS-9973, on RBL-2H3 cell degranulation.	105
Figure 4.29 Effect of the Syk inhibitor, GS-9973, on RBL-2H3 cell morphology and granule localization.	106
Figure 4.30 The Syk inhibitor, GS-9973, reduces GEF-H1 activation in antigen-stimulated RBL-2H3 cells.	107
Figure 4.31 Co-immunoprecipitation analysis of GEF-H1 with Exo70 and vinculin.	109
Figure 4.32 Analysis of colocalization of GEF-H1 with CD63, Exo70 and vinculin.	110
Figure 4.33 Granule co-fractionation of Exo70 depends on GEF-H1.	111
Figure 4.34 A putative model of the GEF-H1-RhoA signaling axis in RBL-2H3 cells of antigen stimulation.	115

List of Tables

Table 2.1	Plasmids	20
Table 2.2	Small molecules and drugs	21
Table 2.3	Antibodies and Protein probes	22
Table 2.4	PCR primers of putative RhoGEFs and GAPDH	24
Table 2.5	qPCR primers of five RhoGEFs and GAPDH	25
Table 2.6	qPCR primers of kinesin-1 cargo adaptors	25
Table 2.7	shRNA oligos of RhoGEFs	26

List of Abbreviations

α/β -PIX: p21-activated kinase interacting exchange factor α/β
AID: autoinhibitory domain
ANOVA: one-way analysis of variance
BM: bone marrow
BMMCs: bone marrow-derived mast cells
BSA: bovine serum albumin
C: cysteine
C1: protein kinase C conserved region 1
CC: coiled-coil
Cdc42: cell division control protein 42
cDNA: complementary DNA
co-IP: co-immunoprecipitation
Dbl: diffuse B-cell lymphoma
DH: Dbl homology
DHR-1/2: DOCK homology region-1/2
DIC: differential Interference Contrast
DMEM: Dulbecco's Modified Eagle Medium
DMSO: dimethyl sulfoxide
DNP: 2,4-dinitrophenol
DOCK: dedicator of cytokinesis
EB3: end-binding protein 3
ERK: extracellular signal-regulated kinases
F-actin: filamentous actin
FA(s): focal adhesion(s)
FAK: focal adhesion kinase
FBS: fetal bovine serum
Fc ϵ RI: the high-affinity IgE receptor
Fyn: proto-oncogene tyrosine-protein kinase Fyn
GDP: guanosine diphosphate
GEF-H1/ARHGEF2: Rho guanine nucleotide exchange factor 2
GFP: green fluorescent protein
GST: glutathione S-transferase
GTP: guanosine triphosphate
HA: hemagglutinin
HEPES: 4-(2-hydroxyethyl)-1-piperazineethanesulfonic acid
HI: heat-inactivated
HTB: HEPES-Tyrode's buffer
IgE: immunoglobulin E

IP3G: isopropyl β -D-1-thiogalactopyranoside
ITAMs: immunoreceptor tyrosine-based activation motifs
JIP/mapk8ip: mitogen-activated protein kinase 8/JUN interacting protein
KD: knockdown
Kif5b: kinesin-1 heavy chain
LAT: linker for activation of T cells
MT(s): microtubule(s)
MTOC: microtubule-organizing center
MUG: 4-methylumbelliferyl N-acetyl- β -D-glucosaminide
LB: lysogeny broth
Lck: lymphocyte-specific protein tyrosine kinase
Lyn: tyrosine-protein kinase Lyn
MARK3: microtubule affinity regulating kinase 3
MCP II: mast cell protease II
MEK: mitogen-activated protein kinase kinase
MEM: Eagle's minimum essential media
mRNA: messenger RNA
NC: nitrocellulose
P-Rex1: phosphatidylinositol 3,4,5-trisphosphate-dependent Rac exchanger 1
PAGE: polyacrylamide gel electrophoresis
PAK1/2/4: p21-activated kinase 1/2/4
PAR1b (MARK2): Polarity-regulating kinase partitioning-defective 1b
PEI: polyethylenimine
PFA: paraformaldehyde
PH: pleckstrin homology
PI3K: phosphoinositide 3-kinase
PIC: protease inhibitor cocktail
PIP2: phosphatidylinositol 4,5-bisphosphate
PKA/C: protein kinase A/C
PLC γ : Phospholipase C gamma
Plekhm: pleckstrin homology and RUN domain containing M
PMSF: phenylmethylsulfonyl fluoride
Polybrene: hexadimethrine bromide
PTMs: post-translational modifications
qPCR: quantitative polymerase chain reaction
R: resting
Rac1: Ras-related C3 botulinum toxin substrate 1
Rac1-G15A: the "nucleotide free" Rac1 mutant
Ras: rat sarcoma/proto-oncogene protein p21
RBL-2H3: rat basophilic leukemia-2H3 cells

RhoA: Ras homolog family member A
RhoA-G14V: the constitutively active RhoA mutant
RhoA-G17A: the "nucleotide free" RhoA mutant
RhoGAP: Rho GTPase-activating protein
RhoGDI: Rho guanine nucleotide dissociation inhibitor
RhoGEF: Rho guanine nucleotide exchange factor
RNAi: RNA interference
ROCK: Rho-associated protein kinase
RT: reverse transcription
RT: room temperature
S: antigen-stimulated
S: serine
SCF: stem cell factor
SDS: sodium dodecyl-sulfate
shRNA: short hairpin RNA
SKIP (Plekhm2): SifA and kinesin-interacting protein
Slp: synaptotagmin-like (Styl)
SOC: super optimal broth
Src: proto-oncogene tyrosine kinase Src
Syk: spleen tyrosine kinase
T: threonine
TEA: triethanolamine
TU: transducing unit
VAV1: Vav guanine nucleotide exchange factor 1

List of Videos

Video 3.1 Lifeact-GFP_LysoTracker Red live-cell imaging in stimulated RBL-2H3 cells

https://drive.google.com/file/d/1Z4Cj8DNAMzy6_JSSkvrepGSLGI3q81Gr/view?usp=sharing

Video 3.2 EB3-GFP_LysoTracker Red live-cell imaging in stimulated RBL-2H3 cells

https://drive.google.com/file/d/1-UgCnQb9GZ1RPynk0em_mz_r3z4Cla5S/view?usp=sharing

Video 3.3 EB3-GFP_LysoTracker Red live-cell imaging of nocodazole treated cells

<https://drive.google.com/file/d/1cqun2qCI84GROY3eO1BDIfRm3F7BoqIT/view?usp=sharing>

Video 3.4 EB3-GFP_LysoTracker Red live-cell imaging of colchicine treated cells

https://drive.google.com/file/d/1nMVwvQOfGEN28rdMtYn7Gg5Qk_hkOHCc/view?usp=sharing

Video 3.5 EB3-GFP_LysoTracker Red live-cell imaging of paclitaxel (taxol) treated cells

<https://drive.google.com/file/d/1qyqH7P4xdeLD-eQaNY9xsFdmRPJ3MSMC/view?usp=sharing>

Video 3.6 EB3-tdTomato_LysoTracker Green live-cell imaging of kinesore treated cells

https://drive.google.com/file/d/1urM3jC_eF1IOamQU9rqQAikKeRReHHA1/view?usp=sharing

Video 3.7 Lifeact-mRuby_LysoTracker Green live-cell imaging of kinesore treated cells

https://drive.google.com/file/d/1SuA7LzVrm_IKIRaUoAC1pzWZROscFvpW/view?usp=sharing

Video 4.1 LysoTracker Red live-cell imaging in stimulated cells of Scrambled shRNA (control)

https://drive.google.com/file/d/1jRYcVwVEh9nD_YgeoJJ7Kco3ICTFaPzF/view?usp=sharing

Video 4.2 LysoTracker Red live-cell imaging in stimulated RBL-2H3 cells of Vav1 knockdown

<https://drive.google.com/file/d/11ZqF9tRvNAXQfPXwb7DF33i8WH6-2goZ/view?usp=sharing>

Video 4.3 LysoTracker Red live-cell imaging in stimulated RBL-2H3 cells of P-Rex1 knockdown

https://drive.google.com/file/d/1ymsqkcA-EWLq6cxnLZ0u_bzQLXjnua0B/view?usp=sharing

Video 4.4 LysoTracker Red live-cell imaging in stimulated RBL-2H3 cells of α -PIX knockdown

<https://drive.google.com/file/d/1Q3AWRQiFoqE0EWWHW5JbLw4za0oqcf4j/view?usp=sharing>

Video 4.5 LysoTracker Red live-cell imaging in stimulated RBL-2H3 cells of β -PIX knockdown

<https://drive.google.com/file/d/1RWXCHaoDE3ABTgkQezTwZMYow0JHZJHa/view?usp=sharing>

Video 4.6 LysoTracker Red live-cell imaging in stimulated cells of FUGW

<https://drive.google.com/file/d/1mNPBrIyxNKtJMkUtIAAnBDJPt5qN1WLYW/view?usp=sharing>

Video 4.7 LysoTracker Red live-cell imaging in stimulated cells of GEF-H1 knockdown

<https://drive.google.com/file/d/1Aa8FIrBJJ-AMVpWXga-BO2ecqlad0JqA/view?usp=sharing>

Video 4.8 Differential Interference Contrast (DIC) live-cell imaging in stimulated cells of FUGW

https://drive.google.com/file/d/1MgUAsJ4MX_4543WGhytpnL8Uz63ogDRZ/view?usp=sharing

Video 4.9 Differential Interference Contrast (DIC) live-cell imaging in stimulated cells of GEF-H1 knockdown

https://drive.google.com/file/d/1Kzc87PPqH_iiu6W32XWdK7QwN5w9WydE/view?usp=sharing

Video 4.10 Lifeact-mRuby live-cell imaging in stimulated cells of FUGW

https://drive.google.com/file/d/1IQni43sjVOu3LFIhcSvC4R0nz_j2ZPhR/view?usp=sharing

Video 4.11 Lifeact-mRuby live-cell imaging in stimulated cells of GEF-H1 knockdown

https://drive.google.com/file/d/1W8PPupWXz80xAFUJB-o89157L7p6_kz_/view?usp=sharing

Chapter 1 Background of Knowledge

1.1 Mast cells

1.1.1 Overview of mast cells

Mast cells are tissue-resident immune cells, first discovered by Paul Ehrlich in 1878, based on their large cytoplasmic granules and unique staining properties [Krystel-Whittemore et al., 2016]. Due to their high acidity, alkaline dyes such as toluidine blue undergo metachromasia and stain granules violet red, a property unique to mast cells and basophils (**Figure 1.1**).

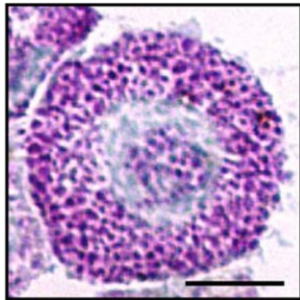


Figure 1.1 A mouse bone marrow-derived mast cell stained with toluidine blue. Mouse bone marrow hematopoietic cells were differentiated into mast cells by culturing in the presence of SCF and IL-3 for four weeks. Note the central nucleus (blue) and the cytosol that is filled with large granules (violet). Scale bar = 10 μ m. Reprinted with permission from Baier et al., 2021.

Mast cells play important roles in multiple cellular processes, including wound healing, inflammation, and immune responses [da Silva et al., 2014]. The activation of mast cells via various antigens specific to IgE, which bind to the mast cell high-affinity IgE receptor, Fc ϵ RI, has been widely recognized and studied [Blank and Rivera, 2004]. When stimulated, mast cells release various pro-inflammatory mediators that are contained inside cytoplasmic granules in a process called degranulation [Blank and Rivera, 2004]. Emerging studies, including results presented in this thesis, have begun to reveal details of the regulatory mechanisms of mast cell activation and degranulation, which primarily aim to alleviate the effects of various mast cell-oriented diseases including allergic inflammation.

1.1.2 Heterogeneity of mast cells

Mast cells exhibit a high degree of phenotypic heterogeneity and plasticity, as a result of their final tissue localization and the influence of each micro-environment and environmental stimuli [da Silva et al., 2014]. In general, mast cells can be broadly classified as either mucosal mast

cells that produce only tryptase, or connective tissue mast cells that produce chymase, tryptase, and carboxypeptidases [Schwartz, 2006]. Mucosal mast cells reside in lungs, intestine and kidney, while connective tissue mast cells reside in skin, joints and vasculature [Krystel-Whittemore et al., 2016; Moon et al., 2010]. Tissue-specific mast cells show a unique but trained memory, which contributes to shaping their functions in the local microenvironment. For example, the most common exposure of antigens to the respiratory tract is via inhalation. Mucosal mast cells in the upper respiratory tract that are activated by antigen can trigger degranulation, releasing histamine that increases vascular permeability and mucus production, which can obstruct nasal airways and lead to congestion [da Silva et al., 2014]. In the lower respiratory tract, mast cell activation leads to the release of tryptase causing muscle contraction and bronchoconstriction producing airflow obstruction and wheezing [Galli et al., 2008].

1.1.3 Development and isolation of mast cells (RBL-2H3 as a mast cell model)

Mast cells originate from bone marrow pluripotent progenitor cells, which differentiate under the influence of the c-kit ligand stem cell factor (SCF) to immature mast cells. Immature mast cells leave the bone marrow and migrate into tissues and then fully differentiate under the influence of cytokines and growth factors present in the local tissue microenvironment [Krystel-Whittemore et al., 2016]. Based on current knowledge, hematopoietic stem cells serially differentiate into common myeloid progenitors and granulocyte/monocyte progenitors that later give rise to both basophils and mast cells which have similar granule contents [Dahlin and Hallgren, 2015]. The majority of these progenitors are found to express the high affinity IgE receptor, FcεRI [Qi et al., 2013]. Mature mast cells are different from basophils which do circulate in the blood, while mast cells eventually reside in various tissues and only then become mature tissue-resident mast cells.

In this study we used rat basophilic leukemia cells, RBL-2H3, as a model mast cell for all the studies. The RBL cell line was obtained from a rat granulocytic leukaemia that was serially passaged through rats by intrapleural injection [Leonard et al., 1971]. While initial isolates of RBL cell lines were more characteristic of basophils, selection based on IgE-mediated histamine release resulted in the clonal selection of RBL-2H3 strain [Kulczycki et al., 1974; Barsumian et al., 1981; Siraganian and Metzger, 1978]. RBL-2H3 cells possess typical properties of mucosal mast cells and express abundant FcεRI, the high affinity IgE receptor, on the cell

surface, and thus, they undergo robust exocytosis after activation by triggering the aggregation of these receptors by stimulated antigens [Passante and Frankish, 2009]. Moreover, RBL-2H3 cells are adherent when cultured and therefore highly amenable to cell-imaging studies for cytoskeleton dynamics and granule movement [Passante and Frankish, 2009; Sheshachalam et al., 2017].

1.1.4 Roles of mast cells in immunity, inflammation, and diseases

Overall, mast cells are involved in many physiological conditions, such as wound healing, inflammation, innate and adaptive immunity, vasodilation and angiogenesis [da Silva et al., 2014]. Mast cells exert protective roles in defense against bacterial and parasitic infection. Because of their positioning at tissue-environmental interface, mast cells are often the first to respond to invading pathogens and react to environmental cues to protect tissues. Mast cells have the capacity to rapidly respond, releasing pre-formed mediators in a highly regulated manner. However, mast cell hyper-responsiveness contributes to inflammatory disorders such as IgE-mediated allergic diseases where the regulation of mast cells is inadequate [Galli and Tsai, 2012]. Moreover, mast cells can regulate the functions of multiple cell types including T cells, B cells, dendritic cells, macrophages, eosinophils, epithelial cells by releasing mediators to facilitate their recruitment and site-specific activation [da Silva et al., 2014; Krystel-Whittemore et al., 2016]. One of the most well-recognized roles of mast cells is the triggering of the pathogenesis of bronchial allergic diseases, for example, asthma [Bradding and Arthur, 2016]. Mast cells, together with eosinophils, are found to critically contribute to asthmatic inflammatory responses by releasing mediators like proteases and eosinophilic basic proteins that directly affect airway epithelial cells leading to the airway damage and remodeling (**Figure 1.2**). Mast cells also produce chemokines that attract other immune cells and cytokines that can affect airway smooth muscle and increase mucus production [Galli et al., 2008; Bradding and Arthur, 2016; da Silva et al., 2014]. Specific treatments targeting the activation of mast cells, such as anti-IgE intervention with omalizumab, have led to some promising results for allergic patients [Bradding and Arthur, 2016]. Therefore, elucidating the detailed roles of how mast cells contribute to inflammation may help curtail various diseases including allergies.

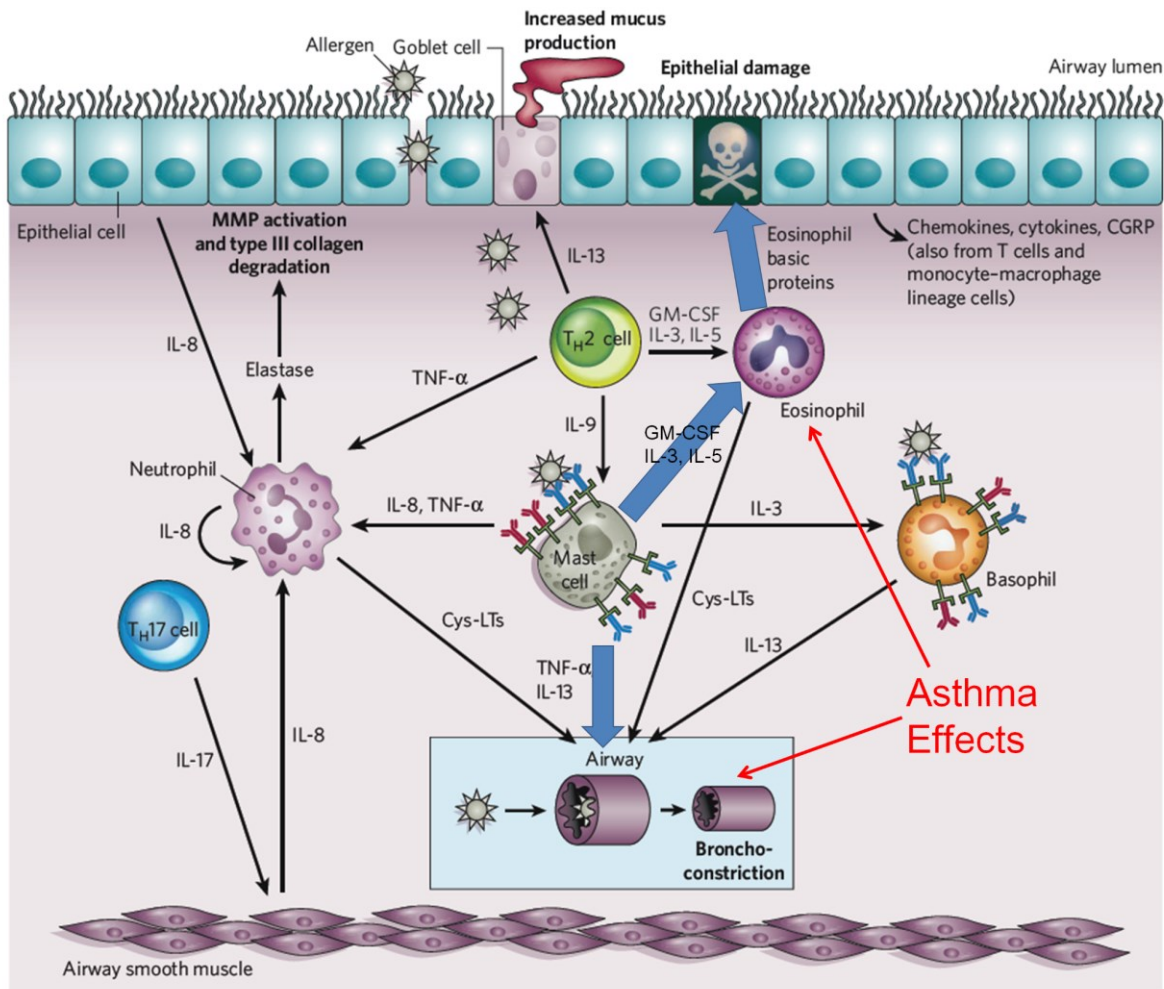


Figure 1.2 Role of mast cells in airway hyper-responsiveness. Mast cells play a central role in allergic diseases through the recruitment and activation of effector immune cells. In asthma, mast cell activation via the FcεRI signaling pathway contributes to the hyper-responsiveness of airways (*thick blue arrows*), triggering bronchial-constriction adding to the difficulty in breathing. Chemokine release during these hyper-responsive reactions also recruits eosinophils which are triggered to release eosinophilic basic proteins which causes damage to the airway epithelia which leads to long-term chronic illness. *Adapted from Galli et al., 2008.*

1.1.5 Regulation of mast cell activation

Mast cells can be activated by diverse stimuli and can produce and release numerous mediator types depending on the stimuli [Blank and Rivera, 2004; Bradding and Arthur, 2016; Redegeld et al., 2018; Wernersson and Pejler, 2014]. The spectrum of mediators mast cells produce include chemical mediators (histamine, serotonin and heparin), enzymes such as proteases and hydrolases (β -hexosaminidase, tryptase, chymase), cytokines (TNF- α), chemokines and

eicosanoids (leukotriene and prostaglandins), growth factors (VEGF) and reactive oxygen species [Galli and Tsai, 2012; Bradding and Arthur, 2016; Mukai et al., 2018]. Mast cells can be activated by both IgE- and non-IgE-mediated signaling pathways [Blank and Rivera, 2004; Redegeld et al., 2018]. The IgE-mediated mast cell activation pathway is well studied and central to the hypersensitivities of allergic reactions [Galli et al., 2008; Galli and Tsai, 2012]. Allergens act as antigens that bind IgE leading to the aggregation of the cell surface receptor, FcεRI [Blank and Rivera, 2004]. Details of this signaling pathway will be discussed later. Mast cells also contain a large repertoire of surface receptors (e.g. Toll-like, Fcγ for IgG, G-protein-coupled receptors (GPCRs) and complement receptors) which facilitate response to various stimuli [Redegeld et al., 2018]. The non-IgE-mediated activation mechanisms in mast cells are complex since distinct stimuli or ligands and act through a diversity of receptors and can trigger a diversity of mast cell responses [Krystal-Whittemore et al., 2016; Mukai et al., 2018]. Certain compounds such as compound 48/80 or calcium ionophore can trigger mast cell activation and exocytosis via direct targeting of the intracellular calcium signaling pathway, rather than through cell surface signaling [Cochrane and Douglas, 1974; Sahara et al., 1990]. These have been helpful experimental tools for dissection of the mast cell activation process [Cochrane and Douglas, 1974; Redegeld et al., 2018].

1.1.6 Mast cell granule exocytosis (degranulation)

Mast cells abundantly express the high affinity IgE receptor, FcεRI, on the cell surface and are sensitized to hyper-reactivity by binding to IgE [Blank and Rivera, 2004]. Cross-linking of IgE-bound FcεRI is initiated by antigens, which triggers robust exocytosis of preformed granules. In vivo this hypersensitivity reaction is the primary effect causing allergic inflammation [Galli et al., 2008; Galli and Tsai, 2012]; hence the regulation of mast cell degranulation via the FcεRI signaling pathway has been well studied [Blank and Rivera, 2004; Wernersson and Pejler, 2014].

Degranulation is the regulated exocytosis of granules, whereby cytoplasmic granules are mobilized to dock and fuse at the plasma membrane, resulting in the release of pro-inflammatory mediators extracellularly [Blank and Rivera, 2004; Wernersson and Pejler, 2014]. This signaling pathway is outlined in **Figure 1.3**. Antigen binding to IgE leads to FcεRI aggregation triggering a downstream signaling cascade [Blank and Rivera, 2004]. Aggregation of FcεRI results in the

cross-phosphorylation of its β and γ subunits by the Src kinase, Lyn, which is associated with the β subunit, followed by the activation of two signaling pathways: one is the Syk-LAT-PLC γ signaling and the other is Fyn-Gab2-PI3K signaling [Costello et al., 1996; Blank and Rivera, 2004]. Activation of PLC γ leads to the hydrolysis of the plasma membrane lipid PIP₂ (phosphatidylinositol-4,5-bisphosphate) to generate IP₃ (inositol 1,4,5-trisphosphate) and DAG (diacylglycerol), which regulates calcium flux and PKC signaling, respectively [Blank and Rivera, 2004]. Calcium is a required co-activator of the SNARE complex which catalyzes granule membrane fusion at the plasma membrane while it is thought that PKC may phosphorylate targets involved in Rab mediated granule docking [Burgoyne and Morgan, 2003; Zhu et al., 2002; Morgan et al., 2005]. Fyn regulates mast cell degranulation in a complementary manner to the Lyn signaling pathway [Parravicini et al., 2002]. Fyn leads to activation of PI3-kinase (PI3K) signaling mechanisms that can initiate cytoskeletal dynamics that contribute to mast cell morphological transitions to an active state and granule mobilization [Sheshachalam et al., 2017; Dráber et al., 2012].

1.2 Cytoskeletal remodeling and its roles in mast cell degranulation

1.2.1 Overview of actin and microtubule polymerization

Actin and microtubule are two major components of the cytoskeleton in the cell [Fletcher and Mullins, 2010]. Actin filaments (F-actin) are the main structural elements that provide for cell shape [Stricker et al., 2010; Pollard, 2016]. Microtubules play important roles in a number of cellular processes, such as intracellular structure organization, cell division, and intracellular transport [Hawkins et al., 2010].

F-actin is a microfilament that is built by two-stranded helical polymers with a diameter of ~ 7 nm [Pollard, 2016]. The actin cytoskeleton consists of biochemically and structurally distinctive actin filament arrays. It can be assembled into actin bundles by crosslinking proteins filamin, villin, spectrin and α -actinin, or branched filaments using effectors actin-related proteins 2/3 (Arp2/3) [Stricker et al., 2010; Pollard, 2016]. Cortical actin surrounds the cell periphery and consists of F-actin filaments, myosin motors, and actin-binding proteins attaching to the plasma membrane via membrane-anchoring proteins called ERM (Ezrin, Radixin, Moesin) proteins

[Pollard, 2016; Ménasché et al., 2021]. The actin cytoskeleton is highly dynamic and its remodeling is actively engaged in various cellular processes including signal transduction, cell motility, cell cycle and cytokinesis, membrane trafficking, the formation of cell adhesion and cell junctions and exocytosis [Stricker et al., 2010; Pollard, 2016; Dráber et al., 2012].

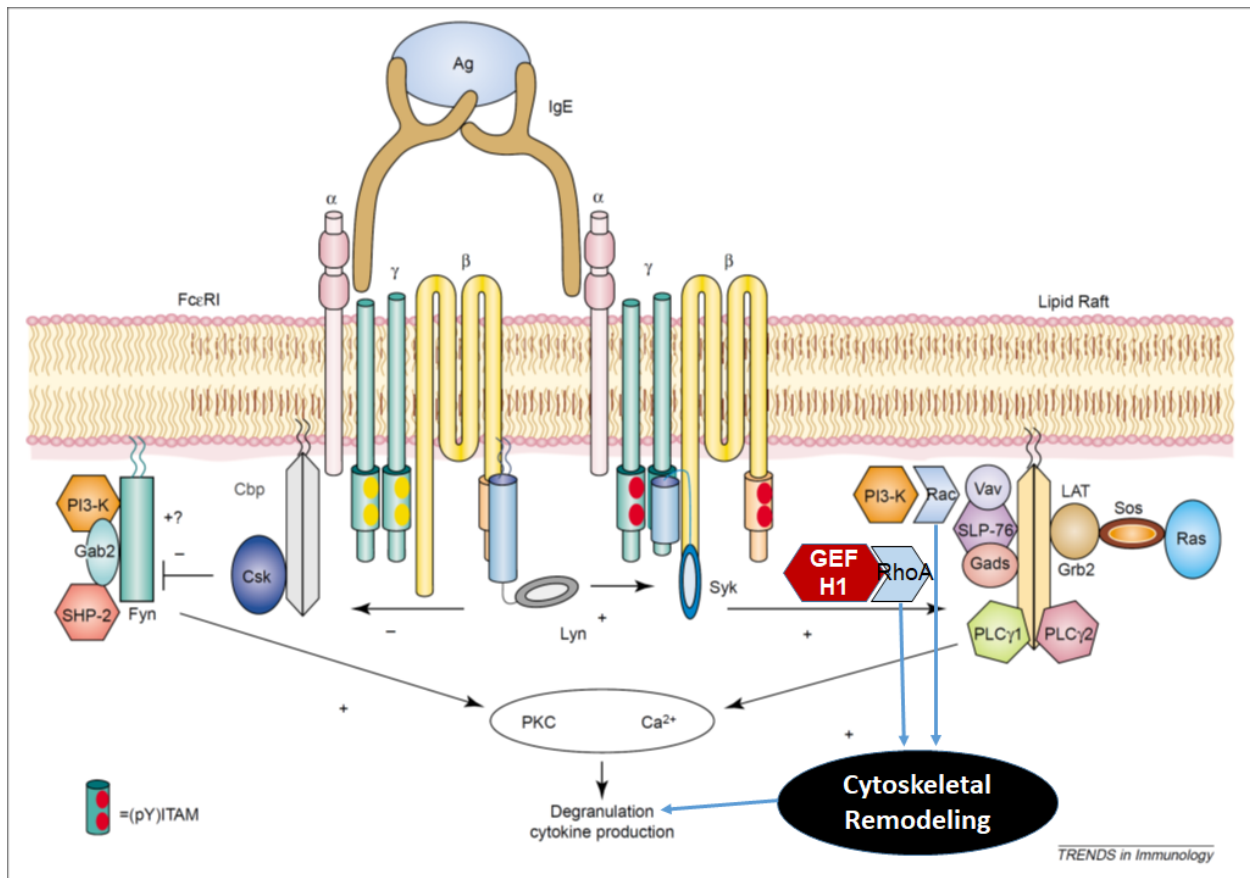


Figure 1.3 Mast cell antigen-activation and FcεRI signaling. Antigen (Ag) binding to FcεRI triggers the aggregation of FcεRI, leading to the phosphorylation of the immunoreceptor tyrosine-based activation motifs (ITAMs). This results in the rapid activations of the Fyn or the Lyn kinases. Fyn activates Grb-2 associated binding-like protein 2 (Gab2) and phosphoinositide 3-kinase (PI3K); while Lyn activates another kinase Syk then activated the linker for activation of T cells (LAT) and phospholipase Cγ (PLCγ). Subsequently, protein kinase C (PKC) and calcium-dependent signaling lead to the outcomes of granule exocytosis (degranulation) and cytokine production. RhoGEFs, such as Vav1, activate Rho proteins which are required for the cytoskeletal remodeling during mast cell exocytosis. The additional knowledge in this thesis is the GEF-H1-RhoA pathway transduces the activation signals of FcεRI to cytoskeletal remodeling during mast cell exocytosis. *Adapted from Blank and Rivera, 2004*

Microtubules are polymers of tubulin consisting of heterodimers of globular α - and β -tubulin subunits assembled into a hollow liner structure [Hawkins et al., 2010]. Microtubules also are highly dynamic that oscillate between phases of growth and shrinkage called “dynamic instability” [Desai and Mitchison, 1997; Hawkins et al., 2010]. New microtubules are nucleated and organized from a centrosome called microtubule organizing center (MTOC) whereby their minus-ends are capped and anchored in the MTOC while the plus-ends grow toward the cell periphery [Akhmanova and Steinmetz, 2015; Ménasché et al., 2021]. Microtubule polymerization at the plus-end contains GTP-bound tubulin which forms a “GTP cap” that is slowly hydrolyzed along the shaft. The GTP cap binds +TIPs end-binding proteins that stabilize microtubules, while GDP-tubulin is inherently unstable which explains the dynamic instability of microtubules [Hawkins et al., 2010; Akhmanova and Steinmetz, 2015]. Microtubule-targeted drugs such as paclitaxel and nocodazole profoundly alter microtubule dynamics and have served as helpful research tools or even treatments for certain diseases [Peterson and Mitchison, 2002; Stanton et al., 2011].

1.2.2 Actin in mast cell degranulation

F-actin dynamics plays an important role in mast cell exocytosis [Dráber et al., 2012; Holowka et al., 2000]; however, the exact roles of actin in exocytosis are controversial. Some studies have suggested actin polymerization acts as a prerequisite for secretory granule capturing and tethering [Nightingale et al., 2011; Wollman and Meyer, 2012; Colin-York et al., 2019], while others have supported actin depolymerization is required for the fusion of secretory granules at the plasma membrane, since cortical F-actin acted as a physiologic barrier [Nishida et al., 2005; Deng et al., 2009; Klein et al., 2019]. Current evidence has indicated there are at least two main functions of the actin cytoskeleton in regulating exocytosis: the tightly and coordinately controlled trafficking of secretory vesicles to their fusion sites at the plasma membrane; and the regulation of the plasma membrane dynamics after vesicle fusion [Porat-Shliom et al., 2013]. Results using the actin depolymerizing drugs, cytochalasin and latrunculin, have demonstrated that actin depolymerization promotes mast cell exocytosis [Narasimhan et al., 1990; Pierini et al., 1997; Frigeri and Apgar, 1999; Sheshachalam et al., 2017].

1.2.3 Role of microtubule dynamics in mast cell granule motility and degranulation

Microtubules also play important roles in mast cell exocytosis [Dráber et al., 2012; Ménasché et al., 2021]. Disruption of microtubules by nocodazole and colchicine has demonstrated the necessity of microtubule polymerization and integrity for calcium influx as well as degranulation in mast cells [Martin-Verdeaux et al., 2003; Oka et al., 2005]. In addition, microtubule-dependent movement has contributed to the mobility of GFP-FasL (Fas ligand)-labeled secretory granules in RBL-2H3 mast cells [Smith et al., 2003]. Nishida et al., revealed two distinct mechanisms in FcεRI-dependent degranulation signaling pathways in mast cells; in particular, a calcium-independent, microtubule-dependent secretory granule trafficking process was mediated by the Fyn/Gab2/RhoA signaling pathway [Nishida et al., 2005]. Further studies have illustrated microtubule-based motor protein, kinesin-1, plays a pivotal role in mast cell exocytosis [Munoz et al., 2016]. Moreover, microtubule-associated proteins along with cell cortex proteins (i.e. ezrin, IQGAP) mediated the interaction between microtubule plus ends and cell periphery, thus regulating the spatial capturing and fusion of secretory granules onto plasma membrane [Noordstra and Akhmanova, 2017]. Interestingly, the acetylation of microtubules contributes to its stability, while inhibition leads to defects in mast cell degranulation [Shiki et al., 2019]. Taken together, microtubule dynamics are critical for mast cell exocytosis.

1.3 The Rho signaling pathway in mast cells

1.3.1 Overview of Rho proteins

Rho proteins are small GTP-binding proteins belonging to the Ras superfamily of GTPases [Mackay and Hall, 1998; Etienne-Manneville and Hall, 2002]. They play an important role in diverse cellular processes including cytoskeletal dynamics, cell polarity and migration, NADPH oxidase activation, membrane trafficking, and transcription [Etienne-Manneville and Hall, 2002]. The Rho gene was originally identified in 1985 [Madaule and Axel, 1985], and its cellular functionalities were later revealed to involve the regulation of the actin cytoskeleton [Ridley and Hall, 1992; Ridley et al., 1992]. There are at least 20 distinct members of the Rho protein family in mammals. Rho protein subfamilies perform different roles; Rac1, Cdc42 and RhoA are the most universally expressed and are functionally essential for the formation of lamellipodia, filopodia and stress fibers respectively [Hodge and Ridley, 2016]. Rho proteins act as molecular

switches that oscillate between GTP-bound activated states or GDP-bound inactivated states [Etienne-Manneville and Hall, 2002; Hodge and Ridley, 2016]. Structurally, most Rho proteins contain an evolutionarily conserved GTPase domain, a hypervariable region towards the C-terminus that often includes a stretch of basic amino acids and a C-terminal CAAX box that is lipid modified by farnesyl or geranylgeranyl isoprenoid lipids [Smithers and Overduin, 2016]. The GTPase domain contains two functional elements: a switch I and switch II regions that are essential for interaction with downstream effectors, while the C-terminal lipid modification, together with the additional C-terminal sequence of the poly-basic domains, target Rho GTPases to specific membranes [Etienne-Manneville and Hall, 2002; Mitin et al., 2012].

1.3.2 Regulation of Rho proteins

The activity of Rho proteins is tightly regulated by multiple molecular pathways [Hodge and Ridley, 2016]. Rho GTPase cycles between active GTP-bound state and an inactive GDP-bound state; this cycling process is regulated by three families of proteins: i) Rho guanine nucleotide exchange factors (RhoGEFs) that facilitate the loading of GTP onto Rho proteins thus leading to their activation [Cook et al., 2014]; ii) Rho GTPase activating proteins (RhoGAPs) that perform a de-activating function by stimulating the hydrolysis of Rho protein-bound GTP [Hodge and Ridley, 2016]; iii) Rho guanine nucleotide dissociation inhibitors (RhoGDIs), which are inhibitors that tightly bind Rho proteins preventing nucleotide exchange and creating a soluble cytoplasmic pool [Garcia-Mata et al., 2011]. In addition, Rho proteins are regulated by several post-translational modifications (PTMs) including lipid modifications, phosphorylation, ubiquitylation and sumoylation, which contribute to their precise spatial and temporal regulation of their localization, turnover and activation [Etienne-Manneville and Hall, 2002; Hodge and Ridley, 2016].

1.3.3 Rho proteins are cytoskeleton regulators

A well-studied role of Rho proteins is their effect on cytoskeleton dynamics [Hall, 1998; Mackay and Hall, 1998]. Significant evidence has illustrated that Rac1, Cdc42 and RhoA are associated with the dynamic formations of lamellipodia, filopodia and stress fiber, respectively [Hall, 1998; Nobes and Hall, 1995; Ridley and Hall, 1992; Ridley et al., 1992]. These formations require the nucleation and branching of the F-actin cytoskeleton and are mediated via the recruitment and

participation of many downstream effectors [Bishop and Hall, 2000]. Lamellipodia are composed of branched actin filaments generated by the Arp2/3 complex which is activated by Rac1 recruitment of the Wave complex [Hahne et al., 2001; Chen et al., 2010; Derivery and Gautreau, 2010; Lebensohn and Kirschner, 2009]. Filopodia are also Arp2/3 branched actin filaments that are formed by Cdc42 recruitment of WASP/WIP complex and tightly connected to membranes by IRSp53 to produce the microspike phenotype [Krugmann et al., 2001; Lim et al., 2008]. The activity of RhoA has been found to regulate the formation of stress fiber nucleated by formins like mDia and activated by ROCK (Rho-associated protein kinase) isoforms [Bishop and Hall 2000; Mackay and Hall, 1998]. These actin bundles have multiple roles in relationship to generation of force and cell adhesion and are important for the assembly and turnover of focal adhesion, which demonstrates the diversely functional roles of RhoA protein [Chrzanowska-Wodnicka and Burridge, 1996; Ridley and Hall, 1992; Wozniak et al., 2004; Yamana et al., 2006].

1.3.4 Rho proteins and mast cell degranulation

Emerging evidence have shown that Rho proteins regulated intracellular vesicle trafficking behavior by targeting actin dynamics in processes of tethering, docking or fusion of vesicles [Ory and Gasman, 2011; Baier et al., 2014; Norman et al., 1996; Sheshachalam et al., 2017]. Previous results have suggested Rho signaling regulated secretory granule trafficking and exocytosis in granulocytes (i.e. neutrophils and eosinophils) and neurons [Mitchell et al., 2008; Lacy, 2005; Sato et al., 2012]. Our recent studies have demonstrated that the Rho proteins, Rac1 and Rac2, regulated mast cell exocytosis by targeting actin dynamics and calcium signaling pathway, respectively [Baier et al., 2014]. In addition, the specific Rho drugs Rhosin and EHT 1864, significantly inhibit mast cell degranulation, in particular by targeting the activation of RhoA and Rac1 [Sheshachalam et al., 2017]. We also have shown that in both neutrophils and mast cells, drugs targeting cytoskeleton rearrangement, including actin or microtubule polymerization, have distinct effects on secretory granule mobility and degranulation [Mitchell et al., 2008; Sheshachalam et al., 2017]. Moreover, Cdc42 has also been found to play pivotal roles in regulating mast cell exocytosis [Hong-Geller and Cerione, 2000; El-Sibai and Backer, 2007]. However, there is still a lack of exact details about the regulatory roles of Rho proteins in mast cells.

1.4 Rho proteins upstream activators, RhoGEFs

1.4.1 Overview of RhoGEFs

RhoGEFs (Rho guanine nucleotide exchange factors) are key activators of Rho proteins. To date, there are 71 Dbl (diffuse B-cell lymphoma) and 11 DOCK (dedicator of cytokinesis) subfamily members of RhoGEFs have been found in mammals, which harbor diverse functions in various biological processes [Schmidt and Hall, 2002; Cook et al., 2014]. The first Dbl RhoGEF to be identified was Dbl (diffuse B-cell lymphoma) [Eva and Aaronson, 1985]; since then, many RhoGEFs have been identified based on the presence of a tandem Dbl-homology (DH) and pleckstrin-homology (PH) domains. RhoGEFs play diverse regulatory functions in many cellular processes including cell migration, membrane trafficking, and oncogenesis [Rossman et al., 2005]. Most RhoGEFs act as signal transducers bridging the extracellular stimuli to their downstream effector via Rho proteins [Cook et al., 2014; Kutys and Yamada, 2015; Schmidt and Hall, 2002].

Structurally, all Dbl members of RhoGEFs have a tandem DH-PH domain, flanked by other functional domains in their N- or C-termini [Cook et al., 2014; Schmidt and Hall, 2002]; while the DOCK members of RhoGEFs consist of the DHR-1 (DOCK homology region-1) and DHR-2 domains [Kunimura et al., 2020]. The DH and DHR-2 domains are mainly responsible for binding Rho proteins and nucleotide exchange, whereas the PH and DHR-1 domains contribute to the localization of RhoGEFs and binding to membrane compartments via interacting with phospholipids [Cook et al., 2014; Rossman et al., 2005; Kunimura et al., 2020].

1.4.2 Roles of RhoGEFs in immune cells and cell secretion

While many RhoGEFs are known oncogenes that promote cell proliferation and migration in cancers [Cook et al., 2014; Gadea and Blangy, 2014; Kunimura et al., 2020], emerging data has revealed important roles for certain RhoGEFs in exocytosis and membrane trafficking [Rossman et al., 2005; Manetz et al., 2001; Pathak et al., 2012; Sulimenko et al., 2015]. Vav1 and P-Rex1, are two Dbl RhoGEFs predominantly expressed in hematopoietic cell lineages [Bustelo, 2014; Welch, 2015]. They have been shown to regulate mast cell degranulation, GLUT4 protein trafficking in adipocytes and dense granule secretion from platelets [Balamatsias et al., 2011;

Manetz et al., 2001; Qian et al., 2012]. ARHGEF10, a RhoA RhoGEF, can interact with Rab6A and Rab8A to mediate the membrane trafficking and the exocytotic pathway [Shibata et al., 2019]. In addition, Intersectin-1L and β -PIX (p21-activated kinase interacting exchange factor β) critically regulate neuroendocrine exocytosis by controlling the activities of Cdc42 and Rac1, respectively [Momboisse et al., 2010]. β -PIX, considered as a Rac and Cdc42 RhoGEF, also modulates the actin-mediated recruitment of vesicles to synapses, and its depletion remarkably disrupts the synaptic vesicle localization [Sun and Bamji, 2011]. Moreover, β -PIX can interact with γ -tubulin to regulate the nucleation/polymerization of microtubules in activated mast cells [Sulimenko et al., 2015]. Several studies also have demonstrated that the RhoA GEF, GEF-H1, is involved in the processes of membrane trafficking in either B cells or epithelial cells [Pathak et al., 2012; Pathak and Dermardirossian, 2013; Sáez et al., 2019]. In mast cells, DOCK5, a Rac GEF from the DOCK subfamily, regulates the remodeling of the microtubule network that is essential for mast cell degranulation; its knockout in mice results in resistance to systemic and cutaneous anaphylaxis [Ogawa et al., 2014]. Therefore, RhoGEFs are important signal transduction modulators for exocytosis in various cells with the potential therapeutic intervention. We assume that certain RhoGEFs will play an important role in regulating mast cell activation and degranulation since our previous studies indicate that Rho proteins are required for these processes [Baier et al., 2014; Sheshachalam et al., 2017].

1.5 GEF-H1, a RhoGEF involved in exocytosis

1.5.1 GEF-H1 overview

GEF-H1 (ARHGEF2), a human homologue to murine Lfc, was firstly discovered as a Dbl-like RhoGEF by screening a human HeLa cell cDNA library [Reddy et al., 1989; Ren et al., 1998] (**Figure 1.4**). It was subsequently demonstrated to have catalytic activity toward RhoA by several studies [Glaven et al., 1996; Ren et al., 1998; Krendel et al., 2002]. Structurally, GEF-H1 possesses an N-terminal C1 domain with a zinc-finger motif that potentially bind diacylglycerol, a tandem Dbl-homology (DH)-Pleckstrin homology (PH) domains, and a C-terminal coiled-coil domain [Birkenfeld et al., 2008; Joo and Olson, 2020]. The DH domain is responsible for its catalytic activity on downstream Rho proteins; whereas the C1, PH and coiled-coil domains participate in its association with microtubules [Birkenfeld et al., 2008; Joo and Olson, 2020].

Several studies have suggested that the binding state of GEF-H1 within the microtubule network is important for its activity [Krendel et al., 2002; Siesser et al., 2012]. In addition, GEF-H1 contains several phosphorylation sites, especially in the coiled-coil domain, that can be phosphorylated by serine/threonine or tyrosine kinases to regulate its function (*see Figure 1.4*) [Birkenfeld et al., 2008; Joo and Olson, 2020].

1.5.2 Roles of GEF-H1 in cellular processes and diseases

GEF-H1 has diverse functionalities in a number of biological processes including many diseases [Birkenfeld et al., 2008]. A role for GEF-H1 has been shown in tumorigenesis [Cao et al., 2019; Liao et al., 2012; Kashyap et al., 2019], immune response against pathogens [Chiang et al., 2014; Zhao et al., 2019], cytokine production [Guo et al., 2012], cytokinesis [Birkenfeld et al., 2007], development [Ravindran et al., 2017; Kang et al., 2009], cell permeability [Birukova et al., 2010; Kakiashvili et al., 2011; Kakiashvili et al., 2009], mast cell degranulation [Kosoff et al., 2013], cell migration [Nalbant et al., 2009] and polarity [Sandí et al., 2017]. Interestingly, this complex of roles in GEF-H1 could enlighten GEF-H1 as an interest of scientific exploration in dissecting its detailed roles in various cellular processes, as well as to be recognized as a novel therapeutic target for many diseases.

1.5.3 Regulation of GEF-H1

The activity of GEF-H1 is regulated by microtubule dynamics, protein phosphorylation and protein-protein interaction [Birkenfeld et al., 2008; Joo and Olson, 2020] (**Figure 1.4**). GEF-H1 coordinates crosstalk between microtubules and RhoA-based actin remodeling [Birkenfeld et al., 2008]. In certain cells, depolymerization of microtubules by microtubule disassociating drugs can trigger the release and activation of GEF-H1, suggesting GEF-H1 activity is dependent on the integrity and stability of microtubules [Chang et al., 2008; Krendel et al., 2002]. Mutation of a conserved cysteine residue (C53R) in the C1 domain abolished its binding to microtubules and resulted in a constitutively active mutant of GEF-H1 [Birkenfeld et al., 2008]. A mutation in DH domain (T393A) resulted in a dominant negative mutant of GEF-H1 that failed to activate RhoA [Krendel et al., 2002; Birkenfeld et al., 2008]. The coiled-coil domain is mainly for the interactions with other proteins, as well as phosphorylation regulations by kinases including p21-activated kinases (PAK) and protein kinase A (PKA) [Meiri et al., 2012; Meiri et al., 2014].

Specifically, phosphorylation of Ser885 and/or Ser959 by PAK1/2/4 and polarity-regulating kinase partitioning-defective 1b (PAR1b) resulted in inhibition on GEF-H1 activity [Callow et al., 2005; Kosoff et al., 2013; Yamahashi et al., 2011; Zenke et al., 2004]; while phosphorylation of Thr678 by extracellular signal-regulated kinases (ERK) is a key for GEF-H1 activation [Fujishiro et al., 2008; Guilluy et al., 2011; Kakiashvili et al., 2011]. Moreover, GEF-H1 can be phosphorylation inhibited by mitotic kinases including Aurora A/B and Cdk1/Cyclin B during cytokinesis [Birkenfeld et al., 2007]. Interestingly, other kinases including PI3K (phosphoinositide 3-kinase), FAK (focal adhesion kinase), and Src kinase at site of Y198, have been reported to regulate the activity of GEF-H1 [Scott et al., 2016; Collins et al., 2012; Azoitei et al., 2019].

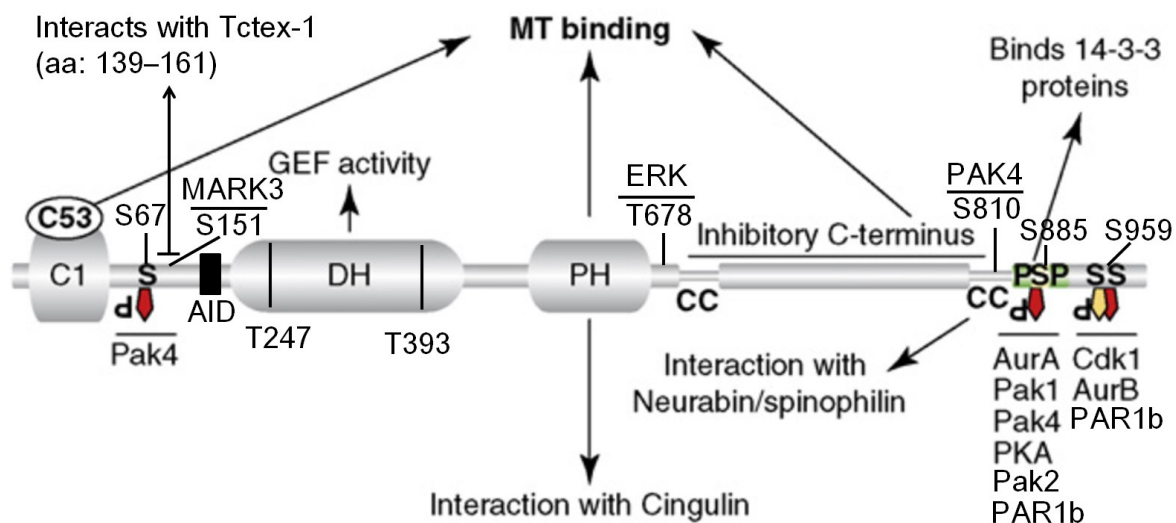


Figure 1.4 Features of the GEF-H1/ARHGEF2 protein. The GEF-H1 protein is 985 amino acids (aa) and possesses multiple functional domains. GEF-H1 can be phosphorylated by various kinases, for both activation and inhibition. Several proteins including 14-3-3 and Tctex-1 (a dynein motor light chain) have been reported to interact with GEF-H1. Domains (start..end): Protein kinase C conserved region 1 (C1), aa 40..85; AID (autoinhibitory domain), aa 190..204 (predicted); DH (Dbl homology, a Rho binding domain), aa 237..431; PH (Pleckstrin homology, a PIP2 binding domain), aa 474..572; coiled-coil (CC), aa 731..876. AurA/B, aurora A/B; Cdk1, cyclin-dependent kinase 1; MARK3, microtubule affinity regulating kinase 3); PAR1b (MARK2), Partitioning-defective 1b; Pak 1/2/4, p21-activated kinase 1/2/4; PKA, Protein kinase A; ERK, Extracellular signal-regulated kinases; C, cysteine; S, serine; T, threonine; T247 and T393 are crucial for the GEF activity. *Adapted from Birkenfeld et al., 2008.*

1.5.4 Interacting partners of GEF-H1

GEF-H1 has been found to interact with various proteins to account for its multiple functionalities [Birkenfeld et al., 2008] (**Figure 1.4**). While the RhoA protein seems to be the main target of GEF-H1, a study has shown that Rac1 behaves as a downstream effector of GEF-H1 [Tonami et al., 2011]. GEF-H1 also interacts with various protein kinases and scaffolding proteins including 14-3-3 [Zenke et al., 2004], the dynein light chain protein Tctex-1 [Meiri et al., 2012] and tight junctions adaptor proteins cingulin and paracingulin [Aijaz et al., 2005; Guillemot et al., 2008]. Several studies have uncovered the exocyst components associated with GEF-H1 [Ahmed et al., 2018; Pathak et al., 2012]. Interestingly, GEF-H1 has been found to be enriched in focal adhesions (FAs) thus targeting myosin-II heavy chain-B (NMIIB, myosin-10) to regulate FAs formation in mesenchymal stem cells (MSCs) during lineage commitment [Huang et al., 2014]. The regulatory roles of active GEF-H1 in myosin IIA filament assembly and the formation of stress fibre-associated focal adhesions has been found under the suppression by the KANK family proteins in HT1080 fibrosarcoma cells [Rafiq et al., 2019]. Altogether, the wide range of effects and binding partners demonstrates how GEF-H1 is diversely regulated and functioning in many cellular processes.

1.5.5 Roles of exocyst in exocytosis and membrane trafficking

The exocyst is an octameric protein complex containing eight subunits: Sec3, Sec5, Sec6, Sec8, Sec10, Sec15, Exo70 and Exo84 [Wu and Guo, 2015; Martin-Urdiroz et al., 2016]. Accumulating evidence has revealed the important roles for the exocyst in the tethering and docking of secretory granules during exocytosis in various cell types [Wu and Guo, 2015]. Sec3 and Sec6 have been shown to mediate vesicle tethering and fusion via the soluble N-ethylmaleimide-sensitive factor (NSF) attachment protein receptor (SNARE) membrane fusion machinery [Yue et al., 2017; Morgera et al., 2012]. Sec5 mediates the recruitment and exocytosis of newcomer insulin granules in rat INS-1 cells [Xie et al., 2013]. In MDA-MB-231 breast cancer cells, the exocyst components Exo70 and Sec8 mediates the secretion of matrix metalloproteinases (MMPs) and Arp2/3-mediated actin dynamics, which are essential for breast cancer invasion [Liu et al., 2009]. In B cells, Exo70 regulates lysosome secretion, while depletion of Exo70 results in the defect of antigen extraction and presentation [Sáez et al., 2019].

In yeast, Exo84p interacts with both Sec5p and Sec10p to essentially regulate the polarized secretion [Guo et al., 1999].

The exocyst can interact with various small G proteins (i.e. Rho GTPases), lipids and cytoskeleton during vesicle trafficking and exocytosis [Synek et al., 2014]. Sec5 binds to DelGef, a protein homologous to Ran guanine nucleotide exchange factor (RanGEF), to modulate secretion in HeLa cells [Sjölander et al., 2002]. Exo70 acts as an effector of both Cdc42 and Rho3 functioning in exocytosis in yeast [Robinson et al., 1999; Wu et al., 2010; Zhu et al., 2019]. In addition, Sec3p in yeast binds to GTP-bound Cdc42 to mediate its polarized exocytosis [Zhang et al., 2001]. Exo70 has also been shown to interact with a Cdc42 homologue, TC10, which mediates Glut4 vesicle trafficking in adipocytes via insulin stimulation [Inoue et al., 2003]. Taken together, the coordinated roles of the exocyst downstream of Rho GTPases in exocytosis led us to investigate its functions in mast cell degranulation.

1.5.6 The exocyst contributes to the function of GEF-H1

Interestingly, recent studies have demonstrated the important roles of GEF-H1 in regulating exocytosis and membrane trafficking via its interaction with the exocyst [Pathak and Dermardirossian, 2013; Sáez et al., 2019; Wu and Guo, 2015]. Specifically, GEF-H1 directly binds to Sec5 leading to its regulatory roles in secretory granule trafficking and exocytosis in a RhoA-dependent manner [Pathak et al., 2012] which is particularly significant since GEF-H1 is a RhoA GEF [Krendel et al., 2002]. Furthermore, GEF-H1 interacts with Exo70 to control the secretion and antigen presentation of B cells at the immune synapses [Sáez et al., 2019]. Given the critical roles of the exocyst in exocytosis, further protein-protein interaction studies were done and have revealed interactions between GEF-H1 and the exocyst components Sec3, Sec5, and Exo70 [Ahmed et al., 2018; Wang et al., 2015]. Additionally, an important study has demonstrated the inhibitory role of PAK2 in mast cell degranulation by phosphorylated inactivation of the GEF-H1-RhoA signaling pathway [Kosoff et al., 2013]. All the aforementioned evidences support the importance of GEF-H1 in controlling exocytosis. It is needed to explore this in mast cell degranulation. Whether GEF-H1 together with its putative interactions with the exocyst play a role in the mast cell exocytotic process is novel and requires further investigations.

1.6 Rationale and Hypothesis

1.6.1 Rationale

Based on the aforementioned background knowledge to date, there is much evidence supporting the dynamics of actin cytoskeleton and microtubules in mast cell degranulation. However, many details of this mechanism have not been shown in regulated granule exocytosis. Moreover, previous studies have demonstrated the involvement of Rho proteins in regulating mast cell degranulation, and further investigation is needed to understand the link between FcεRI receptor signaling and Rho GTPase activation. Certain RhoGEFs, such as Vav1, β-PIX and GEF-H1, together with various exocyst components, have been revealed to regulate membrane trafficking and exocytosis in various cells, but their role in mast cell degranulation has not been determined.

1.6.2 Hypothesis and Research Questions

Here, we hypothesize that Rho GTPases regulate cytoskeletal remodeling during mast cell activation and granule exocytosis, and that critical RhoGEFs transduce mast cell antigen-receptor signals to activate Rho GTPases for the necessary cytoskeletal remodeling events (**Figure 1.5**). The following experimental questions are examined in this thesis work:

- i) Does cytoskeletal dynamics, in particular the microtubule dynamics and associated granule transport via microtubule motors, facilitate granule trafficking and exocytosis in mast cells? (**Chapter 3**)
- ii) Do microtubule-targeted drugs alter the granule trafficking and exocytosis in mast cells? (**Chapter 3**)
- iii) Since Rho GTPases are required for mast cell exocytosis, which RhoGEFs (putatively Vav1, P-Rex1, β-PIX and GEF-H1), regulate mast cell activation, granule trafficking and exocytosis? (**Chapter 4**)
- iv) Does GEF-H1 regulate cytoskeletal dynamics in mast cells by targeting downstream Rho proteins? (**Chapter 4**)
- v) Does GEF-H1 regulate granule trafficking and exocytosis in mast cells and via interacting with the exocyst? (**Chapter 4**)

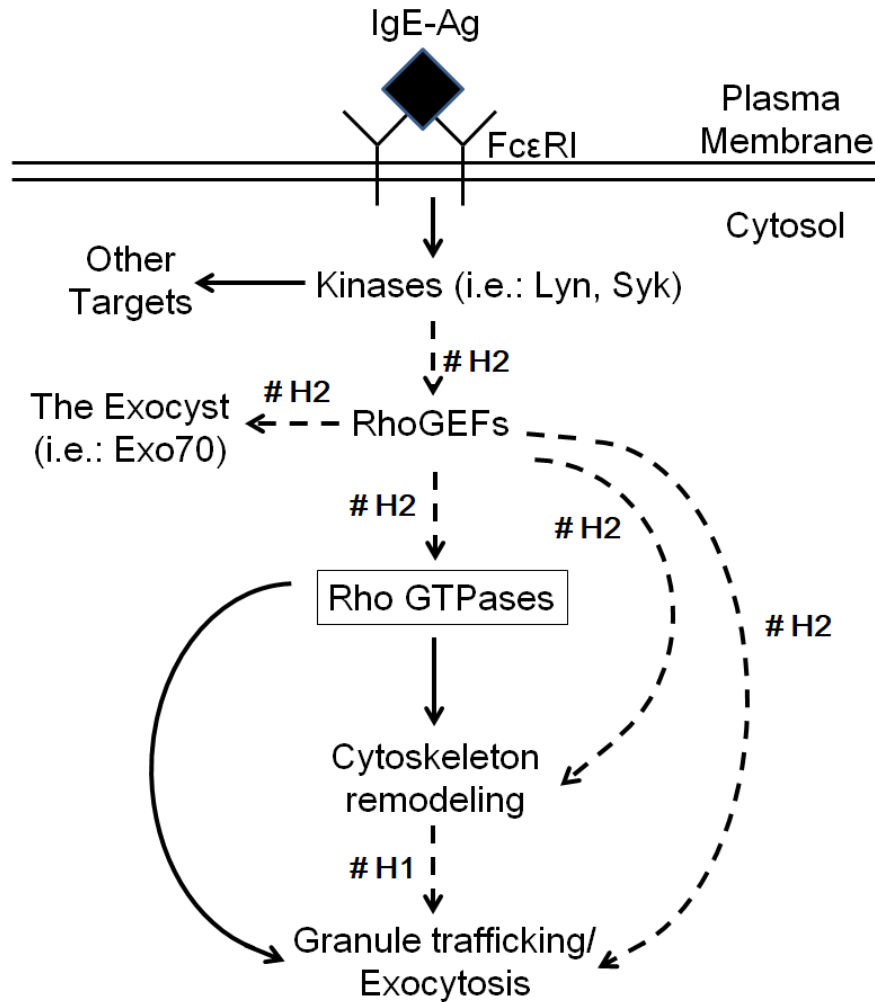


Figure 1.5 A hypothesized model of RhoGEFs and cytoskeleton remodeling in mast cell exocytosis. Rho proteins (i.e. Rac1, RhoA) regulate mast exocytosis. Cytoskeleton (actin or microtubules) remodeling is a downstream process controlled by Rho proteins. In this thesis, cytoskeletal dynamics, particularly involving microtubules and associated motors-based transport machinery (i.e.: kinesin-1 activity) are hypothesized to regulate granule trafficking and exocytosis in mast cells (# **H1**). Microtubules-targeted drugs, including microtubule motor modulators, should therefore affect mast cell exocytosis (# **H1**). Moreover, RhoGEFs, upstream activators of Rho GTPases, are hypothesized to regulate mast degranulation via targeting cytoskeleton remodeling and granule trafficking (# **H2**). RhoGEFs (i.e. GEF-H1) should be activated by receptor proximal kinases thus transduce the activation signals from the surface receptor FcεRI to the exocyst machinery in antigen-stimulated mast cells (# **H2**). GEF-H1 may interact with the Exocyst (i.e. Exo70) to mediate the exocytosis as well (# **H2**). Solid arrows indicated already-known data; dashed arrows are hypothesized signaling pathways; IgE-Ag, IgE-bound antigen complex; RhoGEFs, Rho guanine nucleotide exchange factors.

Chapter 2 Materials and Methods

2.1 Materials

The following section lists the suppliers of key materials. All reagents for common buffers and solutions were obtained from Fisher or Sigma and were of the highest quality available.

2.1.1 Plasmids

Table 2.1 Plasmids

Plasmid	Supplier or Gifts from	Item No.	Backbone	Epitope Tag
Lifect-mRuby	Dr Michael Glogauer	-	-	mRuby
Lifect-GFP	Dr Michael Davidson	-	pEGFP-C1	GFP
EB3-tdTomato	Addgene	50708	tdTomato-N1	tdTomato
EB3-GFP	Dr Michael Davidson	-	pEGFP-C1	GFP
RhoA-G17A	Addgene	69357	pGEX-4T1	GST
RhoA-G14V	UMR cDNA Resource Center	RHO0A0TN C0	pcDNA3.1+	3xHA
pcDNA3.1+	Addgene	-	-	-
pmCherry-C1	Dr Paul Melancon	-	-	mCherry
pEGFP-C1	Addgene	-	-	GFP
mCherry-GEF-H1-full length	custom clone	-	pmCherry-C1	mCherry
mCherry-GEF-H1-RNAi-Resi mutant	custom clone	-	pmCherry-C1	mCherry
GFP-GEF-H1-full length	custom clone	-	pEGFP-C1	GFP
GFP-GEF-H1-RNAi-Resi mut	custom clone	-	pEGFP-C1	GFP
lentiviral shRNA GEF-H1	Addgene	21477	FUGW	GFP

FUGW	Addgene	14883	-	GFP
psPAX2	Addgene	12260	-	-
pMD2.G	Addgene	12259	-	-
Vav1 lenti-shRNA	OriGene Technologies	TL709380	pGFP-C-shLenti	tGFP
P-Rex1 lenti-shRNA	OriGene Technologies	TL708973	pGFP-C-shLenti	tGFP
α -PIX lenti-shRNA	OriGene Technologies	TL700676	pGFP-C-shLenti	tGFP
β -PIX lenti-shRNA	OriGene Technologies	TL708209	pGFP-C-shLenti	tGFP
Scrambled shRNA	OriGene Technologies	TR30021	pGFP-C-shLenti	tGFP

GFP, green fluorescent protein

tGFP, turbo GFP

GST, glutathione S-transferase

HA, human influenza hemagglutinin

mCherry-GEF-H1-RNAi-Resi mut, mCherry-tagged GEF-H1 full-length RNA interference resistant mutant construct

2.1.2 Small molecules and drugs

Table 2.2 Small molecules and drugs

Compounds	Characteristics	Supplier	Item No.	Max Conc. (in DMSO)
Src I1	Src and Lck inhibitor	Tocris Bioscience	3642	10 μ M
PP 2	Lck and Fyn inhibitor	Tocris Bioscience	1407	10 μ M
PD98059	MEK inhibitor	Tocris Bioscience	1213	100 μ M
Ionomycin	Intracellular calcium increaser	MilliporeSigma	I0634	10 μ M
Kinesore	kinesin-1 modulator	Tocris Bioscience	6664	100 μ M
Wortmannin	PI3K inhibitor	MilliporeSigma	W1628	10 μ M

GS-9973	Syk inhibitor	Cayman Chemical	17653	10 μ M
Paclitaxel (taxol)	MTs stabilizer	MilliporeSigma	PHL89806	10 μ M
Nocodazole	MTs de-polymerizer	MilliporeSigma	M1404	10 μ M
Colchicine	MTs de-polymerizer	MilliporeSigma	C9754	10 μ M
PF-573228	FAK inhibitor	MilliporeSigma	PZ0117	10 μ M
Polyethylenimine (PEI)	Transfection reagent	Polysciences	23966-100	1 μ g/ μ l (in water)
Hexadimethrine bromide	Transfection reagent	MilliporeSigma	H9268	10 mg/ml (in water)
DNP-BSA	Mast cell stimulus	Thermo Fisher Scientific	A23018	25 μ g/ml (in HTB)

MTs, microtubules
 FAK, focal adhesion kinase
 Src, Lck, Fyn, Syk, PI3K, MEK are intracellular kinases
 Max Conc., maximum concentration used
 DNP-BSA, albumin from bovine serum (BSA), 2,4-dinitrophenylated
 HTB, HEPES-Tyrode's buffer

2.1.3 Antibodies

Table 2.3 Antibodies and Protein probes

Antibodies or Probes	Supplier	Item No.	Species	Reactivity or Usage
GEF-H1	GeneTex	GTX125893	Rb pAb	Hu, Mo, Rat
Kif5b	Thermo Fisher Sci	21632-1-AP	Rb pAb	Hu, Mo, Rat
α -tubulin (YL1/2)	Novus Biologicals	NB600-506	Rat mAb	Hu, Mo, Rat, ...
β -tubulin (EPR16774)	Abcam	ab179513	Rb mAb	Hu, Mo, Rat, ...

Exo70	MilliporeSigma	MABT186	Mo mAb	Hu, Rat
CD63	BIO-RAD	MCA4754GA	Mo mAb	Rat
Vinculin	Proteintech	66305-1-Ig	Mo mAb	Hu, Mo, Rat, P
Rho A (26C4)	Santa Cruz	sc-418	Mo mAb	Hu, Mo, Rat, ...
Rac1 (23A8)	MilliporeSigma	05-389	Mo mAb	Hu, Mo, Rat
Slp3	Proteintech	22076-1-AP	Rb pAb	Hu, Mo, Rat
SKIP (PLEKHM2)	Novus Biologicals	NBP1-77089	Rb pAb	Hu, Mo, Rat
MCP II	gift	-	Rb pAb	Rat
GST antibody	Home	-	Rb pAb	-
Anit-HA-Biotin (3F10)	Roche	12158167001	Rat mAb	-
Anti-DNP IgE (SPE-7)	MilliporeSigma	D8406	Mo mAb	-
GST-Rhotekin (probe)	Dr Gary Bokoch	-	GST (tag)	RhoA-GTP detection
GST-PAK1 (probe)	Dr Gary Bokoch	-	GST (tag)	Rac1-GTP detection
GST-RhoA-G17A (probe)	Addgene	69357	GST (tag)	Active GEF-H1 detection
GST-Rac1-G15A	Addgene	69355	GST (tag)	Active Rac1 RhoGEFs detection
pGEX-4T-1	Addgene	-	GST (tag)	-
Phalloidin-iFluor 405	Abcam	ab176752	-	F-actin staining
Oregon Green™ 488 Phalloidin	Thermo Fisher Scientific	O7466	-	F-actin staining
Alexa Fluor™ 546	Thermo Fisher	A22283	-	F-actin staining

Phalloidin	Scientific				
LysoTracker™ Red DND-99	Thermo Fisher Scientific	L7528	-		Lysosome or acidic organelles staining
LysoTracker™ Green DND-26	Thermo Fisher Scientific	L7526	-		Lysosome or acidic organelles staining

MCP II, mast cell protease II, a gift from Dr Dean Befus (University of Alberta)
 PAK1, p21-activated kinase 1
 F-actin, filamentous actin
 GST, glutathione S-transferase
 HA, human influenza hemagglutinin
 Hu, human; Mo, mouse; Rb, Rabbit; P, Pig
 mAb, monoclonal antibody; pAb, polyclonal antibody
 DNP, dinitrophenyl

2.1.4 Oligonucleotides

Table 2.4 PCR primers of putative RhoGEFs and GAPDH

Gene	Forward (5'-3')	Reverse (5'-3')	Product (bp)
GAPDH	TGACTCTACCCACGGCAAGT	AGTGGATGCAGGGATGATGT	487
Vav1	TGGAGGTGTGTCAGGAATAC	TCAGCAGTATTCAGAATAGTC	749
Vav2	GAAGAATATTCGCACCTTCC	TAGATCAGGAGCCGTTTCCTT	618
Vav3	CACACTCCATCAATCTGAAG	TCGTGAATCTCTTGCATTAAG	607
P-Rex1	CACTCCTGCTCAAGGAGTTATC	GATACATCACCTGCTCGTTCTT	870
P-Rex2	AGTTCAAGCCAGAGCAAATG	TTTCAGGAAGCAATCAACTTC	617
α -Pix	GCAGATCCTTTTCGGAACCTATT	GGATGTCTTTCTCTCCGTCTTT	634
β -PIX	CAAGAGCTATTACAATGTGGT	ATGGGCTCTGTCAGGATCTG	594
Tiam1	ATTCTTCTGTCACTCCCAGC	GAGTTGGTGGCATTGGATCT	748
Tiam2	ACACCTTCTCACCTGCTATG	AGTTAAGGCTTTGGACTTGC	700

Trio	AGCAGCAGGAGTTGGATTTAG	CGCTGTTCCCTGTGTAGGTATTT	615
GEF-H1/ ARHGEF2	GACATTCCCGAAGAGACAGAAA	GGAGCTAGAAGTGCCTACAATC	723
LARG/ArhGE F12	AGATAGCTCCTCCAAGAAGA	GTTAGGGCATCACCTAATGG	690
Net1	GTACCTGGATGAGAAGCAGAAG	GGAACACACACACTCATACCA	692
Ect2	TGAGGCCAGGATGGATTTATG	CTTCTGCTCTCATCCCAGTTAG	880
Alsin/ALS2	ATGGCTTGGAAAGACGGATATG	GGAGTGTACAGGCCTTTATTA	904
Asef2/Spata13	GACTTCGACAGAGTCCTGAAAC	CTTACCTCCTCCTCCTCTCTT	710
ArhGEF10	CAGCAGGTTGTGAGGAGATAC	CAGCACGTCATTTCAGCATAAAG	768

Table 2.5 qPCR primers of five RhoGEFs and GAPDH

Gene	Forward (5'-3')	Reverse (5'-3')	Product (bp)
GAPDH	ACTCCCATTCTCCACCTTTG	CCCTGTTGCTGTAGCCATATT	105
Vav1	CTGTGCACACCCACTTCTTA	GACTGCAATAACGGCCATAAAC	123
P-Rex1	GCTTCGATCTTGAGGAGAAGAA	GGTCCCTCGTTGATGGAGTAAAT	117
α -Pix	TTTGAGCCTGATGACCTCTATTC	CGTCCACATGGTCTTTCTGATA	110
β -PIX	GAAGCGAGGAGAAGAATGAGAG	TTGGCAGCTTCCCTGATAG	108
GEF-H1	TGTACCAAGGTCAAGCAGAAG	GCTCTCTGGTGGTTGTCTTAC	100

Table 2.6 qPCR primers of kinesin-1 cargo adaptors

Gene	Forward (5'-3')	Reverse (5'-3')	Product (bp)
Styl1	CGAAGGAAGAAGAGCTCTAAGG	CTGCCTCTTCTATGGTGTCTTC	88
Styl2	CCGATGTCTTCTGGGTCTATTC	TCACTGATGATGGATGAACTCTC	101

Styl3	AACCGGAGAGTGGTTCTTTG	TGCTCTGCCTCTGATAAGATTG	104
Styl4	CTCCAGGTGTGGATCAAAGAAG	TCCTCATGGGAAGGAGGTATC	97
Styl5	GGTGGAAGACAAGAGGATAAGG	TTCTGACAGTGAACACAGACTC	108
Plekhm1	TCATAACTGGGACCTCACAAAG	TGCGCTCTACATGCTCATAAC	128
Plekhm2 (SKIP)	CCGTATCCAAAGGAGTCATACC	TCTTCGTGGCATGTGAAGAG	100
JIP1	TGTGTGTTCAAAGAAGGAGAGG	AGTAGTAGCCAGGTGACAAGA	108
JIP2	CTGTGTGGTCAATGGAGAAGAG	GGGTCGTCCACATCTAACTCTA	99
JIP3	AGTTCTTTAGCCGCCTCTTC	CTGTAGTGGGTGACTTGTAGTG	96
JIP4	CAGCACCCATTCAACTACAAAG	GGCAATGCACAGAACATGAG	103

Synaptotagmin-like (Styl), as known as Slp

Plekhm: pleckstrin homology and RUN domain containing M

Plekhm2 also known as SKIP (SifA and kinesin-interacting protein)

JIP, also known as mapk8ip (mitogen-activated protein kinase 8/JUN interacting protein)

JIP4 has another name-- Spag9 (sperm associated antigen 9)

Table 2.7 shRNA oligos of RhoGEFs

Targeted Gene	shRNA oligo sequence	Targeted Region	Supplier	Item No.
Vav1	GGACATTGTGGAACCTACTAAGGCAGAGG	2560-2588	OriGene Technologies	TL709380D
P-Rex1	GCCAAGGTCTCATTGACAGTATCTTCGTG	3191-3219	OriGene Technologies	TL708973D
α -PIX	GAGAAGAGCCTTGTTGATACTGTCTATGC	2119-2147	OriGene Technologies	TL700676A
β -PIX	GATGAAGTCCAAGAGTTACGACAGGATAA	1795-1823	OriGene Technologies	TL708209A
GEF-H1	AACCTTCAATGGCTCCATTGA	2115-2135	Addgene	21477

shRNA, short hairpin RNA

Targeted templates (Gene Accession No.): Vav1, NM_012759.2; P-Rex1, NM_001135718.1; α -PIX, NM_001005565.1; β -PIX, AF044673.1; GEF-H1, NM_001012079.1

Scrambled shRNA (TR30021, OriGene Technologies) as control for Vav1, P-Rex1, α -PIX, β -PIX shRNAs
FUGW (Addgene # 14883) as empty vector control for GEF-H1shRNA

2.2 Methods

2.2.1 Cell culture

RBL-2H3 cells are widely used as a mast cell model cell line [Passante and Frankish, 2009]. RBL-2H3 cells were maintained in Eagle's Minimum Essential Media (MEM) supplemented with 10% (v/v) heat-inactivated Fetal Bovine Serum (HI-FBS) and 1× antibiotic-antimycotic (1× A-A: 100 units/mL of penicillin, 100 µg/mL of streptomycin, and 0.25 µg/mL of amphotericin B) in a humidified incubator set to 5% CO₂ at 37°C. Cells were split by incubation with 0.25% Trypsin/0.53 mM EDTA and replated at a 1:6 dilution every 2-3 days. Rat BMMCs were obtained from the bone marrow of femurs of 8-12 week old Sprague-Dawley rats following the previously described isolation method [Yu et al., 2018]. Rat bone marrow (BM) stromal cells were obtained by the same method but only harvested the attached cells during cell culture. Both BMMCs and BM stromal cells were maintained in RPMI 1640 media supplemented with 10% HI-FBS, 50 ng/mL IL-3 and 50 ng/ml rSCF (GenScript Biotech, Piscataway, NJ, USA). BMMCs were used after 2 weeks of incubation. NRK cells were grown in Dulbecco's Modified Eagle Medium (DMEM) with 10% HI-FBS. 293T cells were maintained in DMEM with 10% FBS and used for lentivirus packaging. To create shRNA knockdown strains, low passage RBL-2H3 cells (less than p10) were transduced by recombinant lentiviruses at an MOI of 10, then maintained in complete MEM media with 0.5 µg/ml puromycin (Sigma).

2.2.2 Drug and small molecule treatment

All small molecule compounds and drugs (**Table 2.2**) were dissolved in DMSO and used at the indicated concentrations in the results. Cells were pretreated 30 min prior to performing degranulation assay or immunofluorescence, or simultaneously with antigen stimulation when performing live-cell imaging.

2.2.3 Total RNA extraction and cDNA synthesis

Total RNA from cultured cells was extracted by Trizol (Invitrogen) following the instruction manual, and complementary DNA (cDNA) was synthesized from mRNA thereafter using oligo dT primers. Briefly, 2-3 million cells were solubilized by adding 1 ml Trizol then 200 µl chloroform was added. The cell homogenate was centrifuged at 12,000×g for 10 min at 4°C. The

top aqueous phase containing total RNA was collected and precipitated by adding 500 μ l isopropanol then centrifuged at 12,000 $\times g$ for 10 min to form the RNA pellet. The pellet was washed with 70% ethanol twice, air-dried, and dissolved in 50-100 μ l RNase-free water. The concentration and purity of extracted RNA was determined by NanoDrop spectrophotometer (ThermoFisher). To synthesize cDNA, 5 μ g of RNA was used in the SuperScript™ II Reverse Transcriptase (Invitrogen) protocol with 0.5 μ g Oligo (dT) 12-18 primer (Invitrogen). cDNA was used for polymerase chain reaction (PCR) or quantitative PCR (qPCR) experiments.

2.2.4 RT-PCR and qPCR

To determine the mRNA profile of putative RhoGEFs in mast cells (with control groups), RT-PCR was performed by using the Taq polymerase (Invitrogen) and cDNA as outlined in **section 2.2.3**. The PCR primers of RhoGEFs were in **Table 2.4**. To verify the knockdown effects by certain RhoGEF shRNAs, as well as to quantify the kinesin-1 cargo adaptors mRNA levels in RBL-2H3 cells, qPCR was performed based on the SensiFAST™ Probe No-ROX Kit (Meridian Bioscience, Memphis, TN, USA). The qPCR primers for certain RhoGEFs and kinesin-1 cargo adaptors were in **Tables 2.5** and **2.6**. PCR and qPCR primers were designed by using the IDT online tool PrimerQuest based on required criteria and then verified by BLAST for specificity. Each 20 μ l PCR reaction contained 5 μ g cDNA template, 1 μ l of 10 μ M dNTPs, 1 μ l of 10 μ M forward and reverse primers, 2 μ l of 10 \times PCR buffer (with Mg²⁺), 0.3 μ l 5 U/ μ l Taq (500 U/100) and water. The PCR condition was as follows: 94°C 1 min (initial denaturation), 94°C 30 s, 55°C 30 s, and 72 °C 1 min for 30 cycles. GAPDH was used as control. PCR products were run on a 1.2% agarose gel containing 0.0001% SYBRsafe (ThermoFisher) and imaged. For qPCR reaction, a two-step thermocycling reaction was performed based on the Mastercycler® ep realplex Real-time PCR System (Eppendorf). The $2^{-\Delta\Delta C_t}$ method was applied to quantify the mRNA levels accordingly (GAPDH as a control) [Livak and Schmittgen, 2001].

2.2.5 Knockdown of Vav1, P-Rex1, α -PIX, β -PIX and GEF-H1 expression

Lentivirus-mediated shRNA interference was used to knockdown the expression of Vav1, P-Rex1, α -PIX, β -PIX and GEF-H/ARHGEF2 in RBL-2H3 cells. As illustrated in **Table 2.7**, the shRNAs for Vav1, P-Rex1, α -PIX, β -PIX were derived from the pGFP-C-shLenti system (OriGene), which uses a puromycin selection cassette; while the GEF-H1 shRNA was from

FUWG shRNA plasmid with a GFP reporter [Kang et al., 2009]. The 2nd generation lentiviral system was used to package lentiviruses expressing desired shRNAs in HEK293T cells. Briefly, 9 µg transfer plasmids containing the shRNAs, 6 µg of psPAX2 packaging plasmid and 3 µg of pMD2.G (VSV-G) envelop plasmid, together with 72 µl PEI (polyethylenimine, 1 µg/µl) were dissolved in 1 ml Opti-MEM then dropwise added into HEK293T cells on a 10 cm plate. Supernatants of recombinant lentiviruses were harvested 48 h post transfection, filtered by 0.45 µm syringe filters and then were either directly used or concentrated 100 times by ultracentrifuge at 20,000×g, 4°C for 2 h. Lentiviruses containing a scrambled shRNA for Vav1, P-Rex1, α-PIX, β-PIX, or an empty vector for GEF-H1, were used for controls. Titration of recombinant viruses was determined by the limiting dilution method or a flow cytometry-based method accordingly [Sena-Esteves et al., 2018]. Viral titres were typically 3-5×10⁶ TU (transducing unit)/ml before concentration. To carry out the viral transduction, 300,000-500,000 of cells were seed in a 6-well plate; the following day lentiviruses with MOI (multiplicity of infection) of 10 and 8-10 µg/ml polybrene (Hexadimethrine bromide, Sigma) were mixed together added onto the cells. For creating stable cell strains of Vav1, P-Rex1, α-PIX, β-PIX or scrambled shRNAs, 0.5 µg/ml puromycin was added for the selection. Knockdown efficiencies were determined by RT-qPCR and western blotting 4-5 d after viral transduction.

2.2.6 Competent cell preparation and plasmid isolation

Competent cells of high transformation efficiency were generated based on previously described methods [Inoue et al., 1990]. Briefly, DH5-alpha or Stbl3 E. coli strains (Invitrogen) were grown in **lysogeny broth** (LB: 1% wt/v tryptone, 0.5% wt/v yeast extract, 170 mM NaCl) or **super optimal broth** (SOC: 2% wt/v tryptone, 0.5% wt/v yeast extract, 10 mM NaCl, 2.5 mM KCl, 10 mM MgCl₂) media to logarithmic growth phase (OD₆₀₀: 0.3~0.4). The cells were immediately cooled on ice and harvested by centrifuging at 8000×g for 5 min, 4°C. Ice-cold **TB buffer** (10 mM Pipes, 55 mM MnCl₂, 15 mM CaCl₂, 250 mM KCl, pH 6.7) was used to wash and resuspend cells, and finally, cells were aliquoted by adding TB buffer containing 6% v/v DMSO, snap-frozen by dry-ice and stored at -80°C for future usage. For heat-shock transformation, 100 µl of competent cells were completely thawed on ice, mixed with 10-100 ng of desired plasmids and incubated on ice for 30 min. The cell-plasmid mixtures were placed in a 42°C water bath for 25 s then recovered with 1 ml SOC media at 37°C for 1 h, and finally plated onto proper LB agar

plates with appropriate antibiotics and grown overnight. To identify or isolate proper plasmids, bacteria colonies were amplified in LB media with appropriate antibiotics and plasmids were extracted by Miniprep (Qiagen, Hilden, Germany).

2.2.7 Transfection of RBL-2H3 cells by electroporation of plasmids

Electroporation is the most efficient method to transfect RBL-2H3 cells [Cohen et al., 2012]. We used this approach to label F-actin using plasmids of fluorescently-tagged Lifeact [Riedl et al., 2008] or microtubules by EB3 (end-binding protein 3) [Stepanova et al., 2003], or to express other proteins as indicated. Briefly, 2-3 million RBL-2H3 cells of good condition were mixed with 10 µg pure plasmid in 400 µl ice-cold **electroporation buffer** (137 mM NaCl, 2.7 mM KCl, 1 mM MgCl₂, 10 mM glucose, 20 mM HEPES, pH 7.4). Cell-plasmid suspension was then transferred to a 4 mm electroporation cuvette and pulsed by electric shock at the setting of 250 V voltage, 950 µF capacitance and R3 resistance (Harvard Apparatus BTX ECM600 Electro Cell Manipulator). Cells were recovered in complete medium for 24-48 h, and were ready for other experiments, such as immunofluorescence or live-cell imaging. With this strategy we have expressed RhoA-G14V or GEF-H1-RNAi-Resi mutant plasmids in RBL-2H3 cells.

2.2.8 Purification of recombinant protein probes

The glutathione S-transferase (GST)-tagged protein probes GST-RhoA-G17A, GST-PAK1 Cdc42/Rac-binding domain, GST-Rhotekin Rho-binding domain [García-Mata et al., 2006; Benard et al., 2002; Ren et al., 2000] (*see Table 2.3*), were prepared by expressing proteins in *E. coli* strain Rosetta™ (DE3) (MilliporeSigma). Briefly, cells with expression plasmids for the protein probes were grown in LB media with appropriate antibiotics at 37°C overnight, then diluted to 0.5 OD₆₀₀ and protein expression was induced by adding 200 µM isopropyl β-D-1-thiogalactopyranoside (IPTG, MilliporeSigma) and growing for another 4-5 h at 30°C. Cells were harvested by centrifugation at 8,000×g for 10 min, 4°C, then lysed by **lysis buffer A** (20 mM HEPES pH 7.5, 1% Triton X-100, 10 mM MgCl₂, 150 mM NaCl, 5% v/v glycerol, 2 mM Na₃VO₄, 5 mM NaF, 1×PIC (1X protease inhibitor cocktail: 10 µg/ml leupeptin, 10 µg/ml pepstatin, 5 mM *o*-phenanthroline) and 0.2 mM PMSF). Protein concentrations were determined by a Bradford assay and stored at -80°C for future usage.

2.2.9 Detection of RhoA-GTP and Rac1-GTP by pulldown assay

GST-PAK1 Cdc42/Rac-binding domain and GST-Rhotekin Rho-binding domain are widely used to detect RhoA-GTP and Rac1-GTP, respectively. Probes were made by binding GST-PAK1 or GST-Rhotekin to glutathione resin (GenScript Biotech). Cell lysates made by solubilization of a 10 cm plate of cells at 80% confluency (5 million cells) in 1 ml **lysis buffer A**. Equal amounts of lysate were incubated with 20 µl of packed resin containing the probe. The mixture was nutated at 4°C for 30-45 min, then washed three times with lysis buffer A. Proteins were eluted from the resin by adding 50 µl 1× Laemmli SDS-PAGE buffer and boiling for 5 min. The eluted fractions together with a sample of the total lysates were subjected to SDS-PAGE and western blot. Rho A (26C4) or Rac1 (23A8) specific antibodies were used for immunoblotting.

2.2.10 Detection of active GEF-H1 by RhoA-G17A pulldown assay

RhoA-G17A, a nucleotide-free RhoA mutant, exerts a high affinity for upstream activators, the RhoGEFs. Thus, it can be used to detect RhoGEF activation [García-Mata et al., 2006]. The GST-RhoA-G17A probe and GST or GST-Rac1-G15A controls were prepared as described for Rho activation probes. Cell lysates were prepared after various stimuli with **lysis buffer A** followed by the addition of RhoA-G17A or control beads. The mixtures were nutated at 4°C for 30-45 min, then washed three times with lysis buffer A. Proteins were eluted from the resin by adding 50 µl 1× Laemmli SDS-PAGE buffer and boiling for 5 min. Eluted fraction and a total lysate (as an input control) were subjected to SDS-PAGE and western blot, recognized by a GEF-H1 specific antibody later. The relative levels of active GEF-H1 were normalized to an input control (by calculating the amount of eluted fractions divided by total lysate).

2.2.11 Co-immunoprecipitation (co-IP) assay

To determine the interacting partners of GEF-H1 a co-IP assay was performed. The RBL-2H3 cells were lysed by **lysis buffer B** (50 mM Tris-Cl pH 7.4, 150 mM NaCl, 1% v/v Triton X-100, 0.1% wt/v SDS, 0.5% wt/v sodium deoxycholate, 5% v/v glycerol, 2 mM Na₃VO₄, 5 mM NaF, 1×PIC and 0.2 mM PMSF). Cells from a 10 cm plate at 80% confluency (8 million cells) were lysed in 500 µl lysis buffer B. 10% of the total lysate was saved for input control and the remaining lysate was incubated with 5 µl of GEF-H1 antibody for 20 min, then immunoprecipitated by adding by 10 µl of protein A agarose (GeneScript). After 2 h of

additional incubation, the resin was washed three times with lysis buffer B, then eluted by boiling with 50 μ l 1 \times Laemmli SDS-PAGE buffer and boiling for 5 min. Eluted fraction and a sample of the input control were subjected to SDS-PAGE and western blot. The presence of α -tubulin, Exo70, vinculin proteins in elution fractions were analyzed by immunoblotting.

2.2.12 Protein extraction and immunoblot analysis

Immunoblot (western blotting) was conducted to determine protein expression levels. Cells were harvested and lysed in **lysis buffer B**. The lysates were cleared by centrifuging at 14,000 \times g at 4°C for 30 min, then protein concentrations were measured and boiled with 1 \times Laemmli SDS-PAGE buffer. 20 μ g of protein samples were subjected to SDS-PAGE and transferred to the 0.45 μ m nitrocellulose (NC) membrane by western blotting. The membrane was blocked with 5% skim milk for 1 h at room temperature, then incubated with various primary antibodies overnight at 4°C or 2 h at room temperature. Blots were washed three times in PBS 0.1% v/v Tween 20 and then incubated with fluorescently labelled secondary antibodies, goat anti-rabbit IgG Dylight 680 conjugated or goat anti-mouse IgG Dylight 800 4 \times PEG conjugated (Invitrogen). Images were captured by an Odyssey® CLx Imaging System (LI-COR Biosciences, Lincoln, NE, USA). The quantification of protein levels was performed by using Image Studio Ver 5.2 software.

2.2.13 Mast cell granule exocytosis assay (degranulation assay)

β -hexosaminidase is an abundant lysosomal-resident enzyme that can be used to assay mast granule exocytosis, which is also commonly described as the degranulation assay [Naal et al., 2004]. 100,000 RBL-2H3 cells or 250,000 of BMBCs were plated in 24 well plates one day before assaying. Cells were sensitized to antigen stimulation by incubation for 4 h with 120 ng/ml anti-DNP IgE (SPE-7, Sigma) in **HTB (HEPES-Tyrode's buffer**: 120 mM NaCl, 5 mM MgCl₂, 1.5 mM CaCl₂, 1 g/liter glucose, 1 g/l BSA, 25 mM HEPES, pH 7.4). Cells were antigen-stimulated by the addition of 25 ng/ml DNP-BSA (ThermoFisher). Percent exocytosis was calculated as the levels of β -hexosaminidase in the supernatant compared to total β -hexosaminidase from HTB, 0.5% v/v Triton X-100 lysed cells. β -hexosaminidase levels were determined by enzyme assay. 100 μ l of cell supernatant or lysate was incubated with 100 μ l 1.2 mM 4-methylumbelliferyl N-acetyl- β -D-glucosaminide (MUG) (Sigma) in 50 mM citrate buffer pH 4.5 for 30 min at 37°C. Reactions were terminated by the addition of 50 μ l of 0.2 M glycine

pH 10. Cleavage of MUG by β -hexosaminidase releases the fluorescent product 4-methylumbelliferone, which was detected with a Synergy-4 fluorometer set to 360 nm \pm 20 nm excitation and 450 nm \pm 20 nm emission (BioTek Instruments). Fluorescence is directly proportional to exocytosis, which was calculated as the percentage of β -hexosaminidase in the supernatant, divided by total β -hexosaminidase as determined from Triton X-100 lysed cells.

2.2.14 Immunofluorescence

Immunofluorescence was used to determine the intracellular distribution of granules, cytoskeleton or the localization proteins in RBL-2H3 cells. Cells grown on coverglass were fixed by 4% wt/v paraformaldehyde (PFA) at room temperature (RT) for 30 min or fixed with 100% ice-cold methanol for 10 min (anti-GEF-H1 and microtubule staining), then permeabilized with 0.2% Triton-X100 for 15 min. Cells were blocked with 1% bovine serum albumin (BSA) dissolved in PBS for 30 min, then incubated with primary antibodies for 2 h at room temperature. Cells were washed 5 times with PBS. Alexa Fluor-conjugated secondary antibodies were added as indicated. Oregon-green 488 or Alexa 546 conjugated phalloidin diluted 1:2000 was used to stain F-actin and DAPI (4', 6-diamidino-2-phenylindol) was used to stain nuclei. Cells were mounted on glass slides with ProLong™ Gold Antifade Mountant (ThermoFisher). Images were captured by a Zeiss Observer Z1 microscope (Carl Zeiss, Oberkochen, Germany) with a \times 63 objective (1.4NA) and processed using Axiovision 4.8 software.

2.2.15 Live-cell imaging

Live-cell fluorescence microscopy was performed on RBL-2H3 cells during stimulation to visualize dynamic change in cell morphology, via cytoskeletal remodeling and granule movement. RBL-2H3 cells were transfected by electroporation (250 V, 950 μ F), as previously described (Cohen et al., 2012), with 8 μ g of Lifeact-GFP (Riedl et al., 2008), EB3-GFP (Stepanova et al., 2003) or EB3-tdTomato (Merriam et al., 2013) plasmids. After transfection cells were plated onto 25 mm round coverslips and grown overnight, then sensitized with anti-DNP-IgE for 4 h and granules were stained using 500 nM LysoTracker Red or LysoTracker Green (ThermoFisher). Coverslips were placed in an Attofluor chamber and growth media was replaced with HTB. After 1 min of imaging, resting cells were stimulated by the addition of 25 ng/ml DNP-BSA and drugs or DMSO were added at the same time. Imaging was done on a Zeiss

AxioObserver M1 microscope using a 63× (1.4 NA) objective. Images were taken every 10 s and processed with Volocity v6.3 software. Images were compiled and exported as videos on windows media at 10 frames/s.

2.2.16 Molecular cloning of GEF-H1-RNAi resistant mutant

To further dissect the roles of GEF-H1 in RBL-2H3 cells, a GEF-H1-RNAi (RNA interference) resistant mutant construct (**GEF-H1-RNAi-Resi**) was cloned and used for re-introduction experiments after knockdown of the endogenous gene. Firstly, the full-length of GEF-H1 from rat RBL-2H3 cell cDNA (complementary DNA) was cloned. PCR using the Phusion polymerase (Invitrogen) was performed. Primers were as follows: forward (flanked with Hind3, underlined): TCTAAAGCTTGTATGTCTCGGATCGAATCCCT, reverse (flanked with Kpn1, underlined): AGTGGTACCTTAGCTCTCTGAGGCCGTAG. The Phusion PCR reactions was as follows (in 20 µl reaction volume): 4 µl 5× GC buffer, 0.4 µl 10 mM dNTPs, 2 µl, forward and reverse primers (10 mM each), 0.6 µl DMSO, 2 µl RBL-2H3 cell cDNA (100-200 ng), 0.2µl Phusion polymerase (10 unit/µl) and water. The parameters were: 98°C 30 s (initial denaturation), 98°C 10 s, 58°C 30 s, 72°C 3 min 30s for 35 cycles, and a 10 min 72°C final extension. The PCR product was run on an agarose gel and isolated by gel extraction (QiaGEN). A-tailing was performed by Taq polymerase (Invitrogen) and subsequent cloning into TOPO-pcr2.1 vector (Invitrogen) following the manufacturer protocol. Sanger sequencing was used to verify the accuracy of the cloned GEF-H1 full length, which was subcloned into either pEGFP-C1 or pmCherry-C1 vector by Hind3-Kpn1 digestion. This clone of GEF-H1 was used as a template for **GEF-H1-RNAi-Resi** cloning. The GEF-H1 shRNA in lentiviral shRNA GEF-H1 was AACCTTCAATGGCTCCATTGA, the RNAi resistant primer was designed as follows: forward: CGGAGAGGCCAGAACCTTTAACGGATCCATTGAGCTCTGTAG, reverse: CTACAGAGCTCAATGGATCCGTAAAGGTTCTGGCCTCTCCG. These primers contained a BamH1 site (underlined) for subsequent verification. A Phusion PCR was performed according to the site-directed mutagenesis strategy previously described [Zheng et al., 2004], followed by Dpn1 treatment and BamH1 verification. Sanger sequencing was used to confirm the accurate cloning of **GEF-H1-RNAi-Resi** (either in pEGFP-C1 or pmCherry-C1).

2.2.17 Focal adhesion isolation and staining

Focal adhesion (FA) can be visualized by immunofluorescence microscopy using vinculin antibodies to label them. We used a method for FA purification and further quantification that was previously described [Kuo et al., 2012]. Briefly, RBL-2H3 cells were grown on coverslips, then treated with 2.5 mM TEA (triethanolamine, Sigma) hypotonic buffer for 3 min at room temperature. The cell bodies were removed by hydrodynamic force using a Waterpik® WP-100 Ultra Water Flosser for 10s. The Waterpik nozzle (with a setting of “3”) was held ~0.5cm and at an approximate 90° angle to the cell surface to flush the cells. The FA fraction remained bound to the substrate. Next, the FAs were fixed with 4% wt/v PFA then labelled with vinculin antibody. The coverslips were mounted and fluorescent images of identical exposure time were captured. The relative quantification of FAs were processed by ImageJ (National Institutes of Health, USA) by measuring the total fluorescent intensity of stained FAs of individual cell contour [Kuo et al., 2012]. Coverslips were co-stained with Phalloidin-iFluor 405 to define the outline of individual cells.

2.2.18 Cell size measurement by ImageJ

RBL-2H3 cells undergo spreading and actin remodeling when stimulated [Passante and Frankish, 2009; Sheshachalam et al., 2017], thus, the degree of cell spreading can be regarded as an indicator of mast cell activation. The measurement of cell size was done using ImageJ using fluorescent images of phalloidin-stained cells. Briefly, the selected area of input RGB image was color threshold, then outlined by the phalloidin-stained area. Next, the outlined region was automatically analyzed in ImageJ (by clicking the “Analyze” menu) with the output values of area, mean and integrated density. Calculated values were exported into an Excel file and statistical analysis was performed thereafter. To compare the differences of cell sizes in various groups, cells from various images ($n \geq 13$) from at least two independent experiments were used.

2.2.19 Granule enrichment and co-fractionation

RBL-2H3 cells were grown in 10 cm plates to 90% confluency. Cells were sensitized and stimulated for 15 min accordingly, then washed, and frozen (-80°C) in 1 ml **sucrose buffer** (0.3 M sucrose, 10 mM HEPES, pH 7.5, 0.2 mM PMSF, 1×PIC). Cells were thawed and scrapped

from plates and the suspension was passaged through a Balch Homogenizer (Isobiotec, Heidelberg, Germany) of 12 μm ball bearings for 20 strokes. Equal amounts of lysates of different samples were transferred to 1.5 ml Eppendorf tubes and centrifuged at $450\times g$ to remove cell debris (pellet 1, P1). 50 μl of this supernatant (Sup 1) was saved as a loading control. The supernatant was serially centrifuged at $4000\times g$ and $20,000\times g$ (each for 20 min, 4°C), and the resulting pellets were named as pellet 2 (P2, 4KgP) and pellet 3 (P3, 20KgP), and supernatants as Sup 2 and Sup 3. Next, the P2 and P3 fractions were washed with sucrose buffer and boiled in 50 μl $1\times$ Laemmli SDS-PAGE buffer. Granules were primarily enriched in the P2 fraction [Kokkonen and Kovanen, 1985]. Equal volumes of all fractions were subjected to SDS-PAGE and western blot. The levels of rat mast cell protease II (RMCP II) [Gibson and Miller, 1986], β -tubulin, Exo70, and vinculin proteins were analyzed by immunoblotting and quantified by using Image Studio Ver 5.2 software.

2.2.20 Statistical analysis

Quantified data are presented as mean \pm SD (standard deviation). All statistical tests used two-tailed unpaired Student *t*-tests, to compare differences between two groups; except where indicated in the figure legend, multi-group comparison was analyzed by one-way analysis of variance (ANOVA). All experiments were performed at least three independent times unless specifically mentioned. Statistical analysis was performed using GraphPad Prism 6.01 (GraphPad Software, San Diego, CA); $p < 0.05$ was considered as statistical significance.

Chapter 3

Mast cell granule motility and exocytosis is driven by dynamic microtubule formation and kinesin-1 motor function

Summary

Mast cells are tissue-resident immune cells that contain numerous cytoplasmic granules containing preformed pro-inflammatory mediators. Upon antigen stimulation, sensitized mast cells undergo profound changes to their morphology and rapidly release pro-inflammatory mediators by regulated exocytosis, also known as degranulation. We have previously shown that Rho GTPases regulate exocytosis, which suggests that cytoskeleton remodeling is involved in granule transport. Here, we used live-cell imaging to analyze cytoskeleton remodeling and granule transport in real-time as mast cells were antigen stimulated. We found that granule transport to the cell periphery was coordinated by de novo microtubule formation and not F-actin. Kinesore, a drug that activates the microtubule motor kinesin-1 in the absence of cargo, inhibited microtubule-granule association and significantly reduced exocytosis. Imaging showed granules accumulated in the perinuclear region after kinesore treatment. Complete microtubule depolymerization with nocodazole or colchicine resulted in the same effect. A biochemically enriched granule fraction showed kinesin-1 levels increase in antigen-stimulated cells, but is reduced by pre-treatment with kinesore. Kinesore had no effect on the levels of Slp3, a mast cell granule cargo adaptor, in the granule-enriched fraction which suggests that cargo adaptor recruitment to granules is independent of motor association. Taken together, these results show that granules associate with microtubules and are driven by kinesin-1 to facilitate exocytosis.

Contributions made to the data in Chapter 3 by Jeremies Ibanga are as indicated in the figure legends.

3.1 Introduction: microtubule dynamics, but not actin remodeling, regulate mast cell granule exocytosis

Mast cells are tissue-resident immune cells localized in epithelial and mucosal tissues that are in contact with the external environment such as the respiratory tract, gastrointestinal tract and skin [Metcalf and Boyce, 2006]. Mast cells are morphologically characterized by the presence of numerous cytoplasmic granules which house pro-inflammatory mediators, such as histamine and proteinases and molecularly characterized by the presence of FcεRI, the high affinity receptor for IgE. Upon activation, mast cells undergo profound changes in cell morphology and granule exocytosis, also known as degranulation, is rapidly triggered. Degranulation is the release of granule contents by regulated exocytosis into the interstitial space [Blank and Rivera, 2004]. Mast cell degranulation gives rise to inflammation which plays an important role in immune defense but also plays a role in the pathophysiology of diseases such as allergic asthma and autoimmune disease [Galli and Tsai, 2012; Xu and Chen 2015].

Antigen binding to IgE bound FcεRI induces receptor aggregation which leads to a signaling cascade involving activation of membrane proximal receptor tyrosine kinases [Gilfillan and Rivera, 2009; Sanderson et al., 2010], downstream Rho GTPases [Sheshachalam et al., 2017] and transient increase in intracellular calcium concentration [Hong-Geller et al., 2001; Cohen et al., 2012]. Calcium transients in conjunction with Rho GTPases modulate cytoskeletal arrangements which facilitate granule exocytosis [Norman et al., 1996; Dráber et al., 2012]. Calcium can act on multiple targets that directly activate actin and microtubule remodeling in mast cells. It has been shown that calcium activates gelsolin and cofilin that sever existing filaments, allowing turnover and the formation of new filaments [Borovikov et al., 1995; Suzuki et al., 2021]. Calcium is required for the organization of microtubule protrusions at the periphery of mast cells [Hájková et al., 2011]. Rho GTPases assemble complexes that generate new F-actin structures: activated Rac1 stimulates the formation of lamellipodia and these protrusions can be seen at the periphery of activated mast cells, while activated RhoA stimulates the formation of stress fibers that establish polarized protrusions where granules traffic [Sheshachalam et al., 2017; Baier et al., 2014].

While actin remodeling facilitates the generation of morphological transitions during mast cell stimulation [Sheshachalam et al., 2017], it has been shown that granule transport depends on microtubule dynamics [Nishida et al., 2005; Smith et al., 2003]. Kinesin-1 is a microtubule motor protein that transports anterograde cargo to the cell periphery; it was shown in a variety of cell types to be involved in transport of secretory cargo to the cell periphery for exocytosis [Arimura et al., 2009; Kurowska et al., 2012; Munoz et al., 2016]. Cargo association with kinesin-1 activates its motor activity and thus movement of granules on microtubules is controlled by cargo adaptors, a large family of proteins that link vesicle transport to cellular signaling. In mast cells, it was recently shown that granules recruit the cargo adaptor, Slp3, via a mechanism that involves signaling through Rab27 [Munoz et al., 2016].

Studies to show the role of cytoskeletal remodeling in cellular processes has been greatly facilitated by the availability of small-molecule inhibitors that perturb actin and microtubule dynamics [Peterson and Mitchison, 2002]. Jasplakinolide and paclitaxel are drugs that directly bind to F-actin and microtubule filaments, respectively, which results in the stabilization of these cytoskeletal elements [Peterson and Mitchison, 2002]. Stabilization of the cytoskeleton has shown a slight reduction in mast cell exocytosis [Oka et al., 2002]. Latrunculin and nocodazole or colchicine are drugs that directly bind to actin and tubulin monomers, respectively, which results in a net depolymerization of these cytoskeletal elements. Mast cell granule trafficking dependent on microtubules and exocytosis inhibited by microtubule depolymerizing agents [Martin-Verdeaux et al., 2003; Oka et al., 2005]. F-actin depolymerization agents have shown variable results but typically cause a slight increase in granule exocytosis [Oka et al., 2002; Nishida et al., 2005; Sheshachalam et al., 2017]. Several studies have shown a role for functional coordination between the remodeling of F-actin and microtubules via Rho signaling proteins [Krendel et al., 2002, Meiri et al., 2012; Sulimenko et al., 2015].

While there is clear evidence of microtubules driving granule exocytosis, the mechanism and molecular machinery involved in recruiting the kinesin motor to mast cell secretory granules is still not understood [Rosa-Ferreira and Munro, 2011; Keren-Kaplan and Bonifacino, 2021]. To investigate this, we utilize a novel small molecule drug, kinesore. Kinesore is a new drug that

targets kinesin-cargo adaptor function that results in aberrant remodeling of the microtubule network and the loss of directional vesicle transport [Randall et al., 2017].

Previously, we have shown that Rho proteins are involved in mast cell degranulation using a combination of genetic deletion [Baier et al., 2014] and acute inhibition with Rho specific drugs [Sheshachalam et al., 2017]. Here, we wanted to examine how mast cell regulated exocytosis involves distinct cytoskeletal dynamics. We used the cytoskeletal probes Lifeact-GFP and EB3-GFP, which bind F-actin and microtubules, to image dynamic cytoskeletal remodeling during mast cell activation. We have previously shown that mast cell activation for pro-inflammatory functions results in cytoskeletal induced changes in cell morphology that increase cell adhesion and create zones of exocytosis linked to cellular projections driven by F-actin remodeling. However, here we show that transport of granules into exocytosis zones requires dynamic microtubule formation and kinesin-1 motor function. Disruption of microtubule dynamics or kinesin motor transport, effectively disrupted granule transport to the cell periphery and subsequent exocytosis.

3.2 Live-cell imaging of cytoskeletal dynamics during mast cell stimulation implicates a role for microtubules in granule exocytosis

We recently showed that drugs targeting Rho proteins inhibit mast cell granule exocytosis and morphological transition into an activated state induced by stimulation via FcεRI aggregation [Sheshachalam et al., 2017]. Rho proteins control actin remodeling which seems to play a role in secretory granule transport and exocytosis in many cell types [Gasman et al., 2004; Tran et al., 2015; Conte et al., 2016] including mast cells [Ménasché et al., 2021]. To examine this in secretory granule-rich mast cells, we used the F-actin probe, Lifeact-GFP [Riedl et al., 2008], to microscopically image the dynamics of actin remodeling during antigen-stimulation. RBL-2H3 cells, an adherent cell line typically used as a model of mast cells [Passante and Frankish, 2009], were transfected with the Lifeact-GFP probe and granules were labelled with LysoTracker red to examine coordination between new F-actin formation and granule transport. Live-cell imaging showed the formation of actin rich lamellipodia approximately 5 min after antigen stimulation (**Figure 3.1A**, 5 min; [Video 3.1](#)). However, granules did not appear in these actin-rich protrusion as they formed (**Figure 3.1B**, *asterisk*); instead granules showed a delay in moving into the

protrusions (**Figure 3.1B**, *arrow*). There was no observable overlapping signal from F-actin and granules. This suggests that F-actin may not facilitate granule transport to the cell periphery or exocytosis.

Next, we examined microtubule dynamics during mast cell antigen-stimulation. RBL-2H3 cells were transfected with EB3-GFP, which labels the growing ends of microtubules [Stepanova et al., 2003], and granules were labelled with LysoTracker red. New microtubules radiated from a juxtannuclear position within the cell, likely representing the microtubule organizing center (**Figure 3.1C**, [Video 3.2](#)). During stimulation granules were observed to project on microtubules to the cell periphery. Granules at the cell periphery moved in a coordinated manner as EB3-GFP positive microtubules grew (**Figure 3.1D**). The velocity at which EB3-GFP puncta and lysotracker red-labelled granules moved was determined using particle tracking software. This showed that microtubules grew at $0.57 \pm 0.048 \mu\text{m/s}$, which is similar to previously determined rates in COS-1 cells [Stepanova et al., 2003]. Granules that were tracked at the cell periphery moved at $0.46 \pm 0.23 \mu\text{m/s}$. Hence granules moved at velocities similar to the rate of microtubule growth suggesting that granules are driven on new microtubules. There was significantly more heterogeneity in granule velocities compared to microtubule growth since not all granules moved.

3.3 Effect of microtubule-targeted drugs on mast cell granule exocytosis

To confirm the role of microtubules in granule transport we examined the effects of microtubule drugs that interfere with microtubule dynamics. Nocodazole and colchicine stimulate microtubule depolymerization while paclitaxel binds and stabilizes microtubules but also arrests their growth [Stanton et al., 2011]. Nocodazole potently inhibited granule exocytosis [**Figure 3.2A**; Sheshachalam et al., 2017]. We also tested colchicine as an alternative microtubule depolymerizing agent, which also inhibited exocytosis, although it was less potent than nocodazole (**Figure 3.2A**). Exocytosis was only partially affected by paclitaxel treatment, with a 30% drop in levels at the highest concentration (**Figure 3.2A**).

We used live-cell imaging to further characterize the dynamic effects of microtubule drugs. RBL-2H3 cells were transfected with EB3-GFP to label nascent microtubules and granules were

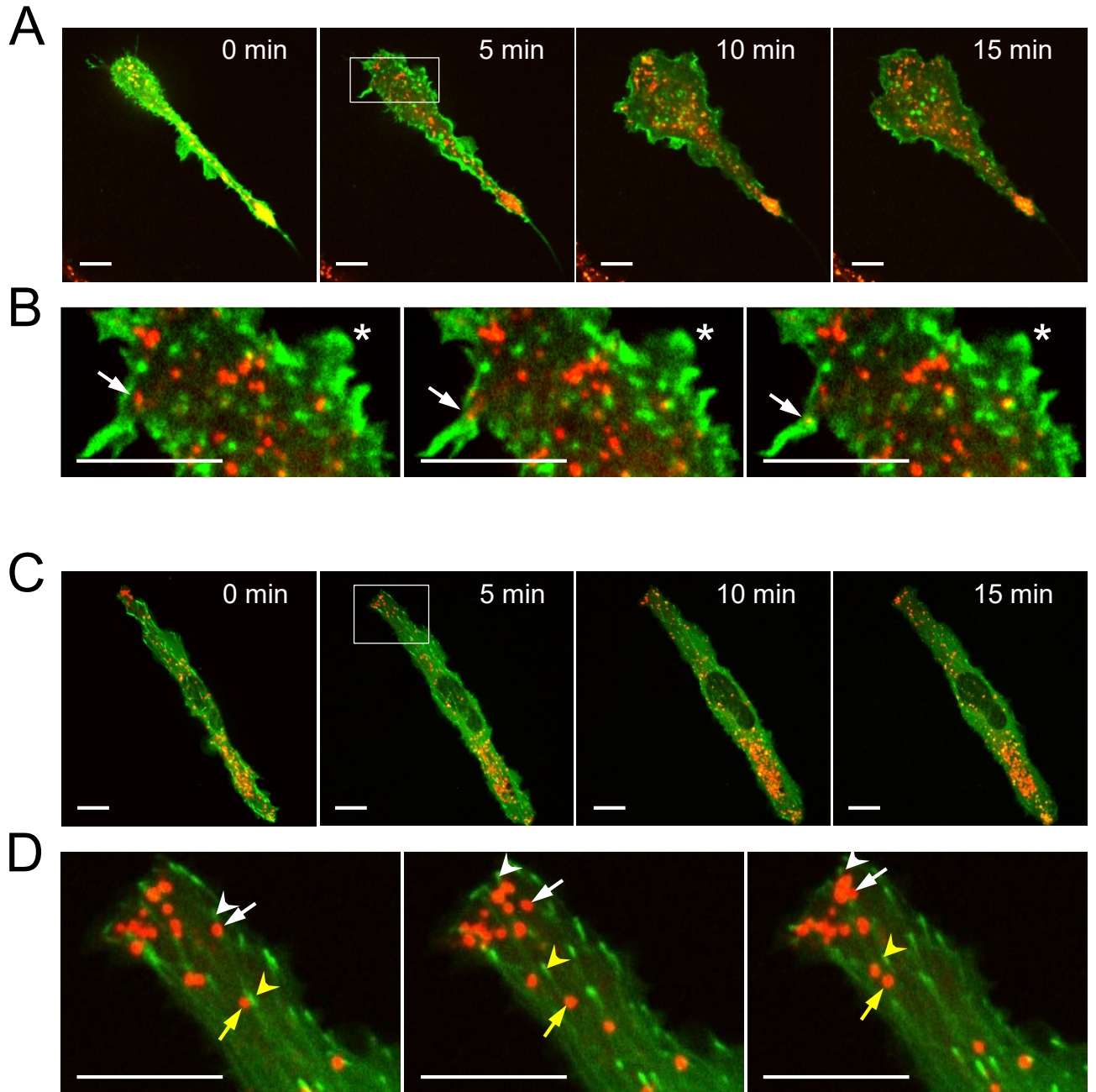


Figure 3.1 Live-cell imaging of cytoskeletal dynamics and granule movement during mast cell stimulation. RBL-2H3 cells were transfected with Lifeact-GFP (A and B) or EB3-GFP (C and D) to label nascent F-actin and microtubules respectively, and granules were stained with LysoTracker Red. (A) Representative confocal images from [Video 3.1](#) of F-actin remodeling and granule movement during a time course after antigen-stimulation. (B) Magnified images from the 5 min time point at 10 s intervals showing the movement of a granule into a pre-existing actin protrusion (*arrow*), and newly forming lamellipodia devoid of granules (*asterisk*). (C) Representative confocal images from [Video 3.2](#) of nascent microtubule formation and granule movement during a time course after antigen-stimulation. (D) Magnified images from the 5 min time point at 10 s intervals showing the movement of granules (*arrows*) is coordinated with the growth of microtubules (*arrowheads*). Scale bar, 10 μm .

Supplemental videos showing live cell imaging are available at the following URLs:

Video 3.1 Lifeact-GFP_LysoTracker Red live-cell imaging in stimulated RBL-2H3 cells

https://drive.google.com/file/d/1Z4Cj8DNAMzy6_JSSkvrepGSLGI3q81Gr/view?usp=sharing

Video 3.2 EB3-GFP_LysoTracker Red live-cell imaging in stimulated RBL-2H3 cells

https://drive.google.com/file/d/1-UgCnQb9GZ1RPynk0em_mz_r3z4Cla5S/view?usp=sharing

co-stained with LysoTracker red. Live-cell imaging of nocodazole and colchicine treated RBL-2H3 cells showed EB3-GFP puncta rapidly dissolved. However, granules still maintained some motility and antigen stimulation resulted in transient peripheral protrusions that were likely F-actin based since they resembled lamellipodia ([Video 3.3](#) and [Video 3.4](#)). Still images at different time points showed changes in granule distribution (**Figure 3.2, B and C**). Paclitaxel treatment rapidly froze microtubule dynamics and caused a slow loss of EB3-GFP puncta; no projections formed and granule movement was static ([Video 3.5](#)). Images from different time points after paclitaxel treatment showed little change in granule distribution and an overall increase in granule number in the perinuclear region showing the lack of exocytosis (**Figure 3.2D**). Particle tracking analysis of granules showed that all paclitaxel reduced granule motility by 52%, while nocodazole and colchicine did not have a significant effect (**Figure 3.2E**). However, granule movement after microtubule depolymerization was no longer directional to the cell periphery and therefore the movement detected was likely stochastic.

3.4 Effect of the microtubule motor modulator, kinesore, on mast cell granule trafficking and exocytosis

Based on the effects of microtubules drugs, granule motility to the cell periphery and subsequent exocytosis seems to be dependent on microtubule dynamics. This observation concurs with work previously demonstrating microtubules are required for granule motility in bone marrow-derived mast cells (BMMCs) and RBL-2H3 cells [Smith et al., 2003; Martin-Verdeaux et al., 2003; Oka et al., 2005; Nishida et al., 2005]. However, microtubules are required for many cellular functions, hence drugs that target microtubules might affect exocytosis indirectly. To directly investigate granule trafficking via microtubule motor proteins, we examined the effect of a recently identified drug, kinesore, a small molecule compound that binds and activates the microtubule motor protein, kinesin-1, in the absence of cargo binding [Randall et al., 2017]. Kinesore pre-treatment showed a dose-dependent inhibition of mast cell exocytosis in both the RBL-2H3 cells and BMMCs (**Figure 3.3A**). The reduction in signal was 41 +/-2.3% for BMMCs and 68 +/-10.4% for RBL-2H3 cells. This may seem modest, however, we used kinesore at concentrations up to its IC₅₀ of 100 µM for blocking interactions with the cargo adaptor SKIP [Randall et al., 2017].

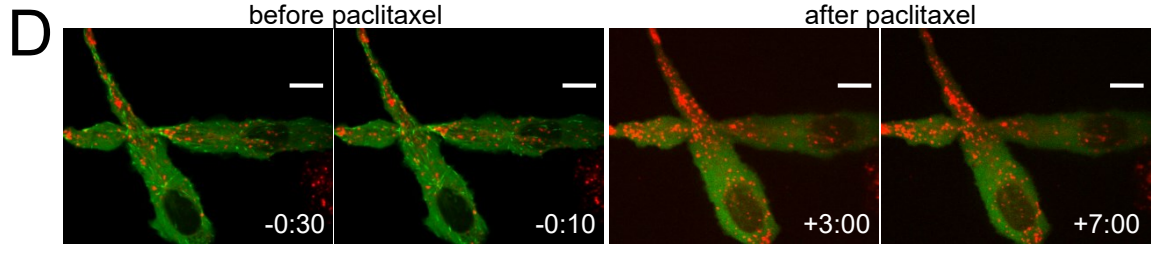
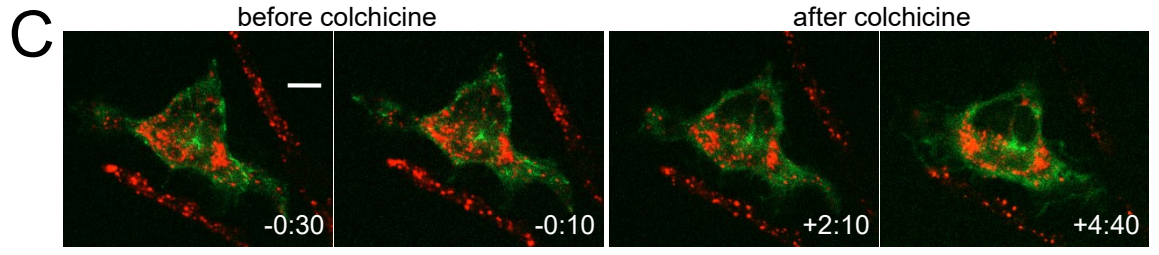
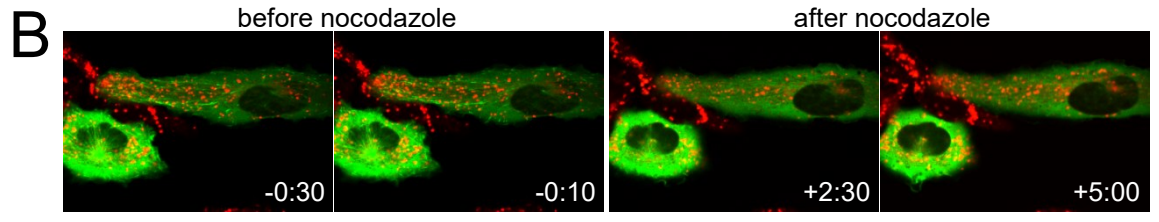
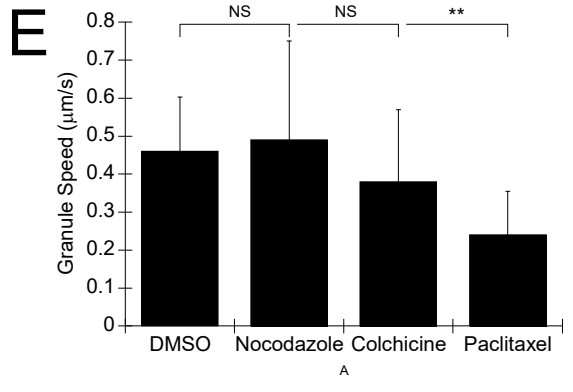
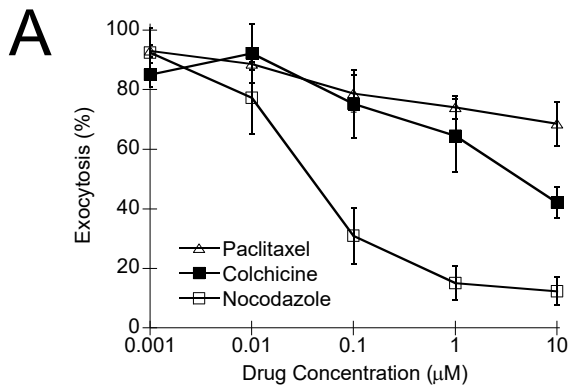


Figure 3.2 Microtubule drugs inhibit mast cell granule exocytosis and affect granule motility. (A) Exocytosis assay of RBL-2H3 cells that were pre-treated with nocodazole, colchicine and paclitaxel for 30 min prior to antigen-stimulation. Exocytosis was assayed as the percent β -hexosaminidase released of total, normalized to vehicle (DMSO) controls (n = 4). (B – D) Representative confocal images from live-cell imaging of microtubule dynamics and granule movement of mast cells treated with 1 μ M nocodazole (B, [Video 3.3](#)), 10 μ M colchicine (C, [Video 3.4](#)), or 10 μ M paclitaxel (D, [Video 3.5](#)). RBL-2H3 cells were transfected with EB3-GFP to label nascent microtubules and incubated with LysoTracker red to label granules. Cells were imaged for 1 min, then antigen-stimulated and concurrently drugs were added, followed by 15 min of imaging. Scale bar = 10 μ m. (E) Granules at the cell periphery were analyzed by particle tracking software. A minimum of 15 granules from 5 cells were tracked. Shown is the mean granule speed \pm standard error. The effect of drugs was compared to the vehicle (0.5% DMSO) control by Student's t-test (NS, not significant; $**p < 0.01$; n = 5). *Jeremies Ibanga provided data for panel A.*

Supplemental videos showing live-cell imaging are available at the following URLs:

Video 3.3 EB3-GFP_LysoTracker Red live-cell imaging of nocodazole treated cells

<https://drive.google.com/file/d/1cqun2qCI84GROY3eO1BDlfRm3F7BoqIT/view?usp=sharing>

Video 3.4 EB3-GFP_LysoTracker Red live-cell imaging of colchicine treated cells

https://drive.google.com/file/d/1nMVwvQOfGEN28rdMtYn7Gg5Qk_hkOHCc/view?usp=sharing

Video 3.5 EB3-GFP_LysoTracker Red live-cell imaging of paclitaxel (taxol) treated cells

<https://drive.google.com/file/d/1qyqH7P4xdeLD-eQaNY9xsFdmRPJ3MSMC/view?usp=sharing>

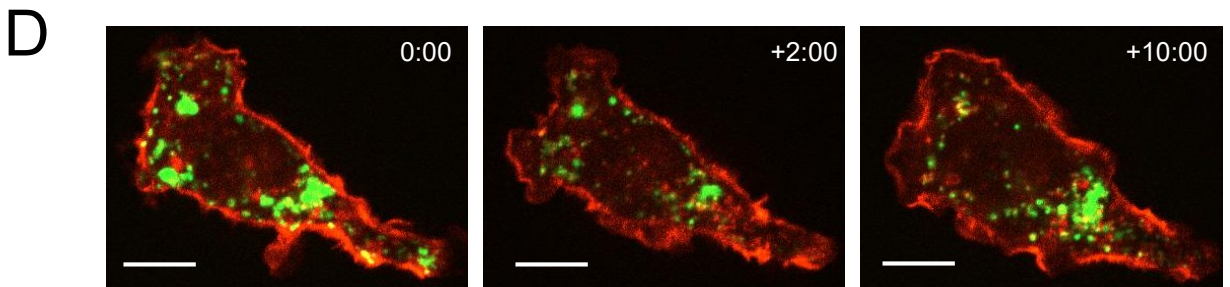
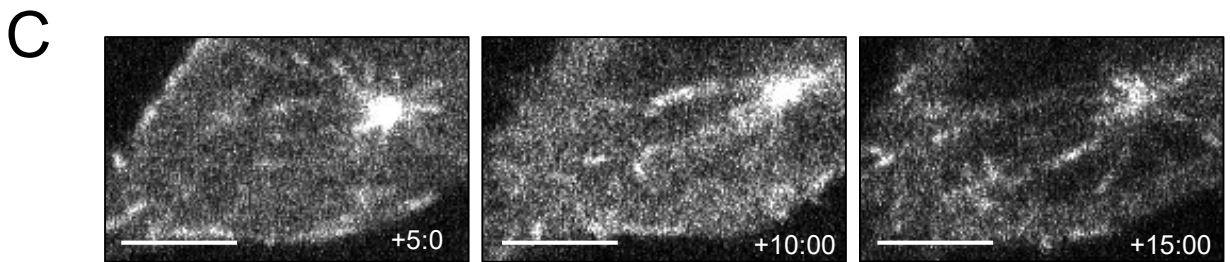
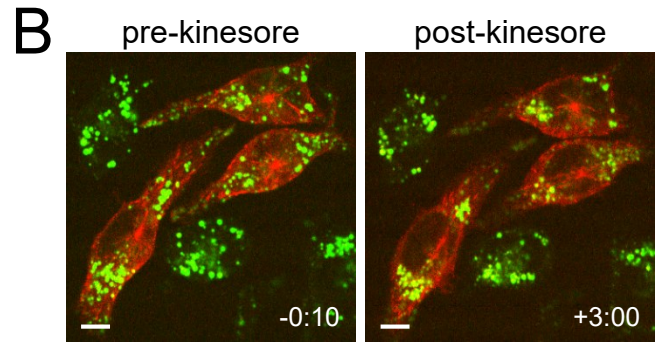
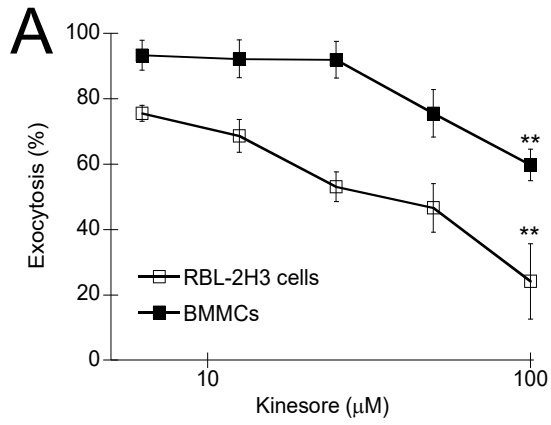


Figure 3.3 Kinesore, a small-molecule activator of microtubule motors, inhibits mast cell granule exocytosis. (A) Exocytosis assay of RBL-2H3 cells and BMMCs that were pre-treated with kinesore for 30 min prior to antigen-stimulation. Exocytosis was assayed as the percent β -hexosaminidase released of total, normalized to vehicle (DMSO) controls. 100 μ M kinesore showed statistically significant inhibition of both RBL-2H3 cell and BMMC exocytosis (** $p < 0.01$; $n = 4$). (B) Representative confocal images from live-cell imaging of microtubule dynamics and granule movement of mast cells treated with 100 μ M kinesore ([Video 3.6](#)). RBL-2H3 cells were transfected with EB3-tdTomato to label nascent microtubules and incubated with LysoTracker green to label granules. Cells were imaged for 1 min, then antigen-stimulated and concurrently 100 μ M kinesore was added, followed by 15 min of imaging. Granules moved to the perinuclear region while microtubules project to the cell periphery. (C) Magnified images from the 5 - 15 min time points showing the formation of EB3-tdTomato puncta were not affected by kinesore. (D) Representative confocal images from live-cell imaging of actin dynamics and granule movement of mast cells treated with 100 μ M kinesore ([Video 3.7](#)). RBL-2H3 cells were transfected with Lifeact-mRuby to label nascent F-actin and incubated with LysoTracker green to label granules. Cells were imaged for 1 min, then antigen-stimulated and concurrently 100 μ M kinesore was added, followed by 15 min of imaging. Scale bar = 10 μ m. *Jeremies Ibanga provided data for panel A.*

Supplemental videos showing live-cell imaging of are available at the following URLs:

Video 3.6 EB3-tdTomato_LysoTracker Green live-cell imaging of kinesore treated cells

https://drive.google.com/file/d/1urM3jC_eF1IOamQU9rqQAikKeRReHHA1/view?usp=sharing

Video 3.7 Lifeact-mRuby_LysoTracker Green live-cell imaging of kinesore treated cells

https://drive.google.com/file/d/1SuA7LzVrm_IKIRaUoAC1pzWZROscFvpW/view?usp=sharing

We performed live-cell imaging of antigen-activated RBL-2H3 cells to characterize the dynamic effects of kinesore on cytoskeletal remodeling and granule motility. EB3-tdTomato and LysoTracker green were used to visualize microtubule dynamics and granule movement, respectively ([Video 3.6](#)). Still images showed that granules were at first spread throughout the cell; however, after kinesore exposure granules no longer projected to the cell periphery and instead accumulated in the perinuclear region (**Figure 3.3B**). EB3-tdTomato labelling of the microtubule network was not affected by kinesore (**Figure 3.3C**). Lifeact-mRuby and LysoTracker green were used to visualize F-actin remodeling and granule movement, respectively, after kinesore treatment ([Video 3.7](#)). Still images of Lifeact-mRuby labelled F-actin showed that kinesore had no effect on actin remodelling (**Figure 3D**). Cell membrane ruffling, an actin remodeling induced phenomena observed in activated mast cells, were consistently observed in antigen-activated RBL-2H3 cells pretreated with kinesore. These results support a role for microtubule-directed granule motility and suggest that kinesin motors play an essential role in the transport of secretory granules.

3.5 Microtubule-targeted drugs do not block cell transition to activated phenotype

We next used immunofluorescence microscopy to examine the effect of microtubule drugs and the microtubule motor modulator drug, kinesore, on F-actin cytoskeletal structures and the distribution of mast cell granules labelled with anti-CD63 antibodies (CD63+) [Köberle et al., 2012]. RBL-2H3 cells were pre-treated with vehicle (0.5% DMSO), nocodazole, colchicine, paclitaxel or kinesore, then left unstimulated or antigen-stimulated for 30 min, fixed and labelled for immunofluorescence microscopy and the distribution of fluorescence signal in a cell analyzed by profile plots (**Figure 3.4, right panels**). Vehicle-treated cells showed typical morphology. Unstimulated cells were elongated with CD63+ granules enriched in the perinuclear region (**Figure 3.4A**) while stimulated cells showed cell spreading and peripheral lamellipodia formation with CD63+ granules spreading to the cell periphery (**Figure 3.4A'**). Unstimulated nocodazole and colchicine-treated cells showed retraction and the formation of numerous filopodia with granule staining that was intensely perinuclear (**Figure 3.4, B and C**). However, stimulated cells pre-treated with colchicine and nocodazole underwent normal cell spreading and formed peripheral lamellipodia as well as prominent stress fibers, particularly in colchicine-treated cells; however, granules remained perinuclear which was much more apparent in

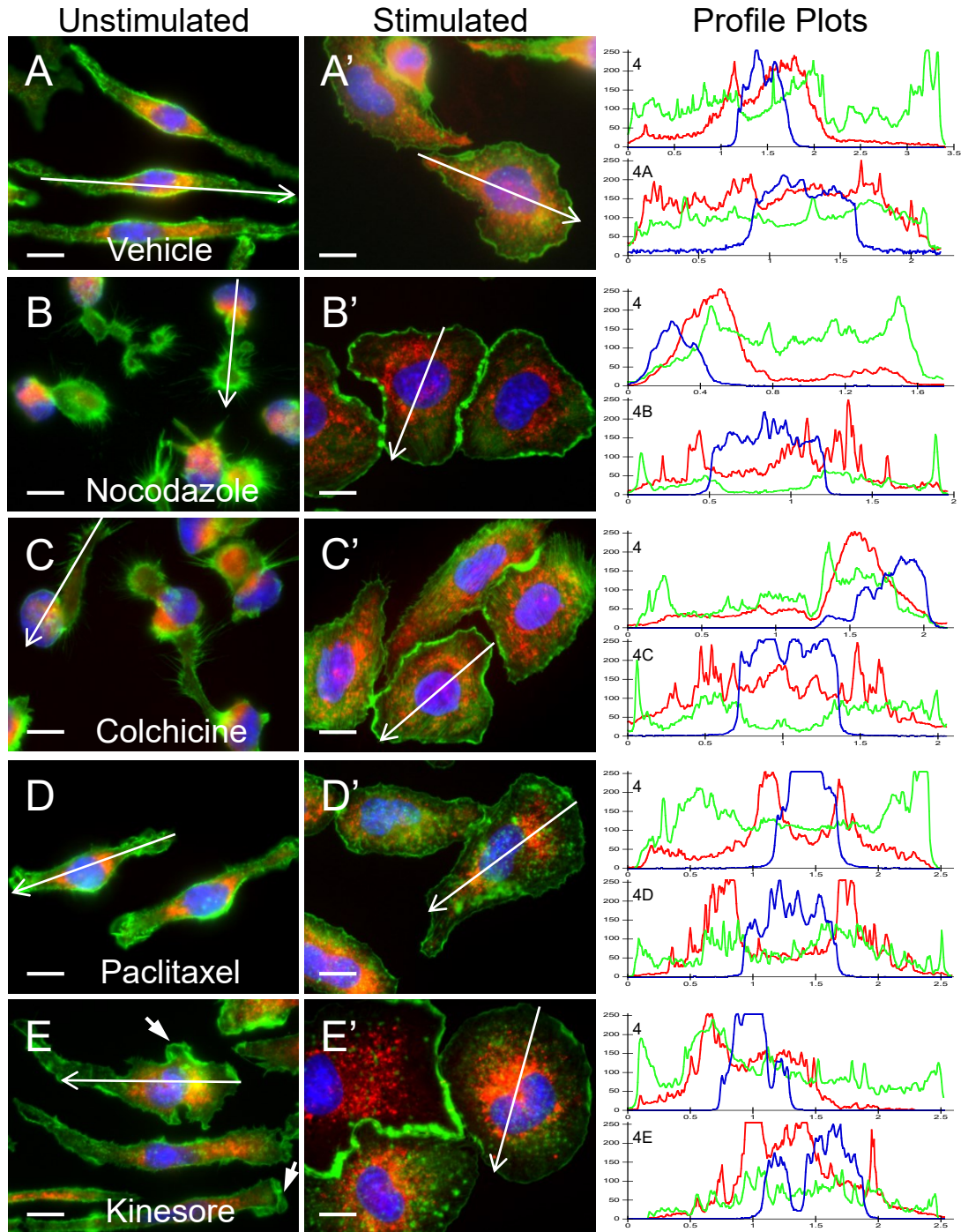


Figure 3.4 Microtubule drugs and the microtubule motor drugs, kinesore, affect cell morphology and granule distribution but not F-actin remodeling. RBL-2H3 cells were pretreated for 30 min with vehicle (DMSO) (A), 1 μ M nocodazole (B), 10 μ M colchicine (C), 10 μ M paclitaxel (D), or 100 μ M kinesore (E). Cells were left unstimulated or antigen-stimulated for 30 min, fixed and stained for nuclei (blue), F-actin (green), or CD63+ granules (red). Scale bar = 10 μ m. Profile plots (right panels) show drug pretreatment does not affect formation of F-actin rich lamellipodia, however CD63+ granules accumulate in the perinuclear region.

nocodazole-treated cells (**Figure 3.4, B' and C'**). Unstimulated paclitaxel-treated cells were elongated and showed actin ruffles but no filopodia (**Figure 3.4D**). After stimulation, actin ruffles persisted and peripheral lamellipodia formed but there was a lack of CD63+ granules at the cell periphery (**Figure 3.4D'**). Interestingly, kinesore-treated cells showed the formation of some peripheral lamellipodia even prior to stimulation (**Figure 3.4E, arrow**). Kinesore pre-treated cells transitioned to an activated morphology after stimulation; cells spread and flattened however CD63+ granules were not in the cell periphery and instead accumulated in the perinuclear region (**Figure 3.4E'**). The profile plots show CD63 signal spreads throughout vehicle-treated stimulated cells, while in drug-treated cells the CD63 signal is predominantly adjacent to the nucleus (**Figure 3.4, left panels**).

Microtubule morphology was also examined in kinesore-treated RBL-2H3 cells by immunofluorescence microscopy. Microtubules project radially from the nuclear region to the cell periphery in unstimulated and stimulated cells, with many CD63+ granules at the cell periphery after stimulation (**Figure 3.5A, Vehicle**). Pretreatment with kinesore resulted in microtubules that rearranged into looping structures in both unstimulated and stimulated cells (**Figure 3.5A, Kinesore**). This morphology is similar to that previously observed in HeLa cells treated with kinesore [Randall et al., 2017]. A time course of kinesore treatment showed that microtubule remodeling into looping structures in RBL-2H3 cells was not apparent after 15 min of incubation, while full disruption of the microtubule network into loops occurred by 60 min of incubation regardless of whether cells were stimulated or unstimulated (**Figure 3.5B**). Therefore, the loss of granule transport to the cell periphery precedes microtubule looping. Together with dynamic imaging of kinesore effects, these results show that microtubule-based motor proteins transport granules to zones of exocytosis that project from the cell periphery.

3.6 Kinesore affects the association of granules with the microtubule motor, kinesin-1

Kinesin-1 is a microtubule motor protein that is activated by binding to cargo via cargo adaptor proteins that link vesicles, such as granules in activated mast cells, to microtubules for transport [Hirokawa et al., 2009]. We examined the levels of expression of several lysosomal and secretory vesicle cargo adaptors in RBL-2H3 cells by quantitative PCR. This showed the expression of low levels of SKIP, Slp2 and Slp3 mRNA compared to GAPDH (**Figure 3.6A**). Previously, it was reported that Slp3 functioned as a secretory granule cargo adaptor in BMDCs

[Munoz et al., 2016], while SKIP functions as a cargo adaptor that is needed for the recruitment of kinesin-1 to lysosomes and melanosomes [Rosa-Ferreira and Munro, 2011; Keren-Kaplan and Bonifacino, 2021; Ishida et al., 2015]. JIP3 and JIP4 were also detected, however they are associated with bidirectional vesicle transport in neurons and were not further examined [Montagnac et al., 2009]. Immunoblot of lysates from a variety of tissue culture cells showed abundant levels of the kinesin-1 heavy chain, kif5b, and the presence of Slp3 immunoreactive bands, however SKIP could not be detected in RBL-2H3 cells (**Figure 3.6B**).

Kinesore activates the microtubule motor kinesin-1 in the absence of cargo binding by mimicking association with cargo adaptors [Randall et al., 2017]. Therefore, the loss of granule transport observed after kinesore treatment suggests that it may functionally inhibit the association of the microtubule motors with cargo adaptors needed for granule transport. To test this, we generated granule-enriched fractions from stimulated and unstimulated mast cells, and probed them for the presence of kif5b (kinesin-1 heavy chain) and the cargo adaptor Slp3. Granule-enriched fractions showed high levels of rat mast cell protease II (RMCP II) when prepared from unstimulated cells, and a 47 +/- 7.2% reduction in RMCP II levels after stimulation for 30 min, likely due to exocytosis (**Figure 3.6C, DMSO**). Kif5b was also associated with granule-enriched fractions. Kif5b was recruited to granule-enriched fractions with levels increasing by 118 +/- 17% when prepared from cells stimulated for 30 min (**Figure 3.6C, DMSO**). Kinesore treatment resulted in no recruitment of kif5b to granule-enriched fractions but an increase in Slp3 levels (**Figure 3.6C, Kinesore**). There was no reduction in the levels of RMCP II in fractions prepared from kinesore-treated cells after stimulation indicating kinesore blocked exocytosis. Therefore, kinesore likely inhibits exocytosis by blocking microtubule motor protein association with granules. Taken together, these results show that granules are dynamically moved by the formation of microtubules tracks in a mechanism that requires the activation of microtubule motors; motor association with granules is via granule-associated cargo adaptors.

3.7 Discussion: microtubule dynamics for granule trafficking in mast cells

Antigen-stimulation of mast cells induces cytoskeletal remodeling and granule exocytosis; also referred to as degranulation. Here we used live-cell imaging of RBL-2H3 cells to examine the

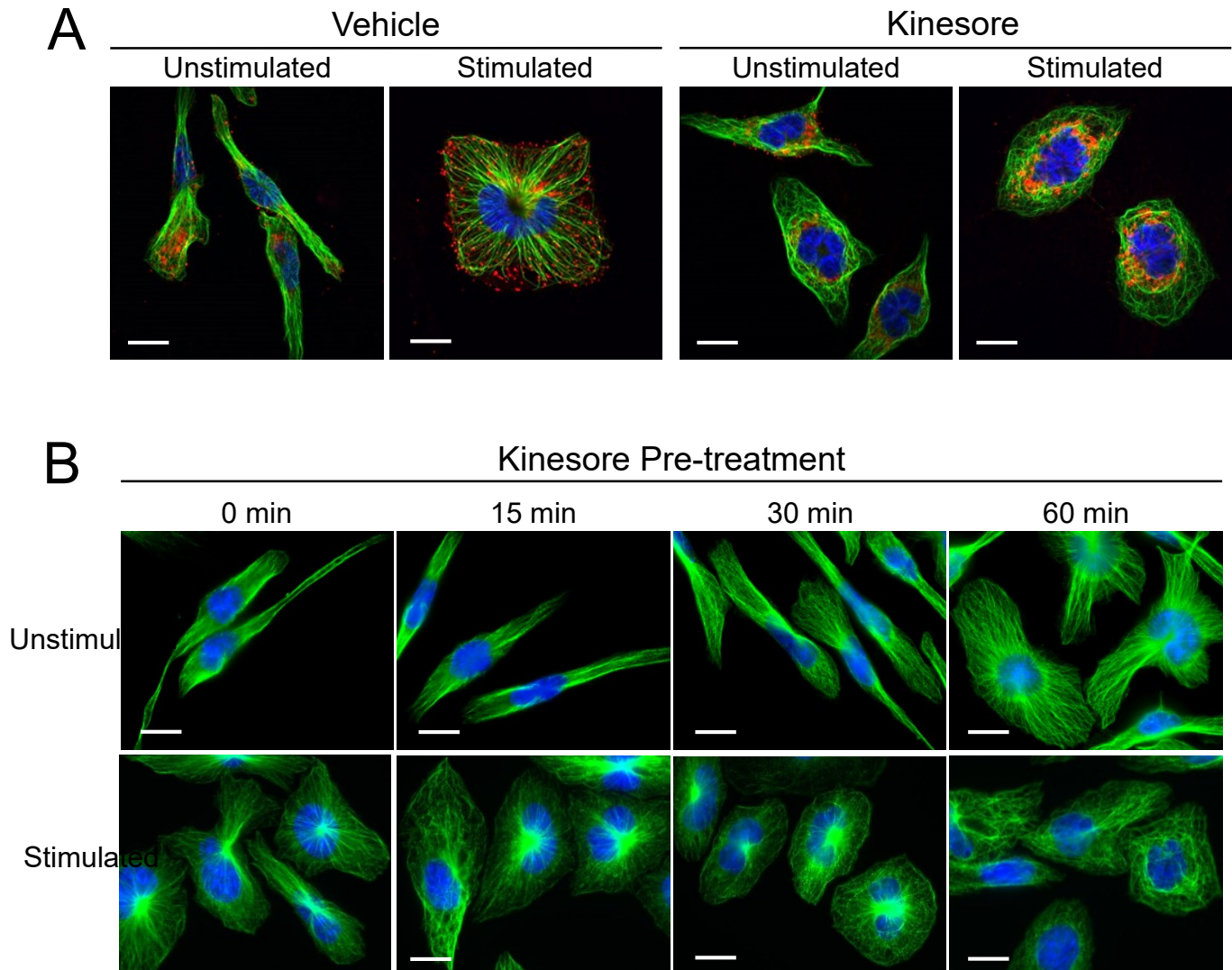


Figure 3.5 Kinesore treatment of mast cells affects microtubule structures independent of its effect on granule distribution. (A) RBL-2H3 cells were pretreated for 30 min with vehicle (DMSO), or 100 μ M kinesore. Cells were left unstimulated, or antigen-stimulated for 30 min, fixed and stained for nuclei (blue), microtubules (green), or CD63+ granules (red). Granule distribution to the cell periphery is disrupted by kinesore treatment. Microtubule structures that normally project linearly to the cell periphery were disrupted by kinesore treatment. (B) RBL-2H3 cells were pre-treated for 0 min, 15 min, 30 min or 60 min with kinesore then fixed (*unstimulated*), or antigen-stimulated for 30 min then fixed and stained for nuclei (blue) and microtubules (green). Microtubule linear structures were disrupted by kinesore after 30 min. Scale bar = 10 μ m. *Jeremies Ibanga provided this data.*

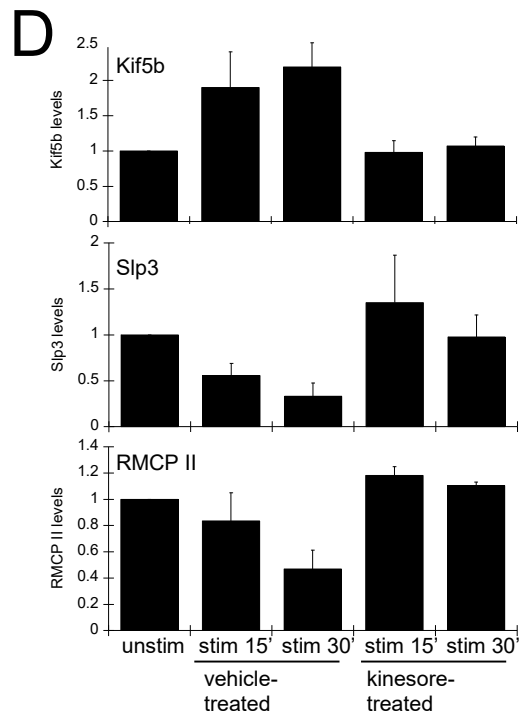
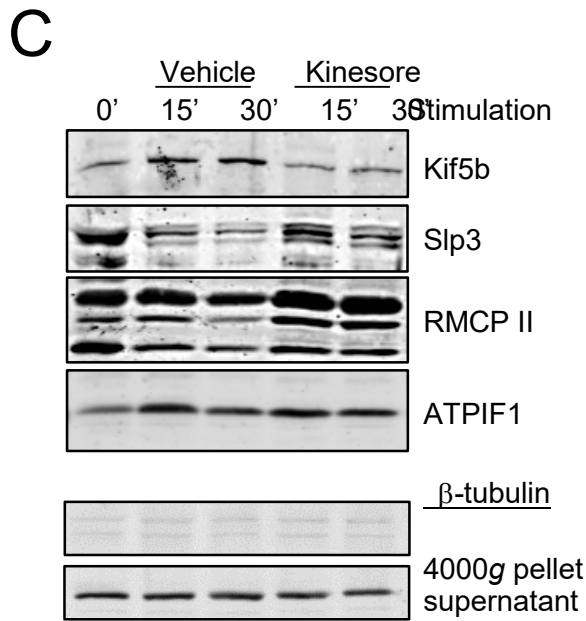
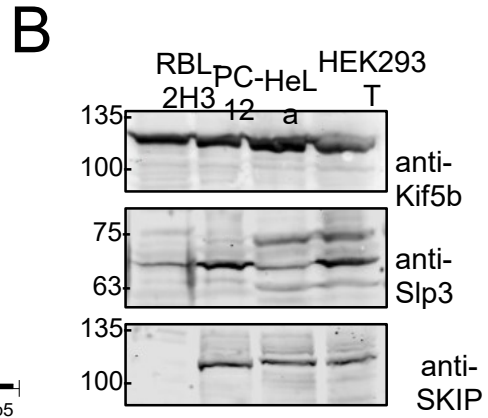
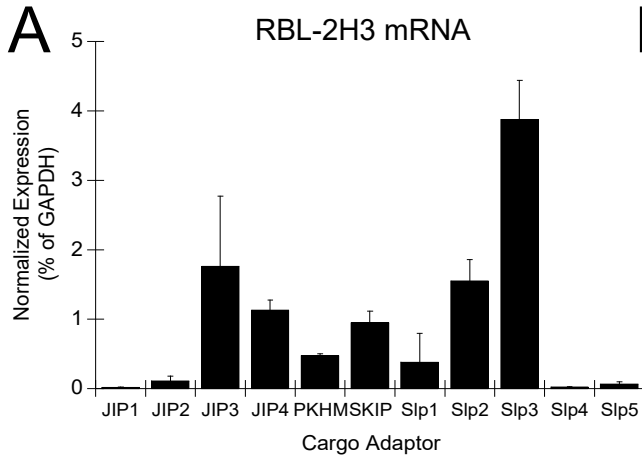


Figure 3.6 Kinesore inhibits granule association of the microtubule motor kinesin-1.

(A) Quantitative PCR analysis of mRNA isolated from RBL-2H3 cells. Gene expression level of cargo adaptors known to associate with secretory granules and lysosomes. (B) Immunoblot of lysates from RBL-2H3, PC-12, HeLa and HEK293T cells (10^7 cells/ml lysate). Lysates were probed for kif5b and two cargo adaptors, Slp3 and SKIP. SKIP was not detected in RBL-2H3 cells. (C) Granule-enriched fractions were prepared by differential centrifugation from unstimulated cells (0'), or from cells that were antigen-stimulated for 15 min and 30 min in the presence of kinesore or vehicle (0.5% DMSO). Fractions were probed by immunoblot for association of the microtubule motor subunit kif5b, the cargo adaptor Slp3, the granule enzyme rat mast cell protease II (RMCP II) and the mitochondrial marker ATP1F1 (*upper panels*). Tubulin was not associated with the granule-enriched fraction and instead was found in supernatant (*lower panels*). (D) Levels of protein associated with granule-enriched fractions were examined by band densitometry of immunoblots. Values were normalized to unstimulated (0 min of antigen stimulation) cells for each experiment (n = 3).

dynamics of cytoskeletal remodeling and granule motility during antigen-stimulation. Actin remodeling at the surface of cells has been proposed to capture vesicles for exocytosis [Eitzen,2003; Malacombe et al., 2006; Nightingale et al., 2012]. However, our results show actin mediated protrusions that form in response to mast cell stimulation are devoid of granules ([Video 3.1](#)). Compounds that depolymerize actin most often enhance exocytosis. This is congruent with a recent study using high resolution microscopy which showed cortical actin disassembly formed exocytosis zones at the surface of mast cells [Colin-York et al., 2019].

Our results support a role for microtubules in the transport and exocytosis mechanism of granule exocytosis. Studies using microtubule depolymerizing agents showed these reduce mast cell degranulation and granule motility [Martin-Verdeaux et al., 2003; Smith et al., 2003; [Videos 3.3](#) and [3.4](#)]. However, the effect of these compounds could be due to gross perturbation of cell morphology since the formation of exocytosis zones has been shown necessary [Sheshachalam et al., 2017; Colin-York et al., 2019]. Here we tested the compound kinesore which has a more targeted effect on the microtubules network, specifically affecting the function of the microtubule motor, kinesin-1 [Randall et al., 2017]. Kinesore-treated cells showed a lack of trafficking of granules to the cell surface ([Video 3.6](#)) and also significant inhibition of granule exocytosis, both in primary mast cells (BMMCs) and in RBL-2H3 cells. Although kinesore also affected cell morphology with the formation of microtubule looping structures, these structures formed progressively after 30 min of incubation while granules accumulated in the perinuclear region prior to the formation of microtubule loops. Therefore, we conclude that the kinesore-mediated inhibition of exocytosis is independent of the morphological effects on microtubule organization. The degree to which looping structures formed in RBL-2H3 cells was significantly less pronounced than that observed in HeLa cells, however it was comparable to other cell lines examined [Randall et al., 2017].

A growing body of research shows that microtubule nucleation is linked to mast cell activation [Sulimenko et al., 2006; Hájková et al., 2011; Sulimenko et al., 2015; Klebanovych et al., 2019]. Such a mechanism would facilitate the regulation of granule exocytosis to cell activation. Our results indicate that the activation of granule transport for exocytosis is microtubule-based. This activation step is regulated by cargo adaptors that can dynamically associate with granules when

antigen-stimulation signals are received [Kurowska et al., 2014]. The role of cargo adaptors is to link cargo (i.e. granules) to microtubule based motors. Therefore, in mast cells, granule association with cargo-binding adaptors allows association with microtubule based motors to drive the degranulation process [Munoz et al., 2016]. We found kinesin-1 was recruited to a granule enriched fraction during antigen stimulation and its levels were reduced by kinesore. Kinesore is known to activate kinesin-1 motor function in the absence of cargo by binding to the cargo adaptor site. Therefore, it is likely that kinesore inhibits the coupling of a granule cargo adaptor and kinesin-1.

Cargo-binding adaptor recruitment is likely a pivotal regulatory step for the activation of granule transport and exocytosis. We detected the expression of numerous cargo adaptors in RBL-2H3 cells and previously it was shown that Slp3 functions as a granule cargo adaptor in BMMCs and can link to kinesin-1 through a PI3 kinase-activated mechanism [Munoz et al., 2016]. SKIP (PLEKHM2) was the cargo adaptor targeted by kinesore [Randall et al., 2017]. SKIP was previously implicated in kinesin-1 activation during salmonella infection [Boucrot et al., 2005]. Recent studies have defined the role of SKIP in lysosomal transport and kinesin-1 activation. SKIP has been shown to serve as a linker protein between lysosomal membrane proteins and the kinesin-1 motor [Rosa-Ferreira and Munro 2011; Keren-Kaplan and Bonifacino, 2021]. SKIP plays a vital role in microtubule plus end directed motility of lysosomes and the lysosome related organelle, melanosomes [Rosa-Ferreira and Munro 2011; Ishida et al., 2015]. Hence, we consider SKIP may be a potential cargo-binding adaptor for mast cell secretory granules.

The molecular machinery involved in motor protein-cargo binding is highly heterogeneous. In melanocytes, SKIP is involved in the transport of both lysosomes and melanosomes [Ishida et al., 2015]. It differentiates between these organelles via binding to different membrane associated-cargo proteins, binding to Arl8 on lysosomes whiles binding to Rab1a on melanosomes. In hematopoietic cells, cargo adaptors can mediate the transport of a variety of granules via binding to different membrane associated-cargo proteins. In cytotoxic T lymphocytes Slp3 facilitates kinesin-1 based transport of terminal lytic granules via binding to Rab27a on lytic granules and to the kinesin-1 motor protein [Kurowska et al., 2012]. Yet in murine BMMCs, it has been demonstrated that Slp3 enables kinesin-1 dependent transport of CD63+ granules via binding to

Rab27b [Munoz et al., 2016]. Therefore, an important future study is to determine the mechanism that activates mast cell cargo-binding adaptors in their recruitment to granules and coupling with the kinesin-1 microtubule motor.

3.8 Supplemental video list with links to online content

Video 3.1 Lifeact-GFP_LysoTracker Red live-cell imaging in stimulated RBL-2H3 cells

https://drive.google.com/file/d/1Z4Cj8DNAMzy6_JSSkvrepGSLGI3q81Gr/view?usp=sharing

Video 3.2 EB3-GFP_LysoTracker Red live-cell imaging in stimulated RBL-2H3 cells

https://drive.google.com/file/d/1-UgCnQb9GZ1RPynk0em_mz_r3z4Cla5S/view?usp=sharing

Video 3.3 EB3-GFP_LysoTracker Red live-cell imaging of nocodazole treated cells

<https://drive.google.com/file/d/1cqun2qCI84GROY3eO1BDlFRm3F7BoqIT/view?usp=sharing>

Video 3.4 EB3-GFP_LysoTracker Red live-cell imaging of colchicine treated cells

https://drive.google.com/file/d/1nMVwvQOfGEN28rdMtYn7Gg5Qk_hkOHCc/view?usp=sharing

Video 3.5 EB3-GFP_LysoTracker Red live-cell imaging of paclitaxel treated cells

<https://drive.google.com/file/d/1qyqH7P4xdeLD-eQaNY9xsFdmRPJ3MSMC/view?usp=sharing>

Video 3.6 EB3-tdTomato_LysoTracker Green live-cell imaging of kinesore treated cells

https://drive.google.com/file/d/1urM3jC_eF1IOamQU9rqQAikKeRReHHA1/view?usp=sharing

Video 3.7 Lifeact-mRuby_LysoTracker Green live-cell imaging of kinesore treated cells

https://drive.google.com/file/d/1SuA7LzVrm_IKIRaUoAC1pzWZROscFvpW/view?usp=sharing

Chapter 4

The Role of RhoGEFs in mast cell exocytosis

Summary

Our former studies revealed the involved roles of RhoA and Rac1 in mast cell exocytosis. Here, we explored the roles of RhoGEFs, activators of Rho proteins, in antigen-stimulated exocytosis, using RBL-2H3 cells as model mast cells. RT-PCR was used to profile RhoGEF levels and selective expression in mast cells; this revealed that Vav1, P-Rex1, α -PIX, β -PIX and GEF-H1 may be putative functional candidates. Depletion of Vav1, P-Rex1, α -PIX, β -PIX by RNA interference (RNAi) did not significantly alter the granule movement and exocytosis, although the activation of Rac1 was suppressed. These observations ruled out an independent functional role for Vav1, P-Rex1, α -PIX or β -PIX in regulating mast cell exocytosis. However, knockdown of GEF-H1 expression by RNAi significantly disrupted cell spreading, granule movement and exocytosis measured by immunofluorescence, live-cell imaging and degranulation assay, respectively. RhoA, but not Rac1, was the main target of GEF-H1. Knockdown of GEF-H1 suppressed stress fiber formation without altering cell ruffling or lamellipodia formation. Re-introduction of Rho-G14V, a constitutively active mutant, restored normal morphology in GEF-H1-depleted cells. Focal adhesion (FA) formation was involved in granule exocytosis; depletion of GEF-H1 led to the reduced FAs after antigen stimulation. GEF-H1 activation was linked to the Fc ϵ RI signaling pathway but was independent of microtubules dynamics since microtubules-targeted drugs did not affect GEF-H1 activation. Instead, GEF-H1 activation relied on the Syk kinase; Syk inhibitor GS-9973 suppressed cell spreading, granule movement and exocytosis in stimulated RBL-2H3 cells. Inhibitors of other kinases including Src, Fyn, Lck, MEK1/2, PI3-kinase (PI3K) and FAK did not affect GEF-H1 activation. Assays of co-localization and co-fractionation in enriched granules did not address the interaction between GEF-H1 and Exo70, an important component of the exocytosis machinery. Taken together, the GEF-H1-RhoA axis transduces antigen stimulation signals from Fc ϵ RI to exocytosis in mast cells, which involves the formation of FAs.

Contributions made to the data in Chapter 4 by Judeah Negre are as indicated in the figure legends.

4.1 Introduction: Signal transductions from RhoGEFs to Rho proteins in mast cell cytoskeleton remodeling and exocytosis

Mast cells are tissue-resident immune cells that contain granule mediators, which play important roles in multiple cellular processes, including wound healing, inflammation, and immune responses [da Silva et al., 2014]. Mast cells can be activated via various stimuli, however, hyper-responsive reactions that lead to allergic disease most often are mediated by IgE and the Fc ϵ RI signaling pathway [Blank and Rivera, 2004; Mukai et al., 2018]. Antigens that activate this pathway lead to the release of potent pro-inflammatory mediators stored in granules; this process of regulated exocytosis is called degranulation [Blank and Rivera, 2004]. Antigen (or allergens) binding to IgE leads to the Fc ϵ RI aggregation triggering a downstream signaling cascade including the Syk-LAT-PLC γ and the Fyn-Gab2-PI3K signaling pathways [Blank and Rivera, 2004]. Emerging studies have begun to reveal details of the regulatory mechanisms of mast cell degranulation, aiming to alleviate the effects of mast cell-oriented diseases including allergic inflammation [da Silva et al., 2014; Galli et al., 2008].

Mast cell exocytosis is under tight regulations by a number of proteins [Blank and Rivera, 2004]. Our recent results suggest that Rho proteins also regulate mast cell exocytosis [Sheshachalam et al., 2017; Baier et al., 2014]. Rho proteins are monomeric G proteins belonging to the Ras superfamily of GTPases that play diverse roles in multiple cellular processes including cytoskeletal dynamics, cell polarity and migration, NADPH oxidase activation, membrane trafficking, and transcription [Etienne-Manneville and Hall, 2002]. Rho proteins cycle between active GTP-bound and inactive GDP-bound states; Rho guanine nucleotide exchange factors (RhoGEFs) that facilitate the loading of GTP which results in their activation [Cook et al., 2014; Hodge and Ridley, 2016]. Rho proteins are important cytoskeleton regulators. Accumulating evidence have demonstrated that Rac1, Cdc42 and RhoA critically regulate the dynamic formations of lamellipodia, filopodia and stress fiber, respectively [Hall, 1998; Nobes and Hall, 1995; Ridley and Hall, 1992; Ridley et al., 1992]. These formations require the nucleation and branching of the F-actin cytoskeleton and are mediated via the recruitment and participation of many downstream Rho effectors [Hahne et al., 2001; Chen et al., 2010; Krugmann et al., 2001; Bishop and Hall 2000]. RhoA has been found to regulate the formation of stress fiber nucleated by formins like mDia and activated by ROCK (Rho-associated protein kinase) [Bishop and Hall

2000; Mackay and Hall, 1998], which are important for the assembly and turnover of focal adhesion, exerting diversely functional roles of RhoA protein [Chrzanowska-Wodnicka and Burridge, 1996; Ridley and Hall, 1992; Wozniak et al., 2004; Yamana et al., 2006].

Previous studies have shown that Rho proteins regulate cytoskeleton remodeling and granule exocytosis in mast cells from the antigen stimulation pathway [Norman et al., 1996; Hong-Geller, 2001; Baier et al., 2014; Sheshachalam et al., 2017]. Our recent studies have also demonstrated that the Rho proteins, Rac1 and Rac2, regulated mast cell exocytosis by targeting actin dynamics and calcium signaling pathway, respectively [Baier et al., 2014]. Moreover, the specific Rho drugs Rhosin and EHT 1864, significantly inhibit mast cell degranulation, in particular by targeting the activation of RhoA and Rac1 [Sheshachalam et al., 2017]. Since Rho proteins are activated by the upstream RhoGEFs, our hypothesis is that RhoGEFs may be important in regulating mast cell exocytosis.

RhoGEFs are a diverse family of proteins consisting of 71 Dbl (diffuse B-cell lymphoma) and 11 DOCK (dedicator of cytokinesis) subfamily members in mammals [Schmidt and Hall, 2002; Cook et al., 2014]. Accumulating studies have revealed the roles of certain RhoGEFs in exocytosis and membrane trafficking [Rossman et al., 2005; Manetz et al., 2001; Pathak et al., 2012; Sulimenko et al., 2015]. For example, Vav1 and P-Rex1, two RhoGEFs predominantly expressed in hematopoietic cells, regulate mast cell degranulation, GLUT4 protein trafficking in adipocytes and dense granule secretion from platelets [Balamatsias et al., 2011; Manetz et al., 2001; Qian et al., 2012]. β -PIX, considered as a Rac and Cdc42 RhoGEF, modulates synaptic vesicle trafficking in conjunction with microtubules dynamics in activated mast cells [Sun and Bamji, 2011; Sulimenko et al., 2015]. DOCK5, a Rac GEF from the DOCK subfamily, regulates the remodeling of the microtubule network that is essential for mast cell degranulation [Ogawa et al., 2014]. GEF-H1, found as a RhoA GEF, is involved in the processes of membrane trafficking in either B cells or epithelial cells [Pathak et al., 2012; Sáez et al., 2019]. However, most roles of RhoGEFs in exocytosis are obscure. We assume that certain RhoGEFs will be important in regulating mast cell activation and degranulation since our previous studies suggest the involvements of Rho proteins [Baier et al., 2012; Sheshachalam et al., 2017].

Here, we investigated the roles of certain RhoGEFs in mast cell granule exocytosis (also known as degranulation). RT-PCR was used to profile RhoGEF levels and selective expression in mast cells. The knockdown of Vav1, P-Rex1, α -PIX, β -PIX by RNA interference (RNAi) did not significantly alter the granule movement and exocytosis. Importantly, the depletion of GEF-H1 significantly disrupted cell spreading, granule movement and exocytosis in stimulated mast cells. RhoA was the main target of GEF-H1, correlating with the suppressed stress fiber formation in GEF-H1-depleted cells. Focal adhesion (FA) formation was found to be involved in granule exocytosis; depletion of GEF-H1 led to the reduced FAs after antigen stimulation. In addition, the GEF-H1 activation was linked to the Fc ϵ RI signaling pathway but was independent of microtubule dynamics; the Syk inhibitor GS-9973 inhibited the GEF-H1 activation along with cell spreading, granule movement in stimulated RBL-2H3 cells. Our data supports the involvement of the GEF-H1-RhoA signaling axis in transducing antigen stimulation signals from Fc ϵ RI to exocytosis in mast cells.

4.2 Profile of RhoGEF expression in mast cells

Previous studies have shown the involvement of Rho protein, such as Rac1 and RhoA, in mast cell exocytosis [Norman et al., 1996; Hong-Geller et al., 2000; Hong-Geller et al., 2001; Baier et al., 2014; Sheshachalam et al., 2017]. To further define the Rho signaling pathway for mast cell exocytosis, we wanted to identify Rho protein upstream activators termed RhoGEFs (Rho guanine exchange factors) that transduce upstream receptor signals to downstream Rho protein activation. Conventional reverse transcription-polymerase chain reaction (RT-PCR) and gel electrophoresis was used to detect the presence and estimate the level of RhoGEF mRNAs in mast cells compared to epithelial control cells. Since mast cell granule exocytosis is a rapid and robust process, theoretically, the critical RhoGEFs should be abundantly expressed possibly in a mast cell-specific manner. Based on this assumption, a shortened PCR cycle (25 cycles) was used to amplify similar sized fragments of RhoGEF mRNAs, allowing a semi-quantitative analysis of their abundance in RBL-2H3 cells, BMMCs (bone marrow-derived mast cells), BM (bone marrow) stromal cells and rat NRK (normal rat kidney epithelial) cells.

Numerous Rac and RhoA specific RhoGEFs were detected in these four cell lines (**Figure 4.1**). Specifically, α -PIX, β -PIX, Tiam1, Trio, GEF-H1, Net1, Ect2, Alsin, and ArhGEF10 were

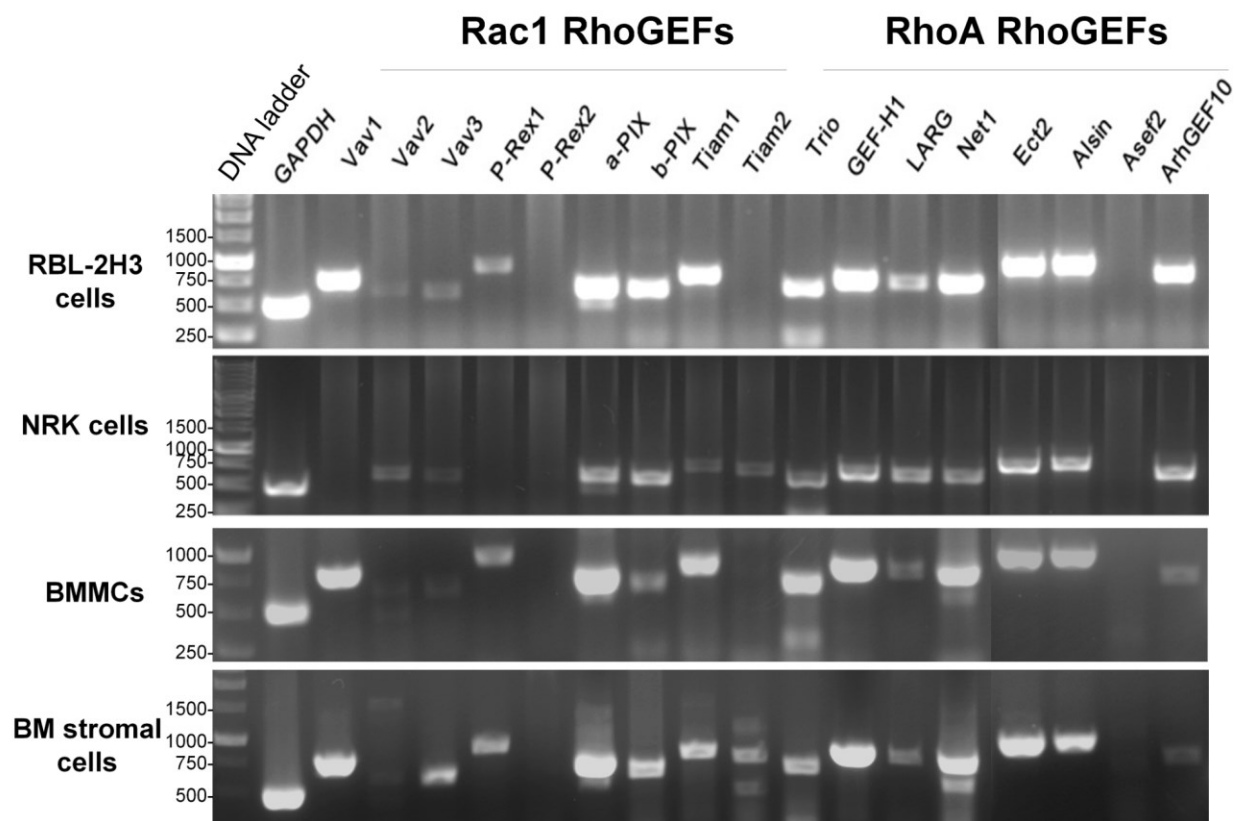


Figure 4.1 RhoGEFs (Rho guanine exchange factors) expressed in RBL-2H3 cells, NRK (normal rat kidney epithelial) cells, BMMCs, and bone marrow (BM) stromal cells. The expression of various RhoGEFs were detected based on RT-PCR assays. α -PIX, β -PIX, Tiam1, Trio, GEF-H1, Net1, Ect2, Alsin, and ArhGEF10 were expressed in all four cell lines, while P-Rex2 and Asef2 expression was absent. By comparison, Vav1 and P-Rex1 were specifically expressed in RBL-2H3 cells, BMMCs and BM stromal cells, while Tiam2 were uniquely expressed in NRK cells but not in RBL-2H3 cells and BMMCs.

abundantly expressed in all cell lines, while P-Rex2 and Asef2 were absent. By comparison, Vav1 and P-Rex1 were specifically expressed in RBL-2H3 cells, BMDCs and BM stromal cells, while Tiam2 were uniquely expressed in NRK cells. Vav1 and P-Rex1, α -PIX, and β -PIX were chosen for further study as they show abundant and selective expression in mast cells. GEF-H1 was also further studied due to its role in microtubule and exocyst association [Pathak and Dermardirossian, 2013; Sáez et al., 2019].

4.3 Knockdown of putative Rac1 RhoGEFs (Vav1, P-Rex1, α -PIX and β -PIX) and the effect on mast cell degranulation

We first analyzed the roles of Vav1, P-Rex1, α -PIX and β -PIX in RBL-2H3 mast cells by creating knockdown cell lines. Lentivirus-mediated shRNAs (short hairpin RNA) were used to silence these RhoGEF mRNAs. ShRNAs specific to Vav1, P-Rex1, α -PIX and β -PIX were cloned in to the commercially-available lentiviral vector, pGFP-C-shLenti (OriGene), with green fluorescence protein (GFP) and puromycin resistant for selection. Lentiviral particles were used to transduce RBL-2H3 cells and GFP/puromycin selection was used for the generation of stably knocked-down (KD) cell lines. qPCR (quantitative reverse transcription-polymerase chain reaction) assays were for the verification of knockdown of these four RhoGEFs. The relative mRNA expressions of Vav1, P-Rex1, α -PIX and β -PIX in stable KD strains of Vav1, P-Rex1, α -PIX and β -PIX, were only at 26.0%, 7.9%, 12.3% and 18.9% of that of scrambled shRNA control cell lines, respectively (**Figure 4.2**). These results verified the successful preparation of stable KD strains of Vav1, P-Rex1, α -PIX and β -PIX.

In order to examine the effects of Vav1, P-Rex1, α -PIX and β -PIX depletion on mast cell granule exocytosis, degranulation assays were performed in both resting and different time points after antigen-stimulation. In the resting state, degranulation of scrambled shRNA strains and four RhoGEF knockdown strains showed no significant differences, suggesting the knockdown (KD) of Vav1, P-Rex1, α -PIX or β -PIX individually does not alter the baseline of degranulation level in mast cells (**Figure 4.3**, *dashed line*). Cells were then antigen-stimulated for 10 min, 15 min, and 30 min, and assayed for degranulation. In non-infected wild-type RBL-2H3 cells, degranulation levels were at $37.4 \pm 12.8\%$, $46.0 \pm 4.7\%$ and $57.1 \pm 10.7\%$ of total, respectively. In the control scrambled shRNA infected cells and the KD strains, levels of degranulation showed

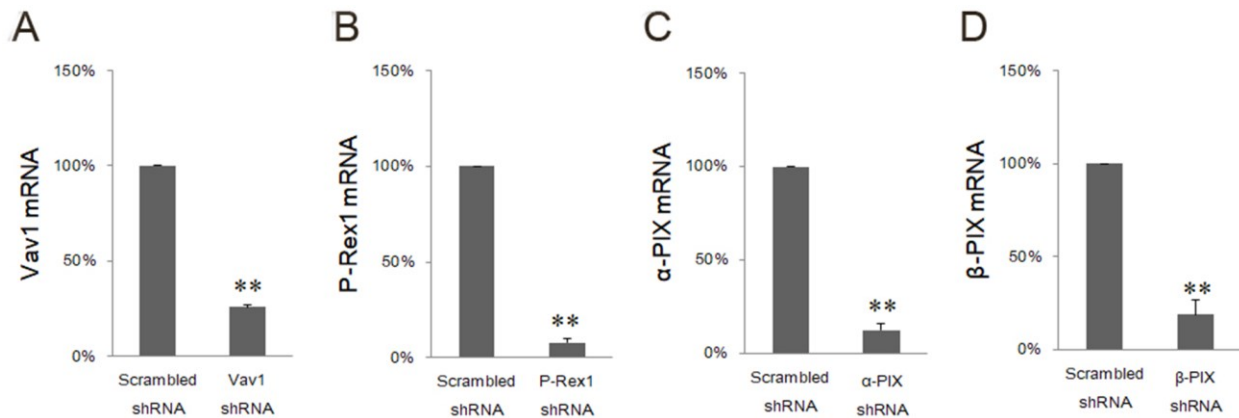


Figure 4.2 Depletion of Vav1, P-Rex1, α -PIX and β -PIX by lentivirus-mediated shRNA knockdown (KD) in RBL-2H3 cells. qPCR assays were used to determine the relative mRNA levels of Vav1 (A), P-Rex1 (B), α -PIX (C) and β -PIX (D) after knockdown with specific shRNA obtained from OriGene. KD strains of Vav1, P-Rex1, α -PIX and β -PIX showed depletion of 74.0%, 92.1%, 87.7% and 81.1%, respectively, compared to scrambled shRNA control groups. All showed significant depletion by unpaired Student's *t*-test (** $p < 0.01$; $n = 3$). *Judeah Negre provided data for panels A - D.*

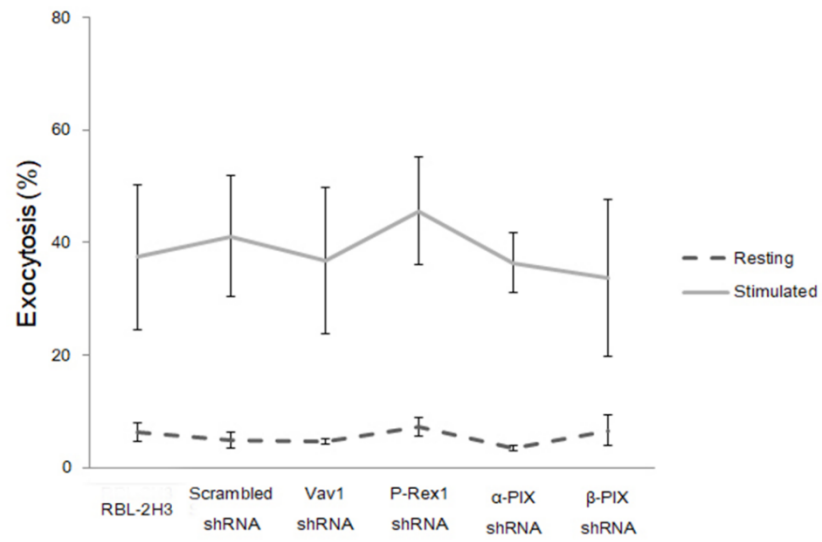
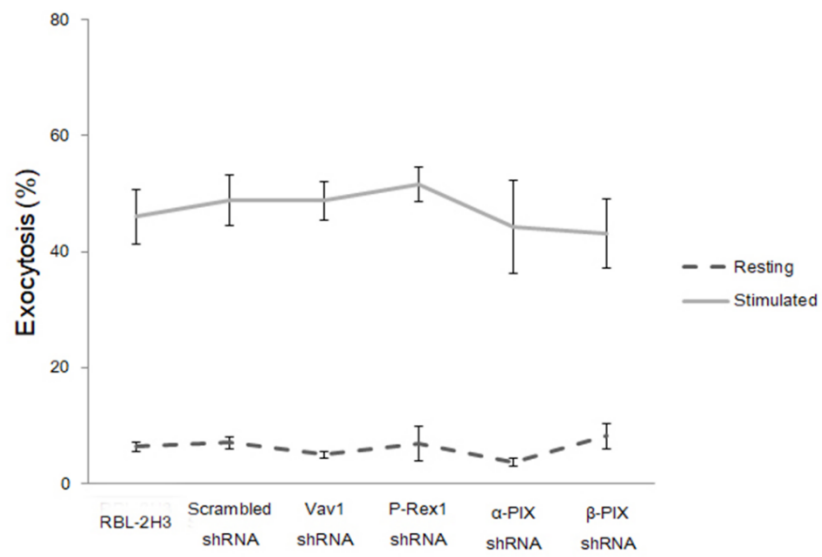
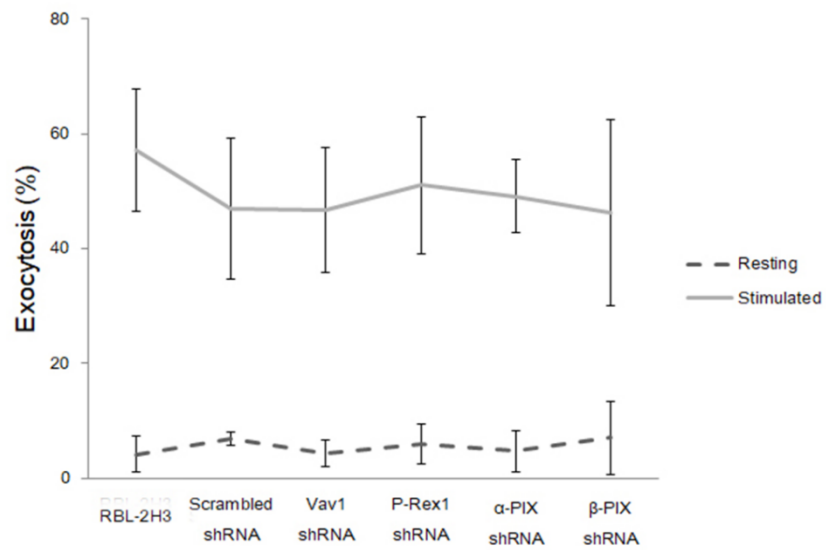
A**B****C**

Figure 4.3 The effects of knockdown of Vav1, P-Rex1, α -PIX and β -PIX on mast cell exocytosis. Exocytosis was examined in RBL-2H3 cells with knockdown of Vav1, P-Rex1, α -PIX and β -PIX expression, together with control groups (non-transfected RBL-2H3 cells and scrambled shRNA). Degranulation assays were used to measure levels of exocytosis in either resting or antigen-stimulated cells that were stimulated for 10 min (A), 15 min (B) and 30 min (C). No statistically significant differences (by ANOVA) were observed between different groups at either resting or stimulated conditions (n = 3). *Judeah Negre provided data for panels A - C.*

no statistically significant differences from wild-type RBL-2H3 cells (**Figure 4.3**, *solid line*). This suggests that KD of Vav1, P-Rex1, α -PIX or β -PIX individually are not required for RBL-2H3 mast cells granule exocytosis when antigen-stimulated.

4.4 Roles of Vav1, P-Rex1, α -PIX and β -PIX in granule trafficking during RBL-2H3 cell activation

Since the activation of Rac1 was found during mast cells of antigen-stimulation [Sheshachalam et al., 2017], Rac1 activation assays were performed in KD strains. RBL-2H3 cells of various RhoGEF KD strains were antigen-stimulated for 10 min then the GST-PAK1-Rho binding domain (RBD) probe was used to precipitate the active Rac1. In the Vav1, P-Rex1 or α -PIX KD strains, levels of Rac1-GTP were reduced as shown by western blot of pulldown fractions (**Figure 4.4A**). Densitometric analysis of multiple blots (**Figure 4.4B**) confirmed that, compared to the scrambled shRNA strain, levels of Rac1-GTP in Vav1, P-Rex1 or α -PIX KD strains were reduced by $40.7 \pm 15.8\%$, $49.6 \pm 21.6\%$ or $52.8 \pm 24.1\%$, respectively. The β -PIX KD strain did not show a statistically difference in Rac1-GTP level. Single depletion of Vav1, P-Rex1, α -PIX or β -PIX did not completely abolish the activation of Rac1 dependent pathways in antigen-activated RBL-2H3 mast cells. Interestingly, there seems to be adequate remaining levels of activated Rac1 in all KD strains to support exocytosis (**Figure 4.3**), suggesting that other RhoGEFs may compensate for a single KD.

We next used live-cell imaging to examine the roles of Vav1, P-Rex1, α -PIX and β -PIX in granule trafficking. Granules were labelled in living RBL-2H3 cells with LysoTracker red and cells were imaged using a spinning-disk confocal microscope during antigen-stimulation. **Figure 4.5** shows still images taken from **Videos 4.1, 4.2, 4.3, 4.4, and 4.5** just prior to antigen-stimulation (0 min) and up to 20 min after stimulation. Control cells (scrambled shRNA) underwent cell spreading and granules were dispersed toward the cell periphery then fused with the plasma membrane. In the individual KD strains, there were no observable differences in cell spreading and granule trafficking. Granule velocities among the different strains were measured without any statistical differences (data not shown). Altogether, single KD of Vav1, P-Rex1, α -PIX or β -PIX in antigen-stimulated RBL-2H3 cells did not prominently alter the granule trafficking, which was consistent with their roles in regulating RBL-2H3 cell degranulation.

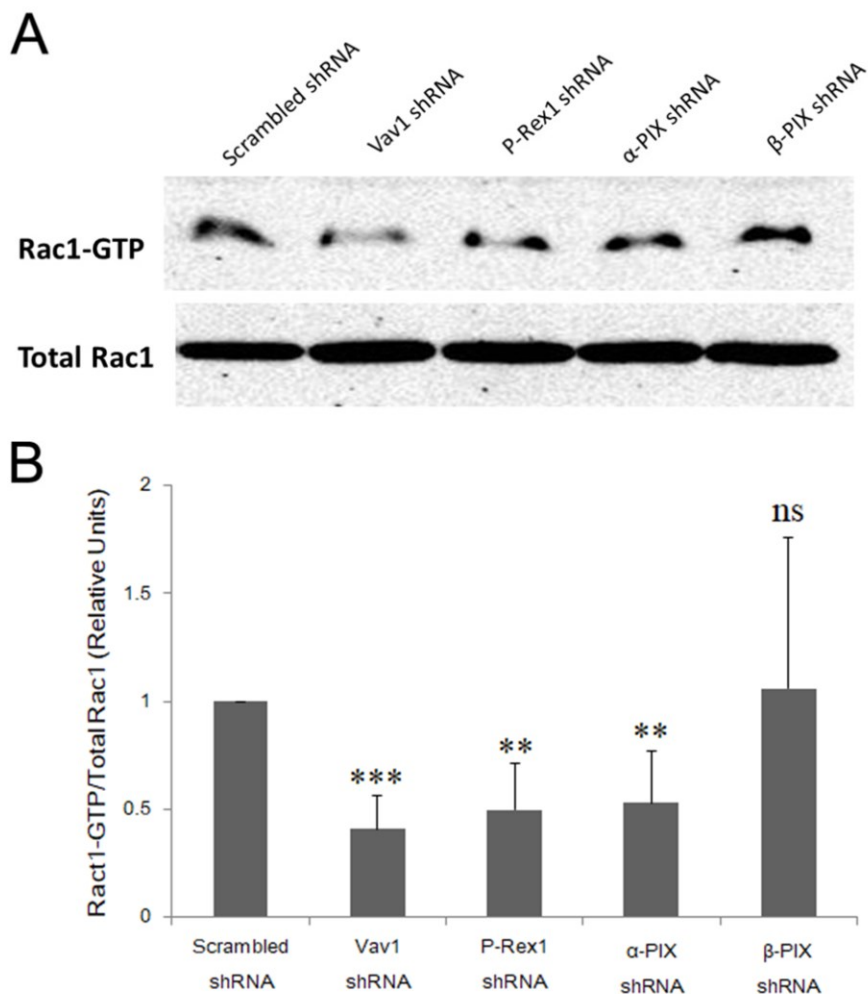


Figure 4.4 Rac1 activation in antigen-stimulated RBL-2H3 cells after the depletion of Vav1, P-Rex1, α -PIX and β -PIX. RBL-2H3 cells were antigen-stimulated for 10 min, lysed and levels of Rac1-GTP were measured by GST-PAK1 RBD pulldown assays (A, western blot) and quantification of band intensity (B). Knockdown of Vav1, P-Rex1 and α -PIX caused significant suppression of Rac1 activation in stimulated RBL-2H3 cells. However, depletion of β -PIX did not show measurable change of Rac1-GTP level. (** $p < 0.01$; *** $p < 0.001$; ns, not significant; compared with Scrambled shRNA; $n = 3$).

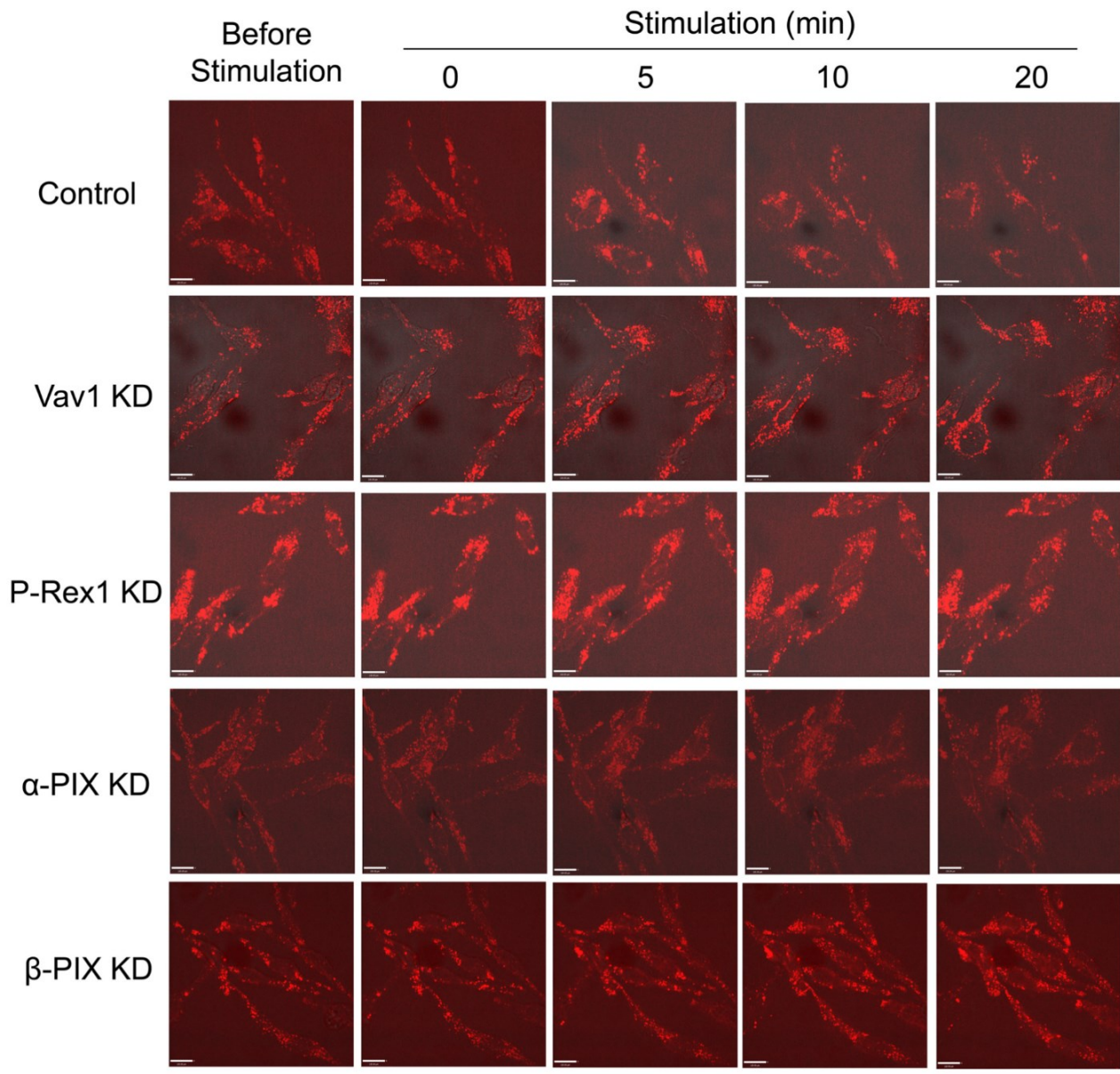


Figure 4.5 Effect of knockdown of Vav1, P-Rex1, α -PIX and β -PIX in granule trafficking in antigen-stimulated RBL-2H3 cells. Granules were stained with LysoTracker Red and live-cell imaged with a spinning-disk confocal microscopy. Shown are representative images from [Video 4.1](#) of control cells (scrambled shRNA), [Video 4.2](#) of Vav1 KD (knockdown) cells, [Video 4.3](#) of P-Rex1 KD cells, [Video 4.4](#) of α -PIX KD cells, and [Video 4.5](#) of β -PIX KD cells after antigen stimulation. No differences in granule distribution or trafficking were observed between various RhoGEFs KD cells and the control cells. Scale bar = 10 μ m.

Supplemental videos showing live-cell imaging of LysoTracker Red are available at the following URLs:

Video 4.1 LysoTracker Red live-cell imaging in stimulated cells of Scrambled shRNA (control)

https://drive.google.com/file/d/1jRYcVwVEh9nD_YgeoJJ7Kco3ICTFaPzF/view?usp=sharing

Video 4.2 LysoTracker Red live-cell imaging in stimulated RBL-2H3 cells of Vav1 knockdown

<https://drive.google.com/file/d/11ZqF9tRvNAXQfPXwb7DF33i8WH6-2goZ/view?usp=sharing>

Video 4.3 LysoTracker Red live-cell imaging in stimulated RBL-2H3 cells of P-Rex1 knockdown

https://drive.google.com/file/d/1ymsqkcA-EWLq6cxnLZ0u_bzQLXjnua0B/view?usp=sharing

Video 4.4 LysoTracker Red live-cell imaging in stimulated RBL-2H3 cells of α -PIX knockdown

<https://drive.google.com/file/d/1Q3AWRQiFoqE0EWWVHW5JbLw4za0oqcf4j/view?usp=sharing>

Video 4.5 LysoTracker Red live-cell imaging in stimulated RBL-2H3 cells of β -PIX knockdown

<https://drive.google.com/file/d/1RWXCHaoDE3ABTgkQezTwZMYow0JHZJHa/view?usp=sharing>

4.5 Double knockdown of Vav1 and P-Rex1 and the effect on mast cell degranulation

Since single Vav1 or P-Rex1 knockdown (KD) strains showed no degranulation defects, we generated a Vav1 and P-Rex1 double knockdown strain, termed V1P1_2KD. Using lentivirus-mediated shRNA knockdown, both Vav1 and P-Rex1 mRNA levels were depleted as confirmed by qPCR (**Figure 4.6A**). Compared to the scrambled shRNA strain, the relative mRNA levels of Vav1 and P-Rex1 were $39.0\pm 3.3\%$ and $28.0\pm 4.2\%$ in V1P1_2KD, respectively. Degranulation assays showed that the V1P1_2KD strain had no significant reduction in granule exocytosis compared to wild-type or scrambled shRNA strains (**Figure 4.6B**). This suggests that Vav1 or P-Rex1 do not significantly regulate in antigen-stimulated granule exocytosis RBL-2H3 cells.

4.6 Establishment of a role for GEF-H1 (ARHGEF2) in mast cell degranulation; depletion of GEF-H1 affects mast cell degranulation

In **Chapter 3**, the role of microtubules in mast cell granule trafficking and exocytosis were examined in detail. GEF-H1 was previously reported as a microtubule-bound RhoGEF [Krendel et al., 2002; Birkenfeld et al., 2008], that may link microtubule remodeling to the activation of Rho proteins such as RhoA and Rac1 [Ren et al., 1998; Krendel et al., 2002; Tonami et al., 2011]. Here, we hypothesize that GEF-H1 may be a putative RhoGEF involved in regulating mast granule exocytosis because of its association with the plasma membrane exocytosis machinery called the exocyst [Pathak et al., 2012; Sáez et al., 2019]. GEF-H1, also known as ARHGEF2, is a multi-domain protein including a tandem the DH (Dbl-homology) and PH (Pleckstrin homology) domain, an N-terminal C1 domain which suggests it can be regulated by diacylglycerol, and two coiled domains. GEF-H1/ARHGEF2 is highly conserved with human and mouse proteins showing high homology to the rat protein. Alignment of GEF-H1 amino acid sequences between human and mouse with rat showed 89% and 98% sequence identity, respectively, with the mouse and rat having a 27 amino acid N-terminal extension not present in the human sequence.

Therefore, we generated a stable RBL-2H3 cell line depleted of GEF-H1 using lentivirus-mediated shRNA knockdown (KD). The lentivirus-transduced cells were 100% GFP labelled indicating efficient infection. qPCR and western blot were used to verify downregulation of GEF-H1 mRNA ($19.9\pm 7.3\%$ compared to the empty vector control (*FUGW*)) and protein levels,

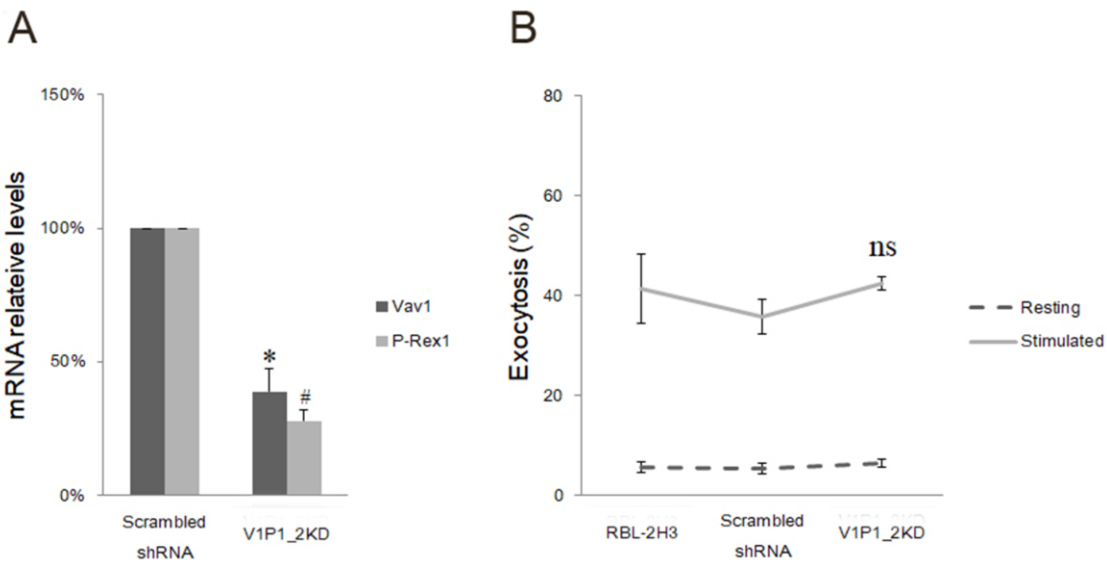


Figure 4.6 Effect of double knockdown of Vav1 and P-Rex1 on mast cell exocytosis. (A) Depletion of both Vav1 and P-Rex1 (V1P1_2KD) mRNA levels in RBL-2H3 cells by lentivirus-mediated shRNA interference was determined by qPCR. Vav1 and P-Rex1 mRNA levels were significantly reduced compared to scrambled shRNA controls as determined by unpaired Student's t-test ($*p < 0.05$, $n = 3$). (B) No significant difference in exocytosis between V1P1_2KD and control groups was observed ($n = 3$). *Judeah Negre provided data for panels A and B.*

respectively (**Figure 4.7**). The effect of GEF-H1 KD on mast cell granule exocytosis was examined by degranulation assay. In the resting state (unstimulated), background levels of exocytosis were similar in all cell lines (**Figure 4.8, dashed line**). However, granule exocytosis was significantly reduced in GEF-H1-depleted cells when antigen-stimulated for either 15 min or 30 min compared to wild-type RBL-2H3 cells (**Figure 4.8, solid line**). Control cells (empty vector FUGW-transduced) showed no significant difference. These results revealed that the knockdown of GEF-H1 triggered a significant reduction in mast cell degranulation, suggesting the important regulatory roles for GEF-H1 in this process.

4.7 Knockdown of GEF-H1 resulted in dysregulated cell activation/spreading and granule trafficking

The activation of RBL-2H3 cells by antigen-stimulation leads to cell spreading [Frigeri and Apgar, 1999; Sheshachalam et al., 2017], which was an indicator of cytoskeletal remodeling and cell activation. As well, the intracellular distribution of secretory granules labeled by a lysosome marker, such as 5G10 antibodies [Smith et al., 2003] shows granule distribution in the cytoplasm toward the cell periphery. Immunofluorescence and live-cell microscopy was used to determine the cellular effects of GEF-H1 depletion on RBL-2H3 cells, such as a putative role in granule trafficking and cell morphology.

Cells transduced with the empty vector (*FUGW*) underwent normal spreading and granules were widely dispersed in the cytoplasm when antigen stimulated (**Figure 4.9A**). However, in GEF-H1-depleted RBL-2H3 cells, antigen-stimulation did not result in cell spreading, though granules remained widely dispersed in the cytoplasm (**Figure 4.9A**). Closer examination revealed that granules seemed to be retained adjacent to the plasma membrane in higher abundance in GEF-H1-depleted cells (**Figure 4.9A, right panel**), which is consistent with the observed reduction in degranulation (**Figure 4.8**). Cell size was quantified by ImageJ software [Schneider et al., 2012]. There was no difference in cell size prior to stimulation, however, GEF-H1-depleted cells showed a significant reduction size after antigen-stimulation (**Figure 4.9B**). This supports the notion that the regulatory roles of GEF-H1 in cell morphology may coordinately regulate granule exocytosis.

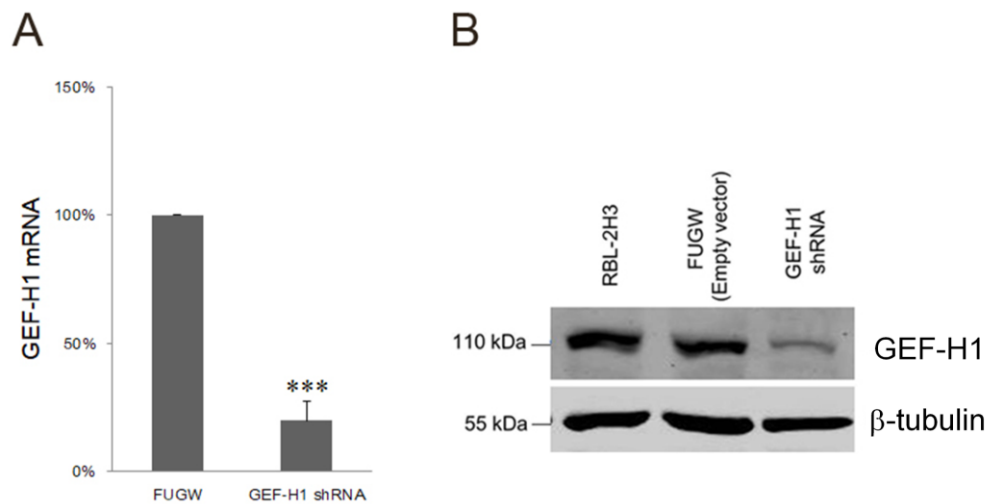


Figure 4.7 Knockdown of GEF-H1 in RBL-2H3 cells by lentivirus-mediated shRNA interference. (A) Levels of GEF-H1 mRNA depletion compared to empty vector control (FUGW) was determined by qPCR assays. An 80.1% reduction in GEF-H1 was achieved ($***p < 0.001$, $n = 3$). (B) Western blot was used to confirm the knockdown effect of GEF-H1 protein (one representative image shown).

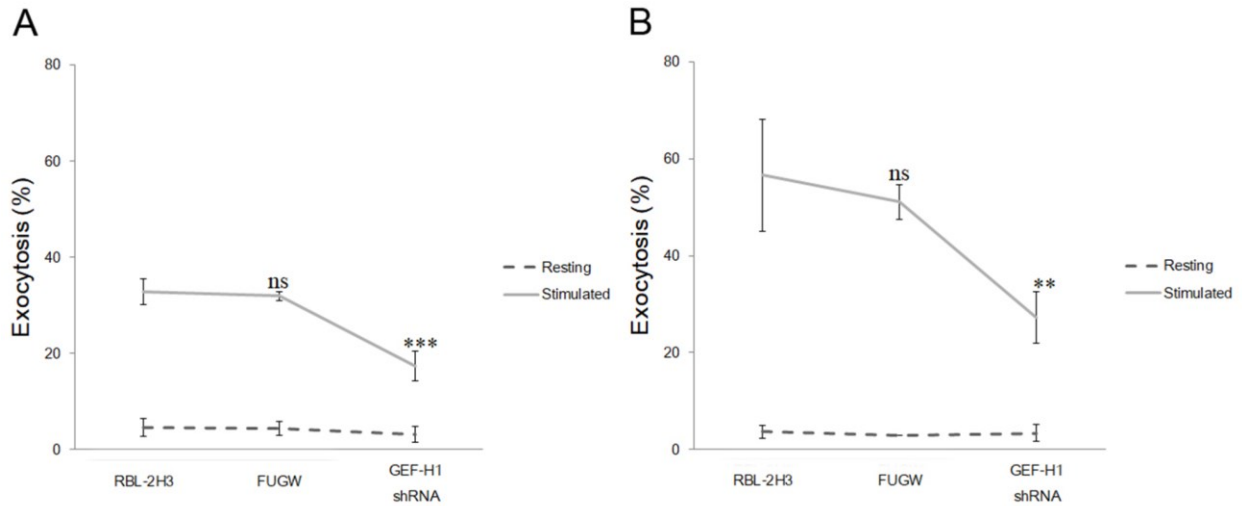


Figure 4.8 Depletion of GEF-H1 reduces antigen-stimulated exocytosis in RBL-2H3 mast cells. Degranulation assays were used to determine the effect of GEF-H1 depletion on mast cell exocytosis compared to wild-type (RBL-2H3) and empty vector control (FUGW) groups after antigen stimulation of 15 min (A) or 30 min (B). There were no differences of degranulation in resting states among these groups. In antigen-stimulated states, GEF-H1 depletion led to significant reduction in exocytosis at both 15 min and 30 min of antigen stimulation (** $p < 0.01$, *** $p < 0.001$, $n = 3$).

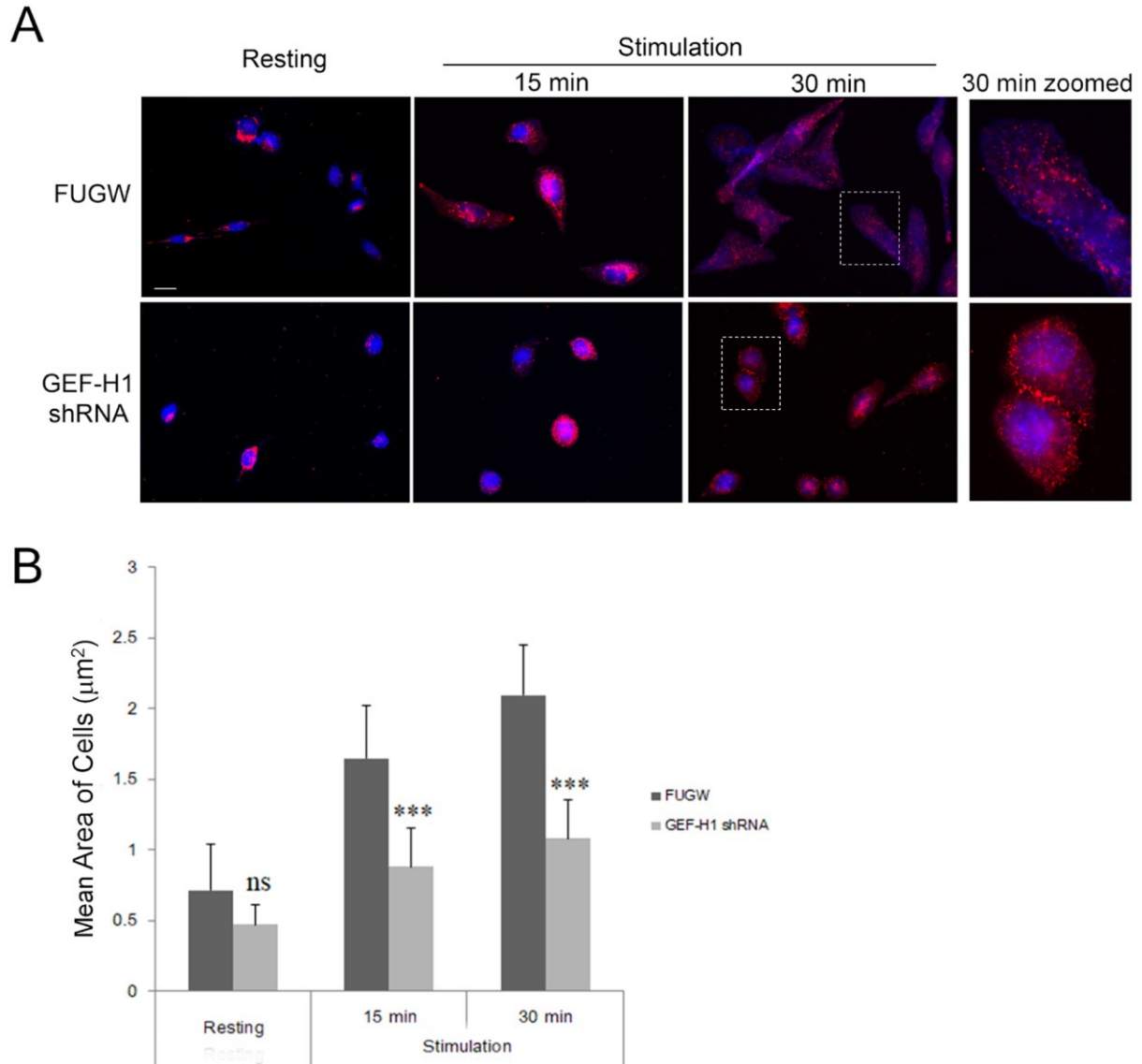


Figure 4.9 Depletion of GEF-H1 causes cell morphology defects. RBL-2H3 cells (FUGW control and GEF-H1-depleted/shRNA) were unstimulated (Resting) or antigen-stimulated (Stimulated) for 15 min or 30 min. (A) Fixed cells were incubated with 5G10 antibody, which labels granules [Smith et al., 2003], and Alexa Fluor 405-phalloidin, which labels F-actin. (B) Quantification of cell size by ImageJ indicates that the depletion of GEF-H1 significantly reduces the cell spreading after antigen stimulation ($***p < 0.001$, ns, not significant, $n \geq 16$). Scale bar = 20 μm .

Next, live-cell imaging was used to examine the role of GEF-H1 in granule trafficking. Granules in both GEF-H1-depleted and empty vector control cells were labeled with LysoTracker Red. Cells were antigen-stimulated during imaging and the granule distribution observed and their velocities were measured using Volocity v6.3 software. The depletion of GEF-H1 in RBL-2H3 cells markedly reduces the dispersing of granules after antigen stimulation (shown in black arrow). Granules accumulated adjacent to the plasma membrane ([Video 4.7](#)). In contrast, granules in control cells rapidly disperse after antigen stimulation and do not accumulate at the plasma membrane ([Video 4.6](#)). **Figure 4.10A** shows still images from [Video 4.6](#) and [Video 4.7](#). Furthermore, velocity analysis revealed significant differences of the granule tracking speeds between these two groups (**Figure 4.10B**). Depletion of GEF-H1 resulted in the significant reduction of tracking speeds of granules ($0.578 \pm 0.434 \mu\text{m/s}$ compared to $0.827 \pm 0.694 \mu\text{m/s}$ in control cells). Thus, the reduced trafficking of secretory granules in GEF-H1-depleted cells coordinated with their reduction of degranulation outcomes illustrated previously.

To confirm the loss of cell spreading and granule trafficking was attributed to the depletion of GEF-H1, we examined whether reintroduction of an RNAi resistant GEF-H1 construct into GEF-H1-depleted cells would rescue these defects. For this we constructed mCherry-GEF-H1-RNAi-Resi (GEF-H1-Resi) which was transfected into both the empty vector control (FUGW) and GEF-H1-depleted cells. mCherry-C1 vector was used as a control. In antigen-stimulated GEF-H1-depleted cells, expression of GEF-H1-Resi restored the defects of both granule distribution and cell spreading while expression of mCherry-C1 alone did not show any rescue effect (**Figure 4.11A**). In empty vector control cells (FUGW), expression of GEF-H1-Resi did not alter cell morphology or granule distribution. Cell size was quantified by ImageJ software which confirmed that, upon antigen-stimulation, depletion of GEF-H1 prevents cell spreading (mCherry-C1 transfected), while expression of GEF-H1-Resi recovers cell spreading (GEF-H1-Resi transfected) (**Figure 4.11B**). Altogether, the restoration of GEF-H1 in GEF-H1-depleted cells confirmed the regulatory roles of GEF-H1 in regulating cell morphology (spreading) and granule trafficking in RBL-2H3 cells when antigen stimulation.

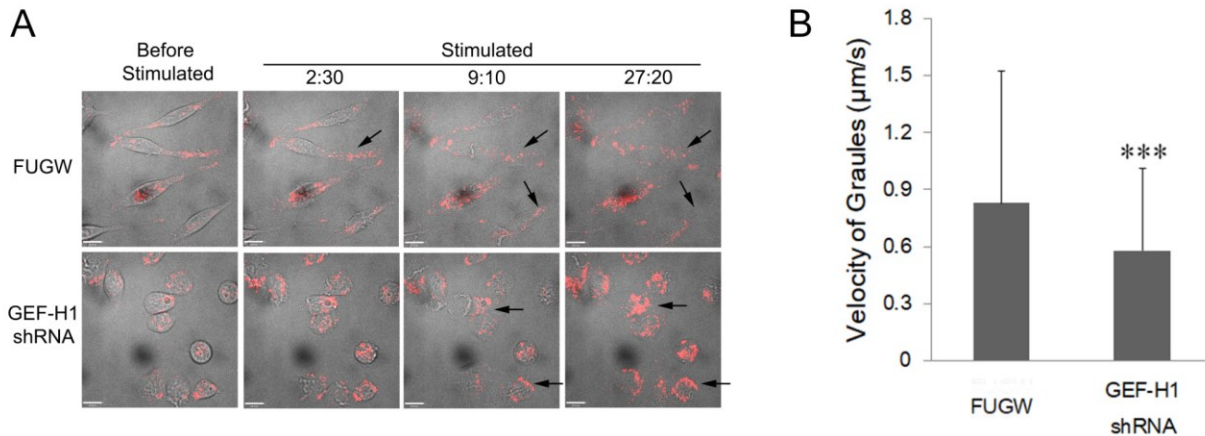


Figure 4.10 Depletion of GEF-H1 affects granule mobility. Granule mobility was examined by labelling granules with LysoTracker Red and imaging live RBL-2H3 cells during antigen stimulation. (A) Representative still images of time points before and after antigen stimulation from [Video 4.6](#) of control cells (*FUGW*) and [Video 4.7](#) of GEF-H1-depleted cells. Compared to the control group, knockdown of GEF-H1 slowed the dispersion of granules and caused their retention adjacent to plasma membrane (*arrows*). (B) Granule velocity was measured using Velocity v6.3 software. Depletion of GEF-H1 significantly reduced the granule speed ($***p < 0.001$, $n \geq 73$). Scale bar = 10 μm .

Supplemental videos showing live-cell imaging of LysoTracker Red are available at the following URLs:

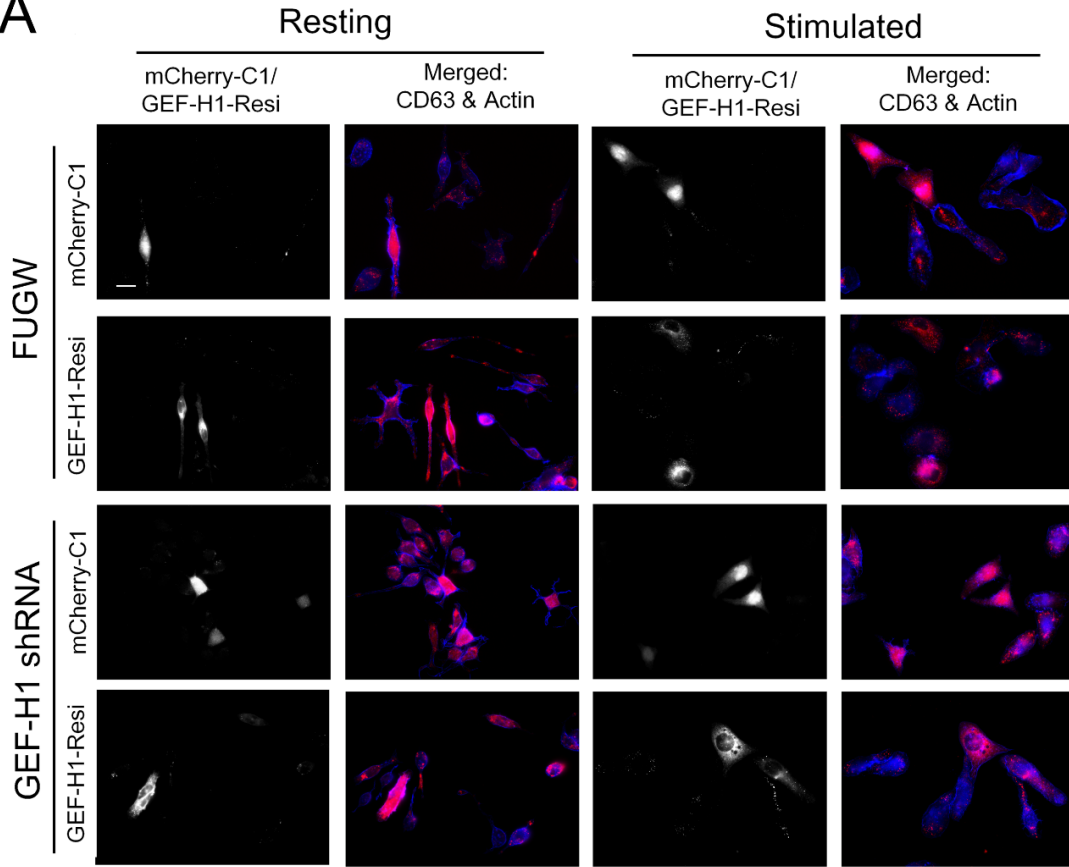
Video 4.6 LysoTracker Red live-cell imaging in stimulated cells of FUGW

<https://drive.google.com/file/d/1mNPBrIyxNKtJMkUtIAnBDJPt5qN1WLYW/view?usp=sharing>

Video 4.7 LysoTracker Red live-cell imaging in stimulated cells of GEF-H1 knockdown

<https://drive.google.com/file/d/1Aa8FIrBJJ-AMVpWXga-BO2ecqlad0JqA/view?usp=sharing>

A



B

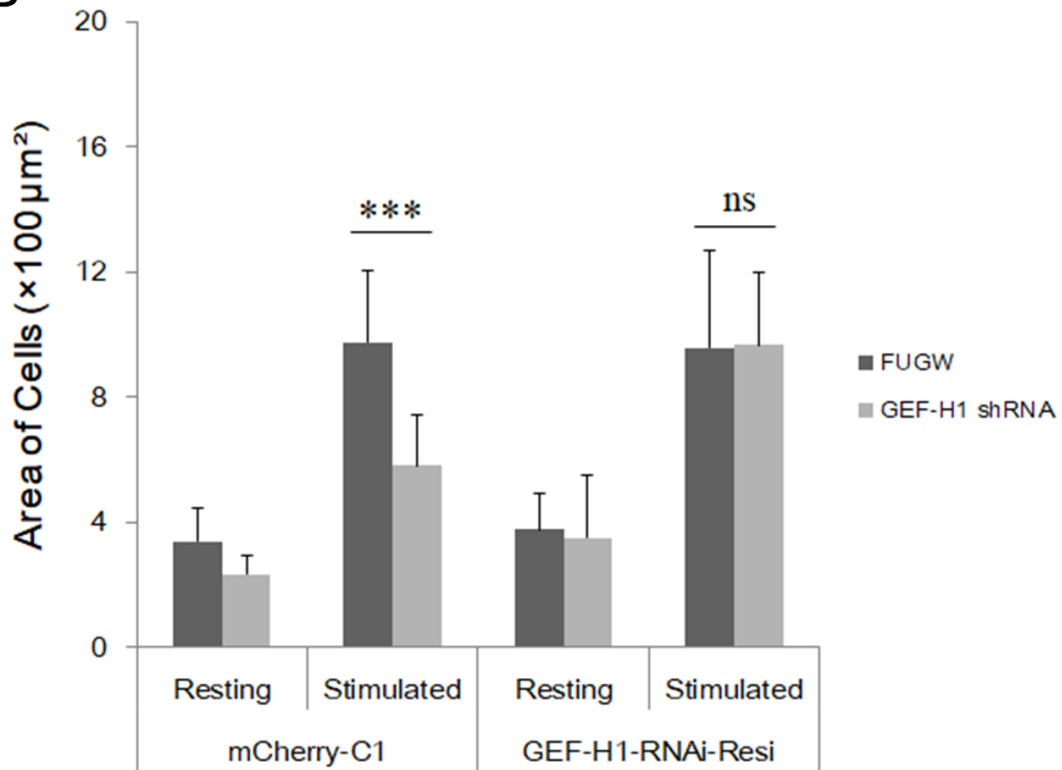


Figure 4.11 Introduction of a GEF-H1 RNAi-resistant construct restores granule distribution and cell spreading in antigen-stimulated GEF-H1-depleted RBL-2H3 cells. The GEF-H1 RNAi resistant construct, mCherry-GEF-H1-Resi, was introduced into both the empty vector control (FUGW) and GEF-H1-depleted (GEF-H1 shRNA) cells by electroporation. mCherry-C1 vector was used as a control. (A) Imaging of granules, labeled with anti-CD63 antibody, and F-actin, labeled with Alexa Fluor 405-phalloidin. In antigen-stimulated GEF-H1-depleted cells, expression of GEF-H1-Resi restored the defects of both granule distribution and cell spreading, compared to the mCherry-C1-transfected group. Scale bar = 20 μm . (B) Quantification of cell size using ImageJ software. When stimulated, knockdown of GEF-H1 prevents cell spreading while expression of GEF-H1-Resi recovers cell spreading ($***p < 0.001$; ns, not significant; $n \geq 16$).

4.8 RhoA, but not Rac1, is a downstream target of GEF-H1

GEF-H1 has previously been reported to be a RhoGEF of RhoA and Rac1 [Ren et al., 1998; Krendel et al., 2002; Tonami et al., 2011], but downstream Rho protein targets in mast cells have not been described. We used a pulldown assay with GST-tagged Rhotekin and PAK1 Rho-Binding-Domains as probes to determine the levels of RhoA and Rac1, respectively. In control cells, antigen-stimulation increases levels of RhoA-GTP and Rac1-GTP (**Figure 4.12 A and B** respectively, *Control, R vs Control, S*). However, in GEF-H1-depleted cells, antigen-stimulation resulted in no increase in Rho-GTP levels while Rac1-GTP levels increased comparably to control (**Figure 4.12 A and B** respectively, *GEF-H1 shRNA, S vs Control, S*). These results suggest that RhoA is the downstream target of GEF-H1 since knockdown of GEF-H1 prevented the activation of RhoA, but not Rac1, after antigen-stimulation.

RhoA is a master regulator of stress fiber formation in various cells [Ridley and Hall, 1992; Hall, 1998], which means the formation of stress fiber could be considered as an indicator of RhoA activity. To further examine RhoA function in antigen-stimulated RBL-2H3 cells, the stress fiber formation was visualized by Alexa Fluor 405-phalloidin staining. No stress fibers were observed in the control and GEF-H1-depleted cells when resting (**Figure 4.13 A and C** respectively). When antigen-stimulated, control cells formed prominent stress fibers across the cell to the cell periphery (**Figure 4.13B**, *red arrows*) while GEF-H1-depleted cells lacked stress fiber formations (**Figure 4.13D**). This result supports the notion that the formation of stress fibers helps project the leading edge of cells for cell spreading. Taken together, the knockdown of GEF-H1 in RBL-2H3 cell resulted in the loss of RhoA activation after antigen stimulation, leading to loss of stress fiber formation and cell spreading.

Rac1 activation triggers lamellipodia formation and cell ruffling [Ridley et al., 1992; Hall, 1998]. To rule out Rac1 as a possible downstream target of GEF-H1, live-cell imaging was used to visualize the dynamic formation of lamellipodia that occurs during RBL-2H3 stimulation [Sheshachalam et al., 2017]. Live-cell imaging via differential interference contrast (DIC) microscopy showed membrane ruffling occurred in both the control cells ([Video 4.8](#), **Figure 4.14**, *top panels*) and similarly in GEF-H1-depleted cells ([Video 4.9](#), **Figure 4.14**, *bottom panels*). Furthermore, actin remodeling in both control and GEF-H1-depleted groups were

imaged in live cells using Lifeact-mRuby. This showed that antigen-stimulation triggered the formation of lamellipodia at the leading edge of control cells ([Video 4.10](#), **Figure 4.15**, *top panels*) and similarly in GEF-H1-depleted cells ([Video 4.11](#), **Figure 4.15**, *bottom panels*). This suggests that Rac1 underwent activation in the absence of GEF-H1. These observations are in agreement with the results of the Rac1 activation assay shown in Figure 4.13B. Taken together, Rac1 was not a major downstream Rho protein regulated by GEF-H1 in RBL-2H3 cells during antigen-stimulation.

To further examine if the effects of GEF-H1 depletion were due to lack of RhoA activation, we transfected cells with a constitutively active RhoA mutant, RhoA-G14V, to see if defects could be rescued. Control and GEF-H1-depleted cells were transfected with a 3×HA-tagged version of RhoA-G14V expressed from a CMV promoter, or empty vector (pcDNA3.1). Cells were either left resting or stimulated for 30 min, then fixed and stained with anti-HA to mark transfected cells, anti-CD63 to mark granules and Alexa Fluor 405-phalloidin to show cell morphology. In control cells (FUGW), transfection with either pcDNA3.1 or RhoA-G14V resulted in granules that were well dispersed and cells that spread after antigen stimulation (**Figure 4.16A**, *upper two rows of images*). In GEF-H1-depleted cells, transfection with empty vector did not rescue these defects, while introduction of RhoA-G14V restored cell spreading after antigen stimulation (**Figure 4.16A**, *bottom two rows of images*). Cell area was quantified by ImageJ software. Control cells were significantly larger than GEF-H1-depleted cells when transfected with empty vector; the ability to spread and increase in size in GEF-H1 was restored to normal levels by transfection with RhoA-G14V (**Figure 4.16B**). RhoA-G14V by itself is likely to mimic and restore the effects of antigen stimulation in GEF-H1-depleted cells. In conclusion, these results support the notion that RhoA is the downstream target of GEF-H1 for activation during antigen-stimulation of RBL-2H3 cells.

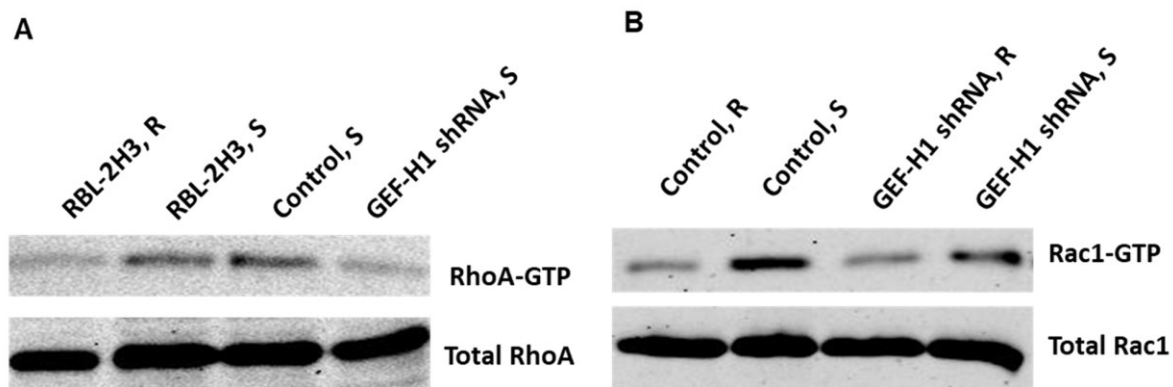


Figure 4.12 RhoA, but not Rac1, is a downstream effector of GEF-H1 in antigen-stimulated RBL-2H3 cells. We previously have revealed Rac1 and RhoA were activated in antigen-stimulated RBL-2H3 cells of 10min and 20 min, respectively [Sheshachalam et al., 2017]. Detection of activated RhoA (A) and Rac1 (B) was performed by pulldown assays using Rhotekin or PAK1 probes that bind RhoA-GTP and Rac1-GTP, respectively. Active levels of both RhoA and Rac1 were increased in either stimulated wild-type RBL-2H3 (*RBL-2H3, S*) or stimulated control cells (*Control, S*). The Depletion of GEF-H1 reduced the activation of RhoA (A, *GEF-H1 shRNA, S*) but did not affect Rac1-GTP levels (B, *GEF-H1 shRNA, S*). Control, RBL-2H3 cells transfected by an empty lentiviral vector FUGW; GEF-H1 shRNA, GEF-H1-depleted cells; R, resting; S, antigen-stimulated for 20 min in panel A and for 10 min in panel B.

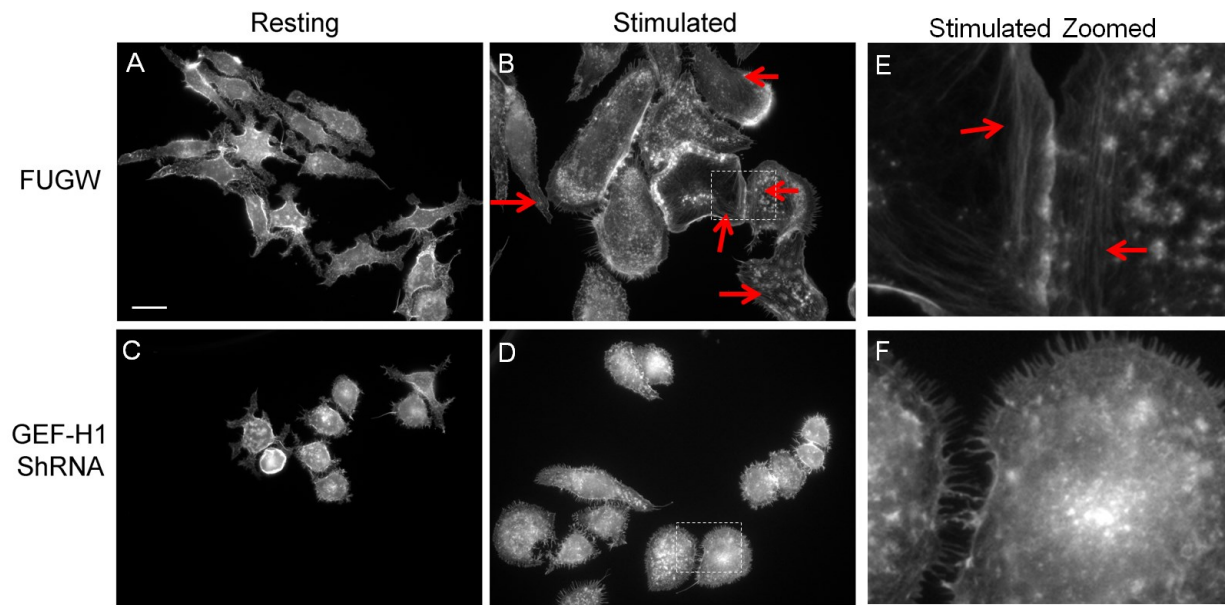


Figure 4.13 Depletion of GEF-H1 affects stress fiber formation in antigen-stimulated RBL-2H3 cells. Alexa Fluor 405-phalloidin was used to label F-actin in resting cells (*left panels*) and antigen-stimulated cells (*middle panels*). (A and B) Control RBL-2H3 cells (*FUGW*), when stimulated, showed the formation of stress fibers in the cytoplasm that project to the plasma membrane (B, *red arrow*). (C and D) GEF-H1 depleted RBL-2H3 cells lacked stress fiber formation and showed reduced cell spreading. E and F (*right panels*) were images of stimulated zoomed. Scale bar = 20 μm .

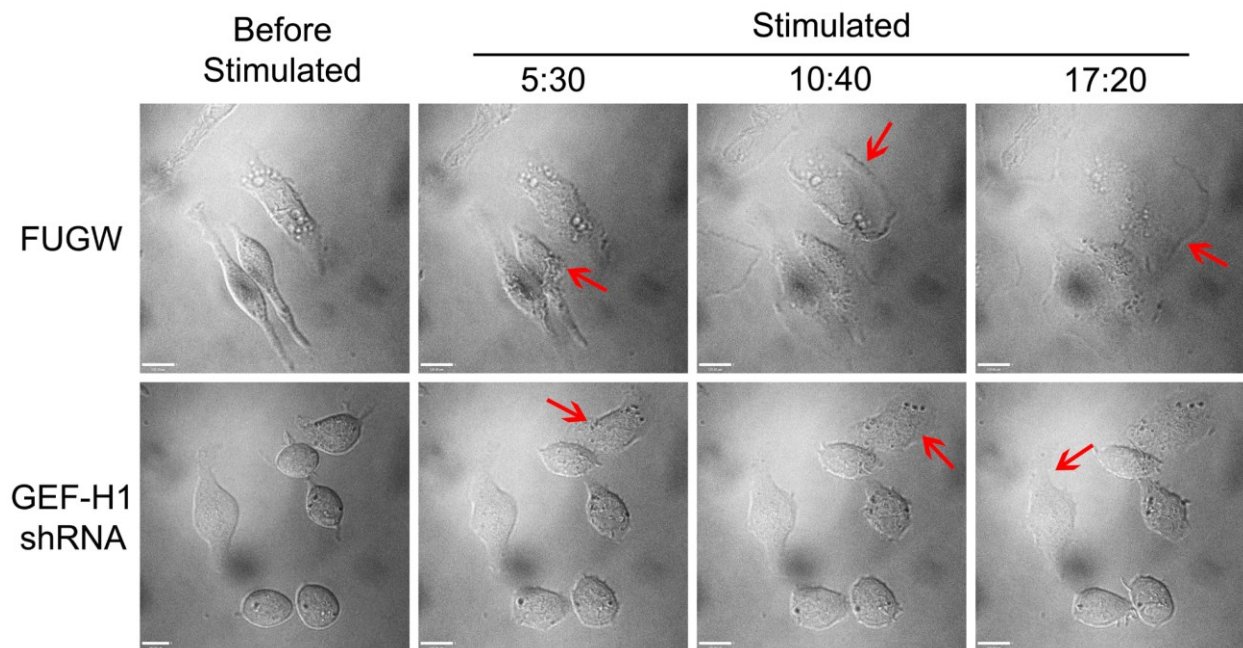


Figure 4.14 Depletion of GEF-H1 does not block membrane ruffling and lamellipodia formation. Membrane ruffling and lamellipodia formation was visualized in live cells during antigen stimulation using Differential Interference Contrast (DIC) microscopy. Shown are representative still images of time points before and after antigen stimulation from [Video 4.8](#) of control cells (*FUGW*) and [Video 4.9](#) of GEF-H1 depleted cells. The formation of membrane ruffling and lamellipodia formation occurred in control and GEF-H1 depleted cells (*red arrows*). Cell spreading was reduced in GEF-H1 depleted cells. Scale bar = 10 μm .

Supplemental videos showing live-cell DIC imaging are available at the following URLs:

Video 4.8 Differential Interference Contrast (DIC) live-cell imaging in stimulated cells of FUGW

https://drive.google.com/file/d/1MgUAsJ4MX_4543WGhytpnL8Uz63ogDRZ/view?usp=sharing

Video 4.9 Differential Interference Contrast (DIC) live-cell imaging in stimulated cells of GEF-H1 knockdown

https://drive.google.com/file/d/1Kzc87PPqH_iiu6W32XWdK7QwN5w9WydE/view?usp=sharing

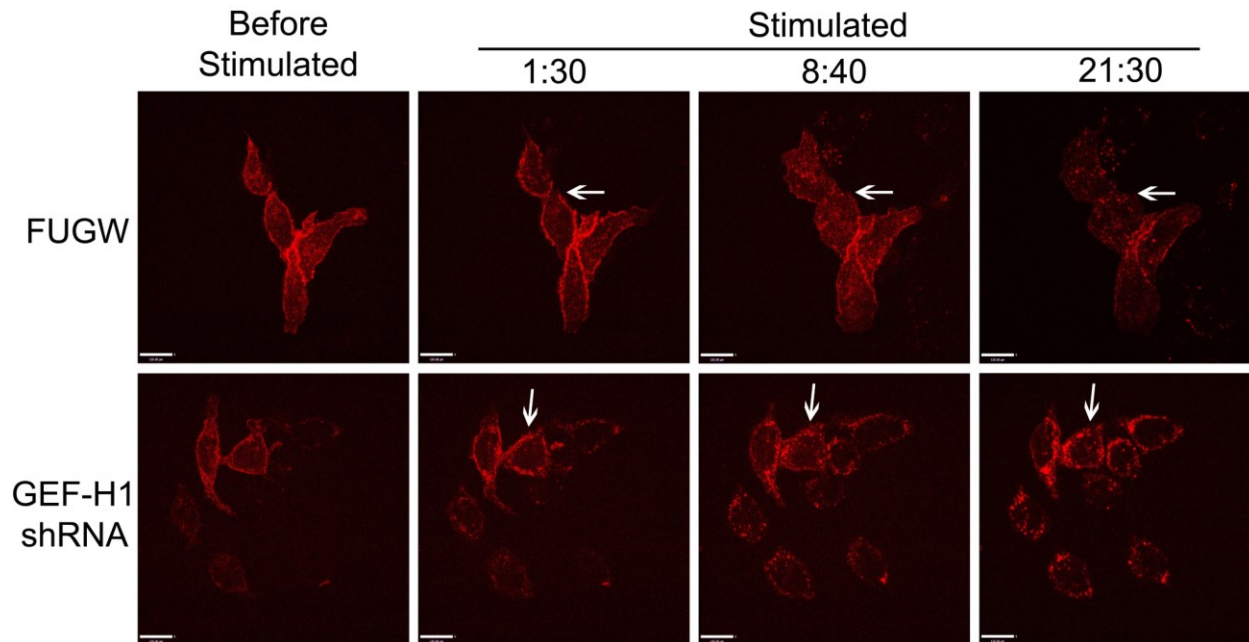


Figure 4.15 Depletion of GEF-H1 does not affect F-actin remodeling at the cell periphery. Actin remodeling was visualized in live cells during antigen stimulation using cells transfected with the F-actin probe Lifeact-mRuby. Shown are representative still images of time points before and after antigen stimulation from [Video 4.10](#) of control cells (*FUGW*) and [Video 4.11](#) of GEF-H1-depleted cells. When antigen-stimulated, control and GEF-H1 depleted cells formed F-actin rich lamellipodia at the leading edge (*white arrow*). Scale bar = 10 μ m.

Supplemental videos showing live-cell imaging of Lifeact-mRuby are available at the following URLs:

Video 4.10 Lifeact-mRuby live-cell imaging in stimulated cells of FUGW

https://drive.google.com/file/d/1IQni43sjVOu3LFIhcSvC4R0nz_j2ZPhR/view?usp=sharing

Video 4.11 Lifeact-mRuby live-cell imaging in stimulated cells of GEF-H1 knockdown

https://drive.google.com/file/d/1W8PPupWXz80xAFUJB-o89157L7p6_kz_/view?usp=sharing

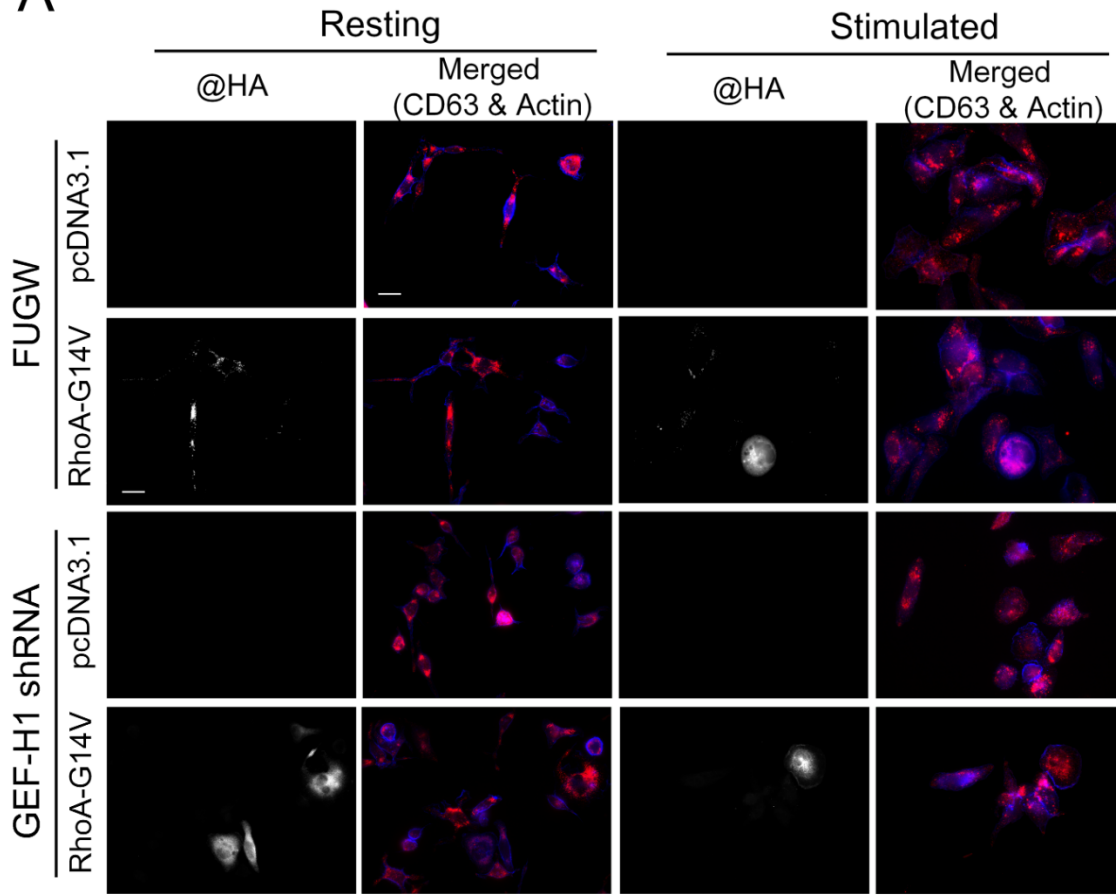
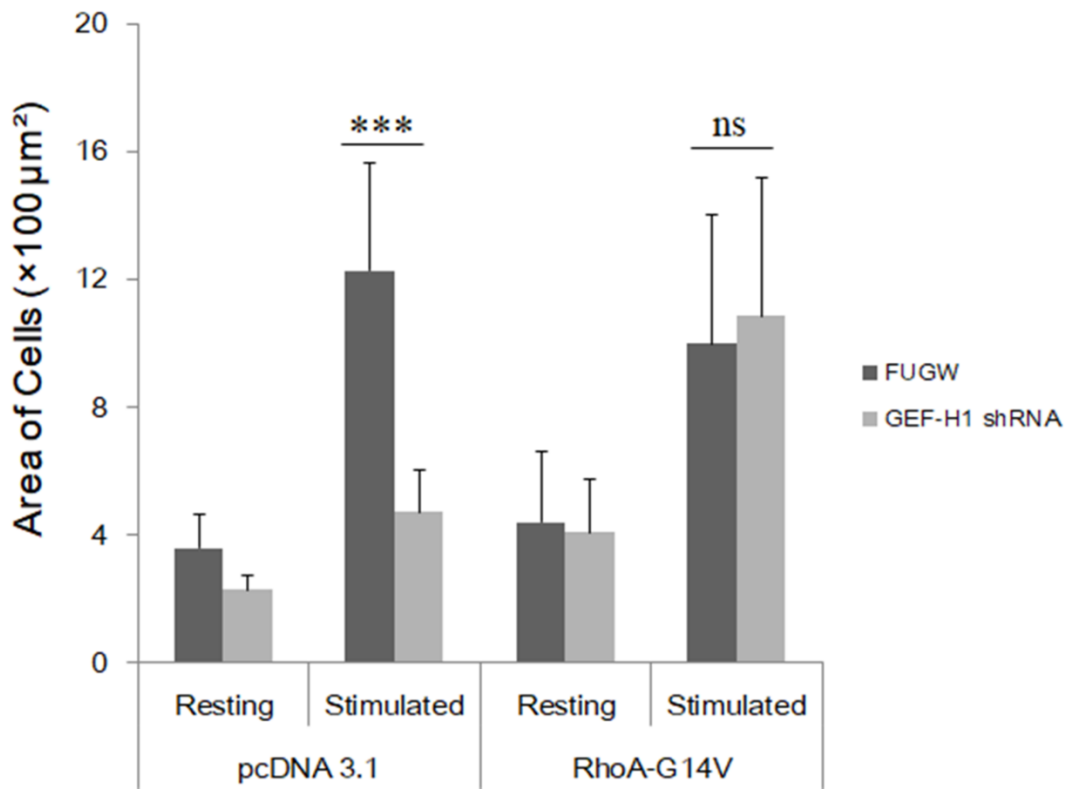
A**B**

Figure 4.16 Expression of constitutively active RhoA-G14V restores the defects of granule distribution and cell spreading in GEF-H1-depleted cells. 3×HA-tagged RhoA-G14V, a constitutively active mutant of RhoA, was introduced into both FUGW (empty vector control) and GEF-H1-depleted (GEF-H1 shRNA) RBL-2H3 cells. pcDNA 3.1 was used as an empty vector control. Granules were labeled with anti-CD63 antibody (*red*) and F-actin was labelled with Alexa Fluor 405-phalloidin (*blue*). Anti-HA labelling indicates transfected cells. (A) Images show expression of 3xHA-RhoA-G14V restores defects of both granule distribution and cell spreading after antigen-stimulation (30 min) of GEF-H1-depleted cells. (B) Quantification of cell sizes by ImageJ software. When stimulated, knockdown of GEF-H1 prevents cell spreading (pcDNA 3.1-transfected cells; *** $p < 0.001$). Transfection of RhoA-G14V restores cell spreading (RhoA-G14V-transfected cells; ns, not significant). Data shown is the mean +/- SD from two independent experiments and quantified from multiple cells ($n \geq 13$). Scale bar = 20 μm .

4.9 The GEF-H1-RhoA signaling axis regulates focal adhesion (FA) formation; role of FAs in mast cell degranulation

Previous studies have shown that RhoA is a key regulator of focal adhesions (FAs) formation [Ridley et al., 1992; Nobes and Hall, 1995; Yamana et al., 2006]. Additionally, focal adhesion kinase (FAK), a key regulator of FA formation, was found to be activated in antigen-stimulated RBL-2H3 cells [Hamawy et al., 1997]. Here, the role of FAs as a downstream target of the GEF-H1-RhoA signaling axis was examined. GEF-H1 was hypothesized to regulate FAs via the RhoA activity. The experimental questions were tested as follows, with the overall goal to determine roles of FAs in exocytosis: 1) Do FAs form during mast cell antigen stimulation? 2) Are FAs involved in RBL-2H3 mast cell degranulation? 3) Does the GEF-H1-RhoA axis regulate FAs formation? A specific FAK inhibitor, PF-573228, was used as a research tool for these studies.

The effect of the FAK inhibitor, PF-573228, on granule exocytosis was examined by degranulation assay. Resting cells preincubated with PF-573228 resulted in no effect on basal levels of degranulation, while after antigen stimulation there was significant inhibition of degranulation with as little as 1 μM (**Figure 4.17A**). Moreover, fluorescence staining of granules with LysoTracker Red and F-actin with Alexa Fluor 405-phalloidin showed that treatment with 10 μM of PF-573228 prevented the cell spreading and granule dispersion (**Figure 4.17B**). This suggests that inhibition of FA formation by PF-573228 disrupted cell activation mechanisms that lead to granule trafficking during antigen stimulation of RBL-2H3 cells.

FAs were purified and quantified in resting and stimulated cells by shearing away cells and staining the remaining adherent FAs with vinculin antibody (**Figure 4.18A**). Antigen-stimulation resulted in a significant increase in the number of FAs while pretreatment with the FAK inhibitor PF-573228 resulted in significantly fewer FAs (**Figure 4.18B**). These results are consistent with the requirement of FAs to support granule exocytosis in antigen-stimulated RBL-2H3 cells.

To determine whether the GEF-H1-RhoA axis regulates FAs formation, immunofluorescence microscopy for FAs was performed on resting and antigen-stimulated RBL-2H3 cells depleted of GEF-H1. FAs were labeled with vinculin antibody and F-actin with Alexa Fluor 405-phalloidin. In resting states of both control (empty vector, FUWG) and GEF-H1-depleted cells, FAs were in

low abundance, mostly adjacent to perinuclear regions (**Figure 4.19, Resting**). In the antigen-stimulated cells, FA staining increased at the periphery of cells (**Figure 4.19, Stimulated**). While the staining levels also increased in GEF-H1 depleted antigen-stimulated cells, the FAs staining region was not as enlarged as that of stimulated control cells. These results suggested the depletion of GEF-H1 disrupted the overall FAs formation during antigen stimulation.

The levels of FA formation in GEF-H1-depleted cells were quantified by shearing away cells and staining the remaining adherent FAs with vinculin antibody (**Figure 4.20A**). Stimulation of control cells (FUGW) showed a robust increase in FAs after antigen stimulation, and while GEF-H1 depleted cells also showed an increase in FAs, it was significantly less when compared to control cells (**Figure 4.20B**). In summary, the depletion of GEF-H1 disrupted the formation of FAs; together with results from **Figures 4.9, 4.18 and 4.20**, suggest a major contribution of the GEF-H1-RhoA signaling axis in regulating RBL-2H3 granule exocytosis correlating with the FAs formation.

4.10 GEF-H1 is activated in mast cells via the FcεRI antigen-stimulated signaling pathway

Our results suggest that the GEF-H1-RhoA axis contributes to FA formation then subsequently regulates the mast cell activation and granule exocytosis via antigen-stimulated FcεRI signaling. We hypothesize that GEF-H1 transduces signals from the cell surface receptor, FcεRI, to downstream Rho proteins (i.e. RhoA). Therefore, we next examined whether activation of GEF-H1 is linked to the FcεRI signaling pathway. To determine the activation of GEF-H1, we used a GST-RhoA-G17A pulldown assay. RhoA-G17A is a nucleotide-free mutant of RhoA that has high binding affinity to RhoA-specific RhoGEFs. To show the efficacy of RhoA-G17A probe to pulldown GEF-H1, cell lysates from control (FUGW) and GEF-H1-depleted cells were incubated with GST-Rho-G17A bound to glutathione resin (with GST only used as a control). GST-RhoA-G17A precipitated GEF-H1 with high specificity, while the GST only probe did not pulldown any GEF-H1 (**Figure 4.21 A and B**). Control pulldowns with a GST-Rac1-G15A probe for active Rac GEFs also did not detect the presence of active GEF-H1 (**Figure 4.21C**). This supports the role of GEF-H1 as a RhoA and not a Rac1 GEF in RBL-2H3 cells, although previous studies indicated GEF-H1 could act as a RhoGEF of either RhoA [Krendel et al., 2002] or Rac1 [Tonami et al., 2011].

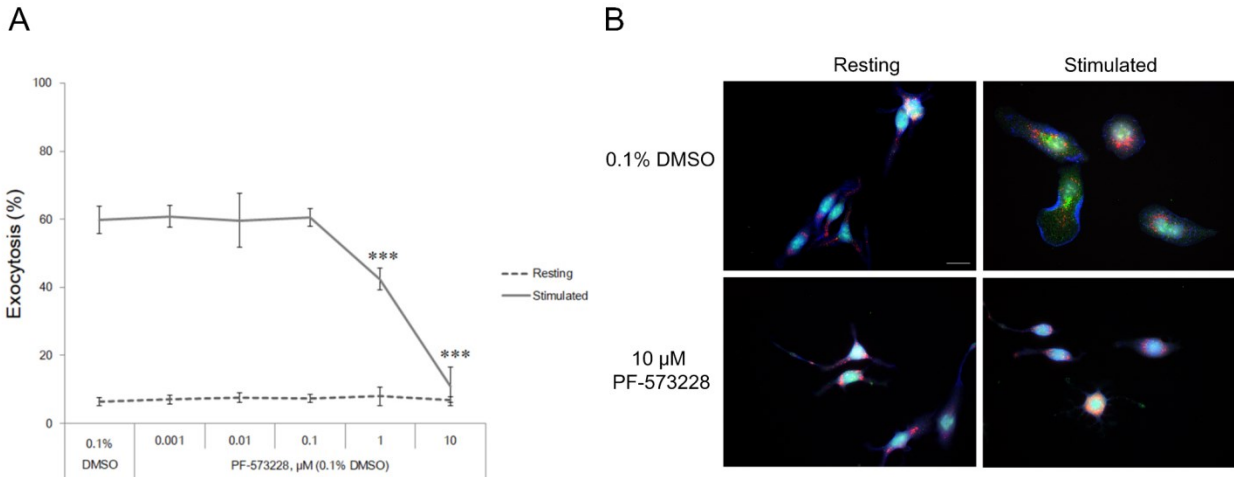


Figure 4.17 Involvement of focal adhesion (FA) formation in RBL-2H3 cell granule exocytosis. (A) The effect of the focal adhesion kinase inhibitor, PF-573228 on RBL-2H3 granule exocytosis. RBL-2H3 cells were preincubated with 1 nM to 10 μ M PF-573228 for 30 min followed by 30 min of antigen-stimulation. Degranulation assays showed a significant reduction in granule exocytosis when RBL-2H3 cells were pretreated with 1 or 10 μ M PF-573228 ($***p < 0.001$ vs. DMSO control, $n = 3$). (B) The formation of FAs in RBL-2H3 cells was visualized by staining with anti-vinculin antibody, together with granule distribution by LysoTracker Red and F-actin by Alexa Fluor 405-phalloidin staining. Inhibition of FA formation by PF-573228 reduced the vinculin staining, and prevented the granule disperse and cell spreading. Scale bar = 20 μ m.

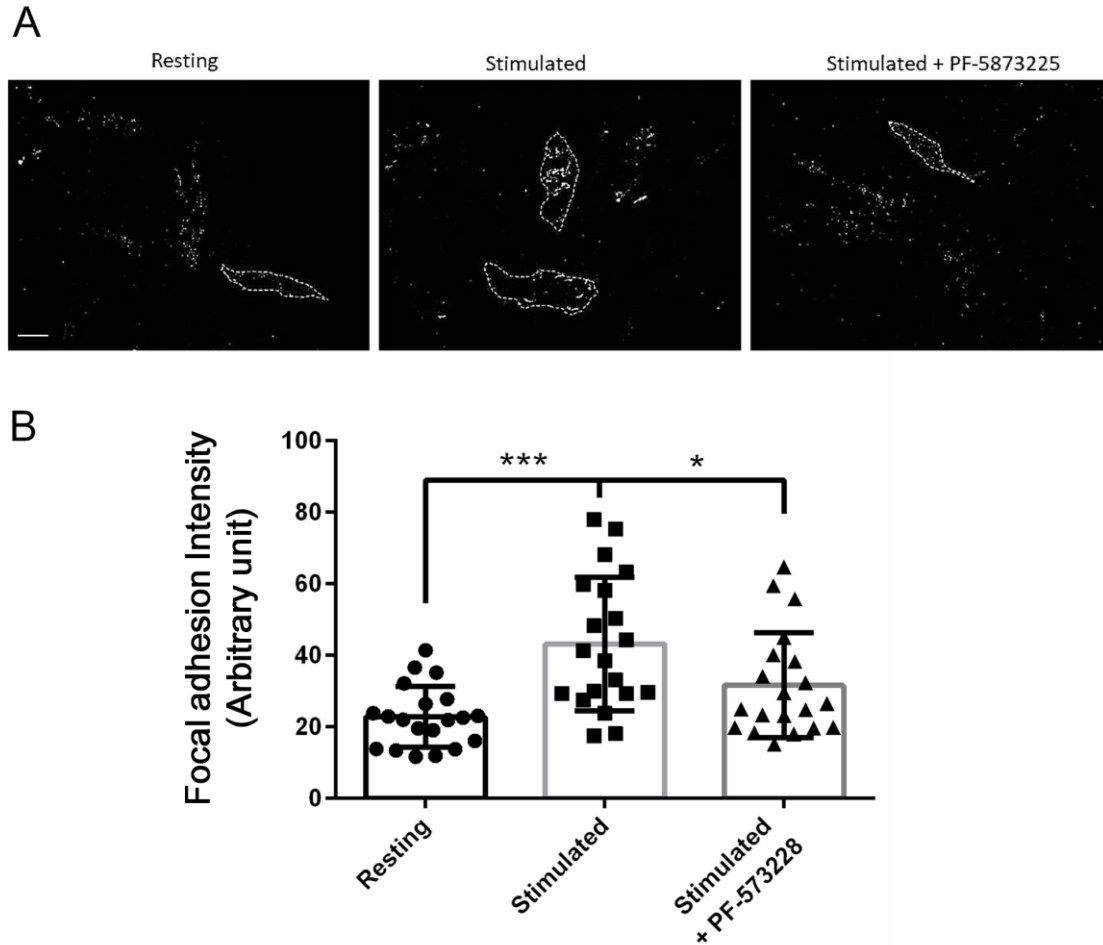


Figure 4.18 Quantification of focal adhesions (FAs) in antigen-stimulated RBL-2H3 cells. FAs were isolated by hypotonic shock of cells (*see Materials and Methods*), followed by anti-vinculin staining. Co-staining with Phalloidin-iFluor 405 was used to define the outline of cell contour. (A) Fluorescence microscope images of resting and antigen-stimulated ($\pm 10 \mu\text{M}$ PF-573228) RBL-2H3 cells after hypotonic shock. The intensity of vinculin signal within a cell contour was increased by antigen-stimulation but reduced by PF-573228-treatment. (B) Quantification of FA intensity per cell was performed using ImageJ software to measure the total vinculin intensity within a cell contour. Antigen stimulation increased FA formation, while pretreatment with PF-573228 prevented FAs formation ($*p < 0.05$, $***p < 0.001$, mean \pm SD). All data were from two independent experiments counting 20 cells per experiment. Scale bar = 20 μm .

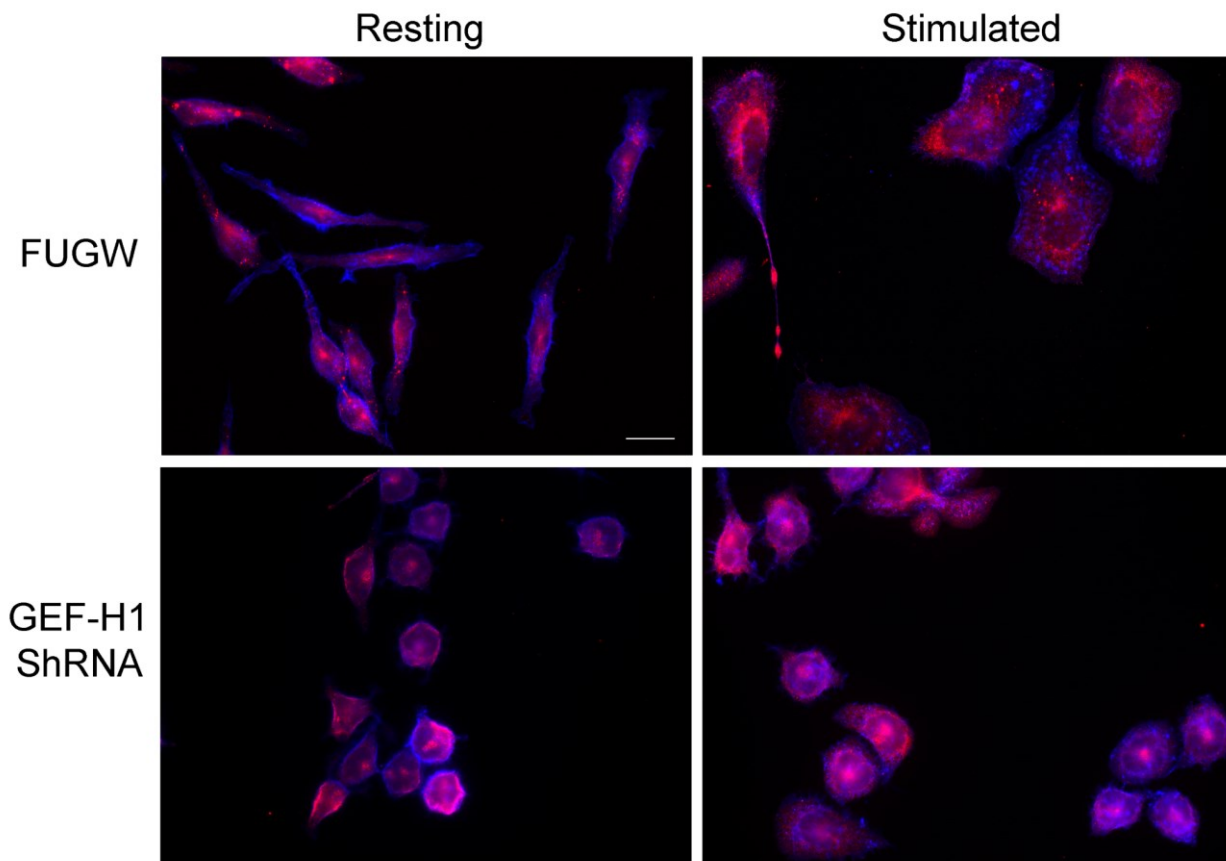


Figure 4.19 Visualization of focal adhesions (FAs) in GEF-H1-depleted RBL-2H3 cells. FAs were stained by anti-vinculin antibody (red), F-actin was stained with Alexa Fluor 405-phalloidin (blue). During antigen stimulation, the overall intensity of vinculin increased in RBL-2H3 control cells (FUGW, empty vector), together with observable cell spreading. However, in GEF-H1-depleted RBL-2H3 cells, antigen stimulation did not show an increase in anti-vinculin staining and cell spreading also did not occur. Scale bar = 20 μ m.

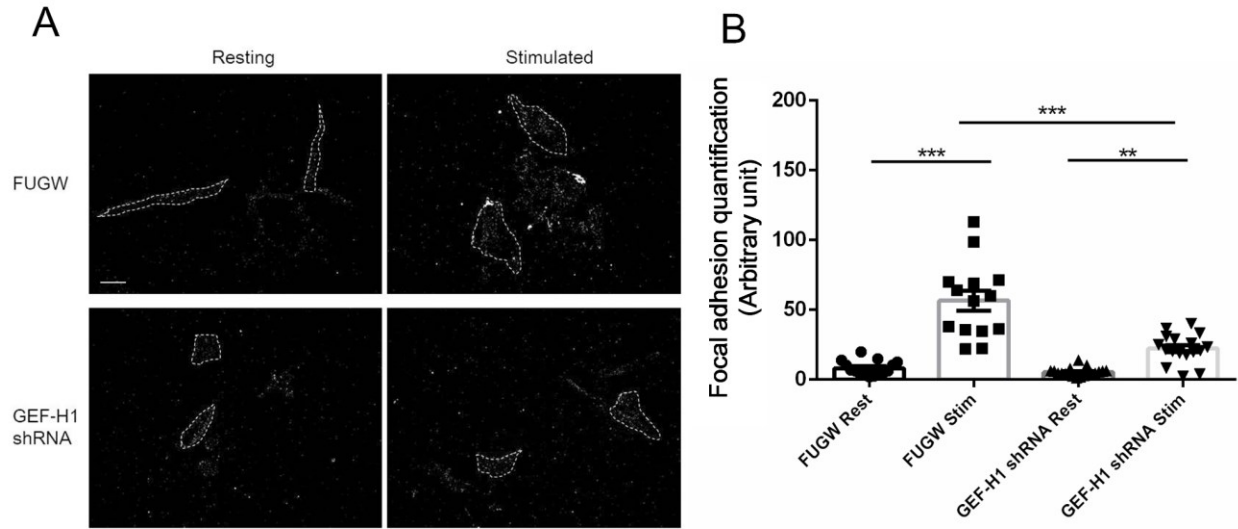


Figure 4.20 Focal adhesions (FAs) are reduced in GEF-H1-depleted RBL-2H3 cells. FAs were isolated by hypotonic shock (*see Materials and Methods*), followed by anti-vinculin staining. Coverslips were co-stained with Phalloidin-iFluor 405 to define the outline of individual cells. (A) Fluorescence microscope images of resting and antigen-stimulated control (FUGW) and GEF-H1 depleted RBL-2H3 cells after hypotonic shock. The intensity of vinculin signal within a cell contour increased after antigen-stimulation in control and GEF-H1 depleted cells but to a lesser extent. (B) Quantification of FA intensity per cell was performed using ImageJ software to measure the total vinculin intensity within a cell contour. Control cells formed significantly more FAs after antigen stimulation compared to GEF-H1 depleted cells (** $p < 0.01$, *** $p < 0.001$, mean \pm SD). All data were from two independent experiments counting 16 cells per experiment. Scale bar = 20 μ m.

The activation of GEF-H1 has been shown to occur by two distinct ways (*see Chapter 1.5.3*): by the microtubule dynamics as GEF-H1 was found to be a microtubule-bound RhoGEF, or by phosphorylation. Active levels of GEF-H1 increased during a time course of antigen stimulation, showing GEF-H1 activation is linked to FcεRI signaling (**Figure 4.22**). Active GEF-H1 was previously shown to be regulated by release from microtubules [Krendel et al., 2002; Birkenfeld et al., 2008]. At 10 min, GEF-H1 was not fully activated, and therefore this time point was used to examine if microtubule drugs could enhance active GEF-H1 levels. Preincubation of cells with the microtubule stabilizing drug, taxol, resulted in no increase in active GEF-H1 levels, while the microtubule destabilizing drug, nocodazole, did increase in active GEF-H1 levels; however, there was not statistically significant (**Figure 4.23**). Whether nocodazole could activate GEF-H1 in resting RBL-2H3 cells was not addressed here, which did not likely occur since it robustly inhibited RBL-2H3 activation and exocytosis (**Chapter 3**). Immunofluorescence of microtubules and GEF-H1 in stimulated RBL-2H3 cells did not show marked colocalization between GEF-H1 and microtubules; preincubation with microtubule drugs did not seem to alter the localization of GEF-H1 (**Figure 4.24**). Immunoprecipitation of GEF-H1 from RBL-2H3 cells over an antigen-stimulation time course failed to co-immunoprecipitate tubulin (**Figure 4.25**). These results suggest that GEF-H1 activation is linked to FcεRI signaling but does not hugely rely on microtubule dynamics during mast cell activation. Thus, the activation of GEF-H1 may depend on other regulatory factors including protein phosphorylation.

4.11 Regulation of GEF-H1 activation by kinases in mast cells

It has been previously shown that GEF-H1 is regulated, both activated and inhibited, by protein phosphorylation [Birkenfeld et al., 2008]. To examine the roles of kinase in the regulation of mast cell GEF-H1, the following specific kinase inhibitors were tested: Src I1, an inhibitor of Src and Lck; PP2, an inhibitor of Fyn and Lck; PD98059, an inhibitor of MEK; wortmannin, an inhibitor of PI3-kinase. Wortmannin was previously found to inhibit the histamine secretion in RBL-2H3 cells [Yano et al., 1993]. Degranulation assays showed all these inhibitors affected RBL-2H3 cell granule exocytosis to varying degrees (**Figure 4.26, solid line**). More than 1 μM of Src I1, PP2 and PD98059 and only 10 nM of wortmannin did significantly inhibit mast cell exocytosis. There was no impact of these four inhibitors on background degranulation levels measured in unstimulated cells (**Figure 4.26, dashed line**).

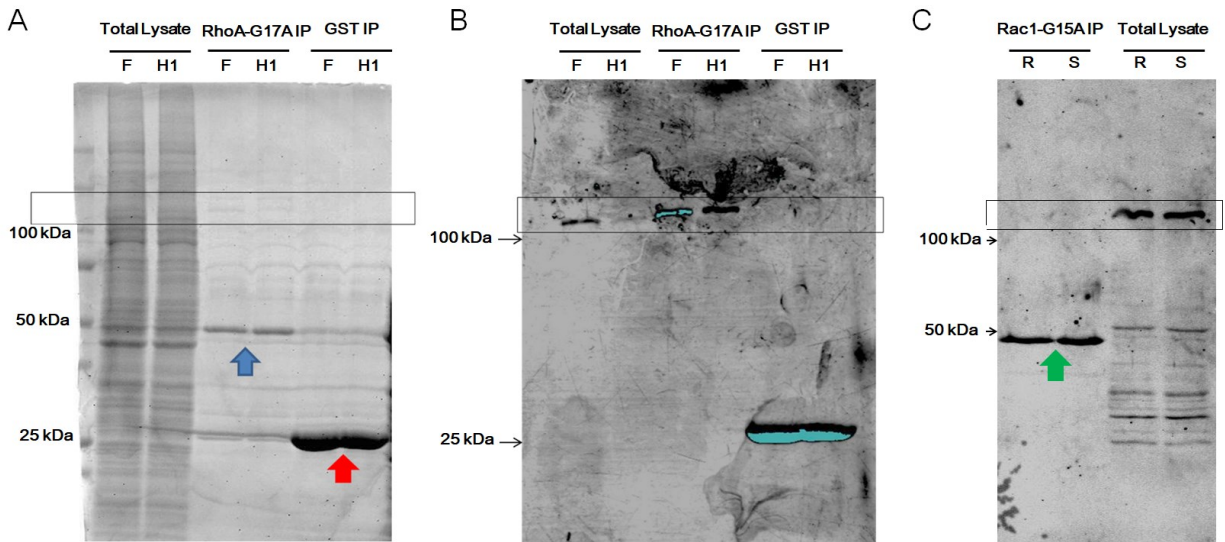


Figure 4.21 Assay for active GEF-H1. Active GEF-H1 was determined by pulldown assay using immobilized GST-RhoA-G17A (RhoA-G17A), a nucleotide-free mutant of RhoA that has high affinity for RhoA-associated active RhoGEFs. RBL-2H3 cell lysates were prepared from control cells (*F*, FUGW empty vector) and GEF-H1 depleted cells (*H1*). (A) Coomassie blue stained gel showing GST-RhoA-G17A was successfully purified (*blue arrow*) compared to GST only (*red arrow*). The rectangular frame indicates the position of GEF-H1. (B) Western blot using anti-GEF-H1 antibody to probe total lysate (5% of the pulldown fraction), GST-RhoA-G17A (*RhoA-G17A IP*) and GST control pulldowns. GST-RhoA-G17A effectively pulled down GEF-H1, while the GST probe did not. (C) GST-Rac1-G15A (Rac1-G15A), a nucleotide-free mutant of Rac1 that has high affinity for active Rac GEFs, was used to pulldown active GEF-H1 in resting (*R*) or antigen-stimulated (*S*) RBL-2H3 cell lysates. The rectangular frame indicated the position of GEF-H1 probed by a GEF-H1 antibody by western blot (Rac1-G15A pull downs and 5% total lysates). GST-Rac1-G15A is indicated by the *green arrow*. GEF-H1 could not be pulled down by GST-Rac1-G15A. IP, immunoprecipitation.

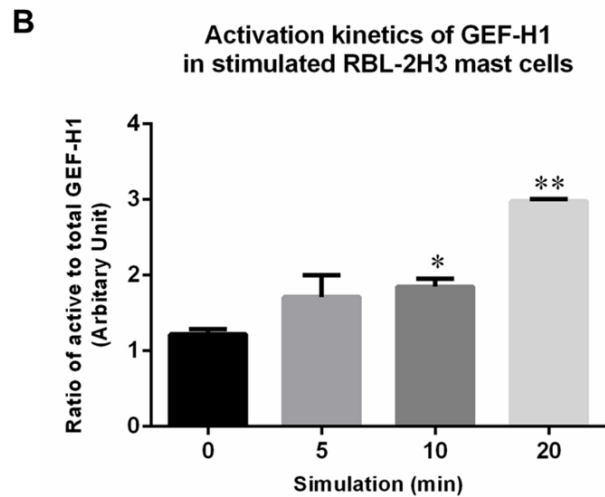
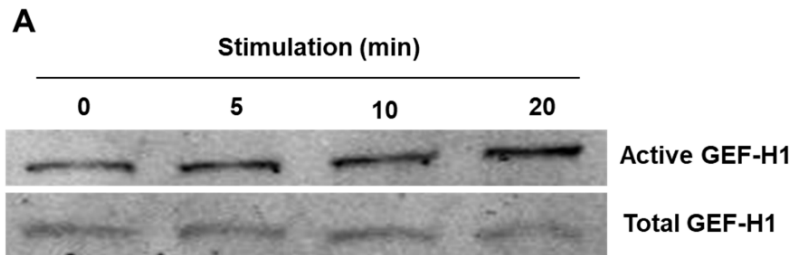


Figure 4.22 Active GEF-H1 levels increase in antigen-stimulated RBL-2H3 cells. Activation of GEF-H1 was measured by GST-RhoA-G17A pulldown assay. (A) Western blot of active GEF-H1 (*upper panel*) and total GEF-H1 from a 5% load control (*lower panel*) of RBL-2H3 cell lysates prepared from antigen stimulated time points of 0, 5, 10, 20 min. (B) Quantification of active GEF-H1 levels by band densitometry of western blots. Levels of active GEF-H1 showed a significant increase after 10 min and 20 min stimulation compared to 0 min of stimulation (* $p < 0.05$, ** $p < 0.01$, $n = 3$).

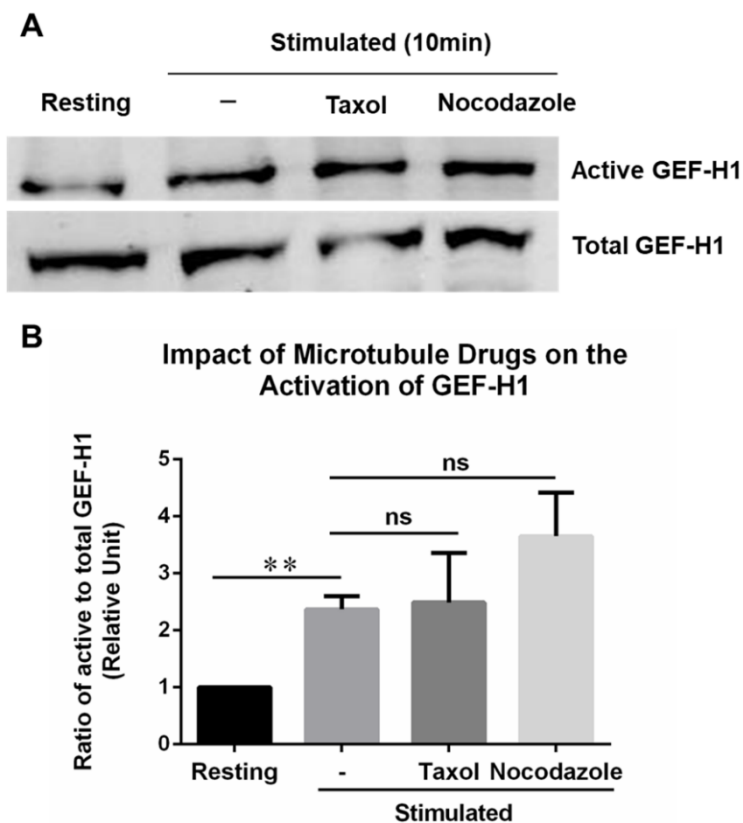


Figure 4.23 Activation of GEF-H1 in stimulated RBL-2H3 cells is not affected by microtubule-targeted drugs. Microtubule-targeted drugs taxol and nocodazole were used to determine the effects of microtubule dynamics on GEF-H1 activation, as measured by GST-RhoA-G17A pulldown assay. (A) Western blot of active GEF-H1 (*upper panel*) and total GEF-H1 from a 5% load control (*lower panel*) of RBL-2H3 cell lysates prepared from cells antigen stimulated for 0 min (*Resting*) or 10 min (-), or stimulated 10 min after pretreatment with 10 μ M taxol or nocodazole. (B) Quantification of active GEF-H1 levels by band densitometry of western blots. Levels of active GEF-H1 showed a significant increase after 10 min of stimulation compared to resting (** $p < 0.01$, $n = 3$) while microtubule-targeted drugs did not show a significant effect compared to 10 min of stimulation (ns, not significant, $n = 3$).

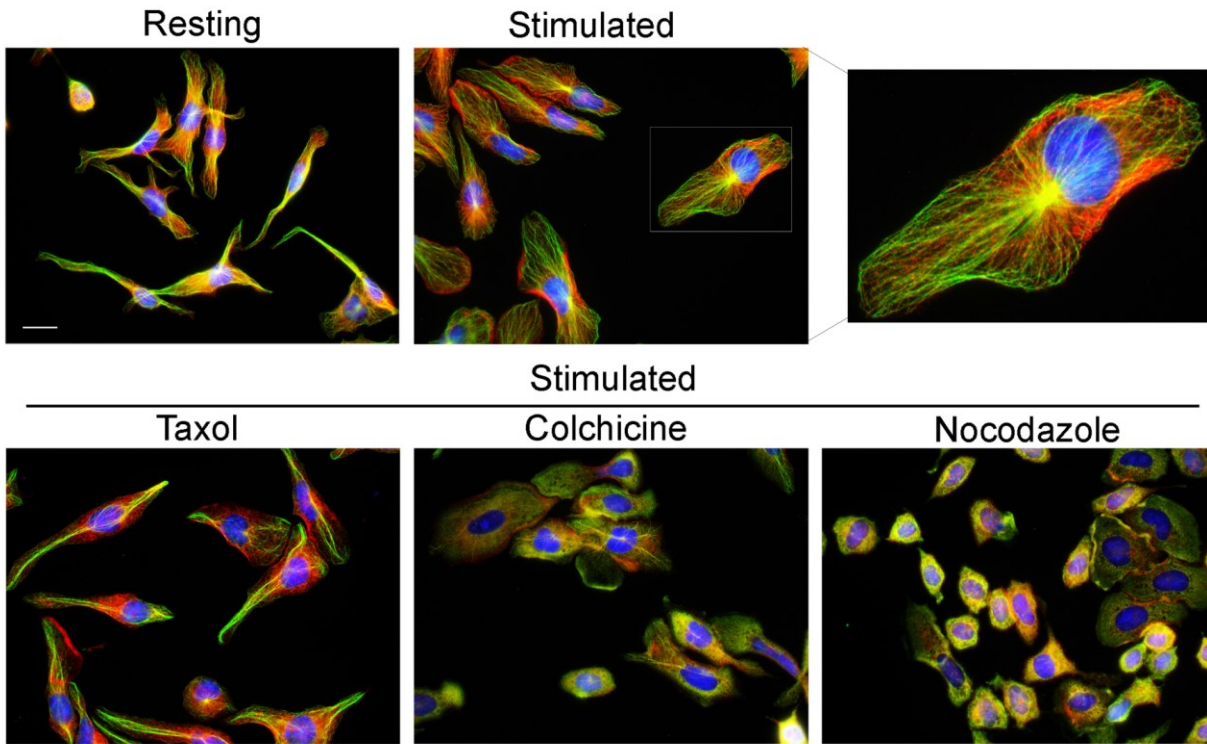


Figure 4.24 Effect of microtubule-targeted drugs on GEF-H1 localization. RBL-2H3 cells were pretreated with 0.1% DMSO (*upper panels*) or 10 μM microtubule-target drugs, then antigen-stimulated for 30 min. Cells were fixed by ice-cold methanol for 10 min to preserve the microtubule network. GEF-H1 was labeled by specific antibody (red), microtubules with β -tubulin antibody (green) and nuclei with DAPI (blue). GEF-H1 was intracellularly dispersed in both resting and antigen-stimulated states. Application of microtubule-targeted drugs altered the microtubule network while the localization of GEF-H1 was not overly changed. Scale bar = 20 μm .

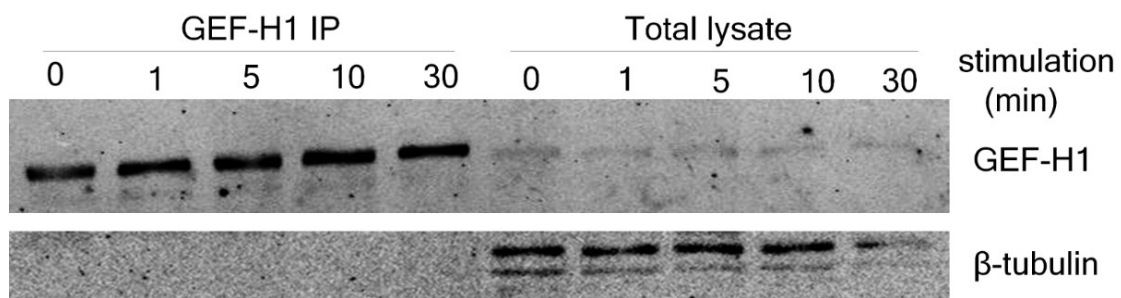


Figure 4.25 Tubulin was not detected in GEF-H1 immunoprecipitates. RBL-2H3 cells were stimulated 0 - 30 min, lysed, and GEF-H1 was immunoprecipitated using GEF-H1 specific antibody. Western blots show no β -tubulin in GEF-H1 IP fractions (left panel), whereas 5% load controls (*Total lysate*) contained β -tubulin and GEF-H1. Images were representatives of three independent experiments.

Next, the effect of these kinase inhibitors on GEF-H1 activation was examined by GST-RhoA-G17A pulldown assays. The FAK inhibitor, PF-573228, was included in these studies since it showed inhibition of degranulation similar to the Src inhibitors (*see* **Figure 4.17**). 1 μ M ionomycin was used as a control stimulus since it robustly triggers degranulation, but bypass the Fc ϵ RI signaling pathway in RBL-2H3 cells [Sahara et al., 1990]. Antigen-stimulation for 10 min significantly increased the active levels of GEF-H1; this required Fc ϵ RI signaling since ionomycin did not increase levels of active GEF-H1 above unstimulated (**Figure 4.27A**). Pretreatment with Src II, PP2, PD98059, wortmannin, or PF-573228 did not significantly alter the active GEF-H1 levels in antigen-stimulated RBL-2H3 cells (**Figure 4.27B**). Therefore, the kinases of Src, Fyn, Lck, MEK, PI3K and FAK do not regulate the activation of GEF-H1 in RBL-2H3 cells via the Fc ϵ RI signaling.

Since multiple Fc receptor-proximal kinases of Src isoforms are involved in mast cell activation [Blank and Rivera, 2004], the putative role of Syk (only a single isoform) was examined. The Syk specific inhibitor, GS-9973, potently inhibited antigen-stimulated degranulation with 1 nM providing approximately 50% inhibition (**Figure 4.28**). In addition, the effect of GS-9973 on cell spreading and granule trafficking were examined. Normal RBL-2H3 cell morphology is resting cells that are elongated and granules that are concentrated in the perinuclear region while stimulated cells increase in size and granules project to the periphery (**Figure 4.29A**). Antigen-stimulated RBL-2H3 cells treated with 1 nM Syk inhibitor showed partial inhibition of the activated morphology; some cell spreading was observed but granules remained perinuclear (**Figure 4.29B, left panel**). Higher concentration resulted in cells that looked like resting cells (**Figure 4.29B, right panel**). Syk regulation of GEF-H1 activation was further demonstrated by GEF activation assay using the GST-RhoA-G17A probe to pulldown active GEF-H1. Levels of active GEF-H1 increased after antigen-stimulation for 10 min, but were significantly inhibited when cells were preincubated with the Syk inhibitor GS-9973 (**Figure 4.30**). These results indicated that the activation of GEF-H1 in antigen-stimulated RBL-2H3 cells was Syk-dependent. Taken together, the inhibition of Syk by GS-9973 also inhibited granule exocytosis; one process the drug affected was GEF-H1 activation which leads to defects in cell spreading when RBL-2H3 cells were antigen-stimulated. While GEF-H1 is known to be regulated by phosphorylation, whether it is a direct Syk substrate requires further investigation.

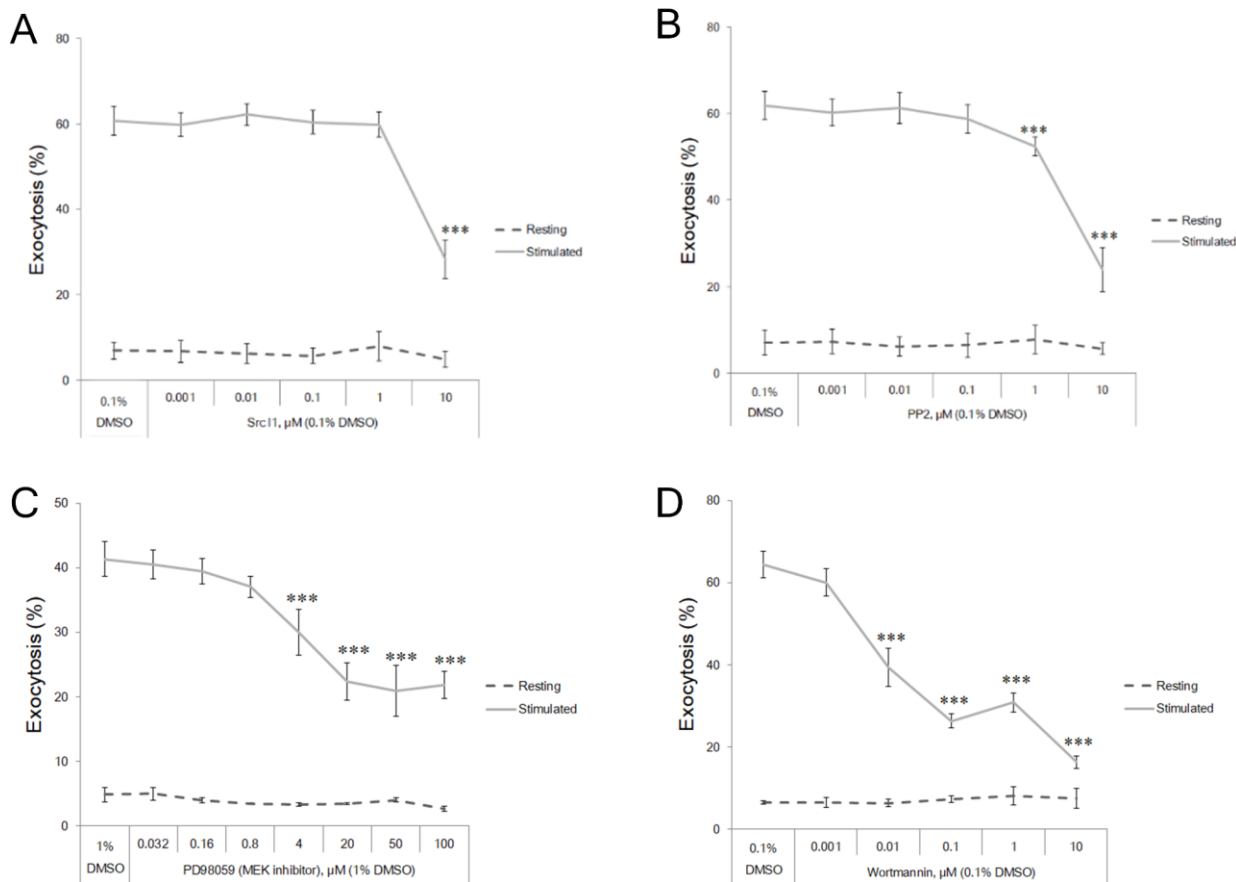


Figure 4.26 Effect of kinase inhibitors on granule exocytosis. RBL-2H3 cells were preincubated for 30 min with kinase inhibitors and their effect on antigen-stimulated exocytosis was examined by degranulation assay. Graphs show dose response for (A) Src 11, an inhibitor of Src and Lck; (B) PP2, an inhibitor of Fyn and Lck; (C) PD98059, an inhibitor of MEK; (D) wortmannin, an inhibitor of PI3-kinase. Wortmannin significantly inhibited exocytosis in as low as 10 nM. Higher doses of Src 11 (10 μM), PP2 (10 μM) and PD98059 (4 μM), were required to achieve significant inhibition of exocytosis (***) $p < 0.001$ compared to DMSO control, $n = 3$).

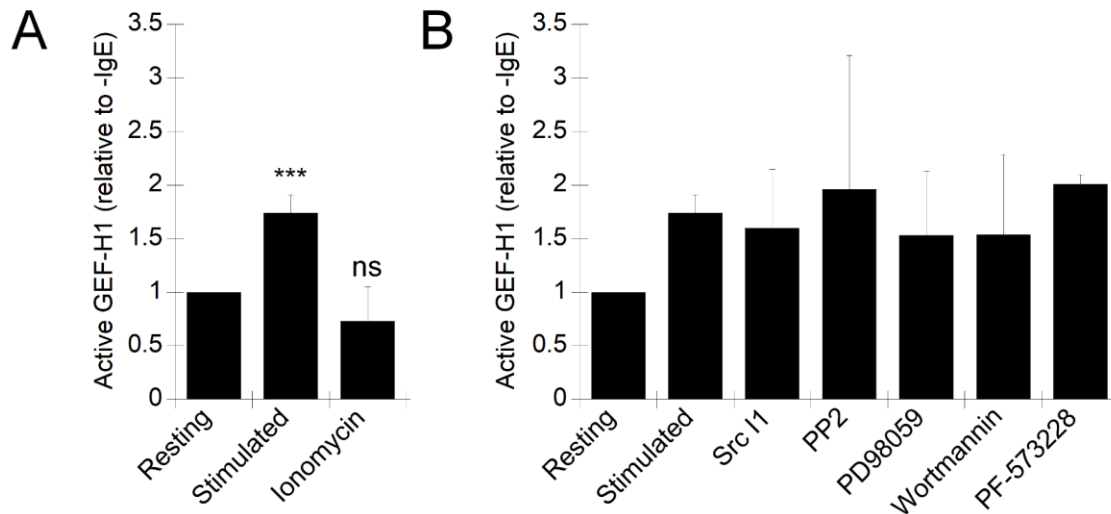


Figure 4.27 Effect of inhibitors on GEF-H1 activation. Active GEF-H1 levels were determined by GST-RhoA-G17A pulldown assays (*see Materials and Methods*). (A) RBL-2H3 cells were antigen-stimulated for 30 min which results in a significant increase in active GEF-H1 levels compared to resting. Stimulation of cells for exocytosis using 1 μ M ionomycin, which bypasses Fc ϵ RI receptor signaling, does not activate GEF-H1. (B) Active GEF-H1 levels were not affected by preincubation with inhibitors and subsequent antigen-stimulation. Src I1 inhibits Src and Lck; PP2 inhibits Fyn and Lck; PD98059 inhibits MEK; wortmannin inhibits PI3-kinase and PF-573228 inhibits FAK. Data were compiled and quantified from three independent western blot experiments by comparing relative band intensities normalized to resting cells (** $p < 0.001$; ns, not significant; $n = 3$). No statistical differences (by ANOVA) between the effects of these kinases on GEF-H1 activation were addressed.

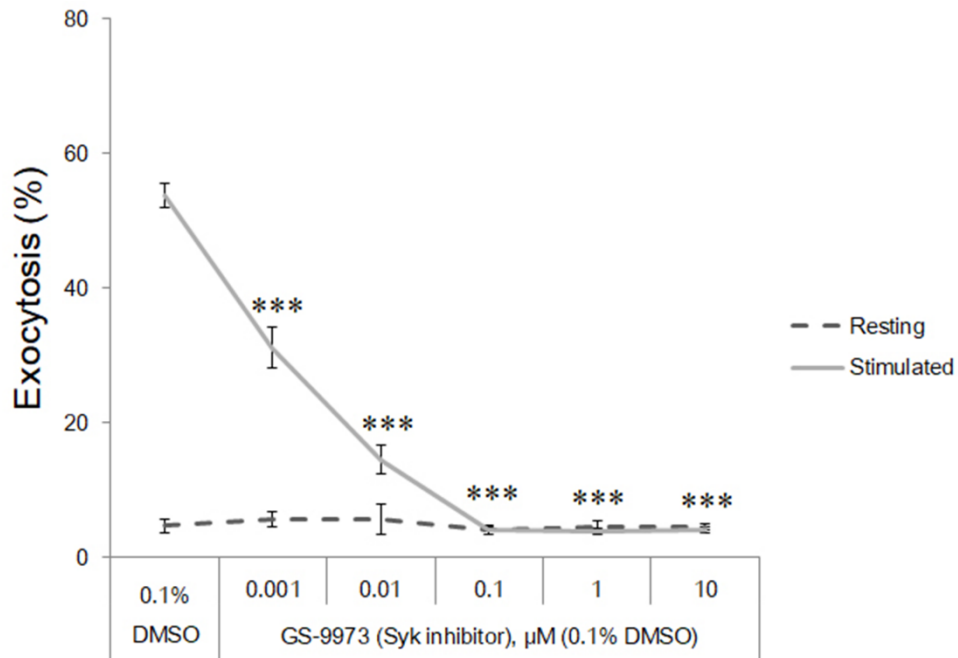


Figure 4.28 Effect of the Syk inhibitor, GS-9973, on RBL-2H3 cell degranulation. RBL-2H3 cells were preincubated for 30 min with varying concentration of GS-9973 and its effect on antigen-stimulated exocytosis was examined by degranulation assays. GS-9973 significantly reduced RBL-2H3 cell granule exocytosis at concentrations as low as 1 nM ($***p < 0.001$ compared to DMSO control, $n = 3$).

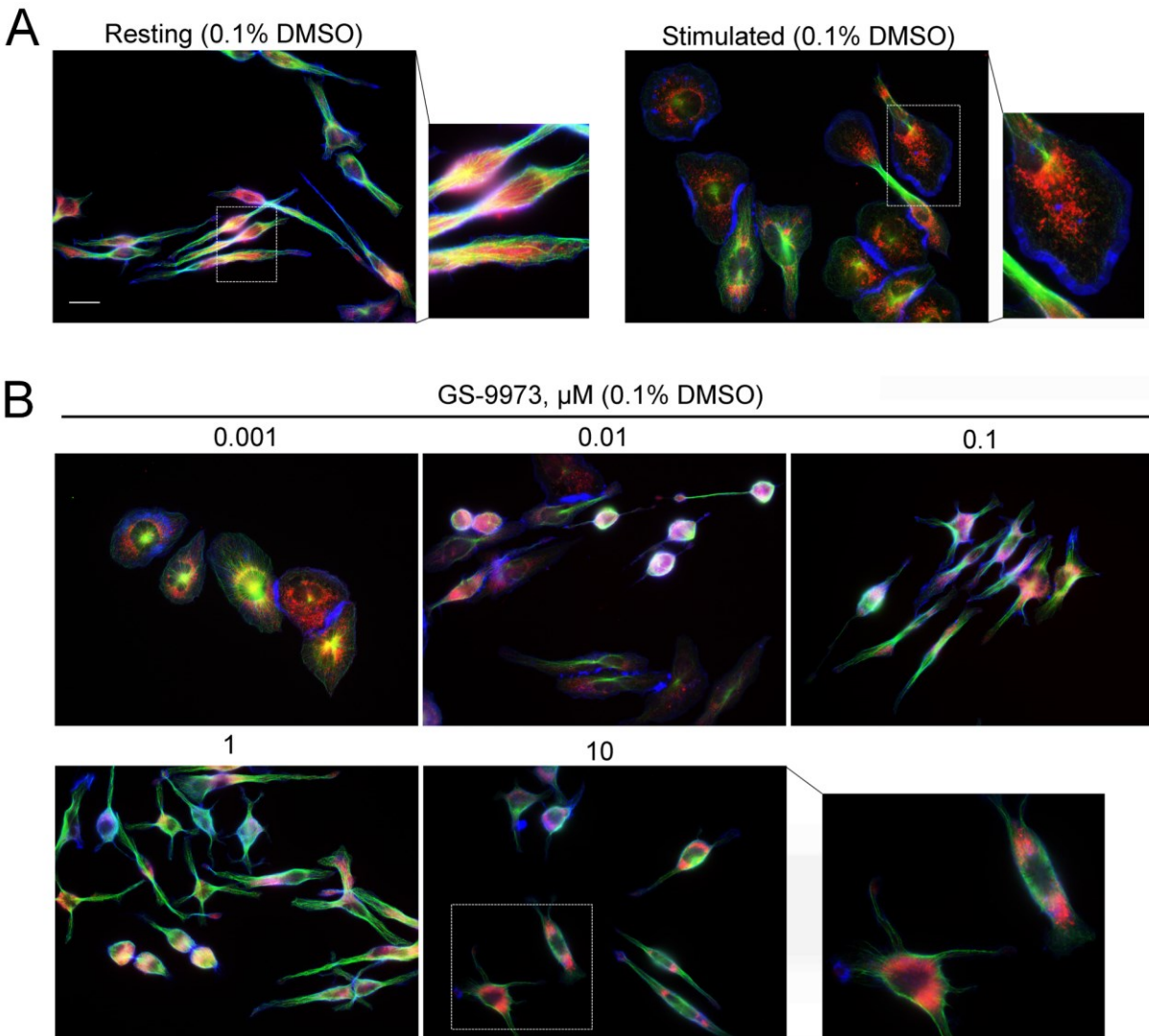


Figure 4.29 Effect of the Syk inhibitor, GS-9973, on RBL-2H3 cell morphology and granule localization. RBL-2H3 cells were preincubated with varying concentrations of GS-9973 or 0.1% DMSO (vehicle control) for 30 min then antigen-stimulated for 30 min. Cells were fixed and stained for granules with anti-CD63 antibody (red), microtubules with β -tubulin antibody (green); and F-actin with Alexa Fluor 405-phalloidin (blue). (A) Vehicle control cells show spreading after stimulation with prominent F-actin lamellipodia formation and granule projection to the periphery (*right panel, enlarged image*). (B) Cells preincubated with GS-9973 show reduced cell spreading and granules remain in the perinuclear region (*right panel, enlarged image*). Scale bar = 20 μm .

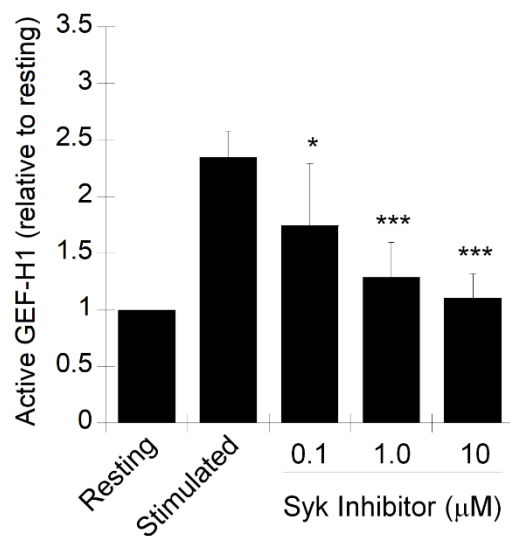


Figure 4.30 The Syk inhibitor, GS-9973, reduces GEF-H1 activation in antigen-stimulated RBL-2H3 cells. Active GEF-H1 levels were determined by GST-RhoA-G17A pulldown assays (see **Materials and Methods**). RBL-2H3 cells were antigen-stimulated for 30 min which results in a significant increase in active GEF-H1 levels compared to resting (see **Figure 4.28A**). Active GEF-H1 levels were significantly reduced when RBL-2H3 cells were preincubated with the Syk inhibitors, GS-9973, and then subsequently antigen-stimulated. (* $p < 0.05$ and *** $p < 0.001$ compared to DMSO stimulated, $n = 3$).

4.12 Interaction of GEF-H1 with Exo70 and its contribution to mast cell granule exocytosis

Previous studies have shown that GEF-H1 was enriched in FAs with functional roles in regulating the formation of FA in response to external stimuli [Nalbant et al., 2009; Huang et al., 2014; Sandíet al., 2017; Rafiq et al., 2019]. GEF-H1 was also shown to interact with the exocyst components to control secretion (i.e. Sec5 or Exo70) [*see Chapter 1.5.6*; Pathak et al., 2012; Wang et al., 2015; Ahmed et al., 2018; Sáez et al., 2019]. We investigated interactions with FAs and the exocyst by co-immunoprecipitation assay. Exo70 was immunoprecipitated from resting and stimulated RBL-2H3 cells to analyze exocyst interactions and vinculin to analyze FA interactions. While these proteins were efficiently immunoprecipitated from lysates, GEF-H1 did not co-immunoprecipitate with either protein, even though it was abundantly present in the lysates (**Figure 4.31**). In addition, Exo70 and vinculin were not present in a mass spectrometry analysis of GEF-H1 immunoprecipitations from either resting or antigen-stimulated RBL-2H3 cell lysates (*data not shown*). Furthermore, there was no correlation between the localization of GEF-H1 and granules (CD63), the exocyst (Exo70) or FA, using CD63, Exo70 and vinculin as markers respectively (**Figure 4.32**). The lack of evidence for colocalization between GEF-H1 and Exo70 or vinculin in might be attributed to transient interactions or the disruption by detergent used during mass spectrometry or co-immunoprecipitation assays. So far, in RBL-2H3 cells of antigen stimulation, there lacked the evident interaction between GEF-H1 and Exo70 or vinculin, suggesting these two proteins may not contribute to the function of GEF-H1 in regulating RBL-2H3 cell exocytosis.

To avoid the pitfalls of detergents for the dissection of GEF-H1 interactions, we performed a study of proteins that co-fractionated with an enriched granule fraction. RBL-2H3 cell granules can be enriched by differential centrifugation. A subset of granules can be precipitated by centrifugation at 4000×g while the remainder precipitate at 20,000×g (**Figure 4.33, MCP II**). The exocyst component, Exo70, was also enriched in these fractions while the FA component, vinculin was not detected (likely due to the mild lysis condition). The levels of Exo70 were found to be slightly reduced in granule-enriched fractions prepared from GEF-H1-depleted cells (*HI*) when compared to control cells (*Fw*) (**Figure 4.33, Exo70**). This suggests that GEF-H1 recruits exocyst components to granule fractions. However, these experiments require repeating and validation by alternative quantitative methods.

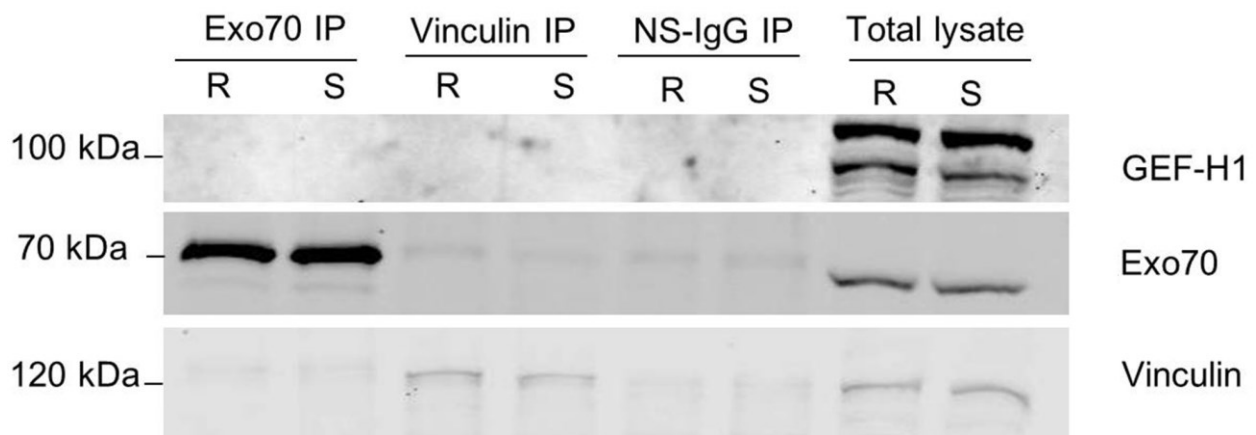


Figure 4.31 Co-immunoprecipitation analysis of GEF-H1 with Exo70 and vinculin. Exo70 and vinculin were immunoprecipitated (*IP*) from RBL-2H3 lysates of resting cells, without antigen stimulation (*R*), or antigen-stimulated for 30 min (*S*). Non-specific IgG (*NS-IgG*) was used as a control. GEF-H1 was not detected in *IP* fractions of either Exo70 or vinculin but was readily detected in the total lysate.

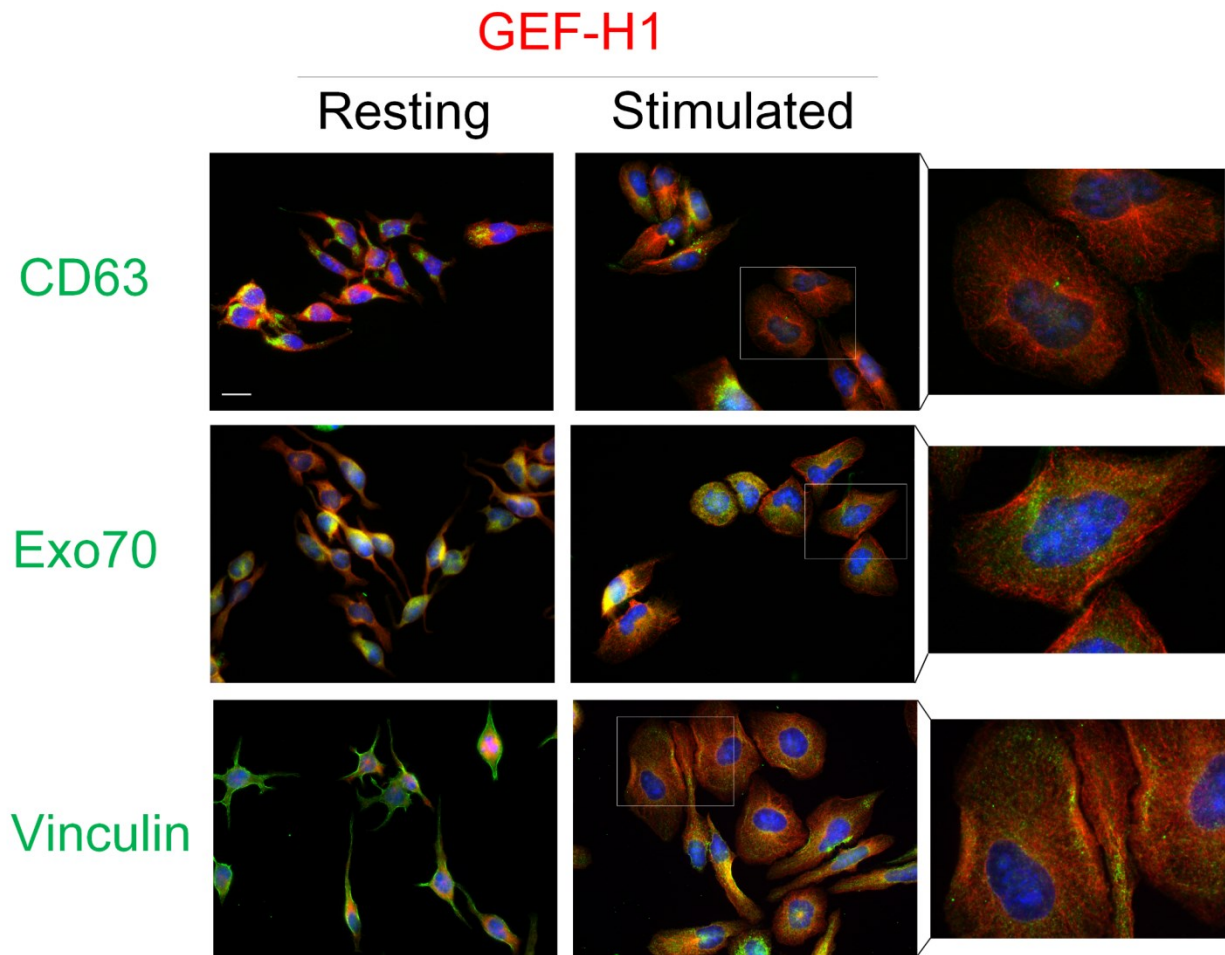


Figure 4.32 Analysis of colocalization of GEF-H1 with CD63, Exo70 and vinculin. RBL-2H3 cells were antigen-stimulated for 30 min (*Stimulated*) or left unstimulated (*Resting*) as a control. Immunofluorescence microscopy was used to examine the intracellular localization of GEF-H1 (red) with respect to granules via CD63 labeling (green, *top panel*), the exocyst via Exo70 labeling (green, *middle panel*) or FA via vinculin labeling (green, *bottom panel*). Nuclei were stained with DAPI (blue). No significant colocalization was detected. Scale bar = 20 μ m.

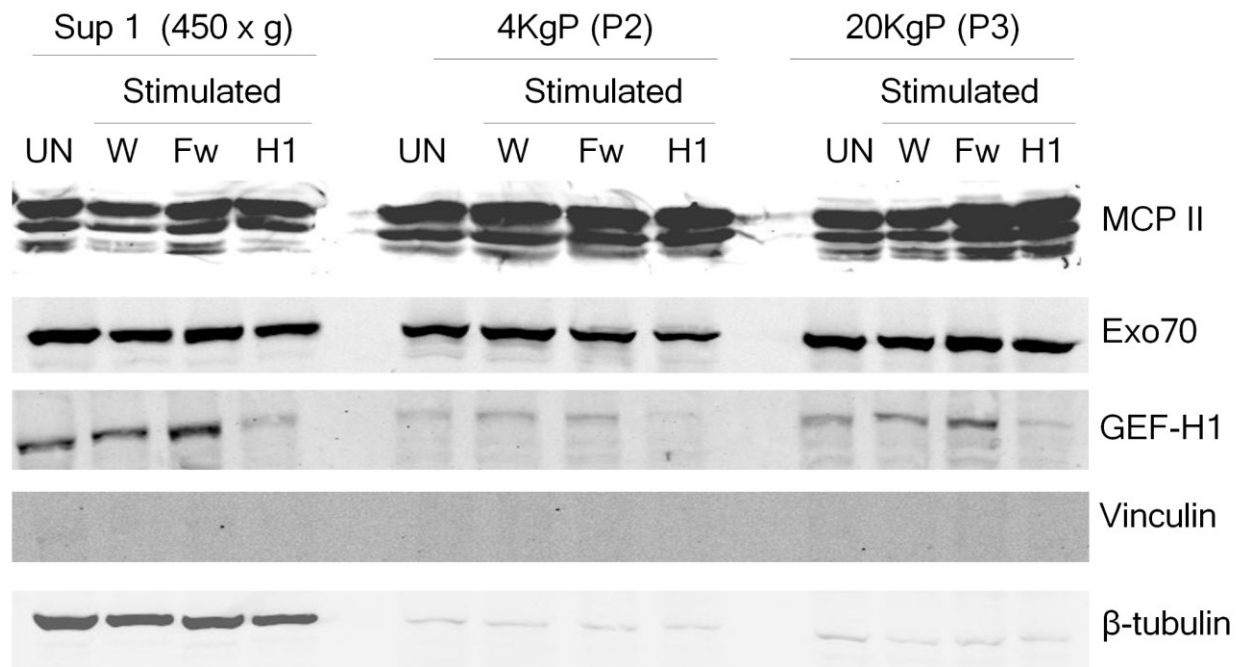


Figure 4.33 Granule co-fractionation of Exo70 depends on GEF-H1. Granule co-fractionation studies via granule enrichment (*see Materials and Methods*) were used to determine the putative protein effectors of GEF-H1. Granule fractions were enriched from wild-type RBL-2H3 cells that were unstimulated (*UN*), or antigen-stimulated (15 min) wild-type (*W*), empty vector control (*FUGW*, *Fw*) or GEF-H1 knock-down (*H1*) RBL-2H3 cells. The isolated pellet fractions from a $4,000 \times g$ (*4KgP*, *P2*) and $20,000 \times g$ (*20KgP* (*P3*)) centrifugation were western blotted with antibodies of β -tubulin, mast cell protease II (MCP II), GEF-H1, vinculin and Exo70. The cleared supernatant (*Sup 1* ($450 \times g$)) is an input control. Microtubules (β -tubulin) were rarely present but MCP II, a granule marker, was present in both P2 and P3 fractions. Vinculin was almost undetectable in S1, P2 and P3 which indicates low solubility in the isolation method. Levels of Exo70 in P2 and P3 fractions increased after antigen stimulation. GEF-H1 knock-down led to a reduction in the recruitment of Exo70 in both P2 and P3 fractions (compare H1 vs. Fw) while similar levels were present in the input control.

4.13 Discussion: the roles of the GEF-H1-RhoA signaling axis in mast cell exocytosis

Here, we define a regulatory role for the GEF-H1-RhoA signaling axis in mast cell granule exocytosis. Since Rho GTPases play a role in mast cell exocytosis, RhoGEFs, the upstream activators of Rho GTPases, were hypothesized to be important signal transducers from external stimuli. RhoGEFs have been shown to function in exocytosis in various cell types in conjunction with cytoskeleton remodeling [Manetz et al., 2001; Momboisse et al., 2010; Balamatsias et al., 2011; Qian et al., 2012; Sulimenko et al., 2015]. Therefore, we explored RhoGEFs in mast cells.

The roles of several specific RhoGEFs were investigated in mast cell exocytosis. By profiling RhoGEF expression in mast cells, Vav1, P-Rex1, α -PIX, β -PIX and GEF-H1 were selected as putative candidates. However, knockdown of Vav1, P-Rex1, α -PIX, or β -PIX did not markedly alter the granule movement or exocytosis in RBL-2H3 mast cells. Importantly for GEF-H1, its depletion significantly disrupted cell spreading, granule movement and exocytosis, together with defects in stress fiber formation without the loss of ruffling or lamellipodia in stimulated cells. GEF-H1 was found to exert its function in this pathway by downstream targeting of RhoA, but not Rac1. Re-introduction of either an RNA interference insensitive mutant of GEF-H1, or a constitutively active mutant of RhoA (Rho-G14V) restored normal morphology in GEF-H1-depleted cells. Moreover, the depletion of GEF-H1 led to the reduced formation of focal adhesions (FAs) after antigen stimulation; FAs were found to be involved in granule exocytosis as well, suggesting that FA formation may be one of the functionalities of the GEF-H1-RhoA signaling axis. The activation of GEF-H1 was linked to the Fc ϵ RI signaling pathway but was independent of microtubules dynamics. Instead, GEF-H1 activation relied on the Syk kinase; with the cell spreading, granule movement and exocytosis in stimulated RBL-2H3 cells were effectively blocked by the Syk inhibitor GS-9973. Inhibitors of other kinases including Src, Fyn, Lck, MEK1/2, PI3-kinase (PI3K) and FAK did not affect GEF-H1 activation. Lastly, a hypothesized interacting protein of the exocyst complex, Exo70, did not address its interaction with GEF-H1 during mast cell exocytosis. Altogether, the GEF-H1-RhoA signaling axis was demonstrated to be important in regulating mast cell exocytosis.

Figure 4.34 provides a schematic model of this signaling pathway based on the aforementioned results. Antigen stimulation triggers the aggregation of IgE-Fc ϵ RI complexes and

phosphorylation of ITAM in FcεRI, leading to the downstream activation of various signaling cascades. Src, Fyn, Lck, MEK1/2, PI3K, and FAK were not involved in the activation of GEF-H1. Instead, Syk was critical for the GEF-H1 activation; thus, aggregation of FcεRI leads to the activation of Syk which then leads to the action of GEF-H1. Previous studies have shown that GEF-H1 can be activated by phosphorylation by either tyrosine or serine/threonine kinases [Birkenfeld et al., 2008; Azoitei et al., 2019]. GEF-H1 exhibited an autoinhibitory domain (AID) containing a central tyrosine (Tyr198) surrounded by negatively charged and lipophilic residues, which was proposed to interact with the DH (Dbl homology) domain to retain its catalytic activity [Azoitei et al., 2019]. GEF-H1 can be activated by Src phosphorylation at Tyr198, leading to free the DH domain [Azoitei et al., 2019]. This was similar to the activation manner of another RhoGEF Vav1 at Tyr174 by phosphorylation to dissociate its DH domain from the AID of Vav1 [Yu et al., 2010]. Antigen stimulation in mast cells could either activate Syk directly, or active Lyn then activate Syk [Blank and Rivera, 2004; Sanderson et al., 2010]. Activated GEF-H1 subsequently activates RhoA, which regulates multiple RhoA-specific downstream events including granule movement, cell spreading/activation, formation of stress fibers and FAs. The inhibition of FA formation by the FAK inhibitor, PF-573228, significantly defects degranulation, suggesting FAs are an important downstream component of the GEF-H1-RhoA signaling axis to regulate the exocytosis outcomes.

Interestingly, disruption of microtubules dynamics using taxol or nocodazole did not significantly alter GEF-H1 activation in stimulated RBL-2H3 cells (**Figure 4.23**). GEF-H1 was found to be a microtubule-bound RhoGEF previously; binding of GEF-H1 to microtubules retained its GEF activity in various cells [Birkenfeld et al., 2008; Joo and Olson, 2020]; while treating with nocodazole dissociated the microtubules leading to the activation release of GEF-H1 [Chang et al., 2018; Kashyap et al., 2019]. GEF-H1 was also associated with microtubules with the aid of scaffolding proteins including 14-3-3 [Zenke et al., 2004] and Tctex-1 [Meiri et al., 2012]. Furthermore, certain kinases, such as PAK1 [Zenke et al., 2004] or PAK4 [Callow et al., 2005], can phosphorylate GEF-H1 at its inhibitory sites (Ser885 or Ser810) to retain its activity. Other studies indicated that GEF-H1 can be phosphorylated activated by certain kinases (i.e. ERK) at Thr678 [Fujishiro et al., 2008; Guilluy et al., 2011; Kakiashvili et al., 2009]. Therefore, there were two activation models of GEF-H1: protein phosphorylation and

microtubules dependent-regulation; either of them could work independently or cooperatively to mediate the activity of GEF-H1. In **Chapter 4**, the active levels of GEF-H1 were shown to significantly increase after antigen stimulation using the RhoA-G17A pull down assays (**Figure 4.22**) [García-Mata et al., 2006]; however, treating with nocodazole did not remarkably activate GEF-H1 after 10 min stimulation, although the active GEF-H1 level tended to increase (**Figure 4.23**). The localization manners of GEF-H1 did not markedly alter between the states of resting and stimulation (+/- microtubules-targeted drugs) (**Figure 4.24**), suggesting GEF-H1 was mainly pooled in cytosol in RBL-2H3 cells regardless of the dynamics of microtubules. This observation led to the dissecting of the Syk-dependent activation of GEF-H1 in stimulated RBL-2H3 cells thereafter (**Figure 4.30**). Since the activation of GEF-H1 was more robust in 20 min of stimulation (**Figure 4.22**), we could not rule out whether longer stimulation conjugating with nocodazole treatment did dramatically increase the active GEF-H1 levels. Further studies need to elucidate the impacts of MT dynamics and/or protein phosphorylation in the regulatory activation of GEF-H1. Taken together, the GEF-H1-RhoA signaling axis transduced the antigen stimulation signals from FcεRI to the exocytosis machinery in mast cells, which involved the formation of FAs.

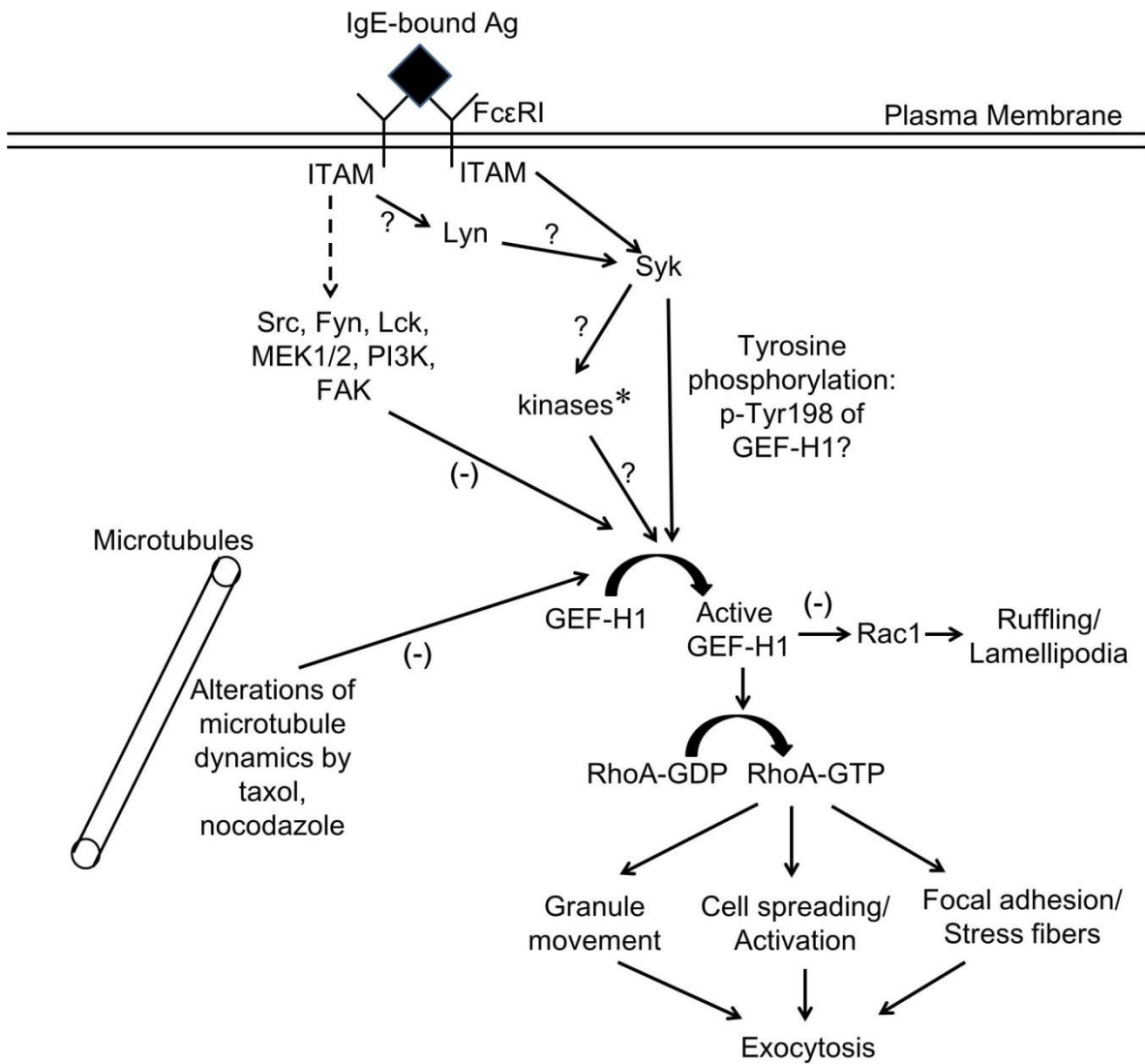


Figure 4.34 A putative model of the GEF-H1-RhoA signaling axis in RBL-2H3 cells of antigen stimulation. When antigen-stimulated, antigen triggers the aggregation of IgE-bound FcεRI. The intracellular ITAM domains in FcεRI are phosphorylated resulting in the activations of multiple downstream signaling cascades. Previous studies have shown the participation of various protein kinases during mast cell activation, including Src, Lyn, Syk, Fyn, Lck, MEK1/2, PI3-kinase and FAK. The activation of GEF-H1 was found to be dependent on the activity of Syk using specific kinase inhibitors. Although the exact activation mechanism of GEF-H1 in mast cells is unclear, our data supports activation signals from the FcεRI via Syk. To activate GEF-H1 it would be likely phosphorylated at Tyr-198 [Azoitei et al., 2019], or by other kinases such as Ser/Thr kinases (indicated with a “(*)” symbol), downstream of Syk. The active GEF-H1 subsequently turns on RhoA by facilitating its GTP loading, leading to the regulation of RhoA-specific downstream events including directed granule movement, cell spreading/activation likely through the formation of stress fibers and FAs. GEF-H1 did not regulate the activity of Rac1, with formations of surface ruffles and lamellipodia at the leading edges still occurring in GEF-H1-depleted cells (indicated with a “(-)” symbol). The inhibition of FAs by the FAK inhibitor PF-573228 significantly affected degranulation when stimulated, suggesting FAs exert a downstream event of the GEF-H1-RhoA signaling axis. Interestingly, alterations of microtubule dynamics using taxol or nocodazole did not significantly alter the activation levels of GEF-H1 in stimulated RBL-2H3 cells. Ag, antigen; ITAM, immunoreceptor tyrosine-based activation motifs. Solid arrows represented the activation flow, dashed arrows suggested the likelihoods of regulation. A “(-)” means negatively correlated. The question mark (“?”) suggested the possibilities.

4.14 Supplemental video list with links to online content

Video 4.1 LysoTracker Red live-cell imaging in stimulated cells of Scrambled shRNA (control)

https://drive.google.com/file/d/1jRYcVwVEh9nD_YgeoJJ7Kco3ICTFaPzF/view?usp=sharing

Video 4.2 LysoTracker Red live-cell imaging in stimulated RBL-2H3 cells of Vav1 knockdown

<https://drive.google.com/file/d/11ZqF9tRvNAXQfPXwb7DF33i8WH6-2goZ/view?usp=sharing>

Video 4.3 LysoTracker Red live-cell imaging in stimulated RBL-2H3 cells of P-Rex1 knockdown

https://drive.google.com/file/d/1ymsqkcA-EWLq6cxnLZ0u_bzQLXjnua0B/view?usp=sharing

Video 4.4 LysoTracker Red live-cell imaging in stimulated RBL-2H3 cells of α -PIX knockdown

<https://drive.google.com/file/d/1Q3AWRQiF0qE0EWWHW5JbLw4za0oqcf4j/view?usp=sharing>

Video 4.5 LysoTracker Red live-cell imaging in stimulated RBL-2H3 cells of β -PIX knockdown

<https://drive.google.com/file/d/1RWXCHaoDE3ABTgkQezTwZMYow0JHZJHa/view?usp=sharing>

Video 4.6 LysoTracker Red live-cell imaging in stimulated cells of FUGW

<https://drive.google.com/file/d/1mNPBrIyxNKtJMkUtIAnBDJPt5qN1WLYW/view?usp=sharing>

Video 4.7 LysoTracker Red live-cell imaging in stimulated cells of GEF-H1 knockdown

<https://drive.google.com/file/d/1Aa8FIrBJJ-AMVpWXga-BO2ecqlad0JqA/view?usp=sharing>

Video 4.8 Differential Interference Contrast (DIC) live-cell imaging in stimulated cells of FUGW

https://drive.google.com/file/d/1MgUAsJ4MX_4543WGhytpnL8Uz63ogDRZ/view?usp=sharing

Video 4.9 Differential Interference Contrast (DIC) live-cell imaging in stimulated cells of GEF-H1 knockdown

https://drive.google.com/file/d/1Kzc87PPqH_iiu6W32XWdK7QwN5w9WydE/view?usp=sharing

Video 4.10 Lifeact-mRuby live-cell imaging in stimulated cells of FUGW

https://drive.google.com/file/d/1IQni43sjVOu3LFIhcSvC4R0nz_j2ZPhR/view?usp=sharing

Video 4.11 Lifeact-mRuby live-cell imaging in stimulated cells of GEF-H1 knockdown

https://drive.google.com/file/d/1W8PPupWXz80xAFUJB-o89l57L7p6_kz_/view?usp=sharing

Chapter 5

Discussion and Future Directions

5.1 Discussion

5.1.1 Roles of microtubules (and associated motors) in mast cell degranulation

The role of the cytoskeleton in mast cell exocytosis has been of long-standing scientific interest. Early studies supported the functions of actin in this process, although actin has been shown to exhibit both positive and negative regulatory roles [Norman et al., 1996; Sullivan et al., 1999; Frigeri and Apgar, 1999; Eitzen, 2003; Dráber et al., 2012]. Emerging studies have demonstrated that microtubules function in the transport of granules via the long-track trafficking machinery in antigen-stimulated mast cells [Dráber et al., 2012; Munoz et al., 2016], and depolymerization of microtubules resulted in a significant reduction of exocytosis in antigen-stimulated mast cells [Nielsen and Johansen, 1986; Stanton et al., 2011; Ménasché et al., 2021]. Here in **Chapter 3**, we first investigated the roles of F-actin and microtubules remodeling in mast cell exocytosis using live-cell imaging to visualize the correlation between the cytoskeleton dynamics and granule trafficking. Polymerization of microtubules but not F-actin coordinated with the movement of secretory granules (**Figure 3.1**; [Video 3.1](#) and [Video 3.2](#)). Microtubules-directed drugs robustly disturbed granule movement during antigen stimulation and exocytosis, especially drugs that depolymerize microtubules (**Figure 3.2**). These observations led to the elucidation of the mechanism of microtubules-associated motors in mast cell exocytosis.

Our data regarding the essential roles of microtubule dynamics in mast cell exocytosis are in agreement with several previous studies [Martin-Verdeaux et al., 2003; Smith et al., 2003; Sulimenko et al., 2006; Hájková et al., 2011; Sulimenko et al., 2015; Klebanovych et al., 2019]. These studies suggest that microtubules critically function in regulating exocytosis by serving as long-distance trafficking tracks for motor proteins that transported secretory granules [Ménasché et al., 2021]. Microtubules-associated motor proteins occupy two large distinct families, dyneins and kinesins [Hirokawa, 1998; Roberts et al., 2013; Boucrot et al., 2005; Hirokawa et al., 2009]. Dyneins are well known for their role in retrograde transport from the microtubule plus end to

the minus end [Roberts et al., 2013], while kinesins conversely drive most cargos (i.e. secretory granules) from the cell body to periphery along microtubules [Vale et al., 1985; Hirokawa et al., 2009]. Thus, the likely roles of kinesin in exocytosis have been proposed, which are linked to neurosecretion or lysosome movement [Hirokawa et al., 2009]. However, the diverse roles of kinesins and their associated cargos or adaptor proteins in exocytosis are largely unclear. Kinesin-1, one of the kinesin family proteins, was found to mediate mast cell degranulation by driving Rab27b+ granules that depended on the activity of PI3-kinase [Munoz et al., 2016]. Here, we used a kinesin-1 specific modulator drug, kinesore [Randall et al., 2017], to further dissect the roles of kinesin-1 function in mast cell exocytosis. The inhibition effect of kinesore on both BMDCs and RBL-2H3 cell exocytosis (**Figure 3.3**) supports the involvement of kinesin-1 function in mast cell degranulation.

5.1.2 Microtubule-based motors and their cargo adaptor proteins

The microtubule-based trafficking machinery requires the engagement of certain motors and their cargo adaptor proteins [Kurowska et al., 2014; Fu and Holzbaur, 2004; Ménasché et al., 2021]. Disturbing the microtubule-motors association was proposed to inhibit this trafficking machinery [Kurowska et al., 2014]. In **Figure 3.3** and [Video 3.6](#) and [Video 3.7](#), treatment by kinesore caused the dysfunctional trafficking of granules to the cell periphery in antigen-stimulated RBL-2H3 cells ([Video 3.6](#)) while the actin remodeling was not impacted ([Video 3.7](#)). Moreover, kinesore treatment remodeled the microtubule network, generating extensive microtubule looping structures which were specific to the activation kinesin-1 function (especially its heavy chain kif5b) (**Figure 3.5**) [Randall et al., 2017]. Therefore, kinesore exhibited a specific modulation of the kinesin-1 motor function in stimulated RBL-2H3 cells, leading to the defects of granule movement and exocytosis.

The association of cargo adaptors with secretory granules is important for the granule transport in response to antigen-stimulation signals [Kurowska et al., 2014; Fu and Holzbaur, 2014]. The engagement of cargo adaptors with granules is likely a pivotal step for the activation of granule transport and exocytosis [Fu and Holzbaur, 2014]. Kinesins engage with a diverse set of cargo adaptors to exert transport functions [Hirokawa et al., 2009]; however, cargo adaptor specificity has remained elusive. Here, the expression of putative kinesin-1-associated cargo adaptors were

quantitatively detected in RBL-2H3 cells, leading to the consideration of SKIP (PLEKHM2) and Slp3 as likely functional candidates (**Figure 3.6**). Although JIP3 was found abundantly expressed (**Figure 3.6**), it mainly functions in vesicle transport in neurons [Fu and Holzbaur, 2014]. SKIP was the cargo adapter targeted by kinesore in HeLa cells [Randall et al., 2017], which participates in the kinesin-1 activation important for salmonella infection [Boucrot et al., 2005]. SKIP also serves as a scaffolding protein between lysosomal membrane proteins and the kinesin-1 motor, which regulates lysosomal transport and kinesin-1 activation [Rosa-Ferreira and Munro, 2011; Keren-Kaplan and Bonifacino, 2021; Ishida et al., 2015]. However, SKIP was undetectable by immunoblotting in RBL-2H3, indicating the likely unstable property of SKIP protein, leading to the difficulty in dissecting its exact roles during mast cell exocytosis (**Figure 3.6**). Slp3 was another kinesin-1-associated cargo adaptor associated with secretory granules (recognized by rat MCP II) during RBL-2H3 cell exocytosis. Kinesore treatment did not affect the association Slp3 with the granule fraction in the stimulated state (**Figure 3.6**). These data support kif5b, kinesin-1 heavy chain, as the specific target of kinesore, and Slp3 as a functional adaptor for secretory granules during mast cell exocytosis. All the data were consistent with those in BMDCs [Munoz et al., 2016]. Furthermore, Slp3 facilitates kinesin-1-based transport of terminal lytic granules in functional cytotoxic T lymphocytes [Kurowska et al., 2012]. However, the detailed roles of Slp3 and kif5b in kinesore-treated antigen-stimulated RBL-2H3 cells required further investigation. Genetic manipulation of either Slp3 or kif5b by RNA interference, or utilization of fluorescence-based labeling of Slp3 or kif5b with granules in stimulated mast cells, would provide useful tools to approach this question. Taken together, kinesore inhibited mast cell exocytosis and granule movement by disrupting kinesin-1 function, suggesting that the modulation of kinesin-1 function could be a potential intervention for mast cells-oriented allergies.

5.1.3 Roles of putative RhoGEFs in mast cell degranulation

The Rho proteins, RhoA and Rac1, have been reported to regulate mast cell degranulation (Sheshachalam et al., 2017); however, the RhoGEFs (Rho guanine nucleotide exchange factors), which are upstream activators of Rho proteins, that are involved in this process are still largely unclear. RhoGEFs exert diverse roles in multiple cellular processes and can be promiscuous in terms of the Rho protein(s) they activate [Cook et al., 2014; Schmidt and Hall, 2002]. By

profiling certain RhoGEFs in rat mast cells versus control cells by RT-PCR, Vav1 and P-Rex1 were found elusively expressed in both RBL-2H3 cells and BMMCs (**Figure 4.1**). Hence, it seemed rational that both of them might play important roles in mast cell degranulation. However, neither the singular knockdown of Vav1 or P-Rex1 (**Figure 4.3**), nor the double depletion of both Vav1 and P-Rex1 (**Figure 4.6B**), were shown to alter the antigen-stimulated degranulation in RBL-2H3 cells. The knockdown of either Vav1 or P-Rex1 did not alter the granule trafficking in RBL-2H3 cells (**Figure 4.5**; [Video 4.2](#) and [Video 4.3](#)). Conversely, previous studies have shown that Vav1 regulated degranulation via phospholipase C γ activation and calcium responses in mouse BMMCs [Manetz et al., 2001]. Reduced degranulation and cytokine production was also found in Vav1-deficient BMMCs [Manetz et al., 2001]. Our discrepancy regarding the role of Vav1 in mast cell degranulation likely can be attributed to the different usages of cells, since the heterogeneous properties of different mast cells were addressed as a pitfall for research [Passante and Frankish, 2009; Moon et al., 2010]. For the roles of α -PIX and β -PIX in regulating mast cell degranulation and granule trafficking in antigen-stimulated RBL-2H3 cells (**Figures 4.3 and 4.5**; [Video 4.4](#) and [Video 4.5](#)), there was no evidence supporting their important roles. β -PIX was found to modulate the synaptic vesicle trafficking [Sun and Bamji, 2011] and negatively regulated the degranulation (measured by β -glucuronidase release) in antigen-stimulated mouse BMMCs [Sulimenko et al., 2015]. The reason regarding the lack of regulatory roles in RBL-2H3 cells might be due to the differential measurement of mediators or the cell heterogeneity. Although the complete inhibition of Rac1 by EHT-1864 significantly reduced cell degranulation in both RBL-2H3 cells and mouse BMMCs [Sheshachalam et al., 2017], the incomplete blocking of Rac1 in the knockdown strains of Vav1, P-Rex1, α -PIX or β -PIX was likely responsible for their ineffective roles in regulating RBL-2H3 cell degranulation. One Rho protein could be tightly regulated by one or more RhoGEFs spatiotemporally [Cook et al., 2014], here, the activation of Rac1 in antigen-stimulated RBL-2H3 cells might be required for other crucial RhoGEFs. This functional redundancy needs further investigation.

The positive roles of GEF-H1 in regulating mast cell degranulation have been determined in this thesis (**Figures 4.8, 4.9 and 4.10 in Chapter 4**), revealing that the GEF-H1-RhoA signaling pathway could regulate cell spreading, stress fiber and focal adhesion formation, granule

trafficking during mast cell exocytosis. Our discoveries were consistent with a previous work done by Kosoff and colleagues [Kosoff et al., 2013]. In this study, PAK2 (P21-activated kinase 2) was found to negatively regulate the IgE-stimulated degranulation in bone marrow-derived mast cells (BMMCs). PAK2 triggered the inhibitory phosphorylation of GEF-H1 to reduce the downstream RhoA activity and related signaling events, leading to the reduction of mast cell exocytosis [Kosoff et al., 2013]. Other studies regarding the interactions between GEF-H1 and the exocyst were linked to regulate exocytosis [Pathak et al., 2012; Sáez et al., 2019; Ahmed et al., 2018; Wang et al., 2015]. Taken together, GEF-H1-mediated mast cell exocytosis was likely involved in various pathways; such underlying regulations would require further investigation.

5.1.4 GEF-H1 subcellular localization: interacted with microtubules

Previous studies have revealed that GEF-H1 was mainly a microtubule-bound RhoGEFs, with its PH and C-terminal coiled-coil domains required for such interactions [Birkenfeld et al., 2008; Joo and Olson, 2020]. The catalytic activity of GEF-H1 could be activated by the dissociation from microtubules, leading to the release of GEF-H1 from the microtubule-bound state to be cytosolic [Krendel et al., 2002]. The intracellular localization of GEF-H1 and its relationship with microtubules were completely unknown in mast cells. In **Figure 4.25 of Chapter 4**, there was no GEF-H1-microtubule interaction detected in antigen-stimulated RBL-2H3 cells, and no tubulin could be detected in a GEF-H1 immunoprecipitation. Moreover, the intracellular localization of GEF-H1 by immunofluorescence in RBL-2H3 cells of either resting or antigen-stimulated states showed mainly cytosolic distribution rather than microtubules-bound (**Figure 4.26**), even the application of microtubules-directed drugs (i.e. taxol, colchicine and nocodazole) did not alter the localization of GEF-H1 in stimulated RBL-2H3 cells. Interestingly, GEF-H1 was activated after antigen stimulation in a process that seemed to be independent of microtubules dynamics. Therefore, GEF-H1 in RBL-2H3 cells is likely regulated in a microtubules-independent manner, which may involve protein-protein interaction or protein phosphorylation as reported before [Birkenfeld et al., 2008].

5.1.5 GEF-H1 in actin remodeling

The depletion of GEF-H1 in RBL-2H3 cells triggered cells to round-up in the resting state, although the alteration of cell size was not significant. Cell spreading was disrupted when

antigen-stimulated (**Figure 4.10**). Together with results of live-cell imaging, the knockdown of GEF-H1, resulted in cells that did not obtain an activated phenotype when antigen-stimulated (**Figure 4.11**; [Video 4.6](#) and [Video 4.7](#)). This suggests that actin remodeling was targeted by GEF-H1 in the cell activation mechanism. GEF-H1 was found to be a RhoA-specific RhoGEF and not a Rac1-specific RhoGEF (**Figure 4.13**). As RhoA is a master regulator of the formation of stress fiber and focal adhesion [Chrzanowska-Wodnicka and Burridge, 1996; Ridley and Hall, 1992; Wozniak et al., 2004; Yamana et al., 2006], the actin remodeling in antigen-stimulated RBL-2H3 cells were considered to mainly rely on the functionality of RhoA. Knockdown of GEF-H1 inhibited the formation of stress fiber formation (**Figure 4.14**). Furthermore, re-introduction of either a GEF-H1 RNAi resistant construct (mCherry-GEF-H1-RNAi-Resi) or a constitutively active RhoA construct (RhoA-G14V) in GEF-H1-depleted RBL-2H3 cells, could restore cell size and the ability for cells to spread (**Figures 4.12** and **4.17**), suggesting the regulatory roles of GEF-H1 on actin remodeling was RhoA-dependent. The loss of RhoA activity prevented the spreading of cell spreading in stimulated RBL-2H3 cells since there was a lack of stress fiber formation and inadequate focal adhesions to facilitate the enlargement of cells [Ridley and Hall, 1992; Nobes and Hall, 1995; Wozniak et al., 2004].

5.1.6 GEF-H1-RhoA axis regulated focal adhesion

Focal adhesions (FAs) are adhesion complexes where integrin and proteoglycan mediated adhesion associations to the actin cytoskeleton [Wozniak et al., 2004]. The components of FAs are extremely diverse including scaffolding protein, structural molecules, GTPases, phosphatases, kinases, and lipases, which are regulated in response to various stimuli [Wozniak et al., 2004]. It was found that RhoA played important roles in regulating the formation of FAs for cell spreading [Gonon et al., 2005]. Moreover, there is some evidence that FAs and the focal adhesion kinase (FAK) may be involved in mast cell activation and degranulation under antigen stimulation [Kawasugi et al., 1995; Hamawy et al., 1997].

The positive roles of FAs remodeling and FAK activity in glucose-stimulated insulin secretion has been extensively studied [Rondas et al., 2011; Rondas et al., 2012; Cai et al., 2012; Arous et al. 2013]. FAK can regulate focal protein dynamics by controlling cortical F-actin depolymerization in response to glucose, leading to insufficient insulin granule trafficking

[Rondas et al., 2012; Cai et al., 2012]. Inhibition of FAK activity blocked glucose-induced actin cytoskeleton remodeling and trafficking of insulin granules to the plasma membrane [Rondas et al., 2012]. The β -cells of FAK knockout in mice exhibited dysfunctional insulin granule trafficking and secretion, together with the suppression of focal adhesion remodeling, and impaired F-actin depolymerization [Alenkvist et al., 2014; Cai et al., 2012]. Moreover, the exocyst, a master protein complex for granule tethering and docking [Wu and Guo, 2015], was found to co-localize and co-purify with FA complex proteins, which was responsible for the functions of FAs in exocytosis [Spiczka et al., 2008].

In **Chapter 4**, the formation of FAs in antigen-stimulated RBL-2H3 cells was found to be involved in degranulation. Inhibiting FA formation by the FAK inhibitor, PF-573228, significantly reduced degranulation. Since previous studies have shown GEF-H1 also regulates FAs formation, mainly via its downstream effector, RhoA [Nalbant et al., 2009; Huang et al., 2014; Sandí et al., 2017; Rafiq et al., 2019], here in **Figures 4.20** and **4.21**, the depletion of GEF-H1 caused a reduction in FA formation contributing to a degranulation defect. These results confirm the notion that the GEF-H1-RhoA axis regulates RBL-2H3 cell degranulation via targeting FA formation. Our studies are in agreement with the discoveries of FA involvement in glucose-stimulated insulin secretion [Rondas et al., 2011; Rondas et al., 2012; Cai et al., 2012; Arous et al. 2013]. Further studies would be required to elucidate the detailed regulatory mechanism of FAs in stimulated RBL-2H3 cells.

5.1.7 GEF-H1 activation by kinases in mast cells

GEF-H1 could be inhibited or activated through protein phosphorylation by various kinases, including p21-activated kinases 1/2/4 (PAK1/2/4), protein kinase A (PKA), polarity-regulating kinase partitioning-defective 1b (PAR1b), extracellular signal-regulated kinases (ERK), Aurora A/B, Cdk1/Cyclin B, PI3K (phosphoinositide 3-kinase), FAK (focal adhesion kinase), and Src in various circumstances [*see Chapter 1.5.3*], which are mostly independent of the microtubule dynamics. Here, by using various kinases inhibitors, the activation of GEF-H1 by phosphorylation was defined. Although the suppressions of Src and Lck (by Src I1), Fyn and Lck (by PP2), MEK (by PD98059), PI3K (by wortmannin), FAK (by PF-573328) exerted significant inhibitions of degranulation in antigen-stimulated RBL-2H3 cells (**Figures 4.18** and **4.27**), none

of these kinases seemed to be involved in the activation of GEF-H1 (**Figures 4.28**). The regulation of GEF-H1 by kinases is complex, since GEF-H1 has multiple phosphorylation sites that provide for both positive and negative regulation [Birkenfeld et al., 2008]. As a surface receptor-proximal kinase, Syk has been found to critically regulate mast cell degranulation and cytoskeleton remodeling [Gilfillan and Rivera, 2009; Blank and Rivera, 2004]. Here, Syk was revealed to critically regulate degranulation, granule localization, cell morphology, and especially GEF-H1 activation in antigen-stimulated RBL-2H3 cells (**Figures 4.29, 4.30 and 4.31**). Therefore, our data suggests the signaling pathway for degranulation in RBL-2H3 cells goes from the cell surface receptor, FcεRI, to the GEF-H1-RhoA axis with the participation of Syk, leading to the formation of focal adhesions involving the degranulation. However, the exact activation mechanism of GEF-H1 remains unknown though we suggest that it involves phosphorylation. Future assays regarding the identification of GEF-H1 phosphorylated sites after antigen-activation, or the application of GEF-H1 phosphorylated mutant constructs, need to be performed.

5.1.8 Interactions of GEF-H1: and roles of Exo70

GEF-H1 has been reported to interact with the exocyst complex (i.e. Exo70) [Inoue et al., 2003; Martin-Urdiroz et al., 2016; Ahmed et al., 2018; Sáez et al., 2019]. Here, Exo70 was hypothesized to be a target effector of the GEF-H1-RhoA axis in antigen-stimulated RBL-2H3 cells, since its roles have been revealed to critically regulate exocytosis in many cell types [Robinson et al., 1999; Wu et al., 2010; Wu and Guo, 2015]. However, Exo70 could not be found to directly interact or co-localize with GEF-H1 (**Figures 4.32 and 4.33**). The interaction between GEF-H1 and Exo70 (or the exocyst complex) might be transient or too weak that the application of detergents might disturb these interactions. By adopting the co-fractionation assay that enrich the granule fractions in **Figure 4.34**, it was found that the depletion of GEF-H1 in antigen-stimulated RBL-2H3 cells led to the reduced engagement of Exo70. Knockdown of GEF-H1 caused a reduction in the co-fractionation of Exo70 with granules, suggesting Exo70 might contribute to the functionalities of GEF-H1. Further studies will be required to dissect the role of Exo70 or other components of the exocyst complex and whether it is involved in the GEF-H1-RhoA axis during mast cell degranulation.

5.1.9 The crosstalk between microtubule dynamics and focal adhesions

The crosstalk between microtubule dynamics and focal adhesions has been recently examined [LaFlamme et al., 2018; Seetharaman and Etienne-Manneville, 2020]. Microtubules can mediate adhesion complex assembly and turnover, especially during cell migration [Bershadsky et al., 1996; Stehbens et al., 2012; Ng et al., 2014]. A number of proteins including liprins, KANKs (Ankyrin repeat domain-containing proteins), the kinesin family member KIF21A, CLASPs (CLIP-associating proteins), EB1 (end-binding protein 1) and LL5 β coordinate the association of microtubules with focal adhesions that border the plasma membrane [LaFlamme et al., 2018; Astro and de Curtis, 2015; Astro et al., 2016; Lansbergen et al., 2006; Bouchet et al., 2016; Stehbens et al., 2014; Zhang et al., 2016]. In addition, the Rho signaling pathway including RhoGEFs (i.e. GEF-H1, Tiam2, Asef) [Kawasaki et al., 2000; Rafiq et al., 2019; Rooney et al., 2010; Malliri, 2010] and Rho proteins [Chang et al., 2008] regulate such crosstalk, suggesting they have important roles. By contrast, the adhesion complex can also regulate microtubule dynamics [LaFlamme et al., 2018; Seetharaman and Etienne-Manneville, 2020]. The integrin components of focal adhesion were shown to promote microtubule nucleation, growth and stabilization, which contributed to the establishment of the front–rear polarity required for multiple cellular processes [LaFlamme et al., 2018; Colello et al., 2012; Palazzo et al., 2004]. Integrin-dependent signaling is known to facilitate microtubule stabilization at the leading edge [Colello et al., 2012; Palazzo et al., 2004]. In this thesis, microtubule dynamics and the motor kinesin-1 (**Chapter 3**), together with GEF-H1 and focal adhesion formation (**Chapter 4**), critically regulated mast cell exocytosis. There were likely crosstalk signalings between microtubule dynamics and GEF-H1 or focal adhesion during mast cell exocytosis. However, the activation of GEF-H1 was not shown to be microtubule-dependent (**Chapter 4**), suggesting there was unlikely a signal transduction mechanism acting from microtubule dynamics to the GEF-H1-RhoA pathway in antigen-stimulate mast cells. Conversely, focal adhesion formation regulated by the GEF-H1-RhoA signaling axis may regulate microtubule dynamics during mast cell degranulation; microtubule-based granule trafficking in stimulated mast cells was likely falicated by the GEF-H1-RhoA-focal adhesion pathway. However, such notions will require further investigation in future.

5.2 Future Directions

5.2.1 BioID/protein proximity ligation to dissect GEF-H1 interacting proteins

In this thesis, the interacting partners of GEF-H1 were still largely undefined in RBL-2H3 cells. Although it was found to be activated in a Syk-dependent manner after antigen stimulation (**Figure 4.31**), we do not know if GEF-H1 is a direct Syk substrate. Co-immunoprecipitation and mass spectrometry sequencing to examine protein-protein interactions were done using RBL-2H3 lysates, but the expected interacting partners such as exocyst components or FA components were not identified. The lack of interactions with GEF-H1 may be because of the detergent usage or the biochemical nature of interactions. GEF-H1 is a multidomain protein, suggesting its interaction manner might be internally regulated, requiring the help of scaffolding proteins. This is the case for GEF-H1 and Vav1 which are autoinhibited by an intramolecular interactions and scaffold interactions are known to maintain Vav1 in its active state [Azoitei et al., 2019; Yu et al., 2010; Sylvain et al., 2011]. Another reason might be transient or spatial-temporal interactions between GEF-H1 and its targeted patterns, leading to challenges in capturing the GEF-H1-interacting protein complex. Direct interaction between GEF-H1 and microtubules in RBL-2H3 cells was also not detected which might be due to the requirements of scaffolding proteins, such as 14-3-3 [Zenke et al., 2004] or Tctex-1 [Meiri et al., 2012].

To overcome the limitations of dissecting transient interacting patterns of GEF-H1, firstly, a proximity ligation/BioID conjugated with subdomains of GEF-H1 would be a highly suitable technique [Li et al., 2017]. Secondly, super-resolution microscopy would be a good technique to overcome spatial resolution challenges since interactions with FAs and the exocyst will be very spatially restricted [Liu et al., 2014].

5.2.2 Biosensor of GEF-H1 to dissect its activation manner

GEF-H1 has been shown to be activated via the dissociation of microtubules or perhaps dissociate from microtubules once activated by protein kinases. Our results in **Chapter 4** examined the involvement of FAK, MEK, PI3K, Src, Fyn, and Lck kinases which were ruled out. However, the receptor proximal kinase Syk was found to regulate the activation of GEF-H1. Considering the complex activation manner of GEF-H1, a sensitive assay would be to use a

GEF-H1 biosensor that reports specific GEF-H1 activating conditions spatially within cells [Azoitei et al., 2019]. The GEF-H1 fluorescent biosensor reports the release of autoinhibition via conformational change resulting in a decrease in FRET [Azoitei et al., 2019]. With this probe the details of GEF-H1 activation might be dissected.

5.2.3 Further investigate the role of Exo70 in mast cell degranulation

Although there is strong evidence demonstrating a functional interaction between GEF-H1 and Exo70 for exocytosis [Ahmed et al., 2018; Sáez et al., 2019], in RBL-2H3 cells we could not detect a direct interaction. Exo70 was found in granule enriched fractions and its recruitment seemed to be affected (reduced) by GEF-H1 depletion. This suggests Exo70 might be regulated by GEF-H1 during antigen-stimulated degranulation (**Figure 4.34**). The roles of Exo70, and by extension the exocyst complex, have been intensively studied to regulate exocytosis in many cell types but not mast cells [Robinson et al., 1999; Wu et al., 2010; Wu and Guo, 2015]. This could be examined through the generation of the knockdown of Exo70 (or other the exocyst components) to see its impacts on mast cell granule trafficking and exocytosis.

5.2.4 In vivo study: utilize primary mast cells of GEF-H1 knockout mice and dissect its role in allergic diseases

In **Chapter 4**, the roles of GEF-H1 in regulating RBL-2H3 cell activation and degranulation were investigated in vitro, and we presented multiple lines of evidence that GEF-H1 played roles in cell activation, actin remodeling and granule trafficking by targeting RhoA and the formation of stress fibers and focal adhesions. To further examine these roles of GEF-H1 and their physiological contribution to diseases, mouse models of allergic asthma [Takeda and Gelfand, 2009; Gold et al., 2015] or atopic dermatitis [Jin et al., 2009], works can be performed using the mouse model of GEF-H1 knockout [Chiang et al., 2014]. Knockout of GEF-H1 in these allergic mouse models and then examining the alteration of subsequent inflammatory responses would provide vital information on the importance of GEF-H1 in diseases. Mast cells can also be derived from these mouse models to perform in vitro studies since these cells are viable for several weeks and amenable to genetic manipulation (e.g. shRNA knockdown via viral transduction). It would be necessary in future directions to link GEF-H1 functions to allergic diseases and therapies.

Bibliography

Ahmed SM, Nishida-Fukuda H, Li Y, McDonald WH, Gradinaru CC, Macara IG. Exocyst dynamics during vesicle tethering and fusion. *Nat Commun.* 2018;9(1):5140.

Aijaz S, D'Atri F, Citi S, Balda MS, Matter K. Binding of GEF-H1 to the tight junction-associated adaptor cingulin results in inhibition of Rho signaling and G1/S phase transition. *Dev Cell.* 2005;8(5):777-86.

Akhmanova A, Steinmetz MO. Control of microtubule organization and dynamics: two ends in the limelight. *Nat Rev Mol Cell Biol.* 2015;16(12):711-26.

Alenkvist I, Dyachok O, Tian G, Li J, Mehrabanfar S, Jin Y, Birnir B, Tengholm A, Welsh M. Absence of Shb impairs insulin secretion by elevated FAK activity in pancreatic islets. *J Endocrinol.* 2014;223(3):267-75.

Arimura N, Kimura T, Nakamuta S, Taya S, Funahashi Y, Hattori A, Shimada A, Ménager C, Kawabata S, Fujii K, Iwamatsu A, Segal RA, Fukuda M, Kaibuchi K. Anterograde transport of TrkB in axons is mediated by direct interaction with Slp1 and Rab27. *Dev Cell.* 2009;16(5):675-86.

Arous C, Rondas D, Halban PA. Non-muscle myosin IIA is involved in focal adhesion and actin remodelling controlling glucose-stimulated insulin secretion. *Diabetologia.* 2013;56(4):792-802.

Astro V, de Curtis I. Plasma membrane-associated platforms: dynamic scaffolds that organize membrane-associated events. *Sci Signal.* 2015;8(367):re1.

Astro V, Tonoli D, Chiaretti S, Badanai S, Sala K, Zerial M, de Curtis I. Liprin- α 1 and ERC1 control cell edge dynamics by promoting focal adhesion turnover. *Sci Rep.* 2016;6:33653.

Azoitei ML, Noh J, Marston DJ, Roudot P, Marshall CB, Daugird TA, Lianza SL, Sandí MJ, Ikura M, Sondek J, Rottapel R, Hahn KM, Danuser G. Spatiotemporal dynamics of GEF-H1 activation controlled by microtubule- and Src-mediated pathways. *J Cell Biol.* 2019;218(9):3077-3097.

Baier A, Ndoh VN, Lacy P, Eitzen G. Rac1 and Rac2 control distinct events during antigen-stimulated mast cell exocytosis. *J Leukoc Biol.* 2014;95(5):763-774.

Balamatsias D, Kong AM, Waters JE, Sriratana A, Gurung R, Bailey CG, Rasko JE, Tiganis T, Macaulay SL, Mitchell CA. Identification of P-Rex1 as a novel Rac1-guanine nucleotide exchange factor (GEF) that promotes actin remodeling and GLUT4 protein trafficking in adipocytes. *J Biol Chem.* 2011;286(50):43229-40.

- Barsumian EL, Isersky C, Petrino MG, Siraganian RP. IgE-induced histamine release from rat basophilic leukemia cell lines: isolation of releasing and nonreleasing clones. *Eur J Immunol.* 1981;11(4):317-23.
- Benard V, Bokoch GM. Assay of Cdc42, Rac, and Rho GTPase activation by affinity methods. *Methods Enzymol.* 2002;345:349-59.
- Bershadsky A, Chausovsky A, Becker E, Lyubimova A, Geiger B. Involvement of microtubules in the control of adhesion-dependent signal transduction. *Curr Biol.* 1996;6(10):1279-89.
- Birkenfeld J, Nalbant P, Bohl BP, Pertz O, Hahn KM, Bokoch GM. GEF-H1 modulates localized RhoA activation during cytokinesis under the control of mitotic kinases. *Dev Cell.* 2007;12(5):699-712.
- Birkenfeld J, Nalbant P, Yoon SH, Bokoch GM. Cellular functions of GEF-H1, a microtubule-regulated Rho-GEF: is altered GEF-H1 activity a crucial determinant of disease pathogenesis? *Trends Cell Biol.* 2008;18(5):210-9.
- Birukova AA, Fu P, Xing J, Yakubov B, Cokic I, Birukov KG. Mechanotransduction by GEF-H1 as a novel mechanism of ventilator-induced vascular endothelial permeability. *Am J Physiol Lung Cell Mol Physiol.* 2010;298(6):L837-48.
- Bishop al., Hall A. Rho GTPases and their effector proteins. *Biochem J.* 2000;348 Pt 2(Pt 2):241-55.
- Blank U, Rivera J. The ins and outs of IgE-dependent mast-cell exocytosis. *Trends Immunol.* 2004;25(5):266-73.
- Borovikov YS, Norman JC, Price LS, Weeds A, Koffer A. Secretion from permeabilised mast cells is enhanced by addition of gelsolin: contrasting effects of endogenous gelsolin. *J Cell Sci.* 1995;108 (Pt 2):657-66.
- Bouchet BP, Gough RE, Ammon YC, van de Willige D, Post H, Jacquemet G, Altelaar AM, Heck AJ, Goult BT, Akhmanova A. Talin-KANK1 interaction controls the recruitment of cortical microtubule stabilizing complexes to focal adhesions. *Elife.* 2016;5:e18124.
- Boucrot E, Henry T, Borg JP, Gorvel JP, Méresse S. The intracellular fate of Salmonella depends on the recruitment of kinesin. *Science.* 2005;308(5725):1174-8.
- Bradding P, Arthur G. Mast cells in asthma--state of the art. *Clin Exp Allergy.* 2016;46(2):194-263.
- Burgoyne RD, Morgan A. Secretory granule exocytosis. *Physiol Rev.* 2003;83(2):581-632.

Bustelo XR. Vav family exchange factors: an integrated regulatory and functional view. *Small GTPases*. 2014;5(2):9.

Cai EP, Casimir M, Schroer SA, Luk CT, Shi SY, Choi D, Dai XQ, Hajmrle C, Spigelman AF, Zhu D, Gaisano HY, MacDonald PE, Woo M. In vivo role of focal adhesion kinase in regulating pancreatic β -cell mass and function through insulin signaling, actin dynamics, and granule trafficking. *Diabetes*. 2012;61(7):1708-18.

Callow MG, Zozulya S, Gishizky ML, Jallal B, Smeal T. PAK4 mediates morphological changes through the regulation of GEF-H1. *J Cell Sci*. 2005;118(Pt 9):1861-72.

Cao J, Yang T, Tang D, Zhou F, Qian Y, Zou X. Increased expression of GEF-H1 promotes colon cancer progression by RhoA signaling. *Pathol Res Pract*. 2019;215(5):1012-1019.

Chang YC, Nalbant P, Birkenfeld J, Chang ZF, Bokoch GM. GEF-H1 couples nocodazole-induced microtubule disassembly to cell contractility via RhoA. *Mol Biol Cell*. 2008;19(5):2147-53.

Chen Z, Borek D, Padrick SB, Gomez TS, Metlagel Z, Ismail AM, Umetani J, Billadeau DD, Otwinowski Z, Rosen MK. Structure and control of the actin regulatory WAVE complex. *Nature*. 2010;468(7323):533-8.

Chiang HS, Zhao Y, Song JH, Liu S, Wang N, Terhorst C, Sharpe AH, Basavappa M, Jeffrey KL, Reinecker HC. GEF-H1 controls microtubule-dependent sensing of nucleic acids for antiviral host defenses. *Nat Immunol*. 2014;15(1):63-71.

Chrzanowska-Wodnicka M, Burridge K. Rho-stimulated contractility drives the formation of stress fibers and focal adhesions. *J Cell Biol*. 1996;133(6):1403-15.

Cochrane DE, Douglas WW. Calcium-induced extrusion of secretory granules (exocytosis) in mast cells exposed to 48-80 or the ionophores A-23187 and X-537A. *Proc Natl Acad Sci U S A*. 1974;71(2):408-12.

Cohen R, Corwith K, Holowka D, Baird B. Spatiotemporal resolution of mast cell granule exocytosis reveals correlation with Ca^{2+} wave initiation. *J Cell Sci*. 2012;125(Pt 12):2986-94.

Colello D, Mathew S, Ward R, Pumiglia K, LaFlamme SE. Integrins regulate microtubule nucleating activity of centrosome through mitogen-activated protein kinase/extracellular signal-regulated kinase/extracellular signal-regulated kinase (MEK/ERK) signaling. *J Biol Chem*. 2012;287(4):2520-30.

Colin-York H, Li D, Korobchevskaya K, Chang VT, Betzig E, Eggeling C, Fritzsche M. Cytoskeletal actin patterns shape mast cell activation. *Commun Biol*. 2019;2:93.

Collins C, Guilluy C, Welch C, O'Brien ET, Hahn K, Superfine R, Burridge K, Tzima E. Localized tensional forces on PECAM-1 elicit a global mechanotransduction response via the integrin-RhoA pathway. *Curr Biol.* 2012;22(22):2087-94.

Conte IL, Hellen N, Bierings R, Mashanov GI, Manneville JB, Kiskin NI, Hannah MJ, Molloy JE, Carter T. Interaction between MyRIP and the actin cytoskeleton regulates Weibel-Palade body trafficking and exocytosis. *J Cell Sci.* 2016;129(3):592-603.

Cook DR, Rossman KL, Der CJ. Rho guanine nucleotide exchange factors: regulators of Rho GTPase activity in development and disease. *Oncogene.* 2014;33(31):4021-35.

Costello PS, Turner M, Walters AE, Cunningham CN, Bauer PH, Downward J, Tybulewicz VL. Critical role for the tyrosine kinase Syk in signalling through the high affinity IgE receptor of mast cells. *Oncogene.* 1996;13(12):2595-605.

da Silva EZ, Jamur MC, Oliver C. Mast cell function: a new vision of an old cell. *J Histochem Cytochem.* 2014;62(10):698-738.

Dahlin JS, Hallgren J. Mast cell progenitors: origin, development and migration to tissues. *Mol Immunol.* 2015;63(1):9-17.

Deng Z, Zink T, Chen HY, Walters D, Liu FT, Liu GY. Impact of actin rearrangement and degranulation on the membrane structure of primary mast cells: a combined atomic force and laser scanning confocal microscopy investigation. *Biophys J.* 2009;96(4):1629-39.

Derivery E, Gautreau A. Generation of branched actin networks: assembly and regulation of the N-WASP and WAVE molecular machines. *Bioessays.* 2010;32(2):119-31.

Desai A, Mitchison TJ. Microtubule polymerization dynamics. *Annu Rev Cell Dev Biol.* 1997;13:83-117.

Dráber P, Sulimenko V, Dráberová E. Cytoskeleton in mast cell signaling. *Front Immunol.* 2012;3:130.

Eitzen G. Actin remodeling to facilitate membrane fusion. *Biochim Biophys Acta.* 2003;1641(2-3):175-81.

El-Sibai M, Backer JM. Phospholipase C gamma negatively regulates Rac/Cdc42 activation in antigen-stimulated mast cells. *Eur J Immunol.* 2007;37(1):261-70.

Etienne-Manneville S, Hall A. Rho GTPases in cell biology. *Nature.* 2002;420(6916):629-35.

Eva A, Aaronson SA. Isolation of a new human oncogene from a diffuse B-cell lymphoma. *Nature.* 1985;316(6025):273-5.

Fletcher DA, Mullins RD. Cell mechanics and the cytoskeleton. *Nature*. 2010;463(7280):485-92.

Frigeri L, Apgar JR. The role of actin microfilaments in the down-regulation of the degranulation response in RBL-2H3 mast cells. *J Immunol*. 1999;162(4):2243-50.

Fu MM, Holzbaur EL. Integrated regulation of motor-driven organelle transport by scaffolding proteins. *Trends Cell Biol*. 2014;24(10):564-74.

Fujishiro SH, Tanimura S, Mure S, Kashimoto Y, Watanabe K, Kohno M. ERK1/2 phosphorylate GEF-H1 to enhance its guanine nucleotide exchange activity toward RhoA. *Biochem Biophys Res Commun*. 2008;368(1):162-7.

Gadea G, Blangy A. Dock-family exchange factors in cell migration and disease. *Eur J Cell Biol*. 2014;93(10-12):466-77.

Galli SJ, Tsai M, Piliponsky AM. The development of allergic inflammation. *Nature*. 2008;454(7203):445-54.

Galli SJ, Tsai M. IgE and mast cells in allergic disease. *Nat Med*. 2012;18(5):693-704.

Garcia-Mata R, Boulter E, Burridge K. The 'invisible hand': regulation of RHO GTPases by RHOGDIs. *Nat Rev Mol Cell Biol*. 2011;12(8):493-504.

García-Mata R, Wennerberg K, Arthur WT, Noren NK, Ellerbroek SM, Burridge K. Analysis of activated GAPs and GEFs in cell lysates. *Methods Enzymol*. 2006;406:425-37.

Gasman S, Chasserot-Golaz S, Malacombe M, Way M, Bader MF. Regulated exocytosis in neuroendocrine cells: a role for subplasmalemmal Cdc42/N-WASP-induced actin filaments. *Mol Biol Cell*. 2004;15(2):520-31.

Gibson S, Miller HR. Mast cell subsets in the rat distinguished immunohistochemically by their content of serine proteinases. *Immunology*. 1986;58(1):101-4.

Gilfillan AM, Rivera J. The tyrosine kinase network regulating mast cell activation. *Immunol Rev*. 2009;228(1):149-69.

Glaven JA, Whitehead IP, Nomanbhoy T, Kay R, Cerione RA. Lfc and Lsc oncoproteins represent two new guanine nucleotide exchange factors for the Rho GTP-binding protein. *J Biol Chem*. 1996;271(44):27374-81.

Gold M, Marsolais D, Blanchet MR. Mouse models of allergic asthma. *Methods Mol Biol*. 2015;1220:503-19.

Gonon EM, Skalski M, Kean M, Coppolino MG. SNARE-mediated membrane traffic modulates RhoA-regulated focal adhesion formation. *FEBS Lett.* 2005;579(27):6169-78.

Guillemot L, Paschoud S, Jond L, Foglia A, Citi S. Paracingulin regulates the activity of Rac1 and RhoA GTPases by recruiting Tiam1 and GEF-H1 to epithelial junctions. *Mol Biol Cell.* 2008;19(10):4442-53.

Guilluy C, Swaminathan V, Garcia-Mata R, O'Brien ET, Superfine R, Burridge K. The Rho GEFs LARG and GEF-H1 regulate the mechanical response to force on integrins. *Nat Cell Biol.* 2011;13(6):722-7.

Guo F, Tang J, Zhou Z, Dou Y, Van Lonkhuyzen D, Gao C, Huan J. GEF-H1-RhoA signaling pathway mediates LPS-induced NF- κ B transactivation and IL-8 synthesis in endothelial cells. *Mol Immunol.* 2012;50(1-2):98-107.

Guo W, Grant A, Novick P. Exo84p is an exocyst protein essential for secretion. *J Biol Chem.* 1999;274(33):23558-64.

Hahne P, Sechi A, Benesch S, Small JV. Scar/WAVE is localised at the tips of protruding lamellipodia in living cells. *FEBS Lett.* 2001;492(3):215-20.

Hájková Z, Bugajev V, Dráberová E, Vinopal S, Dráberová L, Janáček J, Dráber P, Dráber P. STIM1-directed reorganization of microtubules in activated mast cells. *J Immunol.* 2011;186(2):913-23.

Hall A. Rho GTPases and the actin cytoskeleton. *Science.* 1998;279(5350):509-14.

Hamawy MM, Swieter M, Mergenhagen SE, Siraganian RP. Reconstitution of high affinity IgE receptor-mediated secretion by transfecting protein tyrosine kinase pp125FAK. *J Biol Chem.* 1997;272(48):30498-503.

Hawkins T, Mirigian M, Selcuk Yasar M, Ross JL. Mechanics of microtubules. *J Biomech.* 2010;43(1):23-30.

Hirokawa N. Kinesin and dynein superfamily proteins and the mechanism of organelle transport. *Science.* 1998;279(5350):519-26.

Hirokawa N, Noda Y, Tanaka Y, Niwa S. Kinesin superfamily motor proteins and intracellular transport. *Nat Rev Mol Cell Biol.* 2009;10(10):682-96.

Hodge RG, Ridley AJ. Regulating Rho GTPases and their regulators. *Nat Rev Mol Cell Biol.* 2016;17(8):496-510.

Holowka D, Sheets ED, Baird B. Interactions between Fc(epsilon)RI and lipid raft components are regulated by the actin cytoskeleton. *J Cell Sci.* 2000;113 (Pt 6):1009-19.

Hong-Geller E, Cerione RA. Cdc42 and Rac stimulate exocytosis of secretory granules by activating the IP(3)/calcium pathway in RBL-2H3 mast cells. *J Cell Biol.* 2000;148(3):481-94.

Hong-Geller E, Holowka D, Siraganian RP, Baird B, Cerione RA. Activated Cdc42/Rac reconstitutes Fcepsilon RI-mediated Ca²⁺ mobilization and degranulation in mutant RBL mast cells. *Proc Natl Acad Sci U S A.* 2001;98(3):1154-9.

Huang IH, Hsiao CT, Wu JC, Shen RF, Liu CY, Wang YK, Chen YC, Huang CM, del Álamo JC, Chang ZF, Tang MJ, Khoo KH, Kuo JC. GEF-H1 controls focal adhesion signaling that regulates mesenchymal stem cell lineage commitment. *J Cell Sci.* 2014;127(Pt 19):4186-200.

Inoue H, Nojima H, Okayama H. High efficiency transformation of *Escherichia coli* with plasmids. *Gene.* 1990;96(1):23-8.

Inoue M, Chang L, Hwang J, Chiang SH, Saltiel AR. The exocyst complex is required for targeting of Glut4 to the plasma membrane by insulin. *Nature.* 2003;422(6932):629-33.

Ishida M, Ohbayashi N, Fukuda M. Rab1A regulates anterograde melanosome transport by recruiting kinesin-1 to melanosomes through interaction with SKIP. *Sci Rep.* 2015;5:8238.

Jin H, He R, Oyoshi M, Geha RS. Animal models of atopic dermatitis. *J Invest Dermatol.* 2009;129(1):31-40.

Joo E, Olson MF. Regulation and functions of the RhoA regulatory guanine nucleotide exchange factor GEF-H1. *Small GTPases.* 2020:1-14.

Kakiashvili E, Dan Q, Vandermeer M, Zhang Y, Waheed F, Pham M, Szászi K. The epidermal growth factor receptor mediates tumor necrosis factor-alpha-induced activation of the ERK/GEF-H1/RhoA pathway in tubular epithelium. *J Biol Chem.* 2011;286(11):9268-79.

Kakiashvili E, Speight P, Waheed F, Seth R, Lodyga M, Tanimura S, Kohno M, Rotstein OD, Kapus A, Szászi K. GEF-H1 mediates tumor necrosis factor-alpha-induced Rho activation and myosin phosphorylation: role in the regulation of tubular paracellular permeability. *J Biol Chem.* 2009;284(17):11454-66.

Kang MG, Guo Y, Haganir RL. AMPA receptor and GEF-H1/Lfc complex regulates dendritic spine development through RhoA signaling cascade. *Proc Natl Acad Sci U S A.* 2009;106(9):3549-54.

Kashyap AS, Fernandez-Rodriguez L, Zhao Y, Monaco G, Trefny MP, Yoshida N, Martin K, Sharma A, Olieric N, Shah P, Stanczak M, Kirchhammer N, Park SM, Wieckowski S, Laubli H, Zagani R, Kasenda B, Steinmetz MO, Reinecker HC, Zippelius A. GEF-H1 Signaling upon Microtubule Destabilization Is Required for Dendritic Cell Activation and Specific Anti-tumor Responses. *Cell Rep.* 2019;28(13):3367-3380.e8.

Kawasaki Y, Senda T, Ishidate T, Koyama R, Morishita T, Iwayama Y, Higuchi O, Akiyama T. Asef, a link between the tumor suppressor APC and G-protein signaling. *Science.* 2000;289(5482):1194-7.

Kawasugi K, French PW, Penny R, Ludowyke RI. Focal adhesion formation is associated with secretion of allergic mediators. *Cell Motil Cytoskeleton.* 1995;31(3):215-24.

Keren-Kaplan T, Bonifacino JS. ARL8 Relieves SKIP Autoinhibition to Enable Coupling of Lysosomes to Kinesin-1. *Curr Biol.* 2021;31(3):540-554.e5.

Klebanovych A, Sládková V, Sulimenko T, Vosecká V, Čapek M, Dráberová E, Dráber P, Sulimenko V. Regulation of Microtubule Nucleation in Mouse Bone Marrow-Derived Mast Cells by Protein Tyrosine Phosphatase SHP-1. *Cells.* 2019;8(4):345.

Klein O, Krier-Burris RA, Lazki-Hagenbach P, Gorzalczany Y, Mei Y, Ji P, Bochner BS, Sagi-Eisenberg R. Mammalian diaphanous-related formin 1 (mDia1) coordinates mast cell migration and secretion through its actin-nucleating activity. *J Allergy Clin Immunol.* 2019;144(4):1074-1090.

Köberle M, Kaesler S, Kempf W, Wölbing F, Biedermann T. Tetraspanins in mast cells. *Front Immunol.* 2012;3:106.

Kokkonen JO, Kovanen PT. Low density lipoprotein degradation by rat mast cells. Demonstration of extracellular proteolysis caused by mast cell granules. *J Biol Chem.* 1985;260(27):14756-63.

Kosoff R, Chow HY, Radu M, Chernoff J. Pak2 kinase restrains mast cell FcεRI receptor signaling through modulation of Rho protein guanine nucleotide exchange factor (GEF) activity. *J Biol Chem.* 2013;288(2):974-83.

Krendel M, Zenke FT, Bokoch GM. Nucleotide exchange factor GEF-H1 mediates cross-talk between microtubules and the actin cytoskeleton. *Nat Cell Biol.* 2002;4(4):294-301.

Krugmann S, Jordens I, Gevaert K, Driessens M, Vandekerckhove J, Hall A. Cdc42 induces filopodia by promoting the formation of an IRSp53:Mena complex. *Curr Biol.* 2001;11(21):1645-55.

Krystel-Whittemore M, Dileepan KN, Wood JG. Mast Cell: A Multi-Functional Master Cell. *Front Immunol.* 2016;6:620.

Kulczycki A Jr, Isersky C, Metzger H. The interaction of IgE with rat basophilic leukemia cells. I. Evidence for specific binding of IgE. *J Exp Med.* 1974;139(3):600-16.

Kunimura K, Uruno T, Fukui Y. DOCK family proteins: key players in immune surveillance mechanisms. *Int Immunol.* 2020;32(1):5-15.

Kuo JC, Han X, Yates JR 3rd, Waterman CM. Isolation of focal adhesion proteins for biochemical and proteomic analysis. *Methods Mol Biol.* 2012;757:297-323.

Kurowska M, Goudin N, Nehme NT, Court M, Garin J, Fischer A, de Saint Basile G, Ménasché G. Terminal transport of lytic granules to the immune synapse is mediated by the kinesin-1/Slp3/Rab27a complex. *Blood.* 2012;119(17):3879-89.

Kutys ML, Yamada KM. Rho GEFs and GAPs: emerging integrators of extracellular matrix signaling. *Small GTPases.* 2015;6(1):16-9.

LaFlamme SE, Mathew-Steiner S, Singh N, Colello-Borges D, Nieves B. Integrin and microtubule crosstalk in the regulation of cellular processes. *Cell Mol Life Sci.* 2018;75(22):4177-4185.

Lacy P. The role of Rho GTPases and SNAREs in mediator release from granulocytes. *Pharmacol Ther.* 2005;107(3):358-76.

Lansbergen G, Grigoriev I, Mimori-Kiyosue Y, Ohtsuka T, Higa S, Kitajima I, Demmers J, Galjart N, Houtsmuller AB, Grosveld F, Akhmanova A. CLASPs attach microtubule plus ends to the cell cortex through a complex with LL5beta. *Dev Cell.* 2006;11(1):21-32.

Lebensohn AM, Kirschner MW. Activation of the WAVE complex by coincident signals controls actin assembly. *Mol Cell.* 2009;36(3):512-24.

Leonard BJ, Eccleston E, Jones D, Lowe J, Turner E. Basophilic leukemia in the rat induced by a -chloroethylamine--ICI 42464. *J Pathol.* 1971;103(2):Pxxv.

Li P, Li J, Wang L, Di LJ. Proximity Labeling of Interacting Proteins: Application of BioID as a Discovery Tool. *Proteomics.* 2017;17(20).

Liao YC, Ruan JW, Lua I, Li MH, Chen WL, Wang JR, Kao RH, Chen JH. Overexpressed hPTTG1 promotes breast cancer cell invasion and metastasis by regulating GEF-H1/RhoA signalling. *Oncogene.* 2012;31(25):3086-97.

- Lim KB, Bu W, Goh WI, Koh E, Ong SH, Pawson T, Sudhaharan T, Ahmed S. The Cdc42 effector IRSp53 generates filopodia by coupling membrane protrusion with actin dynamics. *J Biol Chem*. 2008;283(29):20454-72.
- Livak KJ, Schmittgen TD. Analysis of relative gene expression data using real-time quantitative PCR and the $2^{-\Delta\Delta C(T)}$ Method. *Methods*. 2001;25(4):402-8.
- Liu J, Yue P, Artym VV, Mueller SC, Guo W. The role of the exocyst in matrix metalloproteinase secretion and actin dynamics during tumor cell invadopodia formation. *Mol Biol Cell*. 2009;20(16):3763-71.
- Liu Z, Xing D, Su QP, Zhu Y, Zhang J, Kong X, Xue B, Wang S, Sun H, Tao Y, Sun Y. Super-resolution imaging and tracking of protein-protein interactions in sub-diffraction cellular space. *Nat Commun*. 2014;5:4443.
- Mackay DJ, Hall A. Rho GTPases. *J Biol Chem*. 1998;273(33):20685-8.
- Madaule P, Axel R. A novel ras-related gene family. *Cell*. 1985;41(1):31-40.
- Malacombe M, Bader MF, Gasman S. Exocytosis in neuroendocrine cells: new tasks for actin. *Biochim Biophys Acta*. 2006;1763(11):1175-83.
- Manetz TS, Gonzalez-Espinosa C, Arudchandran R, Xirasagar S, Tybulewicz V, Rivera J. Vav1 regulates phospholipase cgamma activation and calcium responses in mast cells. *Mol Cell Biol*. 2001;21(11):3763-74.
- Martin-Urdiroz M, Deeks MJ, Horton CG, Dawe HR, Jourdain I. The Exocyst Complex in Health and Disease. *Front Cell Dev Biol*. 2016;4:24.
- Martin-Verdeaux S, Pombo I, Iannascoli B, Roa M, Varin-Blank N, Rivera J, Blank U. Evidence of a role for Munc18-2 and microtubules in mast cell granule exocytosis. *J Cell Sci*. 2003;116(Pt 2):325-34.
- Meiri D, Marshall CB, Greeve MA, Kim B, Balan M, Suarez F, Bakal C, Wu C, Larose J, Fine N, Ikura M, Rottapel R. Mechanistic insight into the microtubule and actin cytoskeleton coupling through dynein-dependent RhoGEF inhibition. *Mol Cell*. 2012;45(5):642-55.
- Meiri D, Marshall CB, Mokady D, LaRose J, Mullin M, Gingras AC, Ikura M, Rottapel R. Mechanistic insight into GPCR-mediated activation of the microtubule-associated RhoA exchange factor GEF-H1. *Nat Commun*. 2014;5:4857.
- Ménasché G, Longé C, Bratti M, Blank U. Cytoskeletal Transport, Reorganization, and Fusion Regulation in Mast Cell-Stimulus Secretion Coupling. *Front Cell Dev Biol*. 2021;9:652077

- Merriam EB, Millette M, Lumbard DC, Saengsawang W, Fothergill T, Hu X, Ferhat L, Dent EW. Synaptic regulation of microtubule dynamics in dendritic spines by calcium, F-actin, and drebrin. *J Neurosci*. 2013;33(42):16471-82.
- Metcalf DD, Boyce JA. Mast cell biology in evolution. *J Allergy Clin Immunol*. 2006;117(6):1227-9.
- Mitchell T, Lo A, Logan MR, Lacy P, Eitzen G. Primary granule exocytosis in human neutrophils is regulated by Rac-dependent actin remodeling. *Am J Physiol Cell Physiol*. 2008;295(5):C1354-65.
- Mitin N, Roberts PJ, Chenette EJ, Der CJ. Posttranslational lipid modification of Rho family small GTPases. *Methods Mol Biol*. 2012;827:87-95.
- Momboisse F, Ory S, Ceridono M, Calco V, Vitale N, Bader MF, Gasman S. The Rho guanine nucleotide exchange factors Intersectin 1L and β -Pix control calcium-regulated exocytosis in neuroendocrine PC12 cells. *Cell Mol Neurobiol*. 2010;30(8):1327-33.
- Montagnac G, Sibarita JB, Loubéry S, Daviet L, Romao M, Raposo G, Chavrier P. ARF6 Interacts with JIP4 to control a motor switch mechanism regulating endosome traffic in cytokinesis. *Curr Biol*. 2009;19(3):184-95.
- Moon TC, St Laurent CD, Morris KE, Marcet C, Yoshimura T, Sekar Y, Befus AD. Advances in mast cell biology: new understanding of heterogeneity and function. *Mucosal Immunol*. 2010;3(2):111-28.
- Morgan A, Burgoyne RD, Barclay JW, Craig TJ, Prescott GR, Ciufo LF, Evans GJ, Graham ME. Regulation of exocytosis by protein kinase C. *Biochem Soc Trans*. 2005;33(Pt 6):1341-4.
- Morgera F, Sallah MR, Dubuke ML, Gandhi P, Brewer DN, Carr CM, Munson M. Regulation of exocytosis by the exocyst subunit Sec6 and the SM protein Sec1. *Mol Biol Cell*. 2012;23(2):337-46.
- Mukai K, Tsai M, Saito H, Galli SJ. Mast cells as sources of cytokines, chemokines, and growth factors. *Immunol Rev*. 2018;282(1):121-150.
- Munoz I, Danelli L, Claver J, Goudin N, Kurowska M, Madera-Salcedo IK, Huang JD, Fischer A, González-Espinosa C, de Saint Basile G, Blank U, Ménasché G. Kinesin-1 controls mast cell degranulation and anaphylaxis through PI3K-dependent recruitment to the granular Slp3/Rab27b complex. *J Cell Biol*. 2016;215(2):203-216.
- Naal RM, Tabb J, Holowka D, Baird B. In situ measurement of degranulation as a biosensor based on RBL-2H3 mast cells. *Biosens Bioelectron*. 2004;20(4):791-6.

- Nalbant P, Chang YC, Birkenfeld J, Chang ZF, Bokoch GM. Guanine nucleotide exchange factor-H1 regulates cell migration via localized activation of RhoA at the leading edge. *Mol Biol Cell*. 2009;20(18):4070-82.
- Narasimhan V, Holowka D, Baird B. Microfilaments regulate the rate of exocytosis in rat basophilic leukemia cells. *Biochem Biophys Res Commun*. 1990;171(1):222-9.
- Ng DH, Humphries JD, Byron A, Millon-Frémillon A, Humphries MJ. Microtubule-dependent modulation of adhesion complex composition. *PLoS One*. 2014;9(12):e115213.
- Nielsen EH, Johansen T. Effects of dimethylsulfoxide (DMSO), nocodazole, and taxol on mast cell histamine secretion. *Acta Pharmacol Toxicol (Copenh)*. 1986;59(3):214-9.
- Nightingale TD, White IJ, Doyle EL, Turmaine M, Harrison-Lavoie KJ, Webb KF, Cramer LP, Cutler DF. Actomyosin II contractility expels von Willebrand factor from Weibel-Palade bodies during exocytosis. *J Cell Biol*. 2011;194(4):613-29.
- Nishida K, Yamasaki S, Ito Y, Kabu K, Hattori K, Tezuka T, Nishizumi H, Kitamura D, Goitsuka R, Geha RS, Yamamoto T, Yagi T, Hirano T. Fc ϵ RI-mediated mast cell degranulation requires calcium-independent microtubule-dependent translocation of granules to the plasma membrane. *J Cell Biol*. 2005;170(1):115-26.
- Nobes CD, Hall A. Rho, rac, and cdc42 GTPases regulate the assembly of multimolecular focal complexes associated with actin stress fibers, lamellipodia, and filopodia. *Cell*. 1995;81(1):53-62.
- Noordstra I, Akhmanova A. Linking cortical microtubule attachment and exocytosis. *F1000Res*. 2017;6:469.
- Norman JC, Price LS, Ridley AJ, Koffer A. The small GTP-binding proteins, Rac and Rho, regulate cytoskeletal organization and exocytosis in mast cells by parallel pathways. *Mol Biol Cell*. 1996;7(9):1429-42.
- Ogawa K, Tanaka Y, Uruno T, Duan X, Harada Y, Sanematsu F, Yamamura K, Terasawa M, Nishikimi A, Côté JF, Fukui Y. DOCK5 functions as a key signaling adaptor that links Fc ϵ RI signals to microtubule dynamics during mast cell degranulation. *J Exp Med*. 2014;211(7):1407-19.
- Oka T, Hori M, Ozaki H. Microtubule disruption suppresses allergic response through the inhibition of calcium influx in the mast cell degranulation pathway. *J Immunol*. 2005;174(8):4584-9.
- Oka T, Sato K, Hori M, Ozaki H, Karaki H. Fc ϵ RI cross-linking-induced actin assembly mediates calcium signalling in RBL-2H3 mast cells. *Br J Pharmacol*. 2002;136(6):837-46.

Ory S, Gasman S. Rho GTPases and exocytosis: what are the molecular links? *Semin Cell Dev Biol.* 2011;22(1):27-32.

Palazzo AF, Eng CH, Schlaepfer DD, Marcantonio EE, Gundersen GG. Localized stabilization of microtubules by integrin- and FAK-facilitated Rho signaling. *Science.* 2004;303(5659):836-9.

Parravicini V, Gadina M, Kovarova M, Odom S, Gonzalez-Espinosa C, Furumoto Y, Saitoh S, Samelson LE, O'Shea JJ, Rivera J. Fyn kinase initiates complementary signals required for IgE-dependent mast cell degranulation. *Nat Immunol.* 2002;3(8):741-8.

Passante E, Frankish N. The RBL-2H3 cell line: its provenance and suitability as a model for the mast cell. *Inflamm Res.* 2009;58(11):737-45.

Pathak R, Dermardirossian C. GEF-H1: orchestrating the interplay between cytoskeleton and vesicle trafficking. *Small GTPases.* 2013;4(3):174-9.

Pathak R, Delorme-Walker VD, Howell MC, Anselmo AN, White MA, Bokoch GM, Dermardirossian C. The microtubule-associated Rho activating factor GEF-H1 interacts with exocyst complex to regulate vesicle traffic. *Dev Cell.* 2012;23(2):397-411.

Peterson JR, Mitchison TJ. Small molecules, big impact: a history of chemical inhibitors and the cytoskeleton. *Chem Biol.* 2002;9(12):1275-85.

Pierini L, Harris NT, Holowka D, Baird B. Evidence supporting a role for microfilaments in regulating the coupling between poorly dissociable IgE-Fc epsilonRI aggregates downstream signaling pathways. *Biochemistry.* 1997;36(24):7447-56.

Pollard TD. Actin and Actin-Binding Proteins. *Cold Spring Harb Perspect Biol.* 2016;8(8):a018226.

Porat-Shliom N, Milberg O, Masedunskas A, Weigert R. Multiple roles for the actin cytoskeleton during regulated exocytosis. *Cell Mol Life Sci.* 2013;70(12):2099-121.

Qi X, J. Hong J, L. Chaves L, Y. Zhuang Y, Y. Chen Y, D. Wang D, J. Chabon J, B. Graham B, K. Ohmori K, Y. Li Y, H. Huang H. Antagonistic regulation by the transcription factors C/EBPalpha and MITF specifies basophil and mast cell fates. *Immunity.* 2013; 39:97-110.

Qian F, Le Breton GC, Chen J, Deng J, Christman JW, Wu D, Ye RD. Role for the guanine nucleotide exchange factor phosphatidylinositol-3,4,5-trisphosphate-dependent rac exchanger 1 in platelet secretion and aggregation. *Arterioscler Thromb Vasc Biol.* 2012;32(3):768-77.

Rafiq NBM, Nishimura Y, Plotnikov SV, Thiagarajan V, Zhang Z, Shi S, Natarajan M, Viasnoff V, Kanchanawong P, Jones GE, Bershadsky AD. A mechano-signalling network linking

microtubules, myosin IIA filaments and integrin-based adhesions. *Nat Mater.* 2019;18(6):638-649.

Randall TS, Yip YY, Wallock-Richards DJ, Pfisterer K, Sanger A, Ficek W, Steiner RA, Beavil AJ, Parsons M, Dodding MP. A small-molecule activator of kinesin-1 drives remodeling of the microtubule network. *Proc Natl Acad Sci U S A.* 2017;114(52):13738-13743.

Ravindran E, Hu H, Yuzwa SA, Hernandez-Miranda LR, Kraemer N, Ninnemann O, Musante L, Boltshauser E, Schindler D, Hübner A, Reinecker HC, Ropers HH, Birchmeier C, Miller FD, Wienker TF, Hübner C, Kaindl AM. Homozygous ARHGEF2 mutation causes intellectual disability and midbrain-hindbrain malformation. *PLoS Genet.* 2017;13(4):e1006746.

Reddy AB, Chatterjee A, Rothblum LI, Black A, Busch H. Isolation and characterization of complementary DNA to proliferating cell nucleolar antigen P40. *Cancer Res.* 1989;49(7):1763-7.

Redegeld FA, Yu Y, Kumari S, Charles N, Blank U. Non-IgE mediated mast cell activation. *Immunol Rev.* 2018;282(1):87-113.

Ren XD, Schwartz MA. Determination of GTP loading on Rho. *Methods Enzymol.* 2000;325:264-72.

Ren Y, Li R, Zheng Y, Busch H. Cloning and characterization of GEF-H1, a microtubule-associated guanine nucleotide exchange factor for Rac and Rho GTPases. *J Biol Chem.* 1998;273(52):34954-60.

Ridley AJ, Hall A. The small GTP-binding protein rho regulates the assembly of focal adhesions and actin stress fibers in response to growth factors. *Cell.* 1992;70(3):389-99.

Ridley AJ, Paterson HF, Johnston CL, Diekmann D, Hall A. The small GTP-binding protein rac regulates growth factor-induced membrane ruffling. *Cell.* 1992;70(3):401-10.

Riedl J, Crevenna AH, Kessenbrock K, Yu JH, Neukirchen D, Bista M, Bradke F, Jenne D, Holak TA, Werb Z, Sixt M, Wedlich-Soldner R. Lifeact: a versatile marker to visualize F-actin. *Nat Methods.* 2008;5(7):605-7.

Robinson NG, Guo L, Imai J, Toh-E A, Matsui Y, Tamanoi F. Rho3 of *Saccharomyces cerevisiae*, which regulates the actin cytoskeleton and exocytosis, is a GTPase which interacts with Myo2 and Exo70. *Mol Cell Biol.* 1999;19(5):3580-7.

Rondas D, Tomas A, Halban PA. Focal adhesion remodeling is crucial for glucose-stimulated insulin secretion and involves activation of focal adhesion kinase and paxillin. *Diabetes.* 2011;60(4):1146-57.

Rondas D, Tomas A, Soto-Ribeiro M, Wehrle-Haller B, Halban PA. Novel mechanistic link between focal adhesion remodeling and glucose-stimulated insulin secretion. *J Biol Chem.* 2012;287(4):2423-36.

Rooney C, White G, Nazgiewicz A, Woodcock SA, Anderson KI, Ballestrem C, Malliri A. The Rac activator STEF (Tiam2) regulates cell migration by microtubule-mediated focal adhesion disassembly. *EMBO Rep.* 2010;11(4):292-8.

Rosa-Ferreira C, Munro S. Arl8 and SKIP act together to link lysosomes to kinesin-1. *Dev Cell.* 2011;21(6):1171-8.

Rossman KL, Der CJ, Sondek J. GEF means go: turning on RHO GTPases with guanine nucleotide-exchange factors. *Nat Rev Mol Cell Biol.* 2005;6(2):167-80.

Sáez JJ, Diaz J, Ibañez J, Bozo JP, Cabrera Reyes F, Alamo M, Gobert FX, Obino D, Bono MR, Lennon-Duménil AM, Yeaman C, Yuseff MI. The exocyst controls lysosome secretion and antigen extraction at the immune synapse of B cells. *J Cell Biol.* 2019;218(7):2247-2264.

Sahara N, Siraganian RP, Oliver C. Morphological changes induced by the calcium ionophore A23187 in rat basophilic leukemia (2H3) cells. *J Histochem Cytochem.* 1990;38(7):975-83.

Sanderson MP, Wex E, Kono T, Uto K, Schnapp A. Syk and Lyn mediate distinct Syk phosphorylation events in FcεRI-signal transduction: implications for regulation of IgE-mediated degranulation. *Mol Immunol.* 2010;48(1-3):171-8.

Sandí MJ, Marshall CB, Balan M, Coyaud É, Zhou M, Monson DM, Ishiyama N, Chandrakumar AA, La Rose J, Couzens AL, Gingras AC, Raught B, Xu W, Ikura M, Morrison DK, Rottapel R. MARK3-mediated phosphorylation of ARHGAP2 couples microtubules to the actin cytoskeleton to establish cell polarity. *Sci Signal.* 2017;10(503):eaan3286.

Sato M, Kitaguchi T, Numano R, Ikematsu K, Kakeyama M, Murata M, Sato K, Tsuboi T. The small GTPase Cdc42 modulates the number of exocytosis-competent dense-core vesicles in PC12 cells. *Biochem Biophys Res Commun.* 2012;420(2):417-21.

Schmidt A, Hall A. Guanine nucleotide exchange factors for Rho GTPases: turning on the switch. *Genes Dev.* 2002;16(13):1587-609.

Schneider CA, Rasband WS, Eliceiri KW. NIH Image to ImageJ: 25 years of image analysis. *Nat Methods.* 2012;9(7):671-5.

Schwartz LB. Diagnostic value of tryptase in anaphylaxis and mastocytosis. *Immunol Allergy Clin North Am.* 2006;26(3):451-63.

Scott DW, Tolbert CE, Burridge K. Tension on JAM-A activates RhoA via GEF-H1 and p115 RhoGEF. *Mol Biol Cell*. 2016;27(9):1420-30.

Seetharaman S, Etienne-Manneville S. Cytoskeletal Crosstalk in Cell Migration. *Trends Cell Biol*. 2020;30(9):720-735.

Sena-Esteves M, Gao G. Titration of Lentivirus Vectors. *Cold Spring Harb Protoc*. 2018;2018(4).

Sheshachalam A, Baier A, Eitzen G. The effect of Rho drugs on mast cell activation and degranulation. *J Leukoc Biol*. 2017;102(1):71-81.

Shibata S, Teshima Y, Niimi K, Inagaki S. Involvement of ARHGEF10, GEF for RhoA, in Rab6/Rab8-mediated membrane traffic. *Small GTPases*. 2019;10(3):169-177.

Shiki A, Inoh Y, Yokawa S, Furuno T. Promotion of microtubule acetylation plays an important role in degranulation of antigen-activated mast cells. *Inflamm Res*. 2019;68(3):181-184.

Siesser PF, Motolese M, Walker MP, Goldfarb D, Gewain K, Yan F, Kulikauskas RM, Chien AJ, Wordeman L, Major MB. FAM123A binds to microtubules and inhibits the guanine nucleotide exchange factor ARHGEF2 to decrease actomyosin contractility. *Sci Signal*. 2012;5(240):ra64.

Siraganian RP, Metzger H. Evidence that the "mouse mastocytoma" cell line (MCT-1) is of rat origin. *J Immunol*. 1978;121(6):2584-5.

Sjölinder M, Uhlmann J, Ponstingl H. DelGEF, a homologue of the Ran guanine nucleotide exchange factor RanGEF, binds to the exocyst component Sec5 and modulates secretion. *FEBS Lett*. 2002;532(1-2):211-5.

Smith AJ, Pfeiffer JR, Zhang J, Martinez AM, Griffiths GM, Wilson BS. Microtubule-dependent transport of secretory vesicles in RBL-2H3 cells. *Traffic*. 2003;4(5):302-12.

Smithers CC, Overduin M. Structural Mechanisms and Drug Discovery Prospects of Rho GTPases. *Cells*. 2016;5(2):26.

Spiczka KS, Yeaman C. Ral-regulated interaction between Sec5 and paxillin targets Exocyst to focal complexes during cell migration. *J Cell Sci*. 2008;121(Pt 17):2880-91.

Stanton RA, Gernert KM, Nettles JH, Aneja R. Drugs that target dynamic microtubules: a new molecular perspective. *Med Res Rev*. 2011;31(3):443-81.

Stehbens S, Wittmann T. Targeting and transport: how microtubules control focal adhesion dynamics. *J Cell Biol*. 2012;198(4):481-9.

- Stehbens SJ, Paszek M, Pemble H, Ettinger A, Gierke S, Wittmann T. CLASPs link focal-adhesion-associated microtubule capture to localized exocytosis and adhesion site turnover. *Nat Cell Biol.* 2014;16(6):561-73.
- Stepanova T, Slemmer J, Hoogenraad CC, Lansbergen G, Dortland B, De Zeeuw CI, Grosveld F, van Cappellen G, Akhmanova A, Galjart N. Visualization of microtubule growth in cultured neurons via the use of EB3-GFP (end-binding protein 3-green fluorescent protein). *J Neurosci.* 2003;23(7):2655-64.
- Stricker J, Falzone T, Gardel ML. Mechanics of the F-actin cytoskeleton. *J Biomech.* 2010;43(1):9-14.
- Sulimenko V, Dráberová E, Sulimenko T, Macurek L, Richterová V, Dráber P, Dráber P. Regulation of microtubule formation in activated mast cells by complexes of gamma-tubulin with Fyn and Syk kinases. *J Immunol.* 2006;176(12):7243-53.
- Sulimenko V, Hájková Z, Černohorská M, Sulimenko T, Sládková V, Dráberová L, Vinopal S, Dráberová E, Dráber P. Microtubule nucleation in mouse bone marrow-derived mast cells is regulated by the concerted action of GIT1/ β PIX proteins and calcium. *J Immunol.* 2015;194(9):4099-111.
- Sun Y, Bamji SX. β -Pix modulates actin-mediated recruitment of synaptic vesicles to synapses. *J Neurosci.* 2011;31(47):17123-33.
- Suzuki R, Inoh Y, Yokawa S, Furuno T, Hirashima N. Receptor dynamics regulates actin polymerization state through phosphorylation of cofilin in mast cells. *Biochem Biophys Res Commun.* 2021;534:714-719.
- Sylvain NR, Nguyen K, Bunnell SC. Vav1-mediated scaffolding interactions stabilize SLP-76 microclusters and contribute to antigen-dependent T cell responses. *Sci Signal.* 2011;4(163):ra14.
- Synek L, Sekereš J, Zárský V. The exocyst at the interface between cytoskeleton and membranes in eukaryotic cells. *Front Plant Sci.* 2014;4:543.
- Takeda K, Gelfand EW. Mouse models of allergic diseases. *Curr Opin Immunol.* 2009;21(6):660-5.
- Tonami K, Kurihara Y, Arima S, Nishiyama K, Uchijima Y, Asano T, Sorimachi H, Kurihara H. Calpain-6, a microtubule-stabilizing protein, regulates Rac1 activity and cell motility through interaction with GEF-H1. *J Cell Sci.* 2011;124(Pt 8):1214-23.
- Vale RD, Reese TS, Sheetz MP. Identification of a novel force-generating protein, kinesin, involved in microtubule-based motility. *Cell.* 1985;42(1):39-50.

Tran DT, Masedunskas A, Weigert R, Ten Hagen KG. Arp2/3-mediated F-actin formation controls regulated exocytosis in vivo. *Nat Commun.* 2015;6:10098.

Wang HL, Yang CH, Lee HH, Kuo JC, Hur SS, Chien S, Lee OK, Hung SC, Chang ZF. Dexamethasone-induced cellular tension requires a SGK1-stimulated Sec5-GEF-H1 interaction. *J Cell Sci.* 2015;128(20):3757-68.

Welch HC. Regulation and function of P-Rex family Rac-GEFs. *Small GTPases.* 2015;6(2):49-70.

Wernersson S, Pejler G. Mast cell secretory granules: armed for battle. *Nat Rev Immunol.* 2014;14(7):478-94.

Wollman R, Meyer T. Coordinated oscillations in cortical actin and Ca²⁺ correlate with cycles of vesicle secretion. *Nat Cell Biol.* 2012;14(12):1261-9.

Wozniak MA, Modzelewska K, Kwong L, Keely PJ. Focal adhesion regulation of cell behavior. *Biochim Biophys Acta.* 2004;1692(2-3):103-19.

Wu B, Guo W. The Exocyst at a Glance. *J Cell Sci.* 2015;128(16):2957-64.

Wu H, Turner C, Gardner J, Temple B, Brennwald P. The Exo70 subunit of the exocyst is an effector for both Cdc42 and Rho3 function in polarized exocytosis. *Mol Biol Cell.* 2010;21(3):430-42.

Xie L, Zhu D, Kang Y, Liang T, He Y, Gaisano HY. Exocyst sec5 regulates exocytosis of newcomer insulin granules underlying biphasic insulin secretion. *PLoS One.* 2013;8(7):e67561.

Xu Y, Chen G. Mast cell and autoimmune diseases. *Mediators Inflamm.* 2015;2015:246126.

Yamashita Y, Saito Y, Murata-Kamiya N, Hatakeyama M. Polarity-regulating kinase partitioning-defective 1b (PAR1b) phosphorylates guanine nucleotide exchange factor H1 (GEF-H1) to regulate RhoA-dependent actin cytoskeletal reorganization. *J Biol Chem.* 2011;286(52):44576-84.

Yamana N, Arakawa Y, Nishino T, Kurokawa K, Tanji M, Itoh RE, Monypenny J, Ishizaki T, Bito H, Nozaki K, Hashimoto N, Matsuda M, Narumiya S. The Rho-mDial pathway regulates cell polarity and focal adhesion turnover in migrating cells through mobilizing Apc and c-Src. *Mol Cell Biol.* 2006;26(18):6844-58.

Yano H, Nakanishi S, Kimura K, Hanai N, Saitoh Y, Fukui Y, Nonomura Y, Matsuda Y. Inhibition of histamine secretion by wortmannin through the blockade of phosphatidylinositol 3-kinase in RBL-2H3 cells. *J Biol Chem.* 1993;268(34):25846-56.

- Yu B, Martins IR, Li P, Amarasinghe GK, Umetani J, Fernandez-Zapico ME, Billadeau DD, Machius M, Tomchick DR, Rosen MK. Structural and energetic mechanisms of cooperative autoinhibition and activation of Vav1. *Cell*. 2010;140(2):246-56.
- Yu T, Liu B, He Z, Yang M, Song J, Ma C, Ma S, Feng J, Wang X, Li J. Short-term in vitro culture of purity and highly functional rat bone marrow-derived mast cells. *In Vitro Cell Dev Biol Anim*. 2018;54(10):705-714.
- Yue P, Zhang Y, Mei K, Wang S, Lesigang J, Zhu Y, Dong G, Guo W. Sec3 promotes the initial binary t-SNARE complex assembly and membrane fusion. *Nat Commun*. 2017;8:14236.
- Zenke FT, Krendel M, DerMardirossian C, King CC, Bohl BP, Bokoch GM. p21-activated kinase 1 phosphorylates and regulates 14-3-3 binding to GEF-H1, a microtubule-localized Rho exchange factor. *J Biol Chem*. 2004;279(18):18392-400.
- Zhang X, Bi E, Novick P, Du L, Kozminski KG, Lipschutz JH, Guo W. Cdc42 interacts with the exocyst and regulates polarized secretion. *J Biol Chem*. 2001;276(50):46745-50.
- Zhang Y, Luo Y, Lyu R, Chen J, Liu R, Li D, Liu M, Zhou J. Proto-Oncogenic Src Phosphorylates EB1 to Regulate the Microtubule-Focal Adhesion Crosstalk and Stimulate Cell Migration. *Theranostics*. 2016;6(12):2129-2140.
- Zhao Y, Zagani R, Park SM, Yoshida N, Shah P, Reinecker HC. Microbial recognition by GEF-H1 controls IKK ϵ mediated activation of IRF5. *Nat Commun*. 2019;10(1):1349.
- Zheng L, Baumann U, Reymond JL. An efficient one-step site-directed and site-saturation mutagenesis protocol. *Nucleic Acids Res*. 2004;32(14):e115.
- Zhu H, Hille B, Xu T. Sensitization of regulated exocytosis by protein kinase C. *Proc Natl Acad Sci U S A*. 2002;99(26):17055-9.
- Zhu Y, Wu B, Guo W. The role of Exo70 in exocytosis and beyond. *Small GTPases*. 2019;10(5):331-335.